Dissertation zur Erlangung des Doktorgrades

der Fakultät für Chemie und Pharmazie

der Ludwig-Maximilians-Universität München

Challenges in the Development of Drug Device Combination Products for Biopharmaceuticals

Fabian Alexander Moll

aus

Heppenheim, Deutschland

2022

Erklärung

Diese Dissertation wurde im Sinne von §7 der Promotionsordnung vom 28. November 2011 von Herrn Prof. Dr. Wolfgang Frieß betreut.

Eidesstattliche Versicherung

Diese Dissertation wurde eigenständig und ohne unerlaubte Hilfe erarbeitet.

Basel, den 01.11.2022

_____

Fabian Moll

Dissertation eingereicht am:	**21.11.2022**
1. Gutachter:	Prof. Dr. Wolfgang Frieß
2. Gutachter:	Prof. Dr. Gerhard Winter
Mündliche Prüfung am:	**08.12.2022**

Für meine Eltern

Acknowledgements

First and foremost, I would like to express my deepest gratitude to my supervisor Prof. Dr. Wolfgang Frieß, who guided me throughout the years and gave me the opportunity to not only grow scientifically, but also on a personal level. Thank you very much for all your advice along the way as well as the support and motivation in less successful times. Besides your contributions to my thesis, you created a great atmosphere within our group, and I always enjoyed my everyday work life.

Many thanks also to Prof. Dr. Gerhard Winter not only for being the co-referee of this thesis, but for providing excellent working conditions at the chair of Pharmaceutical Technology and Biopharmaceutics.

Furthermore, I want to thank Dr. Karoline Bechtold-Peters for her enthusiastic supervision as part of the collaboration with Novartis AG. I highly appreciated the valuable input and support during our scientific discussions and the preparation of the manuscripts. Special thanks also go to Stefan Rapp for the support during my visits in Basel. I would have been lost without you. Many thanks also got to Jürgen Sigg and James Mellman for their contributions especially at the beginning of the project.

Thank you so much to all the colleagues of AK Frieß, AK Winter, and AK Merkel, who contributed to the great working atmosphere during my PhD. I especially will not forget our parties, skiing and hiking trips and most importantly coffee breaks and I will always be grateful for the friendships that were built during this time in my life. Without your support this thesis would have not been possible. My special thanks go to all the members of the Damensauna. I really enjoyed the time with you guys in this lab. Thank you Inas ElBialy, Christoph Marschall and Oliver Blümel for always being there, if needed not only for scientific advice. Of course, this includes the one and only Damensauna award winner Eduard Trenkenschuh. Additionally, I especially want to thank Natalie Deiringer and Dr. Friederike Adams for your help in the lab as well as Omaima Missaoui for her contributions to the last chapter.

I deeply thank my family, my father Dietmar, my mother Angelika, and my sister Sophia for the endless support and love over the years. I am very lucky to always know you by my side.

My greatest thanks go to Ula for always being there over the last years. Especially your patience and encouragement helped me to overcome the downs. I am very grateful to have

you by my side and I will always be thankful for your support in those intensive years – thank you so much.

Funding Acknowledgements

This work was funded by the Novartis AG, Basel.

Table of Contents

Chapter I General Introduction

1 Relevance of Combination Products for Injectables

With the growth of the biopharmaceutical market in the last decades the development of ready-to use drug device combination products (DDCP) for parenterals became increasingly important [1–3]. Especially the market for monoclonal antibodies (mAbs) grew significantly making them the major class of biopharmaceuticals and a mainstream molecular entity [4]. Given the upcoming of biosimilars and considering the pipeline of pharmaceutical companies the sales and prescriptions of biopharmaceuticals are expected to rise further [5,6]. Next to mAbs, various novel protein designs like bispecific antibodies, antibody-drug conjugates or fusion proteins are developed [7]. Additionally, the successful development of mRNA-based vaccines against the severe acute respiratory syndrome coronavirus 2 (SARS-CoV-2) can be expected to give a boost to the development of further RNA therapeutics [8]. All those compounds rely on injection [9]. DDCPs are a preferred packaging system as they ease the handling and administration of parenteral drugs [2,3,10–12]. Compared to vials, they allow injection without further handling steps making the administration easier, safer, and faster. The risk of contamination is significantly reduced, many devices already include safety systems preventing from needle stick injuries, and since the syringes do not need manual withdrawal dosing accuracy is in general higher. The advantages are not only relevant for health care professionals. They eventually enable patient for self-administration, which provides cost savings for the health care sector and increases compliance which is particularly important in treatment of chronic diseases [12,13]. Although the packaging system consists of more components leading to high packaging material costs, this may be at least partially outweighed by the lower overfill volume required in syringes or cartridges which is especially relevant for costly biologics [2]. The first DDCPs were introduced for the delivery of insulin in the 1980s in the form of multidose prefilled and reusable pen injectors [3]. Since then, the use of DDCPs has significantly grown, and this is expected to continue [11,14].

2 DDCP Configurations

DDCPs consists of drug formulation that is packaged in a device so the product comes ready-to use [3]. Strictly speaking, also devices for inhalation or nasal application of drugs can be considered a DDCP. In the context of this work, we focused on devices for the

administration of parenteral predominantly for subcutaneous, but also for intramuscular and intravitreal injections application [10,15]. Devices are often hand-held, although the development of on-body delivery systems becomes increasingly important which allow the injection of large volumes up to 10 mL [2,3,16]. The core of every injection device is the primary container which holds the drug product formulation and consists of a barrel filled with drug product and sealed on two sides (Figure I-1). There is either a crimped cap with a pierceable septum for cartridges or a staked-in needle respectively a luer-lock system for syringes on the top of the container [17].

On the opposite site a rubber plunger is placed. In order to release the drug from the container the plunger needs to be pushed towards the top while opening up the sealing by penetrating through the septum with a needle, removing a rigid needle shield or attaching a needle to the luer lock thread.

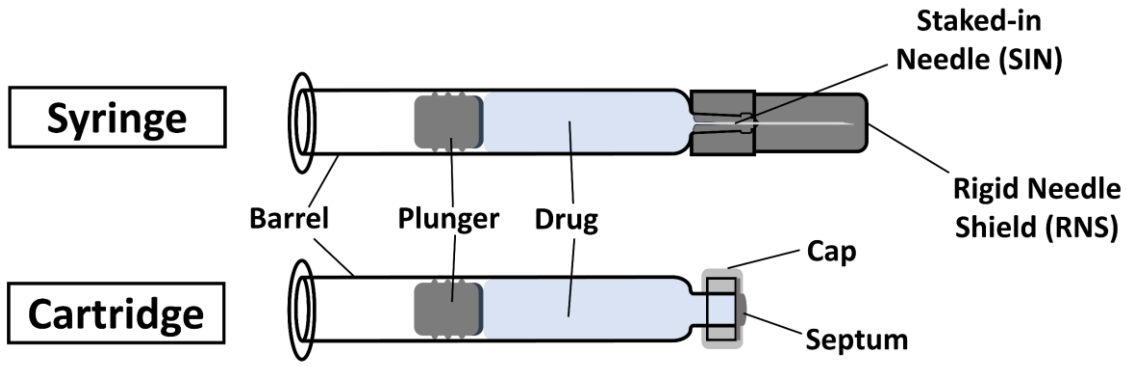

Figure I-1: Schematic construction of the primary container for ready-to use injection devices.

The primary containers are often placed in devices like injection pens, autoinjectors and other large volume on-body delivery injectors [3]. In addition, syringes can be directly combined with accessories like a finger flange, a plunger rod or needle safety systems for the final assembly. Cartridges can be predominantly found in injection pens or patch pumps like for the administration of insulin, where the device can be reused by replacing the primary container. Syringes are more and more utilized as primary containers as they can be placed in autoinjectors but do not necessarily need a further device. The containers can be either based on glass or plastic. In the US and EU, glass is still almost exclusively used material for primary packaging as it shows superior gas barrier properties, higher scratch resistance, and better transparency [12,18]. To ensure an easy and consistent gliding of the plunger the inner surfaces of glass containers are typically coated with silicone oil (SO). With the development of cyclic olefin polymer (COP) and copolymer-based containers the

former issue of low transparency could be overcome for plastic containers [12,18]. Given its inability to brake, the lighter weight and the good leachable and extractable profile the plastic containers became more important in the Japanese market. The plastic containers may be additionally coated with a combination of pure “glass like” silicon dioxide (SiO_2) and organosilicate layers by plasma-enhanced chemical vapor deposition to increase its gas barrier properties to compensate for the low gas barrier properties of the polymer [19].

Although the majority of the DDCPs on the market are liquid formulations, a dual chamber cartridge design allows the packaging of freeze-dried products as well [20,21]. The lyophilizate and the reconstitution medium are separately stored in two chambers divided by an additional plunger and are combined when the plunger is moved, and the liquid can flow through as a bypass channel is opened.

3 Siliconization Methods of Primary Containers

The SO related challenges can be reduced or avoided by using less SO and fixation step after the spray process [22–25]. SO is the most commonly used lubricant on glass barrels to ensure proper functionality. Moreover, it is often applied to the rubber components for better machinability or injection needles as this reduces the friction between needle and skin tissue during penetration. SO can migrate into the drug product solution where it forms microdroplets and potentially interacts with protein molecules. First SO incompatibilities were reported in the 1980s, when clouding and visible particles were observed in siliconized syringes containing insulin [26,27]. Proteins readily adsorb to SO interfaces which can induce unfolding and protein aggregate formation [28–32]. Several studies showed lower protein stability in siliconized syringes compared to vials or silicone oil free (SOF) systems due to the presence of SO microdroplets [33–36]. The formation of mixed SO and protein aggregates may increase the risk of immunogenicity of protein therapeutics [37–40], depending on the protein characteristics [41,42]. SO spiking studies can be performed to assess the tendency of a protein in a certain formulation to interact and be destabilized by SO microdroplets [2,3]. In general, protein interaction with SO can be inhibited by the addition of surfactants like polysorbate 20 and 80 or poloxamer 188 to the formulation [30–32,43–46]. The standard configuration of the primary container in the EU market is still a glass syringe which is siliconized by simply spraying 0.2 – 1 mg raw silicone oil (spray-on siliconization) onto the inner glass barrel surface [47]. Lower SO levels of less than 0.1 mg per barrel are achieved by bake-on siliconization, spraying as

SO-in-water emulsion followed by heat treatment at 300 °C and above which results in water evaporation and a thin, even distribution of the SO on the glass surface [48,49]. Upon baking also low molecular siloxane chains are removed, cross-linking occurs, and the SO is additionally fixed to the surface by covalent bindings [50]. The container systems exhibit much lower tendencies for SO migration due to the fixation and the lower SO levels in the barrels [22,23]. However, this method is not applicable for syringes with staked-in needles as the glue to adhere the needle would at the high baking temperature. Alternatively, the SO may be fixed by irradiation or plasma, which induces cross-linking of the upper regions of the SO layer making it less prone for migration [25,51,52]. Still the SO amounts are higher compared to baked-on siliconized containers as the spray-on process is conducted with raw SO.

SOF container systems were initially COP based [1,35,36,53]. Meanwhile also a SOF glass syringe system is available [54]. The reduction of the friction force is achieved by a complete coating of the syringe plunger with either fluoropolymer or a silicone-based resin [53,55]. The SOF container systems are of particular interest for drugs prone for SO interaction and e.g. for intravitreal administration which requires very low particle counts [2]. In addition, the extrusion force profile over storage is potentially more stable as there is no SO that can be removed.

4 Development Challenges of DDCPs for Biopharmaceuticals

Therapeutic proteins are in general both chemically and physically instable molecules that can degrade via numerous mechanisms [56,57]. They can easily form aggregates due to protein-protein interactions [58]. A suitable formulation typically comprising buffer agents, surfactants, sugars, salts, or antioxidants stabilizes the protein during long-term storage as well as manufacturing, handling and administration [2,3,59–62]. SC administration restricts the injection volume to approx. 2.0 mL, although higher volumes are discussed to be practicable [63,64]. As mAbs require relatively high doses the development of high-concentration protein formulations is essential for a successful therapy via SC injection [65,66]. Higher protein concentrations can come with a higher risk of aggregate formation and an increased viscosity, which could lead to inacceptable high injection forces [2,67–69].

The functionality of a DDCP is an essential requirement that needs to be fulfilled over the complete shelf life [2,70,71]. First of all, the primary container needs to protect the drug product from all external factors that can diminish the products quality and especially prevent microbial contamination as required for parenterals [2]. At the same time the drug product is supposed to be contained, thus the material needs to prevent any kind of permeation, diffusion, or leakage of the product. For example, the plunger of ready-to use primary containers can move during shipment which may compromise product sterility [10]. A variety of different methods is performed to evaluate the requirement summarized as container closure integrity tests [2,59].

In addition, container functionality includes that an appropriately low and consistent force is required to eject the formulation. The extrusion force results from the hydrodynamic resistance of fluid flow through the needle and the friction force between rubber plunger and barrel [71]. The patients with less fine motor skills or strength need to be able to complete a manual injection by themselves. Typically, upper limits for injection forces are between 20 and 25 N guided by product specific human factor studies with the patient population [2,49]. Also, the administration by autoinjectors typically driven by a constant spring mechanism needs to be assured [71]. Injection time may be increased beyond an acceptable level, or the device may completely fail, if forces become too high [2,3,59]. The force required for initiating the plunger movement is defined as the break-loose force, whereas the force needed to keep the plunger moving is referred to as gliding force [71]. It is necessary to apply an SO layer to glass barrels to reduce the friction force between plunger and glass. Upon storage the highly viscous SO can be squeezed out of the contact area between plunger [72] and glass or detach into the drug product solution [23,73], which can result in an increase of both, the break-loose and gliding force, with time. For systems with a staked-in needle the injection forces can be additionally negatively impacted by needle clogging due to the drying or precipitation of drug product that entered the needle and was especially observed for highly concentrated drugs. Leachates from a needle shield rubber were identified as one root cause [74], but also the water vapor transmission through the needle shield plays a role [75,76]. Entering and movement of the formulation in the needle depends on temperature or pressure fluctuations during storage.

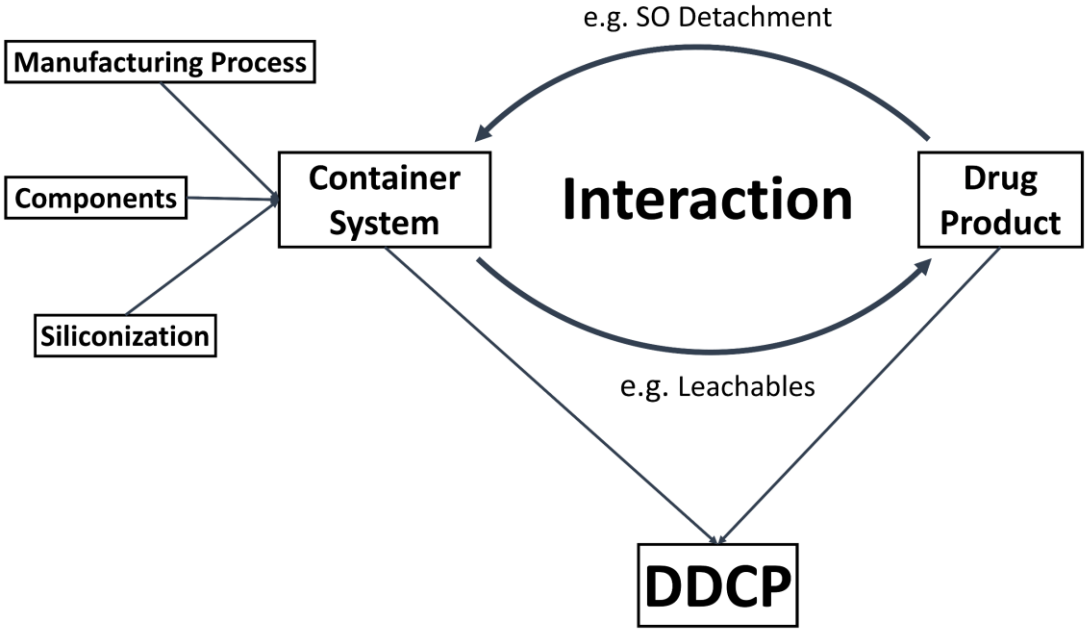

Figure I-2: Interactions between drug product and container system in DDCPs.

Another important issue in the development of DDCPs is the compatibility of the drug product (DP) and the container system (Figure I-2) [2,77]. On the one hand, the DP is confronted with a variety of contact surfaces, materials and leachables. On the other hand the formulation affects the container system e.g. the SO layer which affects the DDCP functionality [73,78]. The choice of the container system and its components needs to be evaluated individually for each DP. One of the most prominent challenges is the presence of SO microdroplets in the DDCP [2,12,22,70,77,79]. Overall, SO migration increases the particle burden, and the SO microdroplets in solution may interact with the biological [22,31,53]. In addition, the process of sloughing off the SO from the inner barrel endangers proper functionality as the direct contact area between rubber plunger and glass is extended. Recent studies suggest that the addition of surfactants to the formulation like polysorbate 80 accelerates this detachment process as a result of the decreased interfacial tension at the SO-formulation interface [73,78,80]. Furthermore, formulation factors like the buffer system, pH and tonicity agents are discussed to affect the container stability [81,82]. Next to SO the DP potentially faces additional leachates released from the different components of the primary container system [77,79]. Residual tungsten respectively tungsten oxide from the needle hole forming process was shown to induce protein denaturation and aggregation leading to increased immunogenicity [83,84]. Other

examples for incompatibilities are the leaching of the adhesive glue from the needles into the drug product causing protein oxidation or leachables from uncoated rubber plungers associated with an increased incidence of pure red cell aplasia [74,85–87].

Finally, the impact of manufacturing processes like washing, drying, siliconization or sterilization of the different components must not be neglected. Certain procedures may impact the physico-chemical properties and affect product stability and quality. For instance, radiation or ethylene oxide (EtO) sterilization were shown to increase protein degradation in polymer-based syringes due to radicals formed or EtO residues in the barrel [88,89]. Besides, the functionality of the container could be affected by physical changes of the stopper or the SO layer. Thus, any changes in the manufacturing processes need to be evaluated for their impact on the product quality and safety [3].

Given the high variety of container systems and novel injectable drugs emerging, the development of DDCPs for biopharmaceuticals will require more attention in the future. Therefore, it is important to understand the differences of the container systems, their interaction propensity with the drug product, and factors impacting functionality.

References

[1] Yoneda, S.; Torisu, T.; Uchiyama, S. Development of Syringes and Vials for Delivery of Biologics: Current Challenges and Innovative Solutions. Expert Opin. Drug Deliv. 2021, 18 (4), 459–470. https://doi.org/10.1080/17425247.2021.1853699.

[2] Warne, N. W.; Mahler, H.-C. Challenges in Protein Product Development. AAPS Advances in the Pharmaceutical Sciences Series; Springer International Publishing: Cham, 2018; Vol. 38. https://doi.org/10.1007/978-3-319-90603-4.

[3] Jameel, F.; Skoug, J. W.; Nesbitt, R. R. Development of Biopharmaceutical Drug-Device Products. AAPS Advances in the Pharmaceutical Sciences Series; Springer International Publishing: Cham, 2020; Vol. 35. https://doi.org/10.1007/978-3-030-31415-6.

[4] Tsumoto, K.; Isozaki, Y.; Yagami, H.; Tomita, M. Future Perspectives of Therapeutic Monoclonal Antibodies. Immunotherapy 2019, 11 (2), 119–127. https://doi.org/10.2217/imt-2018-0130.

[5] Urquhart, L.; Waters, R. World Preview 2020, Outlook to 2026. Evaluate Pharma. 13th Edition - July 2020.

[6] Grilo, A. L.; Mantalaris, A. The Increasingly Human and Profitable Monoclonal Antibody Market. Trends Biotechnol. 2019, 37 (1), 9–16. https://doi.org/10.1016/j.tibtech.2018.05.014.

[7] Elvin, J. G.; Couston, R. G.; Van Der Walle, C. F. Therapeutic Antibodies: Market Considerations, Disease Targets and Bioprocessing. Int. J. Pharm. 2013, 440 (1), 83–98. https://doi.org/10.1016/j.ijpharm.2011.12.039.

[8] Damase, T. R.; Sukhovershin, R.; Boada, C.; Taraballi, F.; Pettigrew, R. I.; Cooke, J. P. The Limitless Future of RNA Therapeutics. Front. Bioeng. Biotechnol. 2021, 9 (March), 1–24. https://doi.org/10.3389/fbioe.2021.628137.

[9] Yu, A. M.; Choi, Y. H.; Tu, M. J. RNA Drugs and RNA Targets for Small Molecules: Principles, Progress, and Challenges. Pharmacol. Rev. 2020, 72 (4), 862–898. https://doi.org/10.1124/pr.120.019554.

[10] Sacha, G.; Rogers, J. A.; Miller, R. L. Pre-Filled Syringes: A Review of the History, Manufacturing and Challenges. Pharm. Dev. Technol. 2015, 20 (1), 1–11. https://doi.org/10.3109/10837450.2014.982825.

[11] Ingle, R. G.; Agarwal, A. S. Pre-Filled Syringe – a Ready-to-Use Drug Delivery System: A Review. Expert Opin. Drug Deliv. 2014, 11 (9), 1391–1399. https://doi.org/10.1517/17425247.2014.923400.

[12] Jezek, J.; Darton, N. J.; Derham, B. K.; Royle, N.; Simpson, I. Biopharmaceutical Formulations for Pre-Filled Delivery Devices. Expert Opin. Drug Deliv. 2013, 10 (6), 811–828. https://doi.org/10.1517/17425247.2013.780023.

[13] Buysman, E.; Conner, C.; Aagren, M.; Bouchard, J.; Liu, F. Adherence and Persistence to a Regimen of Basal Insulin in a Pre-Filled Pen Compared to Vial/Syringe in Insulin-Nave Patients with Type 2 Diabetes. Curr. Med. Res. Opin. 2011, 27 (9), 1709–1717. https://doi.org/10.1185/03007995.2011.598500.

[14] SPECIAL FEATURE - PFS & Parenteral Manufacturing: How COVID-19 Changed the Market - Issue May 2021 (Accessed August 26, 2021). Drug Development and Delivery.

[15] Sassalos, T. M.; Paulus, Y. M. Prefilled Syringes for Intravitreal Drug Delivery. Clin. Ophthalmol. 2019, 13, 695–700. https://doi.org/10.2147/OPTH.S169044.

[16] Furness, A. Wearable Injectors. ONdrugDelivery. Issue No. 111, September 21st , 2020

[17] Sacha, G. A.; Saffell-Clemmer, W.; Abram, K.; Akers, M. J. Practical Fundamentals of Glass, Rubber, and Plastic Sterile Packaging Systems. Pharm. Dev. Technol. 2010, 15 (1), 6–34. https://doi.org/10.3109/10837450903511178.

[18] Werner, B. P.; Schöneich, C.; Winter, G. Silicone Oil-Free Polymer Syringes for the Storage of Therapeutic Proteins. J. Pharm. Sci. 2019, 108 (3), 1148–1160. https://doi.org/10.1016/j.xphs.2018.10.049.

[19] Weikart, C. M.; Pantano, C. G.; Shallenberger, J. R. Performance Stability of Silicone Oxide-Coated Plastic Parenteral Vials. PDA J. Pharm. Sci. Technol. 2017, 71 (4), 317–327. https://doi.org/10.5731/pdajpst.2016.007278.

[20] De Meyer, L.; Lammens, J.; Vanbillemont, B.; Van Bockstal, P. J.; Corver, J.; Vervaet, C.; Friess, W.; De Beer, T. Dual Chamber Cartridges in a Continuous Pharmaceutical Freeze-Drying Concept: Determination of the Optimal Dynamic Infrared Heater Temperature during Primary Drying. Int. J. Pharm. 2019, 570 (April), 118631. https://doi.org/10.1016/j.ijpharm.2019.118631.

[21] Werk, T.; Ludwig, I. S.; Luemkemann, J.; Mahler, H. C.; Huwyler, J.; Hafner, M. Technology, Applications, and Process Challenges of Dual Chamber Systems. J. Pharm. Sci. 2016, 105 (1), 4–9. https://doi.org/10.1016/j.xphs.2015.11.025.

[22] Gerhardt, A.; Nguyen, B. H.; Lewus, R.; Carpenter, J. F.; Randolph, T. W. Effect of the Siliconization Method on Particle Generation in a Monoclonal Antibody Formulation in Pre-Filled Syringes. J. Pharm. Sci. 2015, 104 (5), 1601–1609. https://doi.org/10.1002/jps.24387.

[23] Funke, S.; Matilainen, J.; Nalenz, H.; Bechtold-Peters, K.; Mahler, H.-C.; Friess, W. Silicone Migration From Baked-on Silicone Layers. Particle Characterization in Placebo and Protein Solutions. J. Pharm. Sci. 2016, 105 (12), 3520–3531. https://doi.org/10.1016/j.xphs.2016.08.031.

[24] Felsovalyi, F.; Janvier, S.; Jouffray, S.; Soukiassian, H.; Mangiagalli, P. Silicone-Oil-Based Subvisible Particles: Their Detection, Interactions, and Regulation in Prefilled Container Closure Systems for Biopharmaceuticals. J. Pharm. Sci. 2012, 101 (12), 4569–4583. https://doi.org/10.1002/jps.23328.

[25] Depaz, R. A.; Chevolleau, T.; Jouffray, S.; Narwal, R.; Dimitrova, M. N. Cross-Linked Silicone Coating: A Novel Prefilled Syringe Technology That Reduces Subvisible Particles and Maintains Compatibility with Biologics. J. Pharm. Sci. 2014, 103 (5), 1383–1393. https://doi.org/10.1002/jps.23947.

[26] Chantelau, E.; Berger, M.; Bohlken, B. Silicone Oil Released from Disposable Insulin Syringes. Diabetes Care 1986, 9 (6), 672–673. https://doi.org/10.2337/diacare.9.6.672.

[27] Bernstein, R. K. Clouding and Deactivation of Clear (Regular) Human Insulin: Association With Silicone Oil From Disposable Syringes? Diabetes Care 1987, 10 (6), 786–787. https://doi.org/10.2337/diacare.10.6.786.

[28] Gerhardt, A.; Bonam, K.; Bee, J. S.; Carpenter, J. F.; Randolph, T. W. Ionic Strength Affects Tertiary Structure and Aggregation Propensity of a Monoclonal Antibody Adsorbed to Silicone Oil-Water Interfaces. J Pharm Sci 2013, 102, 429–440. https://doi.org/10.1002/jps.23408.

[29] Jones, L. S.; Kaufmann, A.; Middaugh, C. R. Silicone Oil Induced Aggregation of Proteins. J. Pharm. Sci. 2005, 94 (4), 918–927. https://doi.org/10.1002/jps.20321.

[30] Thirumangalathu, R.; Krishnan, S.; Ricci, M. S.; Brems, D. N.; Randolph, T. W.; Carpenter, J. F. Silicone Oil- and Agitation-Induced Aggregation of a Monoclonal Antibody in Aqueous Solution. J. Pharm. Sci. 2009, 98 (9), 3167–3181. https://doi.org/10.1002/jps.21719.

[31] Kannan, A.; Shieh, I. C.; Negulescu, P. G.; Chandran Suja, V.; Fuller, G. G. Adsorption and Aggregation of Monoclonal Antibodies at Silicone Oil-Water Interfaces. Mol. Pharm. 2021, 18 (4), 1656–1665. https://doi.org/10.1021/acs.molpharmaceut.0c01113.

[32] Mehta, S. B.; Lewus, R.; Bee, J. S.; Randolph, T. W.; Carpenter, J. F. Gelation of a Monoclonal Antibody at the Silicone Oil-Water Interface and Subsequent Rupture of the Interfacial Gel Results in Aggregation and Particle Formation. J. Pharm. Sci. 2015, 104 (4), 1282–1290. https://doi.org/10.1002/jps.24358.

[33] Gerhardt, A.; Mcgraw, N. R.; Schwartz, D. K.; Bee, J. S.; Carpenter, J. F.; Randolph, T. W. Protein Aggregation and Particle Formation in Prefilled Glass Syringes. J. Pharm. Sci. 2014, 103 (6), 1601–1612. https://doi.org/10.1002/jps.23973.

[34] Majumdar, S.; Ford, B. M.; Mar, K. D.; Sullivan, V. J.; Ulrich, R. G.; D'souza, A. J. M. Evaluation of the Effect of Syringe Surfaces on Protein Formulations. Int. J. Drug Dev. Res. 2010, 3 (2), 26–33. https://doi.org/10.1002/jps.

[35] Krayukhina, E.; Tsumoto, K.; Uchiyama, S.; Fukui, K. Effects of Syringe Material and Silicone Oil Lubrication on the Stability of Pharmaceutical Proteins. J. Pharm. Sci. 2015, 104 (2), 527–535. https://doi.org/10.1002/jps.24184.

[36] Waxman, L.; Vilivalam, V. D. A Comparison of Protein Stability in Prefillable Syringes Made of Glass and Plastic. PDA J. Pharm. Sci. Technol. 2017, 71 (6), 462–477. https://doi.org/10.5731/pdajpst.2016.007146.

[37] Chisholm, C. F.; Baker, A. E.; Soucie, K. R.; Torres, R. M.; Carpenter, J. F.; Randolph, T. W. Silicone Oil Microdroplets Can Induce Antibody Responses Against Recombinant Murine Growth Hormone in Mice. J. Pharm. Sci. 2016, 105 (5), 1623–1632. https://doi.org/10.1016/j.xphs.2016.02.019.

[38] Chisholm, C. F.; Soucie, K. R.; Song, J. S.; Strauch, P.; Torres, R. M.; Carpenter, J. F.; Ragheb, J. A.; Randolph, T. W. Immunogenicity of Structurally Perturbed Hen Egg Lysozyme Adsorbed to Silicone Oil Microdroplets in Wild-Type and Transgenic Mouse Models. J. Pharm. Sci. 2017, 106 (6), 1519–1527. https://doi.org/10.1016/j.xphs.2017.02.008.

[39] Uchino, T.; Miyazaki, Y.; Yamazaki, T.; Kagawa, Y. Immunogenicity of Protein Aggregates of a Monoclonal Antibody Generated by Forced Shaking Stress with Siliconized and Nonsiliconized Syringes in BALB/c Mice. J. Pharm. Pharmacol. 2017, 69 (10), 1341–1351. https://doi.org/10.1111/jphp.12765.

[40] Rosenberg, A. S. Effects of Protein Aggregates: An Immunologic Perspective. AAPS J. 2006, 8 (3), 501–507. https://doi.org/10.1208/aapsj080359.

[41] Bai, S.; Landsman, P.; Spencer, A.; Decollibus, D.; Vega, F.; Temel, D. B.; Houde, D.; Henderson, O.; Brader, M. L. Evaluation of Incremental Siliconization Levels on Soluble Aggregates, Submicron and Subvisible Particles in a Prefilled Syringe Product. J. Pharm. Sci. 2016, 105 (1), 50–63. https://doi.org/10.1016/j.xphs.2015.10.012.

[42] Auge, K. B.; Blake-Haskins, A. W.; Devine, S.; Rizvi, S.; Li, Y.-M.; Hesselberg, M.; Orvisky, E.; Affleck, R. P.; Spitznagel, T. M.; Perkins, M. D. Demonstrating the Stability of Albinterferon Alfa-2b in the Presence of Silicone Oil. J. Pharm. Sci. 2011, 100 (12), 5100–5114. https://doi.org/10.1002/jps.22704.

[43] Gerhardt, A.; McUmber, A. C.; Nguyen, B. H.; Lewus, R.; Schwartz, D. K.; Carpenter, J. F.; Randolph, T. W. Surfactant Effects on Particle Generation in Antibody Formulations in Pre-Filled Syringes. J. Pharm. Sci. 2015, 104 (12), 4056–4064. https://doi.org/10.1002/jps.24654.

[44] Khan, T. A.; Mahler, H. C.; Kishore, R. S. K. Key Interactions of Surfactants in Therapeutic Protein Formulations: A Review. Eur. J. Pharm. Biopharm. 2015, 97, 60–67. https://doi.org/10.1016/j.ejpb.2015.09.016.

[45] Basu, P.; Blake-Haskins, A. W.; O'Berry, K. B.; Randolph, T. W.; Carpenter, J. F. Albinterferon A2b Adsorption to Silicone Oil–Water Interfaces: Effects on Protein Conformation, Aggregation, and Subvisible Particle Formation. J. Pharm. Sci. 2014, 103 (2), 427–436. https://doi.org/10.1002/jps.23821.

[46] Höger, K.; Mathes, J.; Frieß, W. IgG1 Adsorption to Siliconized Glass Vials-Influence of PH, Ionic Strength, and Nonionic Surfactants. J. Pharm. Sci. 2015, 104 (1), 34–43. https://doi.org/10.1002/jps.24239.

[47] Loosli, V.; Germershaus, O.; Steinberg, H.; Dreher, S.; Grauschopf, U.; Funke, S. Methods To Determine the Silicone Oil Layer Thickness in Sprayed-On Siliconized Syringes. PDA J. Pharm. Sci. Technol. 2018, 72 (3), 278–297. https://doi.org/10.5731/pdajpst.2017.007997.

[48] Funke, S.; Matilainen, J.; Nalenz, H.; Bechtold-Peters, K.; Mahler, H.-C.; Friess, W. Analysis of Thin Baked-on Silicone Layers by FTIR and 3D-Laser Scanning Microscopy. Eur. J. Pharm. Biopharm. 2015, 96, 304–313. https://doi.org/10.1016/j.ejpb.2015.08.009.

[49] Funke, S.; Matilainen, J.; Nalenz, H.; Bechtold-Peters, K.; Mahler, H.-C.; Friess, W. Optimization of the Bake-on Siliconization of Cartridges. Part I: Optimization of the Spray-on Parameters. Eur. J. Pharm. Biopharm. 2016, 104, 200–215. https://doi.org/10.1016/j.ejpb.2016.05.007.

[50] Funke, S.; Matilainen, J.; Nalenz, H.; Bechtold-Peters, K.; Mahler, H.-C.; Vetter, F.; Müller, C.; Bracher, F.; Friess, W. Optimization of the Bake-on Siliconization of Cartridges. Part II: Investigations into Burn-in Time and Temperature. Eur. J. Pharm. Biopharm. 2016, 105, 209–222. https://doi.org/10.1016/j.ejpb.2016.05.015.

[51] Chillon, A.; Pace, A.; Zuccato, D. Introducing the Alba ® Primary Packaging Platform. Part 1: Particle Release Evaluation . PDA J. Pharm. Sci. Technol. 2018, 72 (4), 382–392. https://doi.org/10.5731/pdajpst.2018.008623.

[52] Thakare, V.; Schmidt, T.; Rupprechter, O.; Leibold, J.; Stemmer, S.; Mischo, A.; Bhattacharjee, D.; Prazeller, P. Can Cross-Linked Siliconized PFS Come to the Rescue of the Biologics Drug Product? J. Pharm. Sci. 2020, 109 (11), 3340–3351. https://doi.org/10.1016/j.xphs.2020.08.018.

[53] Yoshino, K.; Nakamura, K.; Yamashita, A.; Abe, Y.; Iwasaki, K.; Kanazawa, Y.; Funatsu, K.; Yoshimoto, T.; Suzuki, S. Functional Evaluation and Characterization of a Newly Developed Silicone Oil-Free Prefillable Syringe System. J. Pharm. Sci. 2014, 103 (5), 1520–1528. https://doi.org/10.1002/jps.23945.

[54] Silicone-Free Plungers To Enable Delivery of Complex, Sensitive Biologics. W. L. Gore & Associates, Inc. 2019.

[55] When Performance Matters Most - Daikyo Crystal Zenith ® www.westpharm.com.

[56] Manning, M. C.; Chou, D. K.; Murphy, B. M.; Payne, R. W.; Katayama, D. S. Expert Review Stability of Protein Pharmaceuticals : An Update. 2010, 27 (4), 544–575. https://doi.org/10.1007/s11095-009-0045-6.

[57] Chi, E. Y.; Krishnan, S.; Randolph, T. W.; Carpenter, J. F. Physical Stability of Proteins in Aqueous Solution: Mechanism and Driving Forces in Nonnative Protein Aggregation. Pharm. Res. 2003, 20 (9), 1325–1336. https://doi.org/10.1023/A:1025771421906.

[58] Manning, M. C.; Chou, D. K.; Murphy, B. M.; Payne, R. W.; Katayama, D. S. Stability of Protein Pharmaceuticals: An Update. Pharm. Res. 2010, 27 (4), 544–575. https://doi.org/10.1007/s11095-009-0045-6.

[59] Hershenson, S.; Jameel, F. Formulation and Process Development Strategies for Manufacturing Biopharmaceuticals; Jameel, F., Hershenson, S., Eds.; John Wiley & Sons, Inc.: Hoboken, NJ, USA, 2010. https://doi.org/10.1002/9780470595886.

[60] Wang, W. Instability, Stabilization, and Formulation of Liquid Protein Pharmaceuticals. Int. J. Pharm. 1999, 185 (2), 129–188. https://doi.org/10.1016/S0378-5173(99)00152-0.

[61] Goldberg, D. S.; Bishop, S. M.; Shah, A. U.; Sathish, H. A. Formulation Development of Therapeutic Monoclonal Antibodies Using High-Throughput Fluorescence and Static Light Scattering Techniques: Role of Conformational and Colloidal Stability. J. Pharm. Sci. 2011, 100 (4), 1306–1315. https://doi.org/10.1002/jps.22371.

[62] Capelle, M. A. H.; Gurny, R.; Arvinte, T. High Throughput Screening of Protein Formulation Stability: Practical Considerations. Eur. J. Pharm. Biopharm. 2007, 65 (2), 131–148. https://doi.org/10.1016/j.ejpb.2006.09.009.

[63] Mathaes, R.; Koulov, A.; Joerg, S.; Mahler, H. C. Subcutaneous Injection Volume of Biopharmaceuticals—Pushing the Boundaries. J. Pharm. Sci. 2016, 105 (8), 2255–2259. https://doi.org/10.1016/j.xphs.2016.05.029.

[64] Berteau, C.; Filipe-Santos, O.; Wang, T.; Roja, H. E.; Granger, C.; Schwarzenbach, F. Evaluation of the Impact of Viscosity, Injection Volume, and Injection Flow Rate on Subcutaneous Injection Tolerance. Med. Devices Evid. Res. 2015, 8, 473–484. https://doi.org/10.2147/MDER.S91019.

[65] Richter, W. F.; Bhansali, S. G.; Morris, M. E. Mechanistic Determinants of Biotherapeutics Absorption Following SC Administration. AAPS J. 2012, 14 (3), 559–570. https://doi.org/10.1208/s12248-012-9367-0.

[66] Fathallah, A. M.; Balu-Iyer, S. V. Anatomical, Physiological, and Experimental Factors Affecting the Bioavailability of Sc-Administered Large Biotherapeutics. J. Pharm. Sci. 2015, 104 (2), 301–306. https://doi.org/10.1002/jps.24277.

[67] Garidel, P.; Kuhn, A. B.; Schäfer, L. V.; Karow-Zwick, A. R.; Blech, M. High-Concentration Protein Formulations: How High Is High? Eur. J. Pharm. Biopharm. 2017, 119, 353–360. https://doi.org/10.1016/j.ejpb.2017.06.029.

[68] Saluja, A.; Kalonia, D. S. Nature and Consequences of Protein-Protein Interactions in High Protein Concentration Solutions. International Journal of Pharmaceutics. 2008. https://doi.org/10.1016/j.ijpharm.2008.03.041.

[69] Burckbuchler, V.; Mekhloufi, G.; Giteau, A. P.; Grossiord, J. L.; Huille, S.; Agnely, F. Rheological and Syringeability Properties of Highly Concentrated Human Polyclonal Immunoglobulin Solutions. Eur. J. Pharm. Biopharm. 2010, 76 (3), 351–356. https://doi.org/10.1016/j.ejpb.2010.08.002.

[70] Badkar, A.; Wolf, A.; Bohack, L.; Kolhe, P. Development of Biotechnology Products in Pre-Filled Syringes: Technical Considerations and Approaches. AAPS PharmSciTech 2011, 12 (2), 564–572. https://doi.org/10.1208/s12249-011-9617-y.

[71] Rathore, N.; Pranay, P.; Eu, B.; Ji, W.; Walls, E. Variability in Syringe Components and Its Impact on Functionality of Delivery Systems. PDA J. Pharm. Sci. Technol. 2011, 65 (5), 468–480. https://doi.org/10.5731/pdajpst.2011.00785.

[72] Lorenz, B.; Krick, B. A.; Rodriguez, N.; Sawyer, W. G.; Mangiagalli, P.; Persson, B. N. J. Static or Breakloose Friction for Lubricated Contacts: The Role of Surface Roughness and Dewetting. J. Phys. Condens. Matter 2013, 25 (44), 445013. https://doi.org/10.1088/0953-8984/25/44/445013.

[73] Wang, T.; Richard, C. A.; Dong, X.; Shi, G. H. Impact of Surfactants on the Functionality of Prefilled Syringes. J. Pharm. Sci. 2020, 1–10. https://doi.org/10.1016/j.xphs.2020.07.033.

[74] Adler, M. Challenges in the Development of Pre-Filled Syringes for Biologics from a Formulation Scientist's Point of View. American Pharmaceutical Review. 2012. (Accessed 26 September 2019) https://www.americanpharmaceuticalreview.com/Featured-Articles/38372-Challenges-in-the-Development-of-Pre-filled-Syringes-for-Biologics-from-a-Formulation-Scientist-s-Point-of-View/

[75] De Bardi, M.; Müller, R.; Grünzweig, C.; Mannes, D.; Rigollet, M.; Bamberg, F.; Jung, T. A.; Yang, K. Clogging in Staked-in Needle Pre-Filled Syringes (SIN-PFS): Influence of Water Vapor Transmission through the Needle Shield. Eur. J. Pharm. Biopharm. 2018, 127 (February), 104–111. https://doi.org/10.1016/j.ejpb.2018.02.016.

[76] De Bardi, M.; Müller, R.; Grünzweig, C.; Mannes, D.; Boillat, P.; Rigollet, M.; Bamberg, F.; Jung, T. A.; Yang, K. On the Needle Clogging of Staked-in-Needle Pre-Filled Syringes: Mechanism of Liquid Entering the Needle and Solidification Process. Eur. J. Pharm. Biopharm. 2018, 128 (February), 272–281. https://doi.org/10.1016/j.ejpb.2018.05.006.

[77] Jenke, D. R. Extractables and Leachables Considerations for Prefilled Syringes. Expert Opin. Drug Deliv. 2014, 11 (10), 1591–1600. https://doi.org/10.1517/17425247.2014.928281.

[78] Richard, C. A.; Wang, T.; Clark, S. L. Using First Principles to Link Silicone Oil / Formulation Interfacial Tension with Syringe Functionality in Pre-Filled Syringes Systems. J. Pharm. Sci. 2020. https://doi.org/10.1016/j.xphs.2020.06.014.

[79] Bee, J. S.; Randolph, T. W.; Carpenter, J. F.; Bishop, S. M.; Dimitrova, M. N. Effects of Surfaces and Leachables on the Stability of Biopharmaceuticals. J. Pharm. Sci. 2011, 100 (10), 4158–4170. https://doi.org/10.1002/jps.22597.

[80] Fang, L.; Richard, C. A.; Shi, G. H.; Dong, X.; Rase, M. C.; Wang, T. Physicochemical Excipient-Container Interactions in Prefilled Syringes and Their Impact on Syringe Functionality. PDA J. Pharm. Sci. Technol. 2021, pdajpst.2020.012278. https://doi.org/10.5731/pdajpst.2020.012278.

[81] Shi, G. H.; Gopalrathnam, G.; Shinkle, S. L.; Dong, X.; Hofer, J. D.; Jensen, E. C.; Rajagopalan, N. Impact of Drug Formulation Variables on Silicone Oil Structure and Functionality of Prefilled Syringe System. PDA J. Pharm. Sci. Technol. 2018, 72 (1), 50–61. https://doi.org/10.5731/pdajpst.2017.008169.

[82] Fang, L.; Shi, G. H.; Richard, C. Adè.; Dong, X.; Thomas, J. C.; Victor, M. C.; Wang, T.; Shinkle, S.; Zhao, C. Drug Formulation Impact on Prefilled Syringe Functionality and Autoinjector Performance. PDA J. Pharm. Sci. Technol. 2020, 74 (6), 674–687. https://doi.org/10.5731/pdajpst.2020.011627.

[83] Seidl, A.; Hainzl, O.; Richter, M.; Fischer, R.; B??hm, S.; Deutel, B.; Hartinger, M.; Windisch, J.; Casadevall, N.; London, G. M.; Macdougall, I. Tungsten-Induced Denaturation and Aggregation of Epoetin Alfa during Primary Packaging as a Cause of Immunogenicity. Pharm. Res. 2012, 29 (6), 1454–1467. https://doi.org/10.1007/s11095-011-0621-4.

[84] Liu, W.; Swift, R.; Torraca, G.; Nashed-Samuel, Y.; Wen, Z. Q.; Jiang, Y.; Vance, A.; Mire-Sluis, A.; Freund, E.; Davis, J.; Narhi, L. Root Cause Analysis of Tungsten-Induced Protein Aggregation in Pre-Filled Syringes. PDA J. Pharm. Sci. Technol. 2010, 64 (1).

[85] Boven, K.; Stryker, S.; Knight, J.; Thomas, A.; Van Regenmortel, M.; Kemeny, D. M.; Power, D.; Rossert, J.; Casadevall, N. The Increased Incidence of Pure Red Cell Aplasia with an Eprex Formulation in Uncoated Rubber Stopper Syringes. Kidney Int. 2005, 67 (6), 2346–2353. https://doi.org/10.1111/j.1523-1755.2005.00340.x.

[86] Sharma, B. Immunogenicity of Therapeutic Proteins. Part 2: Impact of Container Closures. Biotechnol. Adv. 2007, 25 (3), 318–324. https://doi.org/10.1016/j.biotechadv.2007.01.006.

[87] Liu, D.; Nashed-Samuel, Y.; Bondarenko, P. V.; Brems, D. N.; Ren, D. Interactions between Therapeutic Proteins and Acrylic Acid Leachable. PDA J. Pharm. Sci. Technol. 2012, 66 (1), 12–19. https://doi.org/10.5731/pdajpst.2012.00803.

[88] Funatsu, K.; Kiminami, H.; Abe, Y.; Carpenter, J. F. Impact of Ethylene Oxide Sterilization of Polymer-Based Prefilled Syringes on Chemical Degradation of a Model Therapeutic Protein During Storage. J. Pharm. Sci. 2019, 108 (1), 770–774. https://doi.org/10.1016/j.xphs.2018.09.029.

[89] Kiminami, H.; Krueger, A. B.; Abe, Y.; Yoshino, K.; Carpenter, J. F. Impact of Sterilization Method on Protein Aggregation and Particle Formation in Polymer-Based Syringes. J. Pharm. Sci. 2017, 106 (4), 1001–1007. https://doi.org/10.1016/j.xphs.2016.12.007.

Chapter II Aim and Outline of the Thesis

The thesis compromises multiple topics in context of the development of primary containers for drug device combination products (DDCPs) for biopharmaceuticals. This included a variety of different alternative container systems discussed in the introduction. In all chapters the quality and the performance of primary containers was to be investigated, and the influence on the overall stability and safety of the DDCP was to be discussed.

The first two studies revolve around the development of container systems with baked-on SO layers. In **chapter III** the impact of a change of the spray emulsion for the bake-on siliconization was investigated. Such change may affect the handling properties of the emulsion as well as the obtained SO layer which ultimately affects final product safety and quality. The studies were conducted to scientifically support the transition from the current gold standard emulsion to a new formulation which is in line with the implemented regulation REACh (Regulation concerning the Registration, Evaluation, Authorisation and Restriction of Chemicals) in the European Union. In a next step the impact of steam sterilization on baked-on siliconized containers was evaluated in **chapter IV**. Steam sterilization may be performed in the course of container preparation for filling. Containers with different SO levels were produced and autoclaved at different process parameters. Subsequently, a toolbox of methods was utilized to monitor changes of the SO layer due to autoclavation. Besides, functionality and particle formation of non-autoclaved and autoclaved container systems were compared in an accelerated stability study. Overall, the study aimed to clarify the impact of steam sterilization on the safety and quality of baked-on siliconized container systems for biopharmaceuticals.

To resolve the SO related problems silicone oil free (SOF) container systems were introduced to the market. **In chapter V**, we examined a newly developed glass-based SOF container system and compared it in a long-term stability study to bake-on and cross-linked siliconized container systems to assess its quality and performance compared to novel alternative packaging systems with improved SO migration properties. Functionality and particle formation were monitored upon storage up to 2 years and the state of the SO layer was assessed upon storage. Additionally, we characterized the stopper and evaluated the influence of the surface properties on the container functionality. Friction forces were correlated with contact angle of the fill medium and glass surface energy. The aim was to identify factors that impact container functionality of a SOF container system.

Next to the alternative container systems, we focused on the phenomenon of SO detachment in spray-on siliconized container systems in **chapter VI**. The impact of the fill medium on the container extrusion forces upon accelerated and long-term storage conditions was examined. We tested different formulations factors in the presence of a monoclonal antibody (mAb) as well three different mAbs in one formulation for the purpose of further understanding the role of the formulations components as well as the protein in the SO migration process. The change in gliding forces was linked to the state of the SO layer monitored by SO quantification and layer thickness measurements as well as 3D-laser scanning microscopy (3D-LSM) measurements of the inner surface of the barrel. An additional objective was to find a link between the outcome of the stability studies and the properties of the interface between SO and formulation as analyzed by a profile analysis tensiometer as well as the conformational stability and hydrophobicity of the mAbs.

Chapter III Replacing the Emulsion for Bake-on Siliconization of Containers

This chapter is published* as:

Fabian Moll[1], Karoline Bechtold-Peters[2], James Mellman[2,3], Jürgen Sigg[2], Wolfgang Friess[1]

"Replacing the Emulsion for Bake-on Siliconization of Containers - Comparison of Emulsion Stability and Container Performance in the Context of Protein Formulations"

In PDA Journal of Pharmaceutical Science and Technology; Vol. 76, No. 2, March-April 2022 - https://doi.org/10.5731/pdajpst.2021.012640

1 Pharmaceutical Technology and Biopharmaceutics, Department of Pharmacy, Ludwig-Maximilians-Universität München, 81377 Munich, Germany

2 Technical Research and Development, Novartis Pharma AG, 4002 Basel, Switzerland

3 SHL Medical AG, Zug, Switzerland

* The version included in this thesis is identical with the published article apart from minor changes.

Graphical Abstract

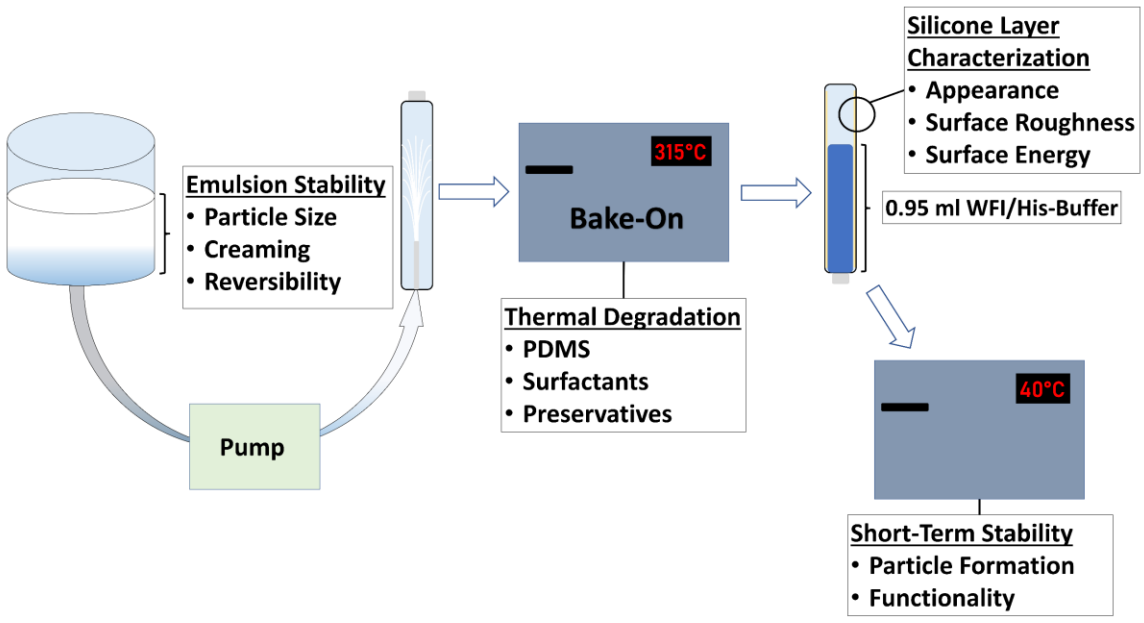

Abstract

Pre-filled syringes have simplified parenteral administration of protein drugs. To ensure an easy and consistent movement of the plunger, the inner glass container surface is typically siliconized. For bake-on siliconization, emulsions are sprayed on and heat treated. Due to the European Union regulation REACh (Regulation concerning the Registration, Evaluation, Authorisation and Restriction of Chemicals) the use of certain emulsion components, partially constituting the gold standard Liveo™ 365 35 % Dimethicone NF Emulsion (Liveo™ 365), becomes restricted and Liveo™ 366 35 % Dimethicone NF Emulsion (Liveo™ 366) has been introduced as an alternative. This change may affect the handling properties as well as the silicone layer formed. The purpose of these studies was to identify any differences that may influence the stability and safety of the final drug/device combination product to enable the use of the new emulsion. We compared silicone emulsions Liveo™ 365 and Liveo™ 366 and dilutions focusing on 1) their general physical stability, 2) the thermal degradation process of the emulsions and their components, and 3) the resulting silicone layer concerning chemistry, morphology, and functionality. The results were linked to the assessment of the final product regarding particle formation and short-term stability. A comparison of the emulsions Liveo™ 365 and Liveo™ 366 for bake-on siliconization is presented to support the transition of the latter as it becomes mandatory with REACh. Our studies show that the two emulsions do not significantly differ with respect to handling and stability, the resultant silicone layer characteristics as well as its functionality. We conclude that the transition to the new emulsion will not significantly impact the final product or the layer performance upon storage and with respect to particle formation.

Keywords

Bake-on siliconization – Protein formulation – Drug/device combination product – Primary packaging – Biopharmaceuticals – Silicone interaction – Silicone layer characterization

1 Introduction

Pre-filled syringes (PFSs), which are often combined with autoinjectors to drug/device combination products, facilitate parenteral administration such as subcutaneous and intravitreal injections of protein drug formulations by reducing handling steps, thereby optimizing dosage accuracy, safety, and sterility assurance. They enable self-administration by the patient or ease application by health care providers (HCPs), thus increase compliance and reduce costs for the health care sector [1–4]. This makes these PFSs highly important for the success of protein drugs that need to be administered parenterally.

Ensuring functionality of ready-to-use devices throughout the product shelf life is a big challenge to the industry [5]. The primary packaging of those devices typically consists of a glass or plastic barrel, a staked-in needle, a luer tip or a cap in combination with a piercing needle sitting on top and a plunger at the bottom [1,3]. The friction forces between plunger and barrel strongly impact the break-loose force to initiate gliding and the force during gliding itself. Together these forces are termed the break-loose gliding forces (BLGF) and used to describe an attribute of the performance from the primary packaging. In order to reduce the friction, inner walls of the barrels are by default siliconized [2]. During storage, silicone oil can migrate into the liquid formulation, resulting in an increase of the BLGF over time [6]. The detached silicone oil may not only lead to higher subvisible particle levels and visible droplets, but in some cases, it may interact with protein molecules with a potential to reduce their overall stability and activity and in worst cases lead to immunogenic reactions by the patient [5,7–14]. Hence, the silicone coating level on the barrel must be optimized, balancing both device functionality and product stability over the product shelf life [1,5]. The most common way to siliconize the primary container is to spray pure silicone oil into the barrel. To reduce the migration of silicone oil droplets, the silicone layer may be cured by heat (bake-on), with plasma or ultraviolet light. Much thinner silicone layers compared with “spray-on” siliconized containers can be achieved by bake-on siliconization, resulting in less particle formation while ensuring device functionality [6,15]. Accordingly, the bake-on siliconization is particularly of interest for the development of products for intravitreal injection to conform to USP <789> [5]. After spraying 1.5 % to 3.5 % silicone oil emulsions onto the glass container, water is evaporated, and the silicone oil spreads at high temperatures of 300 °C–320 °C [15–18]. Dow Corning 365 35 % Dimethicone NF Emulsion (DC 365) used to be the gold standard for bake-on siliconization [16,17]. It contains 35 % polydimethylsiloxane (PDMS), methyl and propyl

paraben as preservatives, and the surfactants polysorbate 20 and Triton X-100 as well as propylene glycol to prevent the emulsion from braking [17,19–22]. However, Triton X-100 was recently added to the Authorisation List (Annex IV) of the European Union regulation REACh (Regulation concerning the Registration, Evaluation, Authorisation and Restriction of Chemicals). REACh is a European Union regulation concerned with the protection of human health and the environment from harm caused by chemicals [19,23]. The European Chemicals Agency has set the January 4, 2021, to be the sunset date for the surfactant. Consequently, Dow Corning Corporation (renamed Dow Silicones Corporation in 2017) introduced a similar product, Dow Corning 366 35 % Dimethicone NF Emulsion (DC 366), to replace DC 365. Both DC 366 and DC 365 are now Liveo™-branded products owned by DuPont subsidiaries by virtue of the DowDuPont merger in 2017, corporate reorganizations, and subsequent separations in 2018–2019. In Liveo™ 366, Triton X-100 is substituted by polyethylene glycol [5] undeceth ether also known as Undeceth-5 [20]. Additionally, the formulation contains phenoxyethanol instead of the formerly used parabens as preservatives [20,23]. As the replacement of Liveo™ 365 by Liveo™ 366 becomes inevitable, a thorough assessment of the effect of the conversion for pharmaceutical products intended for the European market is important. For this purpose, we compared the physical stability and the thermal degradation behavior of the two emulsions and studied the characteristics of the formed silicone oil layer as well as the product performance in a small stability study. The stability of the diluted emulsion is particularly important to observe as creaming and coalescence could alter the silicone oil amount applied onto the glass wall, potentially affecting functionality. Creaming was assessed and particle size and size distribution were monitored upon stress for both emulsions. We assessed the bake-on process of the emulsion and the decomposition of the substituted and newly added excipients as well as their thermal stability at different temperatures. The excipient ought to be removed during the bake-on process to mitigate the risk of interactions of residuals or decomposition products with the drug products [24]. During the bake-on process, the PDMS is partly volatilized, depolymerized, and binds covalently to the glass surface to a certain extent [17,21,25–29]. The thermal degradation is significantly affected by oxygen [30] and can be accelerated by the ingredients contained in the emulsion formulation [17]. An altered thermal degradation behavior of the PDMS could make different bake-on conditions necessary to achieve the desired film characteristics along the length of the barrel. Therefore, glass cartridges as an example for any siliconized glass barrel body were siliconized with both emulsions, and the appearance

as well as the physical properties of the formed silicone layer were characterized by 3D-laser scanning microscopy and contact angle measurements. Additionally, the cartridges were filled with placebo formulations, and particle formation and functionality were tested on a short-term stability study.

2 Materials and Methods

The following material was used in this study.

2.1 Materials

Liveo™ 365 and Liveo™ 366 were purchased, and Undeceth-5 was kindly provided by Dow Silicones Corporation (Midland, MI, USA). Dilutions were prepared using highly purified water (HPW). Non-siliconized 1 mL long cartridges were provided by Nuova Ompi S.r.l. (Piombino Dese, Italy). Additional chemicals used were polysorbate 20 (Merck KGaA, Darmstadt, Germany), Triton X-100, propylene glycol, methyl and propyl paraben, L-histidine monohydrochloride, L-histidine, sucrose and polysorbate 80 (Sigma-Aldrich Chemie GmbH, Steinheim, Germany), phenoxyethanol (Roth GmbH & Co KG, Karlsruhe, Germany), and ethylene glycol (Grüssing GmbH, Filsum, Germany). Diiodomethane and the microscope slides were purchased from VWR International GmbH (Darmstadt, Germany).

2.2 Physical Stability of Diluted Emulsion

Creaming Effect

4.5 mL of emulsion diluted with HPW to 1.75 % (w/w) were filled into 15 mL Falcon tubes and stored at 25 °C protected from light for 60 days. To identify a creaming effect, visual inspection was performed. Additionally, 850 µL samples were taken from the bottom as well as the middle of a redispersed sample and transferred to 2 R vials to evaporate the water at 70 °C in an incubator. Samples were redispersed by shaking 10 times. The residual silicone oil was dissolved in 1 mL n-heptane and quantified using a FTIR Tensor 27 (Bruker Corp., Billerica, MA, USA) equipped with a 250 µm path length transmission liquid cell. Absorption spectra based on 100 scans with a resolution of 4 cm^{-1} between 3000 and 900 cm^{-1} were used. The area under the curve (AUC) of the symmetrical Si-CH_3 deformation vibration at 1261 cm^{-1} was used for quantification [31]. Silicone oil 1000 cSt (Sigma-Aldrich Chemie GmbH, Steinheim, Germany) solutions in n-heptane between 0.5 mg/mL and 16.67 mg/mL were used for calibration (Supplementary data, Figure S III-1). (n = 3)

Coalescence

Emulsions diluted to 1.75 % and 3.5 % (w/w) were stored in the same container type and with the same fill volume at 60 °C for 5 and 20 days or stressed by five freeze-thaw cycles

between 25 °C and -20 °C. For the latter, samples were stored in a deep freezer overnight and thawed during the day. The droplet size was determined with Zetasizer Nano ZS (Malvern Panalytical Ltd, Malvern, UK) in backscattering mode after redispersion of the samples as stated previously. Samples were redispersed by heavily shaking the container manually 10 times. (n = 3)

Creaming Velocity

Diluted emulsions of 1.75 % and 3.5 % (w/w) were analyzed using a LUMiSizer® 651 (LUM GmbH, Berlin, Germany). Based on transmission, the movement of the phase boundary upon centrifugation is monitored. The slope of the linear fit from the start to the end of the creaming process is defined as the creaming velocity. Samples were measured at 25 °C and 4000 rpm for 125 min and at 1500 rpm for 875 min. Particle size distribution was assessed following ISO 13,318 at 7 °C at "constant position". The intensity of transmitted light is hereby measured along the whole length of the sample container while being centrifuged. The particle size distribution can be calculated based on the concentration, density, and refractive index of the dispersed phase using the STEP™ Technology (Space- and time resolved extinction profiles) [32,33]. (n = 2)

Particle Size Distribution via Analytical Centrifugation

To determine the cumulative volume weighted particle size distribution (Q3[x]), the extinction of diluted emulsions of 0.35 % (w/w) alongside the complete sample length was measured at λ = 870 nm at increasing rotational speed between 300 and 4000 rpm (rpm increment every 10 s followed with measurement at 4000 rpm for 1500 s) using a LUMiSizer® 651. Particle size density was based on a density of 0.972 g/cm^3 and a refractive index of 1.404 for silicone oil. (n = 2)

2.3 Thermal Degradation of Emulsions and Their Components

The thermal degradation of the emulsions and their components was analyzed with thermogravimetric analysis and ^{1}H-nuclear magnetic resonance spectroscopy (^{1}H-NMR).

Thermogravimetric Analysis

The thermal degradation of the two undiluted emulsions as well as ingredients of Liveo™ 365 and Liveo™ 366 were assessed with a Hi-Res TGA 2950 (TA Instruments, Eschborn, Germany). Samples of approximately 10 mg were heated at 2 °K/min from room temperature to 400 °C, respectively, until they were decomposed completely. In a second

setup, polysorbate 20, Triton X-100, and Undeceth-5 were heated in isothermal mode at 285 °C, 300 °C, and 315 °C for 360 min after a 30 °C/min ramp with an intermediate hold at 105 °C for 30 min to allow complete water evaporation. Analysis was performed in dry air at a flow rate of 100 mL/min to reflect the industrial bake-on process.

^{1}H-Nuclear Magnetic Resonance Spectroscopy

Residuals of surfactant in the baked-on silicone oil were assessed with ^{1}H-nuclear magnetic resonance (^{1}H-NMR) spectroscopy. Silicone oil was baked-on at 105 °C for 2 h or at standard parameters (see 2.4.1. Siliconization Process) and extracted with toluol for further analysis after the bake-on process. For the extraction, the cartridges were closed on one side with West Novapure syringe plungers (West Pharmaceutical Services, Inc., Exton, PA, USA) and filled with toluol (HPLC Grade, VWR International GmbH, Darmstadt, Germany). After 20 min, the extracts of three cartridges were pooled in a 2 R vial, and toluol was evaporated with a flowtherm evaporator from Barkey GmbH & Co. KG (Leopoldshöhe, Germany) at 100 °C and a constant nitrogen flow of 100 mL/min. The extraction procedure followed by the evaporation step was repeated for another two times to enhance the extraction efficiency. The residue was dissolved in 0.6 mL $CDCl_3$ and ^{1}H-NMR spectroscopy was performed with a Bruker Avance 400 (Bruker Corp., Billerica, MA, USA) at 400 MHz.

2.4 Silicone Layer Characterization

To evaluate the impact of the change of the emulsions on the final product glass cartridges as well as microscopic slides were siliconized, and the resulting silicone layer was characterized.

Siliconization Process

Cartridges were siliconized with 10 mg of 1.75 % (w/w) Liveo™ 365 or Liveo™ 366 emulsion using a diving nozzle on a Siliconization Stand SVS9061 (Bausch+Ströbel Maschinenfabrik Ilshofen GmbH+Co. KG, Ilshofen, Germany). Bake-on was performed in a heating oven (Binder APT.line FED 115, Binder GmbH, Tuttlingen, Germany) at 315 °C for 15 min.

Imaging of the Silicone Layer

Images of the silicone layer were taken from outside the glass barrel with a Keyence VKX250 3D-Laser Scanning Microscope (Keyence International NV/SA, Mechelen,

Belgium) equipped with a CF Plan 10x/0.30 Nikon OFN WD 16.5 objective and stitching 4 images together.

Surface Roughness

For surface roughness measurements, the cartridges wrapped in adhesive tape were broken and individual fragments of approximately 0.5 cm size were removed from the tape. The inner surface was scanned using the microscope stated previously equipped with a CF Plan 100x/0.80 EWLD ∞/0 Epi OFN 25 WD 2.0 Nikon objective. Cartridges were analyzed at the top, middle, and the bottom. Arithmetic mean height (Sa) and maximum height (Sz) of the surface for an area of 150 x 50 µm were determined with the MultiFileAnalyzer software version 1.3.1.120 from Keyence. In total, nine of those areas per cartridge were analyzed. For evaluation, the reference surface was set, and the surface shape was corrected using the integrated surface shape correction tool (Sec curved surf.). Image artefacts were reduced with a height cut level filter at medium cut level. Additionally, the surface roughness of a non-siliconized glass cartridge was determined. (n = 3)

Surface Free Energy

The surface free energy (SFE) of the siliconized cartridges as well as of microscope glass slides siliconized by manually spraying on 1.75 % (w/w) emulsions followed by bake-on at 315 °C for 15 min was determined. Therefore, contact angles of HPW, ethylene glycol, and diiodomethane were measured using a Drop Shape Analyzer 25 (Krüss GmbH, Hamburg, Germany). The liquids (2 µL) were pipetted onto the surfaces. Images were taken 20 s after deposition of the droplet, and contact angles were determined using the fitting mode Ellipse (Tangent-1). SFE was calculated following the method of Owens-Wendt-Rabel-Kaelble [34]. (n = 3)

2.5 Short-Term Stability Studies

The siliconized cartridges were filled and stored to evaluate the impact of the change of the emulsion on the final product quality in regards of particle formation and container functionality.

Sample Preparation

For the stability study, cartridges were capped with Weststar® 8 mm lined seal metal caps (West Pharmaceutical Services, Inc., Exton, PA, USA) and filled with 0.95 mL WFI or placebo formulation consisting of 20 mM histidine-buffer pH 5.5, 240 mM sucrose, and

0.04 % (v/w) polysorbate 80 into 1 mL long glass cartridges following ISO 11040-4 standard dimensions [2]. After insertion of 1 mL long West Novapure syringe plungers (West Pharmaceutical Services, Inc., Exton, PA, USA), the cartridges were stored at 40 °C for 12 weeks. Plungers were set with a plunger setting device at a constant height resulting in a constant head space ("entrapped air"). The distance between the liquid surface and the syringe plunger was 5.9 mm.

Container Functionality

BLGFs were determined using a Texture Analyzer TA.XT Plus (Stable Micro Systems Ltd., Surrey, UK). The septum of the caps was pierced with needles provided by Cambridge Consultant Ltd (Cambridge, UK) and connected through a male-luer-lock-to-thread adapter (¼ - 28 UNF) from Cole Parmer GmbH (Wertheim, Germany) with a BD Microlance 3 27G x ½" (0.4 x 13mm) cannula. The cartridges were expelled at 190.2 mm/min until a trigger force of 30 N. Break-Loose Force was defined as the maximum force required for the plunger over the first 2 mm. Gliding Force was determined by averaging the force needed to move the plunger in the distance from 2 mm to 33 mm. (n = 5)

Subvisible Particle Analysis

Samples were collected in prewashed Eppendorf tubes by extrusion at the previously stated speed but without the cannula. To reduce contamination with silicone oil through the piercing needle, the needles were incubated in n-heptane and HPW before sample collection. Particle formation was determined with a FlowCam 8100 (Fluid Imaging Technologies, Inc., Scarborough, ME, USA) using a 10 x magnification objective. Sample Volume was set to 150 µL with a flow rate of 150 µL/min and an efficiency of 72 %. Additionally, light obscuration (PAMAS SVSS, Partikel- und Analysensysteme GmbH, Rutesheim, Germany) was used as an orthogonal method. Four times 0.2 mL per sample with a prerinse of 0.3 mL and 5 mL rinse with HPW in between measurements were assessed. (n = 3)

Turbidity

The turbidity of the samples was determined using a Nephla LPG239 turbidimeter (Hach Lange GmbH, Düsseldorf, Germany); 2 mL were filled into prewashed glass tubes and analyzed according to the DIN EN 27,027 at a wavelength of 860 nm and temperature of 25 °C. (n = 3)

3 Results and Discussion

The physical stability of both emulsions was evaluated monitoring particle size, particle size distribution as well as the creaming effect.

3.1 Physical Stability of Liveo™ 365 and Liveo™ 366 Dilutions

In general, emulsions are thermodynamically unstable and prone to phase separation as the reduction of the interfacial area minimizes the free energy of the system [35–39]. Creaming, coalescence, and flocculation can be observed as intermediate steps [36,38,40]. For silicone oil-in-water emulsions, creaming emanates from the density difference between the two phases (Density silicone oil: 0.97 g/mL) [20,22,38]. A higher silicone oil concentration at the top of a container can enhance the tendency for the silicone oil droplets to flocculate and coalesce thus eventually resulting in emulsion breakdown [41]. Inconsistencies in silicone oil concentrations could result in variations regarding the sprayed-on silicone oil amount per container. A sufficient amount of silicone oil is critical to prevent functionality failure [42]. Creaming was studied upon static storage conditions as well as with an analytical centrifuge. Particle size and particle size distribution were assessed with DLS (Dynamic Light Scattering) to monitor coalescence. We compared the physical stability of emulsions Liveo™ 365 and Liveo™ 366 diluted to 1.75 % or 3.5 % as concentrations typically utilized in the siliconization of primary packaging material [42].

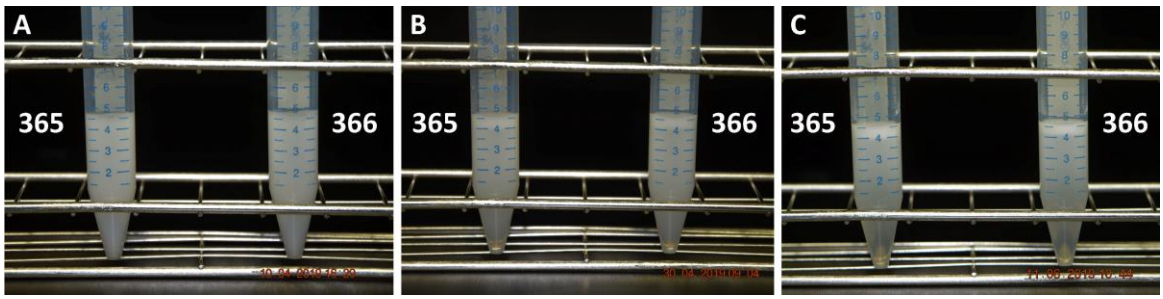

Figure III-1: Falcon tubes filled with 1.75 % Liveo™ 365 and 366 at T0 [A] and stored at 25 °C for 20 [B] and 60 days [C].

Upon storage, a creaming for both diluted emulsions became evident. This observation was assessed at room temperature, mimicking actual conditions during the spray process. When emulsions were filled in 15 mL Falcon tubes, the creaming effect was first visible after 20 days and became distinctly apparent after 60 days (Figure III-1).

Besides a visual inspection, silicone oil concentration was monitored at the bottom of the storage container over time (Figure III-2). For both emulsions, the silicone oil concentration

decreased already after 3 days from approximately 15 mg/mL to 11.7 mg/mL and 10.4 mg/mL, respectively, for Liveo™ 365 and Liveo™ 366. After 60 days, the silicone oil concentrations at the bottom of the container were reduced to 3 mg/mL and 2.3 mg/mL, respectively, for Liveo™ 365 and Liveo™ 366 (Figure III-2A). Both emulsions could be easily redispersed over the 60 days, rendering a homogenous silicone oil concentration (Figure III-2B).

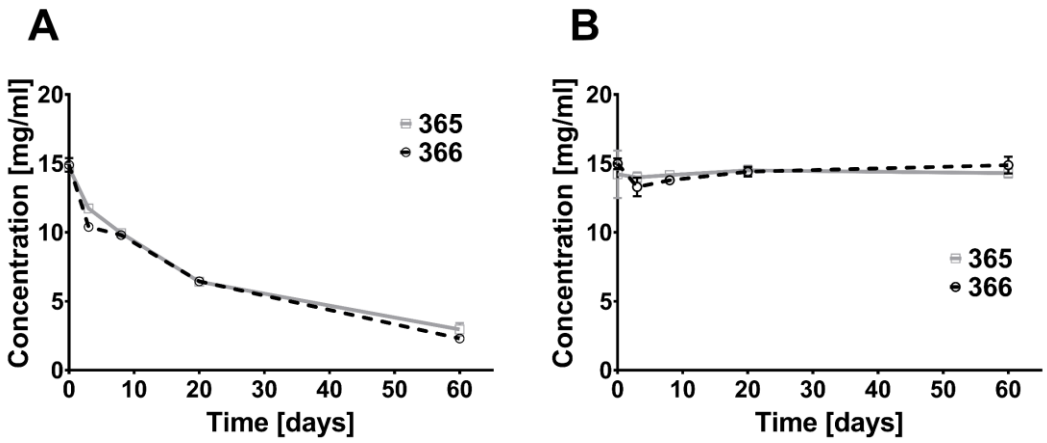

Figure III-2: Silicone oil concentration of 1.75 % dilutions of Liveo™ 365 and 366 at the bottom after storage in Falcon tubes for up to 60 days at 25 °C [A] and after manual homogenization by shaking [B].

For DLS measurements, samples were stored at 60 °C for 20 days and freeze-thaw cycles were applied to accelerate possible instabilities. The previously mentioned creaming effect was also observed at higher temperatures and already visible after 5 days.

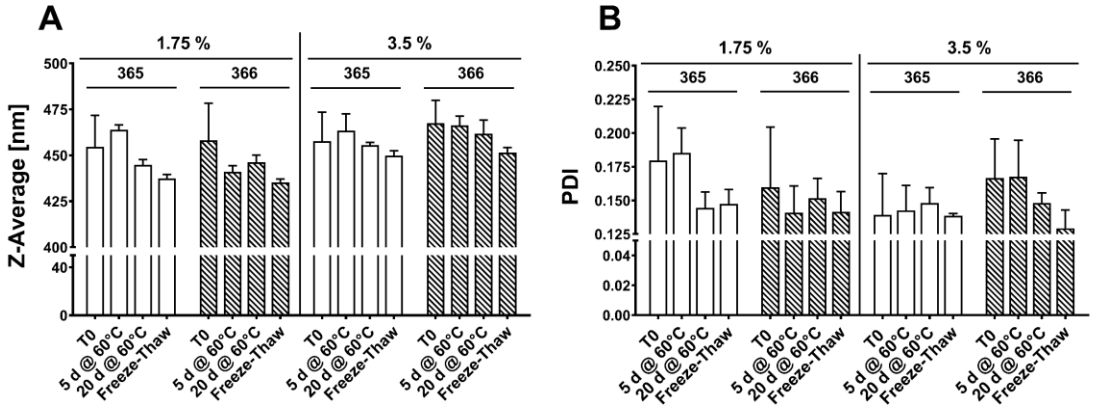

Figure III-3: Z-Average [A] and PDI [B] of 1.75 % and 3.5 % dilutions of Liveo™ 365 and 366 after 5 and 20 days at 60 °C as well as after freeze-thaw stress. PDI = Polydispersity Index.

The particle measurements were consequently measured after redispersion of the samples. At T0, particle size and particle size distribution of both emulsions, Liveo™ 365 and 366, were considered the same. Z-Average ranged from 455 nm to 468 nm independent of the emulsion and concentration. The PDI (Polydispersity Index) of 0.15 and 0.18 in average indicated monodispersity in all samples. This did not change upon storage at 60 °C for 20 days after redispersion nor freeze-thaw stress (Figure III-3).

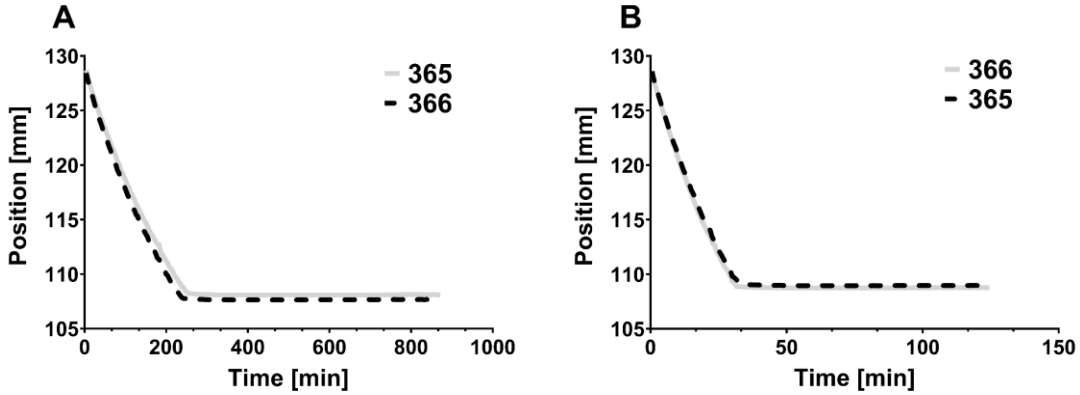

Figure III-4: Movement of the phase boundary of 1.75 % dilutions of Liveo™ 365 and 366 upon centrifugation at rotational speeds 1500 rpm [A] and 4000 rpm [B].

Dilution	Creaming Velocity [µm/min]			
	1500 rpm		4000 rpm	
	365	366	365	366
1.75 % (w/w)	82.8 / 83.7	87.1 / 87.0	619.7 / 620.0	635.3 / 641.1
3.50 % (w/w)	54.1 / 54.4	56.8 / 56.1	385.1 / 388.0	407.1 / 403.4

Table III-1: Creaming Velocity of 1.75 and 3.5 % Liveo™ 365 and 366 at Rotational Speeds of 1500 rpm and 4000 rpm.

In contrast, there was a small decrease toward less variability and lower PDI values observable after 20 days. Thus, DLS measurements indicated high emulsion stability and the absence of large droplets resulting from coalescence after redispersion [37,38,41]. The stability of diluted emulsions was further assessed by analyzing the creaming velocities via analytical photocentrifuge. In the case of silicone oil-in-water emulsions, the transmission drastically increases in the regions without the dispersed lipophilic phase (Figure III-4). The phase boundary consistently moves until the creaming layer becomes so dense that silicone droplet movement is hindered and comes to a hold [32]. The transmission profiles for 1.75 % and 3.5 % were independent of whether formed from

Liveo™ 365 or 366. A 3 % – 5 % faster creaming was observed for Liveo™ 366 (Table III-1). Because the velocity of the flow is dependent on the density difference between the two phases and the particle size distribution, the results underline the outcome of the previously mentioned DLS measurements.

In a second setup of the analytical photocentrifuge, particle size distribution was evaluated as well. Liveo™ 365 and Liveo™ 366 showed the same cumulative volume weighted particle size distribution with size medians of 425.8 and 443.8 nm, respectively (Figure III-5). The observations supported the previously mentioned DLS measurements.

In general, both emulsions showed high stability. Although creaming may occur, it is easy to cope with through redispersion by shaking. Coalescence could not be observed for both diluted emulsions despite the increase in concentration at the top of the storage containers. Thus, we conclude that the handling of the silicone emulsion during the spray process will not be affected by changing from Liveo™ 365 to Liveo™ 366.

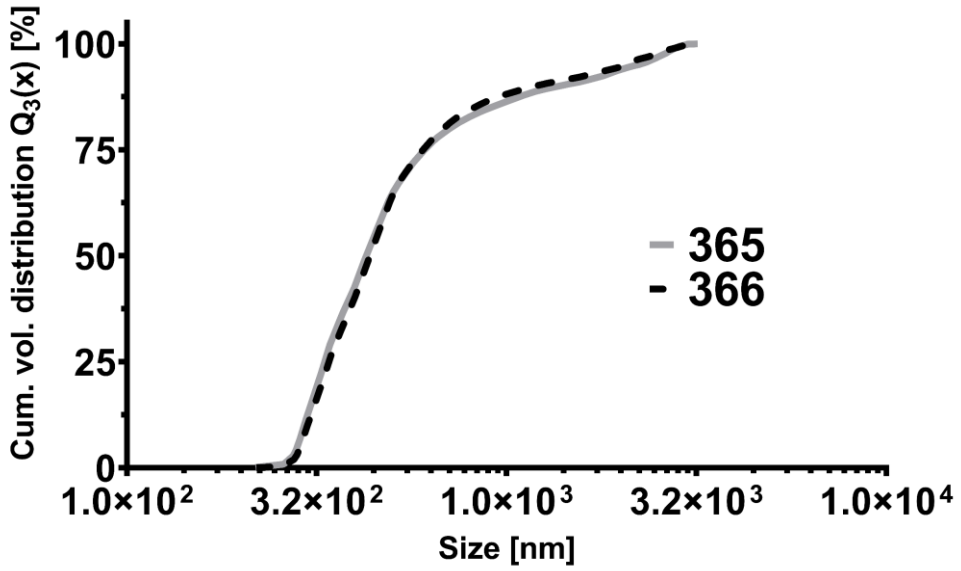

Figure III-5: Cumulative volume weighted particle size distribution of Liveo™ 365 and 366.

A kinetically stable emulsion is achieved by a high-energy barrier for the droplets to flocculate and coalescence through steric or electrostatic repulsion [36,38,41]. Stability can be enhanced by using mixtures of surfactants [38,43–45]. Given the use of two surfactants for Liveo™ 365 [17,21], the results indicate Liveo™ 366 may also contain a surfactant mixture. For the following studies, we assumed the presence of polysorbate 20 also in Liveo™ 366, because Dow Corning Corporation stated the replacement only for Triton X-100 [23].

3.2 Thermal Degradation Process of the Emulsions and Its Component

The emulsions and their different components were further compared in their thermal degradation behavior using thermogravimetric analysis and ^{1}H-NMR spectroscopy.

3.2.1 Thermogravimetric Analysis

The thermal degradation of the undiluted emulsions as well as its individual ingredients was assessed with thermogravimetric analysis (TGA) (Figure III-6). We first evaluated thermal degradation in a ramp mode setting at 2 °C/min, comparing the degradation behavior of the two undiluted emulsions and the ingredients. Subsequently, the more critical ingredients were monitored at different isothermal holds mimicking the actual bake-on process.

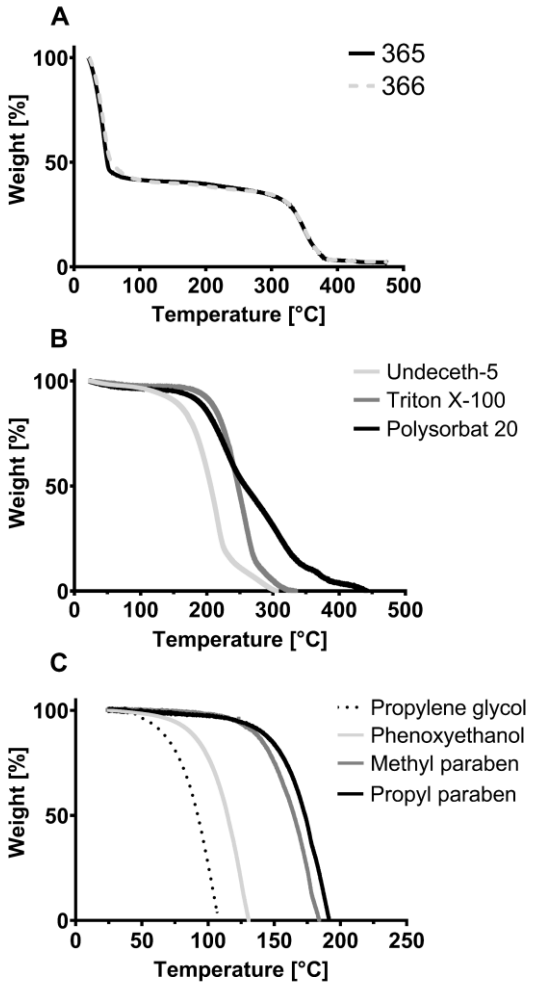

Figure III-6: Thermal degradation of silicone emulsions Liveo^{TM} 365 and 366 [A], preservatives and propylene glycol [B] and the contained surfactants [C] in air – Ramp 2 °C/min.

In the ramp mode setting, the two emulsions rapidly lost approximately 55 % mass at 50 °C due to the evaporation of the water (Figure III-6A) followed by 13 % mass loss between 50 °C and 300 °C. The second weight loss is partly due to the removal of residual preservatives, co-solvents, as well as surfactants. Besides the removal of individual ingredients, also small chain and cyclic PDMS fractions start to volatilize between 150 °C and 250 °C [17,28]. At 300 °C, degradation of PDMS in the presence of oxygen sets in. Depolymerization of siloxane chains takes place by formation of cyclic oligomers that eventually volatilize as well as the occurrence of thermal oxidation, resulting in cross-linking of the siloxane- chains and the formation of SiO_2 [21,25–27,29]. Approximately 2.1 % (Liveo™ 365) and 2.3 % (Liveo™ 366) mass was left, and a white powder could be found in the aluminum pan. The curve progressions indicate a high similarity of the thermal degradation behavior of PDMS of both emulsions. According to Mundry et al. [17], ingredients play a significant role as catalysts, decreasing the activation energy of the thermo-oxidative and depolymerization reactions taking place. Overall, the decomposition temperatures are lower for the emulsion system than for pure PDMS [17].

The least critical ingredient to be removed by the bake-on process with a degradation onset temperature of 60 °C and complete removal at 108 °C was propylene glycol, which is present in both emulsions (Figure III-6B). Also, the preservatives used in both emulsions are removed well below the bake-on temperature. Phenoxyethanol started to evaporate at 90 °C and was already removed at 130 °C. The parabens contained in Liveo™ 365 showed a complete removal at 180 °C and 190 °C, respectively. All the aforementioned substances showed a fast degradation in one step. The chronology of degradation can be derived from their boiling points [46–49] with propylene glycol having the lowest and propyl paraben the highest, which indicates an evaporation of the substances as already known from parabens [21,50]. In comparison, the surfactants appeared to be the most thermally stable emulsion excipients and thus most critical for potential interaction later in the filled primary container (Figure III-6C). For the new surfactant Undeceth-5, mass loss started at 160 °C and was completed at 305 °C. Two steps can be discerned. A faster mass loss of approximately 80 % until 225 °C is associated with an oxidation and degradation process of the polyoxyethylene (POE) chains as described for other nonionic surfactants like polysorbate 20 and 80 [24,51–54]. Above 225 °C, the removal rate slows down and Santacesaria et al. [55] postulated a slow oxidative pyrolysis of the alkyl chains. Given the similarity in the molecular structures of Triton X-100 and Undeceth-5, it can be assumed

that the thermal degradation mechanism is similar. A thermal degradation in two steps was observed for Triton X-100, too, as reported before [56], with a later onset temperature for weight loss of around 190 °C and a complete removal at 330 °C. Both surfactants consist of a small POE chain linked through an ether group to lipophilic hydrocarbon chains. In contrast, polysorbate 20 are esters of fatty acids and POE sorbitan. The products on the market are in general mixtures of POE sorbitans esterified with different fatty acids. According to the specifications of the European Pharmacopoeia, at least 40 % – 60 % of them need to be lauric acid, but also unsaturated acids, which are prone to autooxidation via radical mechanism [52,57], are accepted to some extent. This can be a reason for the different thermal degradation behavior of polysorbate 20, because a fatty acid chain difference can delay the onset of the POE chain degradation reaction [51]. Polysorbate 20 started to decompose earlier than Triton X-100 at 180 °C but was not completely removed until 440 °C. The thermal degradation of the surfactants Triton X-100, Undeceth-5, and polysorbate 20 was assessed additionally by isotherms at 285 °C, 300 °C, and 315 °C over 6 h to reflect the actual bake-on process. In this setup, Undeceth-5 was removed the fastest at all temperatures and did not form any kind of residue (Figure III-7A, Supplementary data, Figure S III-2). In ramp mode, Undeceth-5 started to degrade at approximately 160 °C. After heating to standard bake-on temperatures of 300 °C and 315 °C, within approximately 7 min at 30 °C/min only 9.4 % and 3.6 %, mass respectively, were left. After 15 min, Undeceth-5 was completely removed at these two target temperatures (Figure III-7B). At 285 °C, the weight loss was significantly reduced; 41.3 % mass was left when reaching this target temperature after the 30 °C/min ramp, and the surfactant was not completely removed after 15 min (3.4 % remainder) but fully degraded after 30 min. Triton X-100 showed similar degradation behavior to Undeceth-5 but at a lower rate. It was also removed completely after 15 min at 315 °C, but in contrast to Undeceth-5 at a target temperature of 285 °C, 63.4 % of Triton X-100 remained after the ramp and after 15 min, 6.9 % was left. Polysorbate 20 showed the slowest thermal degradation. 71.1 % remained after the ramp to 285 °C, and it also formed a residue at all temperatures stable for 360 min. After 15 min at 315 °C, 12.3 % mass was left.

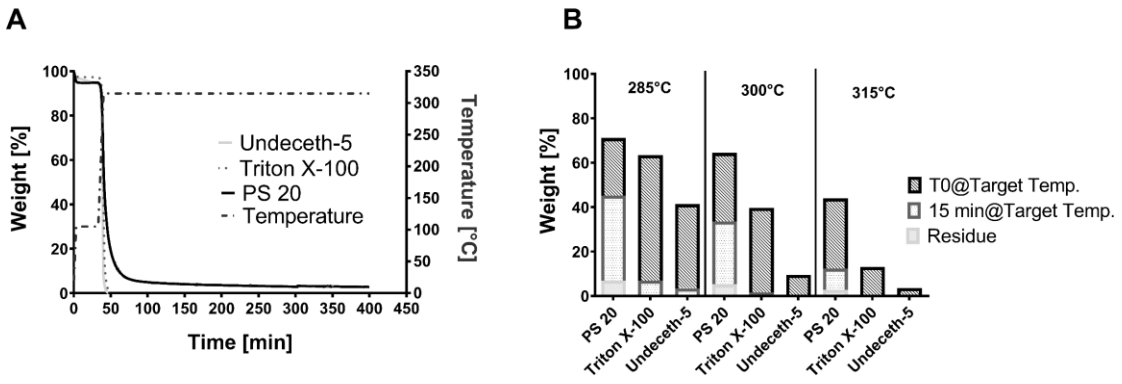

Figure III-7: Thermal degradation of Undeceth-5, Triton X-100, and PS20 at 315 °C [A] and time-dependent degradation at 285 °C, 300 °C, and 315 °C [B] in air.

The residue after 360 min is unlikely to consist of the surfactant itself but rather nonvolatile decomposition products like fatty acids. A variety of different fatty acids like myristic, palmitic, stearic and oleic acid, that have been identified as degradation products of polysorbate 20 [24], show higher boiling points than the bake-on temperature [58–61]. Additionally, olefinic sites present in polysorbate 20 are prone to oxidation via a radical mechanism [51,52]. Consequently, carboxylic acids with even longer aliphatic chains as well as long alkyl chains are potential degradation products with higher thermal stability as the result of a radical termination reaction [55]. Finally, little is known about the thermal degradation behavior of sorbitan. The high boiling point of 442.5 °C stated by some of the suppliers [62] indicates that some of the residue originates from the molecule's backbone.

3.2.2 ^{1}H-NMR Measurements

The presence of Undeceth-5 or residues formed via degradation in the baked-on silicone layers was assessed by ^{1}H-NMR. Mundry et al. [17] were able to detect traces of surfactant in an emulsion mixture down to 1 µg. The total amount of Undeceth-5 per barrel can be estimated as roughly 13 µg given a concentration of 2.5 % in the undiluted emulsion [20]. The amount was sufficient to find distinct signals at 3.64 ppm and 3.44 ppm in a sample dried at 105 °C (Figure III-8) [63,64]. Those signals are characteristic of protons of the POE group of alcohol ethoxylates and were detectable for the Undeceth-5 reference. After the heat treatment at 315 °C for 15 min, those signals were not detectable anymore. The lack of distinct signals for POE chains indicates the removal of the second surfactant possibly contained in Liveo™ 366, polysorbate 20, as well. The Undeceth-5 aliphatic chain signals could not be used for evaluation as they overlapped with signals derived from the non-siliconized glass barrel itself (0.88 ppm, 1.25 ppm, and 1.57 ppm) [17,63,64]. Thus, a

complete removal also of decompositions products cannot be concluded from these observations.

In summary, polysorbate 20 is the ingredient for both emulsions with the highest risk of interaction in the final drug/device combination product by remaining in the baked-on silicone layer. As pointed out by Funke et al. [21], this risk is mitigated by the dilution of the sprayed-on emulsion and removal by the bake-on process to a minimum. Undeceth-5 as well as the other newly added component, phenoxyethanol, showed a faster removal upon the bake-on process. Given the same degradation behavior of the two emulsions as well as the results regarding the thermal stability of the contained components, an impact on the bake-on process and the resulting silicone layer is implausible. However, the slower removal at lower temperatures implies control of the bake-on conditions to ensure the complete removal of the ingredients.

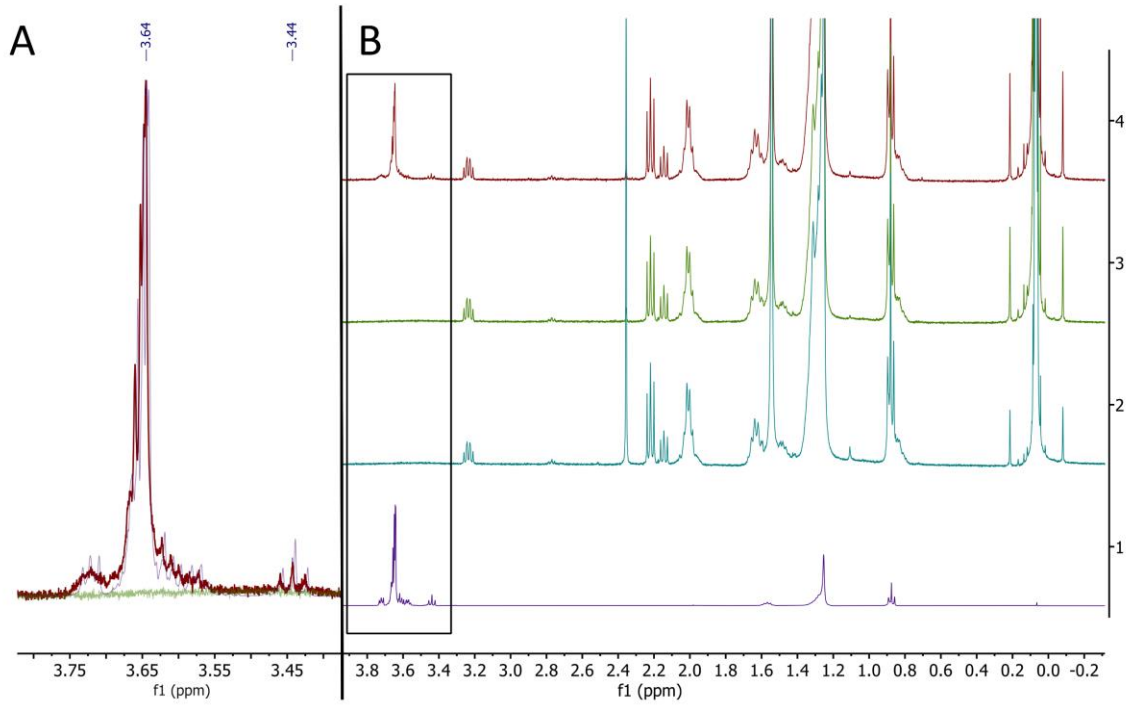

Figure III-8: ^{1}H-NMR spectra of Undeceth-5 reference (1), non-siliconized cartridge extract (2), bake-on siliconized cartridge extract at 315 °C for 15min (3), and siliconized cartridge extract dried at 105 °C for 2 h (4) [B] and superimposed spectra of (1, 3) and (4) [A].

3.3 Characterization of Baked-on Silicone Layers

In the next step, the silicone coatings from Liveo^{TM} 365 and Liveo^{TM} 366 were baked-on at 315 °C, 15 min and were characterized by 3-D-LSM and contact angle measurements.

3.3.1 Silicone Layer Morphology

3D-LSM has been recently established as a tool for the characterization of the silicone oil distribution and its quality in terms of thickness and morphology [16,65]. Measurements were taken from outside the barrel as a quick and nondestructive method to evaluate the silicone distribution along the whole length of the barrel. For both emulsions, an evenly spread film was observed with a few circular spots of accumulations. Samples dried at only 105 °C showed a discontinuous surface (Supplementary data, Figure S III-3).

Surface roughness influences the adsorption behavior of proteins [66,67]. Analysis of the inside of the cartridges after breaking demonstrated that the surface roughness of the silicone layer formed was independent of the silicone emulsion used (Figure III-9). The mean Sa values were the same with 0.022 ± 0.004 µm for Liveo™ 365 and 0.021 ± 0.004 µm for Liveo™ 366. Given the mean Sa of the non-siliconized glass barrels as 0.012 ± 0.002 µm, the mean surface height (Sa) of around 10 nm was comparable with the standard deviation for measurements of the layer thickness of approximately 9 nm to 15 nm [16].

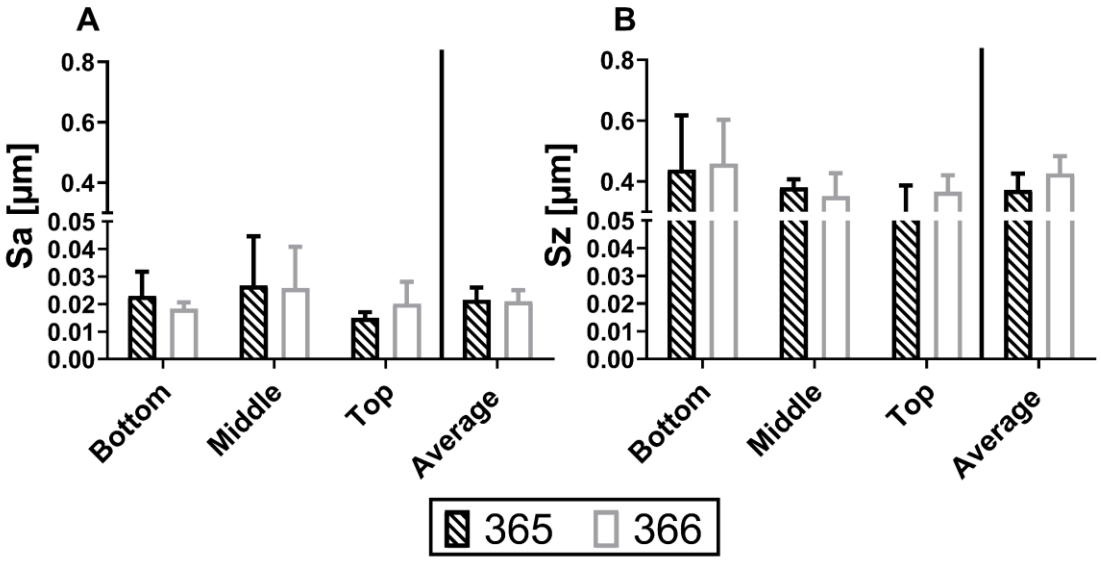

Figure III-9: Surface roughness Sa [A] and Sz [B] of silicone oil layers baked-on to 1mL long glass cartridges using Liveo™ 365 and 366. Sa: mean height; Sz: maximum height.

For Liveo™ 365 and Liveo™ 366, the average maximum height difference (Sz) was not significantly different and was 0.372 ± 0.054 µm and 0.426 ± 0.057 µm, respectively. The overall appearance of the silicone layer when looking from the inside reflected the

visualization from the outside (Figure III-10). Although most of the silicone oil was distributed evenly, some areas showed irregularities.

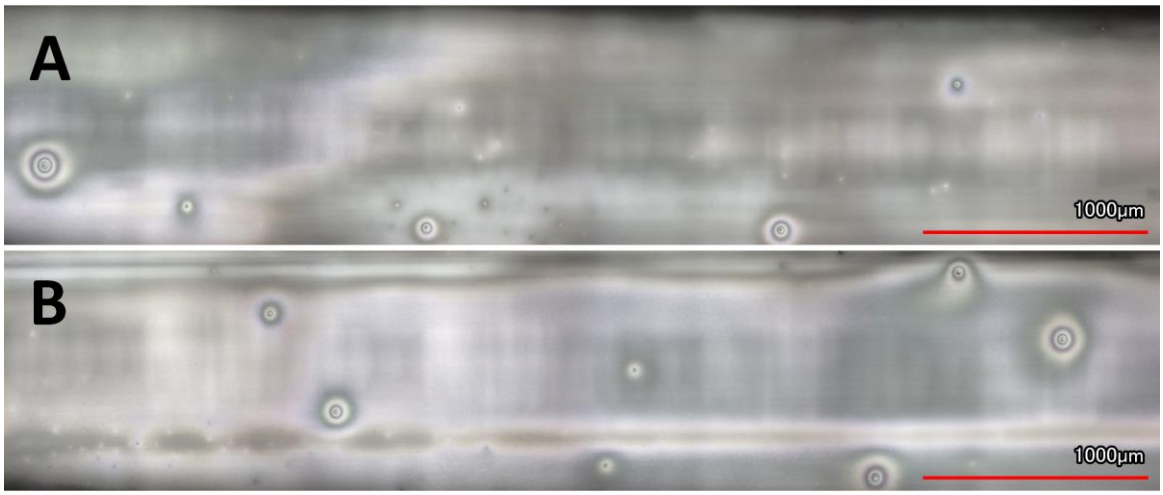

Figure III-10: 3D-LSM images of the silicone oil layer baked-on 1mL long glass cartridges using Liveo™ 365 [A] and Liveo™ 366 [B].

3.3.2 SFE of the Silicone Oil Layer

Contact angles for water, diiodomethane, and ethylene glycol were determined for cartridges and microscope slides siliconized with Liveo™ 365 and Liveo™ 366 by a Drop Shape Analyzer (Supplementary data, Figure S III-4). The SFE was determined following the method of Owens-Wendt-Rabel-Kaelble [34] divided into the polar and the dispersive component. The contact angles of the different liquids were independent of the silicone oil emulsion used (Table III-2). The SFE was approximately 19.8 mN/m for both emulsions and both substrates. The results demonstrate the desired hydrophobization effect independent of the emulsion used [17,68].

	H_2O [°]	**Ethylene Glycol [°]**	**Diiodomethane [°]**	**γ_s [mN/m]**	**γ_p [mN/m]**	**γ_d [mN/m]**
365 MS	108.5 ± 2.2	88.1 ± 1.7	75.1 ± 1.6	19.9	0.3	19.6
366 MS	107.8 ± 1.8	85.4 ± 4.2	76.3 ± 2.0	19.9	0.4	19.4
365 C	107.3 ± 0.7	89.2 ± 2.5	75.0 ± 1.7	19.7	0.4	19.3
366 C	106.6 ± 0.5	88.1 ± 0.7	75.2 ± 1.2	19.7	0.5	19.2

Table III-2: Contact angles of water, ethylene glycol, and diiodomethane on siliconized samples as well as corresponding surface free energy. γ_s = Surface tension of the solid, γ_p = Polar component; γ_d = Dispersive component; MS = Microscopic Slide; C = Cartridge. Samples were siliconized with Liveo™ 365 or 366.

3.4 Short-Term Stability

Subvisible particle (SvP) formation originating from silicone oil detachment and device functionality with respect to BLGF were analyzed.

3.4.1 Subvisible Particle Formation in Siliconized Cartridges

In order to compare the performance upon exchange of Liveo™ 365 against Liveo™ 366, siliconized cartridges were filled with placebo and stored at 40 °C for up to 12 weeks. The SvP numbers of expelled cartridges filled with WFI and 20 mM His-Buffer containing 0.04 % PS80 were analyzed with flow imaging (FI) and light obscuration (LO) as an indication of silicone oil detachment. The samples were generated through extrusion of the cartridges at controlled speed. The expelling of a solution through a siliconized container induces higher particle count in comparison with simply pouring it out, and the count is affected by the extrusion speed [5,6,69]. Migrated silicone oil particles originating from the siliconized primary container can potentially trigger the formation of protein aggregates by adsorption and change of conformation [8,12]. Furthermore, a high and rising number of silicone oil particles can indicate a decreasing performance for the PFS product over its shelf life [5].

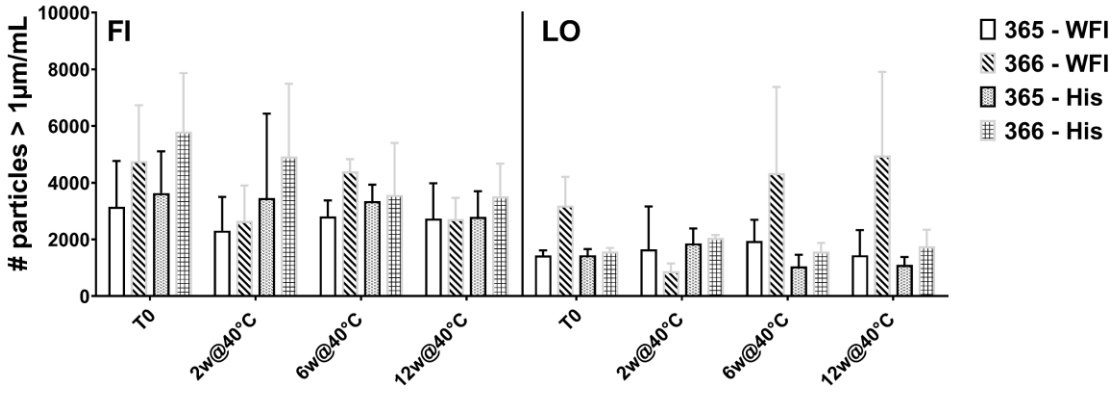

Figure III-11: Particle concentration > 1mm/mL of expelled cartridges siliconized with Liveo™ 365 or 366 and filled with water for injection (WFI) or 20 mM histidine buffer containing 0.04 % PS80 (His) after storage at 40 °C measured with flow imaging [FI] and light obscuration [LO].

For both samples, the number of particles > 1 µm per milliliter was low with numbers ranging from 3000 to 6000 particles/mL in FI and 1500 to 5000 particles/mL in LO (Figure III-11). The numbers of particles ≥ 10 µm and ≥ 25 µm, which are relevant from compendial perspective of actual products on the market (Table III-3), were exceptionally

low as well [5,70,71]. Turbidity measurements supported the results by low values of < 1 FNU for all time points (data not shown).

The samples originating from different emulsions did not show a difference at T0 regarding particles > 1 µm per milliliter. Furthermore, the silicone layer formed by both emulsions appeared to be stable, displayed by steady particle count numbers over the storage time for 12 weeks. Images of the particles in the FI analysis derived from both silicone layers were considered silicone oil-like and did not differ in image morphology parameters like aspect ratio, circularity, or sigma intensity (data not shown).

Emulsion Type	Fill Medium	Particle Size	T0	2 w.	6 w.	12 w.
365	WFI	≥ 10 µm/mL	5 ± 1	10 ± 8	10 ± 8	8 ± 6
		≥ 25 µm/mL	1 ± 1	0 ± 0	<1 ± <1	0 ± 0
	His	≥ 10 µm/mL	17 ± 1	24 ± 3	13 ± 7	14 ± 7
		≥ 25 µm/mL	2 ± 1	2 ± 1	1 ± 1	1 ± 1
366	WFI	≥ 10 µm/mL	5 ± 6	5 ± 1	10 ± 13	21 ± 3
		≥ 25 µm/mL	2 ± 4	<1 ± <1	<1 ± <1	<1 ± <1
	His	≥ 10 µm/mL	29 ± 14	17 ± 5	31 ± 10	35 ± 5
		≥ 25 µm/mL	8 ± 6	2 ± 4	3 ± 1	5 ± 1

Table III-3: SvP Concentration (Mean) ≥ 10 µm and ≥ 25 µm/mL by light obscuration of expelled cartridges after storage at 40 °C for 12 Weeks. Siliconized with Liveo™ 365 or 366 and filled with Water for Injection (WFI) or 20 mM Histidine Buffer Containing 0.04 % PS80 (His).

3.4.2 Functionality of Siliconized Cartridges

In addition to SvP formation, functionality of the previously mentioned samples was assessed over the same storage time and at the same time points. One part of the usability of a drug/device combination product is that they consistently meet their acceptance criteria for functionality over their shelf life. Patients and HCPs rely on a smooth and easy injection, and the use of autoinjectors limits the forces that can be applied. Typical target forces are well below 25 N [5].

For both emulsions, the BLGFs were well below critical limits. The mean break-loose force at T0 was approximately 3 N. This increased over time to 4.5 N for both emulsions, which can be related to a gradual dewetting of the surface by the pressure of the plunger being pressed to the glass [72]. The gliding force stayed between 1.5 and 2 N (Figure III-12). The forces required were similar with regards to the mean values and progression for both surrogate solutions independent of the emulsion used.

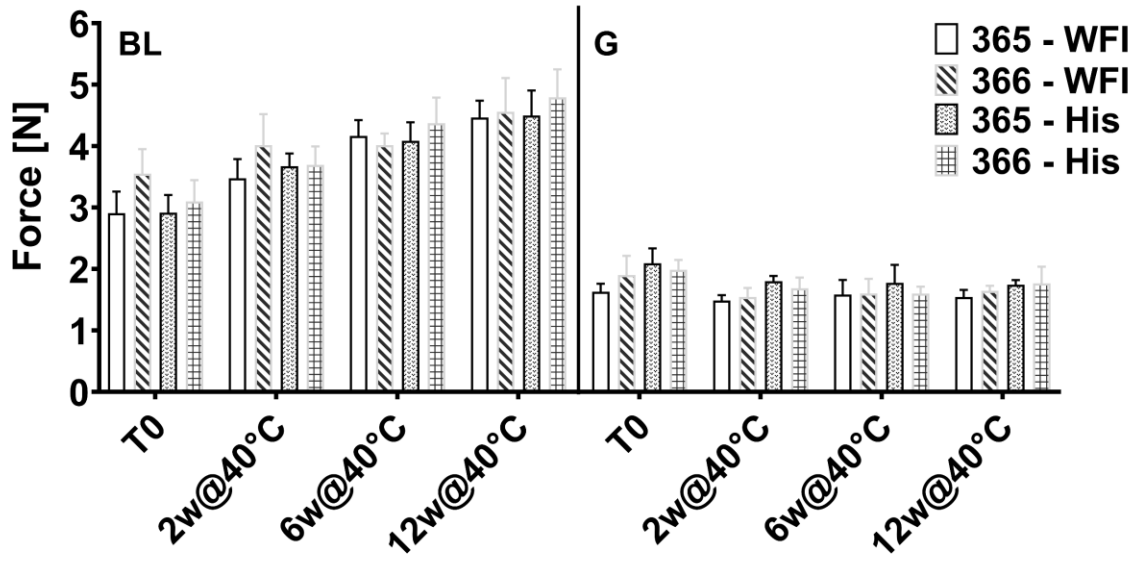

Figure III-12: Impact of storage at 40 °C on break-loose [BL] and gliding forces [G] of bake-on siliconized cartridges with Liveo™ 365 and 366 and filled with water for injection (WFI) or 20mM histidine buffer containing 0.04 % PS80 (His).

The constant gliding forces imply an evenly distributed silicone oil film for both emulsions along the whole length of the barrel [42,73,74]. It can be assumed that irregularities regarding the functionality are more likely to appear through changes in the spray parameters like air pressure, spray amount, or kinetics of the nozzle movement rather than the choice of the emulsion [42].

4 Conclusion

The bake-on siliconization process is established in the pharmaceutical industry to achieve functionality of ready-to-use devices. It is vital for a drug/device combination product to be safe and for the drug product not to interact with the primary packaging material. One of the surfactants used in Liveo™ 365, Triton X-100, has been replaced with Undeceth-5, because it has been indexed on the REACh Authorisation List. Beside the surfactant, the preservatives methyl- and propylparaben were substituted with phenoxyethanol. In this study, we wanted to find out whether there are differences between the two emulsions, Liveo™ 365 and Liveo™ 366, that could influence the quality and safety of the final product. We compared physical stability, thermal degradation behavior of the emulsions, as well as their ingredients, the silicone layer formed upon the bake-on process, and product performance of cartridges siliconized with both emulsions.

The stability of the diluted emulsions used for siliconization was not influenced by the change in formulation for the concentrates Liveo™ 365 and Liveo™ 366. The diluted emulsions showed the same silicone droplet size and equivalently high stability. Droplet size was not affected by storage at 60 °C nor freeze-thaw cycles. Creaming occurred over 20 days at room temperature, but slight shaking was sufficient for easy rehomogenization. Thermal degradation demonstrated that Undeceth-5, the surfactant newly added in Liveo™ 366 to replace Triton X-100, is completely removed by the bake-on process. Undeceth-5 showed a faster thermal degradation than the previously used surfactants. Phenoxyethanol evaporated at even lower temperature than the temperatures at which the substituted parabens evaporated and decomposed. Surface morphology and roughness as well as SFE of the baked-on silicone layer were identical for Liveo™ 365 and Liveo™ 366. This reflects the fact that all components but the silicone oil itself are removed upon heat treatment [19,20].

Finally, a short-term stability study of siliconized cartridges filled with WFI and polysorbate containing histidine buffer underlined that Liveo™ 365 and Liveo™ 366 do not differ in performance. SvP formation was exceptionally low and not affected upon storage at elevated temperatures for both emulsions. Additionally, the BLGF values were remarkably low and consistent for cartridges siliconized using the two different emulsions over the 12 weeks storage at 40 °C. The comparability in functionality corresponds to the overall identical characteristics of the silicon oil film [42]. In summary, we conclude that

the change from Liveo™ 365 to Liveo™ 366 for the bake-on siliconization process of primary containers is not critical with respect to handling of the sprayed-on diluted emulsions, the bake-on process parameters, as well as the performance of the baked-on silicone coating.

Supplementary Data

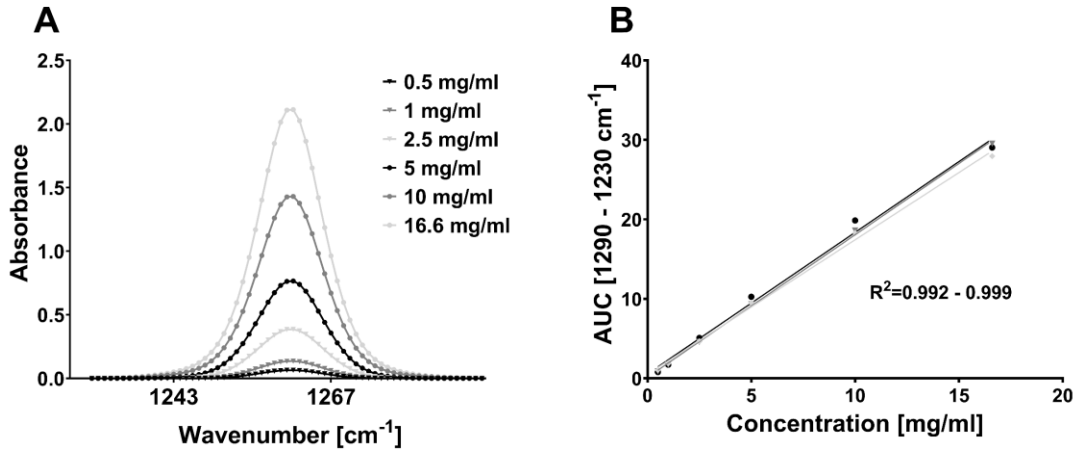

Figure S III-1: Silicone oil quantification of silicone oil in heptane by FTIR. Concentration dependent infrared absorbance spectra of silicone oil in heptane solutions (0.5 – 16.6 mg/mL) [A] and silicone oil concentration calibration curve (R^2=0.992 – 0.999) [B].

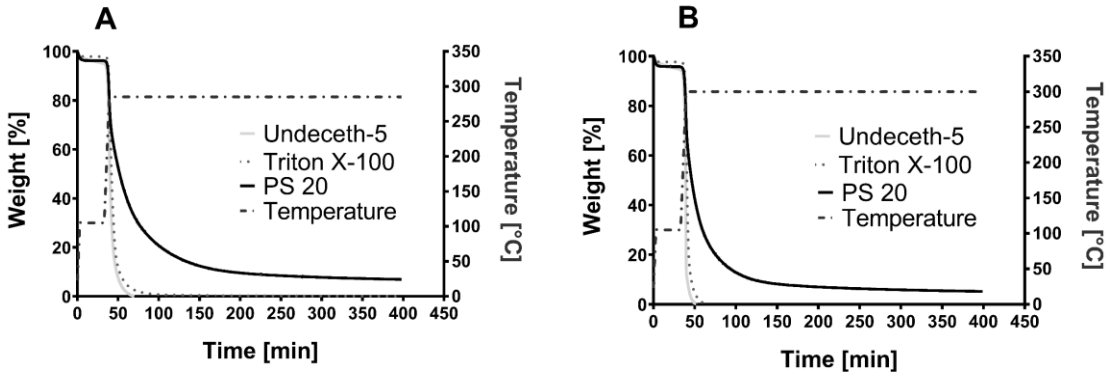

Figure S III-2: Thermal degradation of Undeceth-5, Triton X-100, and PS20 at 285 °C [A] and 300 °C [B] in air.

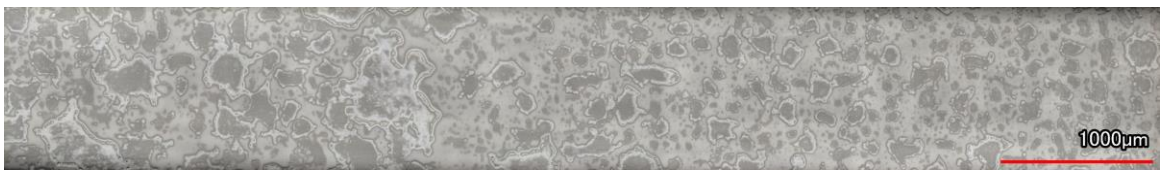

Figure S III-3: 3D-LSM image of the silicone oil layer dried onto glass cartridge at 105 °C for 2 h using 1.75 % Liveo™ 366.

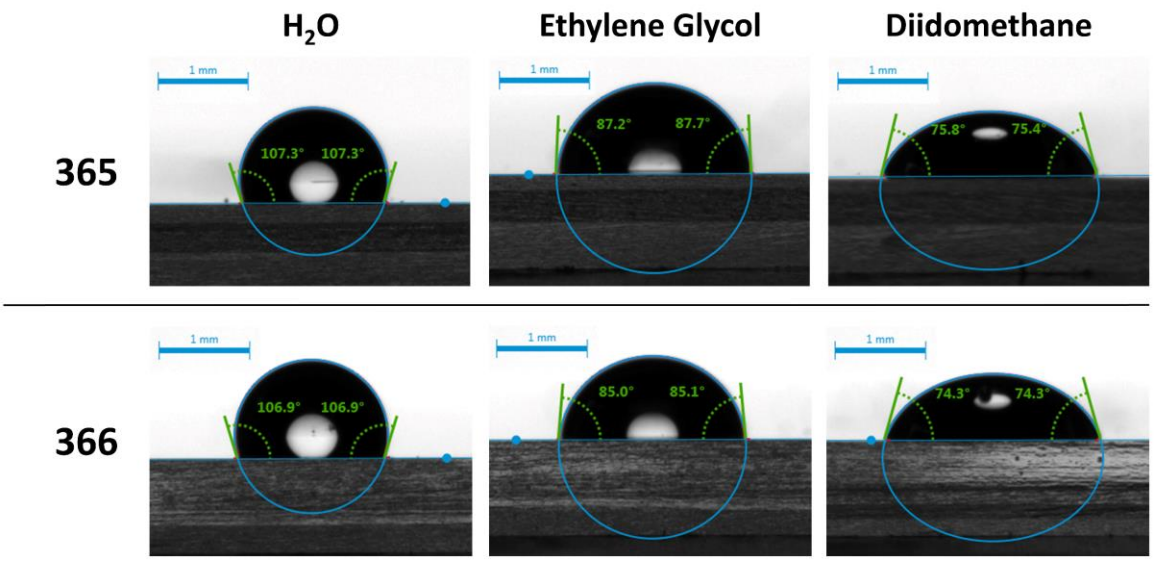

Figure S III-4: Exemplary contact angles of water, ethylene glycol, and diiodomethane on microscopic glass slides bake-on siliconized with 1.75 % Liveo™ 365 and 366.

Acknowledgements

The authors gratefully acknowledge support and funding from Novartis AG, especially Marc Rohrschneider in this regard. We also thank Dow Corning Corporation and DDP Specialty Products Germany Gmbh & Co. KG. DDP and Specialty Electronic Materials US 9 LLC (collectively, DuPont) and Nuova Ompi S.r.l. for providing valuable material to this project.

Abbreviations

BLGF	Break-Loose Gliding Force
DC 365	Dow Corning 365 35 % Dimethicone NF Emulsion
DC 366	Dow Corning 365 35 % Dimethicone NF Emulsion
DLS	Dynamic Light Scattering
FI	Flow Imaging
HCP	Health Care Provider
HPW	Highly Purified Water
Liveo™ 365	Liveo™ 365 35 % Dimethicone NF Emulsion
Liveo™ 366	Liveo™ 366 35 % Dimethicone NF Emulsion
LO	Light Obscuration
PDI	Polydispersity Index
PDMS	Polydimethylsiloxane
PFS	Pre-filled Syringe
POE	Polyoxyethylene
REACh	Regulation concerning the Registration, Evaluation, Authorisation and Restriction of Chemicals
SFE	Surface Free Energy
Sa	Surface Arithmetic Mean Height
SvP	Subvisible Particle
Sz	Surface Maximum Height
TGA	Thermogravimetric Analysis
WFI	Water for Injection

References

[1] Ingle, R. G.; Agarwal, A. S. Pre-Filled Syringe – a Ready-to-Use Drug Delivery System: A Review. Expert Opin. Drug Delivery 2014, 11 (9), 1391–1399. https://doi.org/10.1517/17425247.2014.923400.

[2] Sacha, G.; Rogers, J. A.; Miller, R. L. Pre-Filled Syringes: A Review of the History, Manufacturing and Challenges. Pharm. Dev. Technol. 2015, 20 (1), 1–11. https://doi.org/10.3109/10837450.2014.982825.

[3] Sacha, G. A.; Saffell-Clemmer, W.; Abram, K.; Akers, M. J. Practical Fundamentals of Glass, Rubber, and Plastic Sterile Packaging Systems. Pharm. Dev. Technol. 2010, 15 (1), 6–34. https://doi.org/10.3109/10837450903511178.

[4] Makwana, S.; Basu, B.; Makasana, Y.; Dharamsi, A. Prefilled Syringes: An Innovation in Parenteral Packaging. Int. J. Pharm. Invest. 2011, 1 (4), 200–206. https://doi.org/10.4103/2230-973X.93004.

[5] Warne, N. W.; Mahler, H. C. Challenges in Protein Product Development. AAPS Advances in the Pharmaceutical Sciences Series Vol. 38; Springer, Cham, 2018. https://doi.org/10.1007/978-3-319-90603-4.

[6] Funke, S.; Matilainen, J.; Nalenz, H.; Bechtold-Peters, K.; Mahler, H.-C.; Friess, W. Silicone Migration from Baked-on Silicone Layers. Particle Characterization in Placebo and Protein Solutions. J. Pharm. Sci. 2016, 105 (12), 3520–3531. https://doi.org/10.1016/j.xphs.2016.08.031.

[7] Gerhardt, A.; Mcgraw, N. R.; Schwartz, D. K.; Bee, J. S.; Carpenter, J. F.; Randolph, T. W. Protein Aggregation and Particle Formation in Prefilled Glass Syringes. J. Pharm. Sci. 2014, 103 (6), 1601–1612. https://doi.org/10.1002/jps.23973.

[8] Jones, L. S.; Kaufmann, A.; Middaugh, C. R. Silicone Oil Induced Aggregation of Proteins. J. Pharm. Sci. 2005, 94 (4), 918–927. https://doi.org/10.1002/jps.20321.

[9] Shah, M.; Rattray, Z.; Day, K.; Uddin, S.; Curtis, R.; van der Walle, C. F.; Pluen, A. Evaluation of Aggregate and Silicone-Oil Counts in Pre-Filled Siliconized Syringes: An Orthogonal Study Characterising the Entire Subvisible Size Range. Int. J. Pharm. 2017, 519 (1-2), 58–66. https://doi.org/10.1016/j.ijpharm.2017.01.015.

[10] Li, J.; Pinnamaneni, S.; Quan, Y.; Jaiswal, A.; Andersson, F. I.; Zhang, X. Mechanistic Understanding of Protein-Silicone Oil Interactions. Pharm. Res. 2012, 29 (6), 1689–1697. https://doi.org/10.1007/s11095-012-0696-6.

[11] Badkar, A.;Wolf, A.; Bohack, L.; Kolhe, P. Development of Biotechnology Products in Pre-Filled Syringes: Technical Considerations and Approaches. AAPS PharmSciTech 2011, 12 (2), 564–572. https://doi.org/10.1208/s12249-011-9617-y.

[12] Thirumangalathu, R.; Krishnan, S.; Ricci, M. S.; Brems, D. N.; Randolph, T. W.; Carpenter, J. F. Silicone Oil- and Agitation-Induced Aggregation of a Monoclonal Antibody in Aqueous Solution. J. Pharm. Sci. 2009, 98 (9), 3167–3181. https://doi.org/10.1002/jps.21719.

[13] Basu, P.; Blake-Haskins, A. W.; O'Berry, K. B.; Randolph, T. W.; Carpenter, J. F. Albinterferon a2b Adsorption to Silicone Oil–Water Interfaces: Effects on Protein Conformation, Aggregation, and Subvisible Particle Formation. J. Pharm. Sci. 2014, 103 (2), 427–436. https://doi.org/10.1002/jps.23821.

[14] Chisholm, C. F.; Baker, A. E.; Soucie, K. R.; Torres, R. M.; Carpenter, J. F.; Randolph, T. W. Silicone Oil Microdroplets Can Induce Antibody Responses against Recombinant Murine Growth Hormone in Mice. J. Pharm. Sci. 2016, 105 (5), 1623–1632. https://doi.org/10.1016/j.xphs.2016.02.019.

[15] Gerhardt, A.; Nguyen, B. H.; Lewus, R.; Carpenter, J. F.; Randolph, T. W. Effect of the Siliconization Method on Particle Generation in a Monoclonal Antibody Formulation in Pre-Filled Syringes. J. Pharm. Sci. 2015, 104 (5), 1601–1609. https://doi.org/10.1002/jps.24387.

[16] Funke, S.; Matilainen, J.; Nalenz, H.; Bechtold-Peters, K.; Mahler, H.-C.; Friess, W. Analysis of Thin Baked-on Silicone Layers by FTIR and 3DLaser Scanning Microscopy. Eur. J. Pharm. Biopharm. 2015, 96, 304–313. https://doi.org/10.1016/j.ejpb.2015.08.009.

[17] Mundry, A. T. Einbrennsilikonisierung Bei Pharmazeutischen Glaspackmitteln - Analytische Studien Eines Produktionsprozesses. Ph.D. Thesis, Humboldt-Universität zu Berlin, 1999.

[18] Mundry, T.; Surmann, P.; Schurreit, T. Surface Characterization of Polydimethylsiloxane Treated Pharmaceutical Glass Containers by X-Ray-Excited Photo- and Auger Electron Spectroscopy. Fresenius' J. Anal. Chem. 2000, 368 (8), 820–831. https://doi.org/10.1007/s002160000593.

[19] DDP Specialty Products Germany Gmbh & Co. Kg. Sicherheitsdatenblatt, Dow Corning™ 365 35 % Dimethicone NF Emulsion, Version: 3.0, Oct 13, 2018.

[20] DDP Specialty Products Germany Gmbh & Co. Kg. Sicherheitsdatenblatt, Dow Corning™ 366 35 % Dimethicone NF Emulsion, Version: 2.0, Jan 18, 2019.

[21] Funke, S.; Matilainen, J.; Nalenz, H.; Bechtold-Peters, K.; Mahler, H.-C.; Vetter, F.; Müller, C.; Bracher, F.; Friess, W. Optimization of the Bake-on Siliconization of Cartridges. Part II: Investigations into Burn-in Time and Temperature. Eur. J. Pharm. Biopharm. 2016, 105, 209–222. https://doi.org/10.1016/j.ejpb.2016.05.015.

[22] Dow Corning Corporation. Product Information Dow Corning® 360 Medical Fluid; Form No. 51-0374O-01.

[23] Dow Corning Corporation. Dow Corning® 365, 35 % Dimethicone NF Emulsion and Dow Corning® 366 35 % Dimethicone NF Emulsion Frequently Asked Questions; Form No. 52-1040C-01.

[24] Kishore, R. S. K.; Kiese, S.; Fischer, S.; Pappenberger, A.; Grauschopf, U.; Mahler, H.-C. The Degradation of Polysorbates 20 and 80 and Its Potential Impact on the Stability of Biotherapeutics. Pharm. Res. 2011, 28 (5), 1194–1210. https://doi.org/10.1007/s11095-011-0385-x.

[25] Camino, G.; Lomakin, S. M.; Lazzari, M. Polydimethylsiloxane Thermal Degradation Part 1. Kinetic Aspects. Polymer 2001, 42 (6), 2395–2402. https://doi.org/10.1016/S0032-3861(00)00652-2.

[26] Camino, G.; Lomakin, S. M.; Lageard, M. Thermal Polydimethylsiloxane Degradation. Part 2. The Degradation Mechanisms. Polymer 2002, 43 (7), 2011–2015. https://doi.org/10.1016/S0032-3861(01)00785-6.

[27] Thomas, T. H.; Kendrick, T. C. Thermal Analysis of Polydimethylsiloxanes. I. Thermal Degradation in Controlled Atmospheres. J. Polym. Sci. A-2 Polym. Phys. 1969, 7 (3), 537 549. https://doi.org/10.1002/pol.1969.160070308.

[28] Ballistreri, A.; Garozzo, D.; Montaudo, G. Mass Spectral Characterization and Thermal Decomposition Mechanism of Poly(Dimethylsiloxane). Macromolecules 1984, 17 (7), 1312–1315. https://doi.org/10.1021/ma00137a003.

[29] Grassie, N.; Macfarlane, I. G. The Thermal Degradation of Polysiloxanes-I. Poly(Dimethylsiloxane). Eur. Polym. J. 1978, 14 (11), 875–884. https://doi.org/10.1016/0014-3057(78)90084-8.

[30] Clarson, S. J.; SemLyen, J. A. Studies of Cyclic and Linear Poly(Dimethyl-Siloxanes): 21. High Temperature Thermal Behaviour. Polymer 1986, 27 (1), 91–95. https://doi.org/10.1016/0032-3861(86)90360-5.

[31] Pretsch, E.; Bühlmann, P.; Badertscher, M. Structure Determination of Organic Compounds, Springer: Berlin, Heidelberg, 2009. https://doi.org/10.1007/978-3-540-93810-1.

[32] Detloff, T.; Sobisch, T.; Lerche, D. Particle Size Distribution by Space or Time Dependent Extinction Profiles Obtained by Analytical Centrifugation. Part. Part. Syst. Charact. 2006, 23 (2), 184–187. https://doi.org/10.1002/ppsc.200601028.

[33] Detloff, T.; Sobisch, T.; Lerche, D. Particle Size Distribution by Space or Time Dependent Extinction Profiles Obtained by Analytical Centrifugation (Concentrated Systems). Powder Technol. 2007, 174 (1-2), 50–55. https://doi.org/10.1016/j.powtec.2006.10.021.

[34] Owens, D. K.; Wendt, R. C. Estimation of the Surface Free Energy of Polymers. J. Appl. Polym. Sci. 1969, 13 (8), 1741–1747. https://doi.org/10.1002/app.1969.070130815.

[35] Schramm, L. L. Emulsions, Foams, and Suspensions; Wiley-VCH: Weinheim, Germany, 2005. https://doi.org/10.1002/3527606750.

[36] Dörfler, H.-D. Grenzflächen und Kolloid-Disperse Systeme, Springer: Berlin, Heidelberg, 2002.

[37] Goodarzi, F.; Zendehboudi, S. A Comprehensive Review on Emulsions and Emulsion Stability in Chemical and Energy Industries. Can. J. Chem. Eng. 2019, 97 (1), 281–309. https://doi.org/10.1002/cjce.23336.

[38] Emulsion Formation and Stability; Tadros, T. F., Ed.; Wiley-VCH: Weinheim, Germany, 2013. https://doi.org/10.1002/9783527647941.

[39] Lauth, G. J.; Kowalczyk, J. Einführung in die Physik und Chemie der Grenzflächen und Kolloide; Springer: Berlin, Heidelberg, 2016. https://doi.org/10.1007/978-3-662-47018-3.

[40] Pharmaceutical Emulsions and Suspensions; Nieloud, F.; Marti-Mestres, G., Eds.; Marcel Dekker: New York, 2000.

[41] Modern Aspects of Emulsion Science; Binks, B. P., Ed.; Royal Society of Chemistry: Cambridge, 1998. https://doi.org/10.1039/9781847551474.

[42] Funke, S.; Matilainen, J.; Nalenz, H.; Bechtold-Peters, K.; Mahler, H.-C.; Friess, W. Optimization of the Bake-on Siliconization of Cartridges. Part I: Optimization of the Spray-on Parameters. Eur. J. Pharm. Biopharm. 2016, 104, 200–215. https://doi.org/10.1016/j.ejpb.2016.05.007.

[43] McClements, D. J.; Jafari, S. M. Improving Emulsion Formation, Stability and Performance Using Mixed Emulsifiers: A Review. Adv. Colloid Interface Sci. 2018, 251 55–79. https://doi.org/10.1016/j.cis.2017.12.001.

[44] Vilasau, J.; Solans, C.; Gómez, M.; Dabrio, J.; Mújika-Garai, R.; Esquena, J. Stability of Oil-in-Water Paraffin Emulsions Prepared in a Mixed Ionic/Nonionic Surfactant System. Colloids Surf., A 2011, 389 (1-3), 222–229. https://doi.org/10.1016/j.colsurfa.2011.08.023.

[45] Buszello, K.; Harnisch, S.; Müller, R. H.; Müller, B. W. The Influence of Alkali Fatty Acids on the Properties and the Stability of Parenteral O/W Emulsions Modified with Solutol HS 15®. Eur. J. Pharm. Biopharm. 2000, 49 (2), 143–149. https://doi.org/10.1016/S0939-6411(99)00081-8.

[46] Sigma-Aldrich Chemie GmbH. Sicherheitsdatenblatt Gemäß Verordnung (EG) Nr. 1907/2006 Propylene Glycol; April 26, 2020.

[47] Roth GmbH. Sicherheitsdatenblatt Gemäß Verordnung (EG) Nr. 1907/2006 (REACH), Geändert Mit 2015/830/EU 2-Phenoxyethanol ≥99 % Zur Synthese; Aug 10, 2018.

[48] Roth GmbH. Sicherheitsdatenblatt Gemäß Verordnung (EG) Nr. 1907/2006 (REACH), 4-Hydroxybenzoesäure-Methylester ROTICHROM® Working Standard; Jan 14, 2016.

[49] Sigma-Aldrich Chemie GmbH. Sicherheitsdatenblatt Gemäß Verordnung (EG) Nr. 1907/2006 4-Hydroxybenzoesäure-Propylester; Apr 17, 2019.

[50] Chatterjee, K.; Dollimore, D.; Alexander, K. A New Application for the Antoine Equation in Formulation Development. Int. J. Pharm. 2001, 213 (1-2), 31–44. https://doi.org/10.1016/S0378-5173(00)00644-X.

[51] Kishore, R. S. K.; Pappenberger, A.; Dauphin, I. B.; Ross, A.; Buergi, B.; Staempfli, A.; Mahler, H.-C. Degradation of Polysorbates 20 and 80: Studies on Thermal Autoxidation and Hydrolysis. J. Pharm. Sci. 2011, 100 (2), 721–731. https://doi.org/10.1002/jps.22290.

[52] Kerwin, B. A. Polysorbates 20 and 80 Used in the Formulation of Protein Biotherapeutics: Structure and Degradation Pathways. J. Pharm. Sci. 2008, 97 (8), 2924–2935. https://doi.org/10.1002/jps.21190.

[53] Donbrow, M.; Azaz, E.; Pillersdorf, A. Autoxidation of Polysorbates. J. Pharm. Sci. 1978, 67 (12), 1676–1681. https://doi.org/10.1002/jps.2600671211.

[54] Nonionic Surfactants: Physical Chemistry; Schick, M. J., Ed.; Surfactant Science Series Vol 23; Marcel Dekker: New York, 1987.

[55] Santacesaria, E.; Gelosa, D.; Di Serio, M.; Tesser, R. Thermal Stability of Nonionic Polyoxyalkylene Surfactants. J. Appl. Polym. Sci. 1991, 42 (7), 2053–2061. https://doi.org/10.1002/app.1991.070420733.

[56] Mitsuda, K.; Kimura, H.; Murahashi, T. Evaporation and Decomposition of Triton X-100 under Various Gases and Temperatures. J. Mater. Sci. 1989, 24 (2), 413–419. https://doi.org/10.1007/BF01107420.

[57] Council of Europe, Polysorbat 20. In European Pharmacopoeia (Ph. Eur.), 9th Edition, Council of Europe: Strasbourg, France, 2007; pp 5054–5055.

[58] Roth GmbH. Freiwillige Sicherheitsinformation in Anlehnung an das Sicherheitsdatenblattformat Gemäß Verordnung (EG) Nr. 1907/2006 (REACH) – Myristinsäure ≥ 98 %, Für die Biochemie; Mar 3, 2020.

[59] Roth GmbH. Freiwillige Sicherheitsinformation in Anlehnung an das Sicherheitsdatenblattformat Gemäß Verordnung (EG) Nr. 1907/2006 (REACH) - Palmitinsäure ≥98 %, Reinst; Dec 12, 2019.

[60] Roth GmbH. Freiwillige Sicherheitsinformation in Anlehnung an das Sicherheitsdatenblattformat Gemäß Verordnung (EG) Nr. 1907/2006 (REACH) - Stearinsäure ≥98 %; Dec 12, 2019.

[61] Roth GmbH. Freiwillige Sicherheitsinformation in Anlehnung an das Sicherheitsdatenblattformat Gemäß Verordnung (EG) Nr. 1907/2006 (REACH) – Ölsäure ROTICHROM® GC; Aug 8, 2019.

[62] Santa Cruz Biotechnology, Inc. Safety Data Sheet 1,4-Anhydro-D-Sorbitol; Revision Date Nov 20, 2014.

[63] Christenson, H.; Friberg, S. E. Spectroscopic Investigation of the Mutual Interactions between Nonionic Surfactant, Hydrocarbon, and Water. J. Colloid Interface Sci. 1980, 75 (1), 276–285. https://doi.org/10.1016/0021-9797(80)90369-0.

[64] Nilsson, P. G.; Wennerstroem, H.; Lindman, B. Structure of Micellar Solutions of Nonionic Surfactants. Nuclear Magnetic Resonance Self-Diffusion and Proton Relaxation Studies of Poly (Ethylene Oxide) Alkyl Ethers. J. Phys. Chem. 1983, 87 (8), 1377–1385. https://doi.org/10.1021/j100231a021.

[65] Loosli, V.; Germershaus, O.; Steinberg, H.; Dreher, S.; Grauschopf, U.; Funke, S. Methods to Determine the Silicone Oil Layer Thickness in Sprayed-On Siliconized Syringes. PDA J. Pharm. Sci. Technol. 2018, 72 (3), 278–297. https://doi.org/10.5731/pdajpst.2017.007997.

[66] Rechendorff, K.; Hovgaard, M. B.; Foss, M.; Zhdanov, V. P.; Besenbacher, F. Enhancement of Protein Adsorption Induced by Surface Roughness. Langmuir 2006, 22 (26), 10885–10888. https://doi.org/10.1021/la0621923.

[67] Lord, M. S.; Foss, M.; Besenbacher, F. Influence of Nanoscale Surface Topography on Protein Adsorption and Cellular Response. Nano Today 2010, 5 (1), 66–78. https://doi.org/10.1016/j.nantod.2010.01.001.

[68] Mathes, J. M. Protein Adsorption to Vial Surfaces – Quantification , Structural and Mechanistic Studies. Ph.D. Thesis, LMU Munich, 2010.

[69] Felsovalyi, F.; Janvier, S.; Jouffray, S.; Soukiassian, H.; Mangiagalli, P. Silicone-Oil Based Subvisible Particles: Their Detection, Interactions, and Regulation in Prefilled Container Closure Systems for Biopharmaceuticals. J. Pharm. Sci. 2012, 101 (12), 4569–4583. https://doi.org/10.1002/jps.23328.

[70] Singh, S. K.; Afonina, N.; Awwad, M.; Bechtold-Peters, K.; Blue, J. T.; Chou, D.; Cromwell, M.; Krause, H.-J.; Mahler, H.-C.; Meyer, B. K.; Narhi, L.; Nesta, D. P.; Spitznagel, T. An Industry Perspective on the Monitoring of Subvisible Particles as a Quality Attribute for Protein Therapeutics. J. Pharm. Sci. 2010, 99 (8), 3302–3321. https://doi.org/10.1002/jps.22097.

[71] Zölls, S.; Tantipolphan, R.; Wiggenhorn, M.; Winter, G.; Jiskoot, W.; Friess, W.; Hawe, A. Particles in Therapeutic Protein Formulations, Part 1: Overview of Analytical Methods. J. Pharm. Sci. 2012, 101 (3), 914–935. https://doi.org/10.1002/jps.23001.

[72] Lorenz, B.; Krick, B. A.; Rodriguez, N.; Sawyer, W. G.; Mangiagalli, P.; Persson, B. N. J. Static or Breakloose Friction for Lubricated Contacts: The Role of Surface Roughness and Dewetting. J. Phys.: Condens. Matter 2013, 25 (44), 445013. https://doi.org/10.1088/0953-8984/25/44/445013.

[73] Eu, B.; Cairns, A.; Ding, G.; Cao, X.; Wen, Z.-Q. Direct Visualization of Protein Adsorption to Primary Containers by Gold Nanoparticles. J. Pharm. Sci. 2011, 100 (5), 1663–1670. https://doi.org/10.1002/jps.22410.

[74] Chan, E.; Hubbard, A.; Sane, S.; Maa, Y.-F. Syringe Siliconization Process Investigation and Optimization. PDA J. Pharm. Sci. Technol. 2012, 66 (2), 136–150. https://doi.org/10.5731/pdajpst.2012.00856.

Chapter IV Impact of Autoclavation on Baked-on Siliconized Containers for Biologics

Graphical Abstract

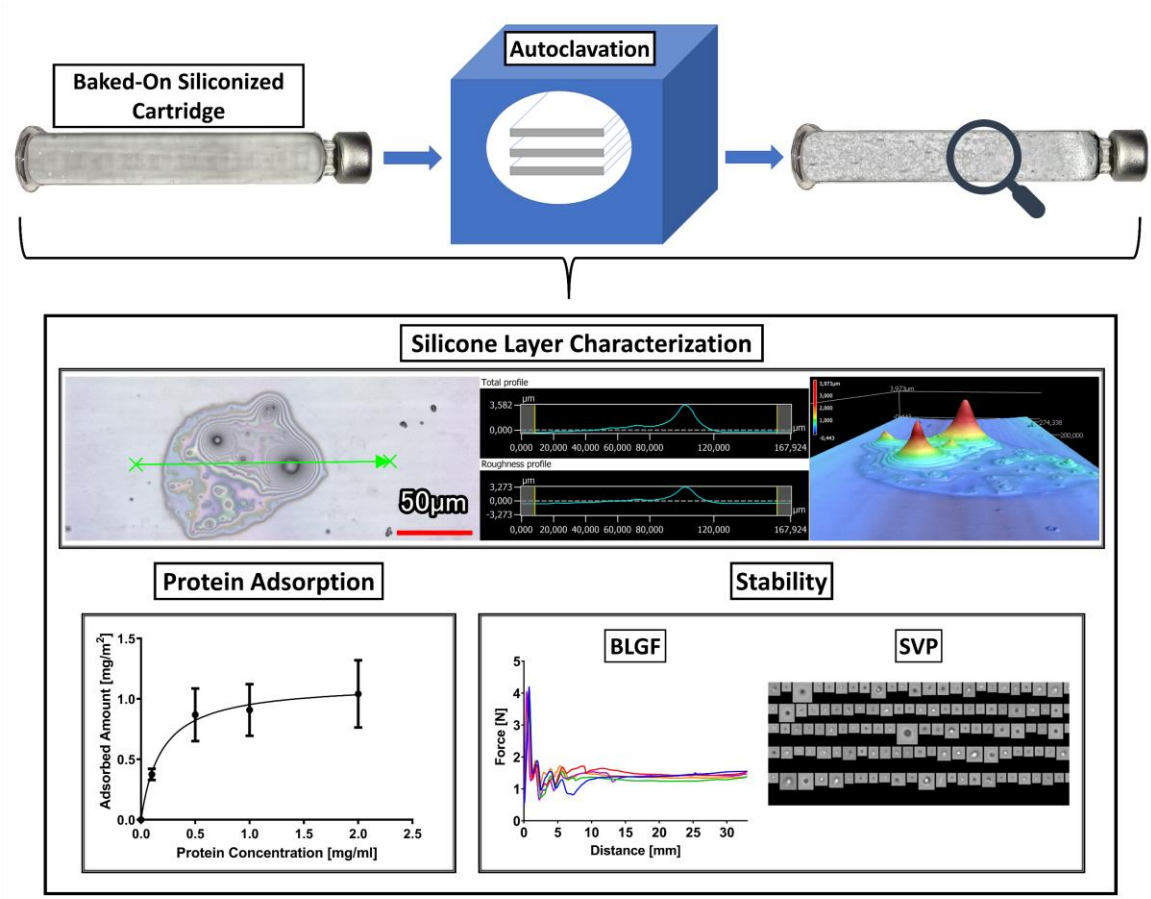

Abstract

Many pharmaceutical manufacturing units utilize pre-sterilized ready-to fill primary containers for parenterals. The containers may have been sterilized by the supplier via autoclavation. This process can change the physicochemical properties of the material and the subsequent product stability. We studied the impact of autoclavation on baked on siliconized containers for biopharmaceuticals. We characterized the container layers of different thickness before and after autoclavation for 15 min at 121 °C and 130 °C. Furthermore, we analyzed the adsorption of a mAb to the silicone layer and subjected filled containers to 12 weeks storage at 40 °C monitoring functionality and subvisible particle formation of the product. Autoclavation turned the initially homogenous silicone coating into an incoherent surface with uneven microstructure, changed surface roughness and energy, and increased protein adsorption. The effect was more pronounced at higher sterilization temperatures. We did not observe an effect of autoclavation on stability. Our results did not indicate any concerns for autoclavation at 121 °C for safety and stability of drug/device combination products using baked-on siliconized containers.

Keywords

Primary Packaging – Biopharmaceuticals – Sterilization – Bake-on Siliconization – Drug/Device Combination Product – Silicone Layer Characterization – Autoclavation

1 Introduction

It is common practice in pharmaceutical industry to use the primary packaging material for parenterals ready-to-fill [1]. The containers come already sterilized from the supplier in nests/tubs or in trays that are compatible with the fill and finish line of the pharmaceutical manufacturer. In general, the assignment of process development related tasks to the supplier of primary packaging material reduces the validation effort for the pharmaceutical manufacturer. The use of nest formats hereby increase flexibility regarding the fill and finish manufacturing as the refitting for different products is not necessarily needed or more easily achieved. Typically, the packaging supplier sterilizes the containers in the sealed tubs or trays at the end of the production cycle after washing, optional siliconization, depyrogenation, and nesting/traying [1,2].

The most common methods for sterilization of glass containers are steam and ethylene oxide treatment (EtO). In contrast, radiation is widely used for containers made out of a polymer like cyclic olefin polymer or cyclic olefin copolymer [1–4]. The sterilization methods have their advantages and drawbacks. The use of EtO requires higher safety measures for personnel and environment [5]. Additionally, EtO residues can remain in the packaging material, which may form adducts with therapeutic proteins [6–8]. Radiation can lead to discoloration of glass [9,10] and, radicals persisting after sterilization can lead to protein oxidation, aggregation, and particle formation [4]. Autoclavation of glass containers does not come with these risks for biopharmaceuticals [4,8], but the impact of steam sterilization on the silicone layer of ready-to-fill siliconized packaging material has not been published in detail yet.

In the following work we report on the impact of autoclavation on baked-on silicone layers in glass cartridges for the first time. Baked-on siliconized primary packaging containers are a valuable alternative to the standard sprayed-on containers for biopharmaceuticals providing several advantages. Utilizing the bake-on process, the silicone oil amount required for plunger movement is significantly reduced [11–13]. Due to the reduced amount of silicone oil needed as well as the heat fixation to the glass surface migration of silicone oil microdroplets into the aqueous product is diminished [1,12–15]. Hence, the risk of a functionality failure due to a lack of lubricant is mitigated. In addition, the risk of critical interactions between free silicone microdroplets and protein drugs is reduced. Furthermore,

products with stricter acceptance criteria regarding particulate matter like ocular products will less likely be out of specifications [16–21].

Silicone oil on the container surface forms a highly viscous layer that could be altered by autoclavation [13]. Heat, steam, and pressure may result in a redistribution or even removal of the silicone layer. This may lead to an inacceptable increase of the break-loose gliding forces (BLGF) [11]. Additionally, a change in surface roughness and hydrophobicity may affect the interaction of the protein drug with the silicone surface and could cause enhanced silicone and protein particle formation during storage. Surface roughness and hydrophobicity are known to influence protein adsorption behavior [22,23]. As adsorption often comes with a conformational change and aggregation of the protein a reduced protein stability could result [24–26].

The purpose of this study was to assess the impact of autoclavation on the quality of baked-on siliconized container systems for biopharmaceuticals. Next to baked-on siliconized cartridges from a supplier (SC) we assessed packaging material siliconized in house (IHC) enabling us to vary silicone levels and sterilization process parameters. We characterized the silicone layer after the autoclavation process and conducted a short-term stability study comparing non-autoclaved and autoclaved material. The silicone layer morphology was evaluated utilizing 3D-laser scanning (3D-LSM) as well as Raman microscopy. Additionally, the silicone distribution and amount per barrel were monitored with combined white light and laser interferometry and Fourier-transform infrared spectroscopy (FTIR). Siliconized microscopic slides served as model to investigate the impact of autoclavation on the surface energy. Furthermore, the adsorption behavior of a monoclonal antibody (mAb) towards the different container surfaces was investigated. For the stability study, container systems from the supplier were filled with surrogate solutions, stored at elevated temperatures for 12 weeks at 40 °C, and compared in terms of particle formation and functionality.

We could show that autoclavation induced obvious changes in the appearance of baked-on silicone layers, but no severe differences were observed in the stability study. In the following, we describe the extent of the change and clarify the consequences for baked-on siliconized container systems used for biopharmaceuticals.

2 Materials and Methods

2.1 Materials

Liveo™ 366 35 % Dimethicone NF Emulsion (Liveo™ 366) for siliconization was obtained by Dow Corning Inc. (Midland, MI, USA). Dilutions of this emulsion were prepared with highly purified water (HPW). 1 mL long non-siliconized and baked-on siliconized cartridges either autoclaved or non-autoclaved were provided by Nuova Ompi S.r.l. (Piombino Dese, Italy) as technical batches from the same production line. 1 mL long West Novapure® syringe plungers (West Pharmaceutical Services, Exton, PA, USA) were inserted for the stability study and functionality tests. Additional chemicals used were L-histidine monohydrochloride, L-histidine, sucrose, sodium dodecyl sulfate (SDS), polysorbate 80 (PS80) all from Sigma-Aldrich, Taufkirchen, Germany, ethylene glycol from Grüssing, Filsum, Germany, diiodomethane and Na_2HPO_4 from VWR, Darmstadt, Germany and NaH_2PO_4 and NaCl from Merck, Darmstadt, Germany. A monoclonal antibody (IgG, pI=8.3) was kindly provided by Novartis AG, Basel, Switzerland.

2.2 Silicone Layer Characterization

Siliconization Process

For the in-house bake-on siliconization process of glass cartridges 4, 8, 10 or 16 mg emulsion (1.75 % (w/w)) was sprayed onto the inner surface of non-siliconized containers with a Siliconization Stand SVS9061 (Bausch+Ströbel, Ilshofen, Germany) equipped with a diving nozzle. The following bake-on process was performed in an APT.line FED 115 Binder at 315 °C for 15 min. For contact angle measurements silicone emulsion was sprayed onto the surface of microscopic slides (SuperFrost™, Fisher Scientific, Schwerte, Germany) and afterwards baked-on at 315 °C for 15 min. Prior to siliconization the microscopic slides were washed with soap, highly purified water (HPW) and acetone to remove impurities from the glass surface. Autoclavation was performed at 121 °C for 15 min (Standard) as well as at a 130 °C (130 - 135 °C/High Temp.) for 15 min using a Varioklav 65T (H+P Labortechnik, Oberschleißheim, Germany).

Combined White Light and Laser Interferometry (WLI)

Silicone oil distribution was assessed with combined white light and laser interferometry (WLI) using the RapID Layer Explorer UT (rap.ID Particle Systems, Berlin, Germany) in UT Mode (limit of detection: 20 nm). Silicone layer thickness was determined

at least along 8 lines of 40 mm length with a resolution of 0.4 mm/step. The baseline was recorded prior to measurements with a non-siliconized cartridge from the same batch. Datapoints below LOD or without signal detectable (n.d.) were counted as 20 nm for data evaluation. Based on the average silicone oil layer thicknesses, the container interior surface (1077 mm^2) and the silicone oil density (0.972 g/cm^3) [27] a silicone oil amount per cartridge was calculated. (n = 3)

Fourier Transform Infrared Spectroscopy (FTIR)

The amount of silicone oil per barrel was determined via Fourier Transform Infrared Spectroscopy (FTIR) with a Bruker FTIR Tensor 27 (Bruker, Billerica, MA, USA) after solvent extraction with n-heptane. Extraction was carried out 3 times with 1.6 mL n-heptane per capped cartridge. The solvent extracts were pooled, and the solvent was evaporated using a Flowtherm Evaporator (Barkey GmbH & Co.KG, Leopoldshöhe, Germany) at 100 °C and nitrogen flow of 100 mL/min. The dried extract was redissolved in 500 µl n-heptane and filled into a 250 µm path length transmission liquid cell. 100 scans with a resolution of 4 cm^{-1} were performed between 3000 and 900 cm^{-1}. After baseline correction the area under the curve (AUC) of the absorption spectrum of the symmetrical Si-CH_3 deformation vibration at 1261 cm^{-1} was determined with Brukers OPUS software (Version 7.5.18). For the calibration silicone oil solutions with ranging concentration from 0.05 mg/mL to 3.33 mg/mL were assessed (R^2=0.9999). (n = 3)

3D-Laser Scanning Microscopy (3D-LSM)

The silicone layer was examined with a Keyence VK-X250 3D-Laser Scanning Microscope (Keyence, Mechelen, Belgium). Images were taken with 10x magnification from outside the barrel or with 100x magnification for surface roughness measurements of the silicone layer from the glass inside after breakage of the glass. Images from outside were stitched together with the VK Image Stitching software. Surface roughness was determined with the MultiFileAnalyzer software as recently reported [28] at 9 spots evenly distributed over the container for the in-house cartridges (IHC) and 3 spots for the supplier's cartridges (SC). (n = 3)

Confocal Raman Imaging

The silicone layer of baked-on siliconized cartridges from the supplier were examined with a Raman microscope alpha300 R (WITec, Ulm, Germany). A depth scan (x,z) of 45 µm (length) x 10 µm (depth) was performed using a 50x objective. The laser was set to 35 ms beam time at 532 nm and 20 mW resulting in a resolution of 30 x 135 pts. The resulting scan was further evaluated by clustering the 2D-image into areas with similar spectra using the Project Five software (WITec, Ulm, Germany). The spectra obtained were further compared to the KnowItAll Raman Spectral Database Collection (John Wiley & Sons, NJ, USA).

Drop-Shape Analyzer

Surface energy of siliconized microscopic slides was determined with a Drop Shape Analyzer (Krüss, Hamburg, Germany). 2 µl of HPW, ethylene glycol and diiodomethane were pipetted onto the surface and contact angles were determined 20 s after deposition in ellipse mode (tangent-1) using the Krüss Advance 1.1.02 software. Following the method of Owens-Wendt-Rabel-Kaelble the surface free energy (SFE) was determined (R^2 = 0.92 - 0.93). Prior to contact angle measurements images of the microscopic slides were taken with a Keyence BZ-8100E microscope (Keyence, Mechelen, Belgium) at 10x magnification. (n = 3)

Texture Analyzer

Container functionality (BLGF) of empty cartridges was assessed with a Texture Analyzer TA.XT Plus (Stable Micro Systems, Surrey, UK) at a speed of 3.17 mm/s. Break-loose force (BLF) was considered the maximum of the force required in the distance between 0 and 2 mm. Gliding force (GF) was defined as the average force required from 2 to 33.5 mm. Cartridges were measured empty and uncapped in order to access the actual friction force of the plunger without the influence of a fill medium. (n = 5)

2.3 mAb Adsorption

Adsorption studies followed a method developed by Saller et al. [23]. Cartridges siliconized with a spray amount of 10 mg were incubated with a 2 mg/mL mAb in 20 mM His-buffer pH 5.4 solution for 24 h without surfactant as well as including 0.04 % (w/v) PS80. After 3 washing steps with the same buffer the protein adsorbed to the surface was desorbed for 24 h using a 10 mM phosphate buffer pH 7.4 with 145 mM NaCl and containing

0.05 % (w/w) SDS. The protein concentration in the desorption medium was determined by HP-SEC using a TSKgel G3000 SWXL column (Tosoh Bioscience, Griesheim, Deutschland) at a flowrate of 0.7 mL/min with detection via UV at 210 nm. 400 µl sample were injected on the column. The mobile phase was identical to the desorption buffer. ($n \geq 3$)

2.4 Short-Term Stability Study

Sample Preparation

Supplier's cartridges both autoclaved and non-autoclaved were filled with 0.95 mL of water for injection (WFI) or 20 mM histidine-buffer pH 5.5, 240 mM sucrose, and 0.04 % (w/v) polysorbate 80 (His-Buffer). After plunger insertion the cartridges were stored at 40 °C for 12 weeks.

Container Functionality

The functionality was evaluated with piercing needles (Cambridge Consultant, Cambridge, UK) connected through a male luer integral lock ring to ¼-28 UNF thread adapter (Cole Parmer GmbH, Wertheim, Germany) to a BD Microlance 3 27G x 1/2 " (0.4 x 13 mm) cannula (see 4.3.2 Texture Analyzer). (n =5)

Particle Analysis

For subvisible particle (SvP) count and turbidity additional samples were expelled at 3.17 mm/s into a 2 mL pre-washed Eppendorf tube only using the piercing needle prerinsed and cleaned with n-heptane. Particle count was monitored by flow imaging (FI) with a FlowCam 8100 (Fluid Imaging Technologies, Scarborough, ME, USA) and light obscuration (LO) using a PAMAS SVSS system (Partikel- und Analysensysteme, Rutesheim, Germany) as describe before [28]. Prior to particle measurements the turbidity of the samples was monitored at a wavelength of 860 nm following DIN EN 27027 with a Nephla LPG239 turbidimeter (Hach Lange, Düsseldorf, Germany). (n = 3)

3 Results

The baked-on silicone layers of the IHC and the SC samples were assessed in terms of silicone layer thickness, silicone oil amount, and morphology of the surface to investigate the impact of autoclavation on the quality of the primary container systems. For the IHC samples additional friction force measurements were performed.

3.1 Silicone Layer Thickness

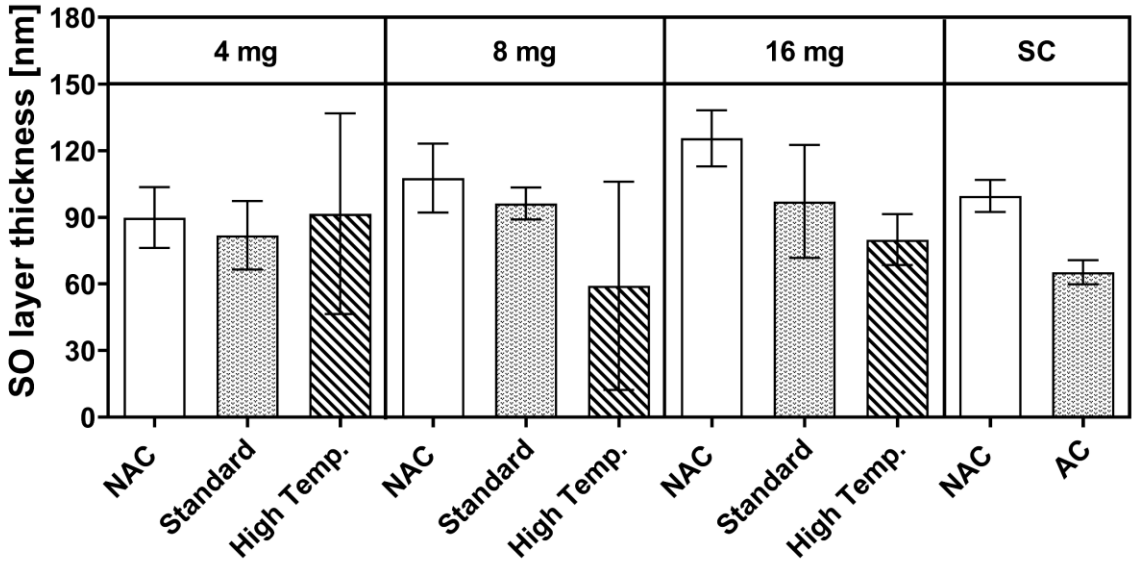

Figure IV-1: Silicone oil (SO) layer thickness of siliconized IHCs and SCs non-autoclaved (NAC) and after autoclavation (AC) at 121 °C 15 min (Standard) or 130 °C 15 min (High Temp.).

The silicone layer thickness was determined with combined white light and laser interferometry (WLI). IHC samples did not show consistent results after autoclavation (Figure IV-1). With increasing spray amount[a] the average silicone layer thickness of the non-autoclaved samples increased steadily from 90 ± 14 nm for the 4 mg spray amount to 108 ± 16 nm and 126 ± 13 nm for the 8 mg respectively 16 mg spray amount. A clear trend towards lower silicone layer thickness was not observable after autoclavation with the thickness ranging roughly between 60 nm and 100 nm. Only for the samples with the high spray amount of 16 mg and autoclaved at the high temperature of 130 °C the layer thickness obviously decreased to 80 ± 12 nm. In comparison, the 4 mg and 8 mg IHC samples did not decrease in the average values, but we observed higher variances after autoclavation at the high temperature. SC samples showed silicone a layer thickness in the same range, but

[a]Amount of 1.75 % (w/w) SO emulsion sprayed on to glass barrel (see 2.2.1.)

a lower layer thickness was detected for the autoclaved samples of 65 ± 5 nm compared to non-autoclaved samples with 100 ± 7 nm.

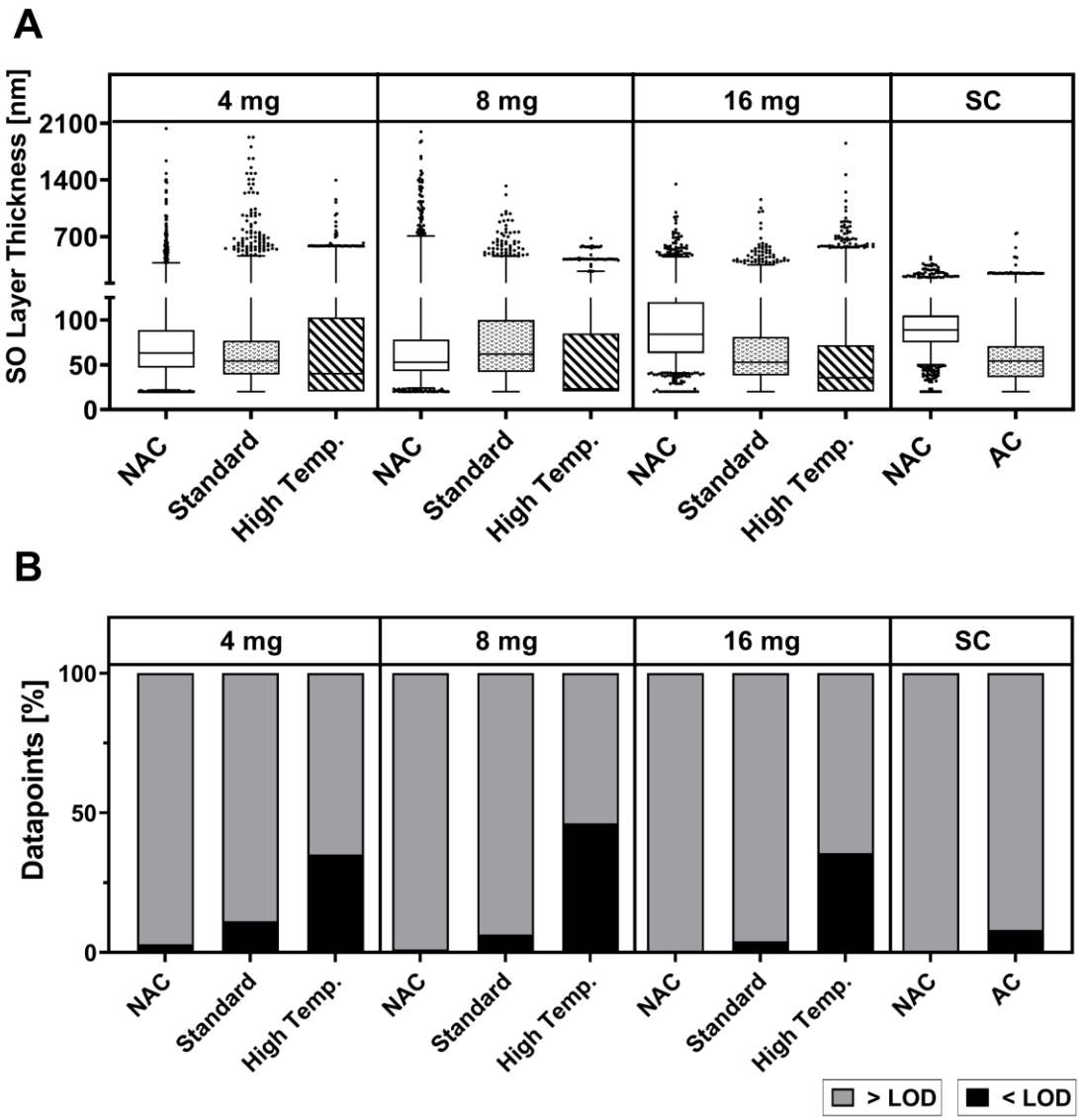

Figure IV-2: Silicone oil (SO) layer thickness data of siliconized IHCs and SCs non-autoclaved (NAC) and after autoclavation (AC) at 121 °C, 15 min or 130 °C 15 min (High Temp.) displayed by boxplots (2.5 – 97.5 percentile) [A] and percentage of data points below and above LOD (20 nm) [B].

We noticed a higher variability for the high temperature samples (Figure IV-2, A). For the lower spray amounts the samples autoclaved at 130 °C showed distinct changes in the median from 63 to 40 nm (4 mg) and from 53 to 23 nm (8 mg). Additionally, the 1st quartile was equal or below LOD (20 nm) for all spray amounts at this high temperature. For the highest spray amount of 16 mg the layer thickness median decreased at the standard process of 121 °C, 15 min from 84 to 53 nm and even more to 36 nm for the high temperature

samples. Autoclavation conditions induced a shift of the box towards smaller values respectively lower 1st quartiles for this spray amount. A clear trend for the median or data distribution displayed by the box plots could not be observed for the other IHC samples, which showed silicone layer median values ranging from 53 nm to 84 nm. Noticeably, the number of datapoints below LOD increased distinctly upon autoclavation, dependent on the process parameters (Figure IV-2, B). For non-autoclaved samples, between 1 % and 3 % were below LOD compared to 4 % to 11 % after autoclavation at 121 °C.

3.2 Silicone Oil Amount per Cartridge

The silicone oil amount per cartridge was calculated based on the results of the layer thickness measurements. In addition, for the IHC samples the values were verified by FTIR measurements. In general, the results obtained by FTIR confirmed the WLI results (Figure IV-3).

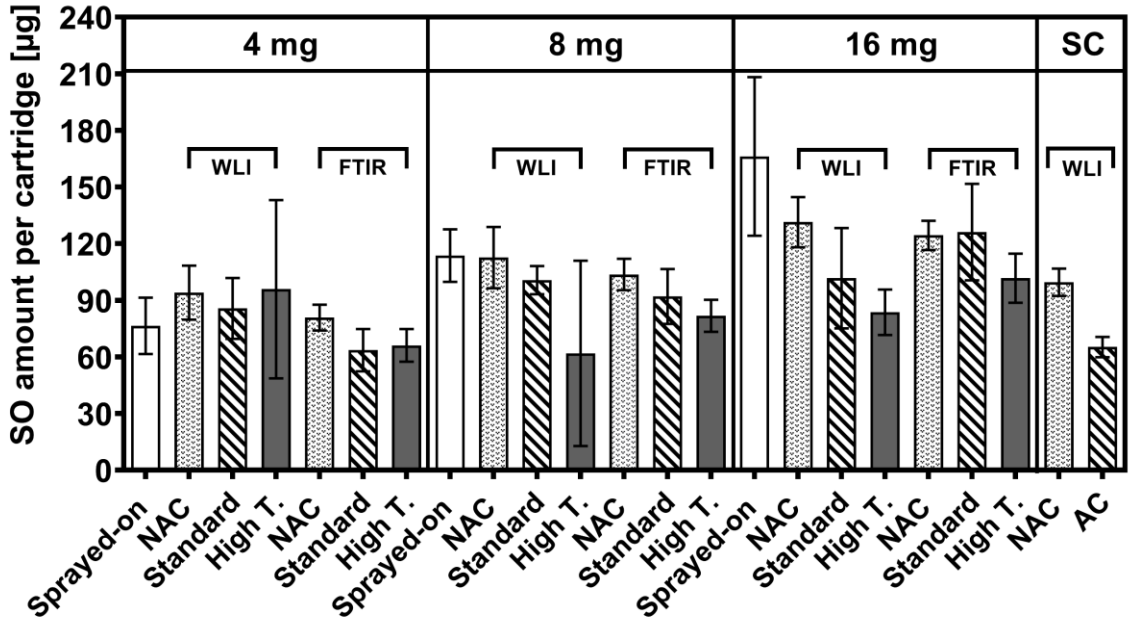

Figure IV-3: Silicone Oil (SO) amount per barrel of siliconized IHCs and SCs non-autoclaved (NAC) and after autoclavation (AC) at 121 °C 15 min (Standard) or 130 °C 15 min (High Temp.) according to WLI and FTIR as well as based on silicone oil emulsion sprayed-on the barrel (Sprayed-on).

Both methods showed no distinct decrease of the silicone oil amount upon autoclavation. According to WLI the silicone amount per barrel for non-autoclaved samples increased with higher spray amounts from 94 ± 14 µg for the 4 mg spray amount to 113 ± 16 µg and 132 ± 13 µg for the 8 mg and 16 mg spray amount. FTIR measurements showed values in the same range with 81 ± 7 µg, 104 ± 8 µg, and 124 ± 8 µg per barrel. These silicone oil

levels were in line with the sprayed-on amounts of silicone oil emulsions monitored with a microbalance during siliconization.

A slightly a greater loss of silicone oil resulted for the highest spray amount for which, based on weighing, a silicone oil amount of 166 ± 42 µg was expected. After standard autoclavation at 121 °C for 15 min, the silicone oil amount per cartridge did not change systematically. Only for the higher autoclavation temperature of 130 °C FTIR analysis showed a tendency towards slightly lower average silicone oil amounts of 66 ± 9 µg, 82 ± 9 µg, and 102 ± 13 µg according to the different spray amounts. The results obtained by WLI did not clearly differ but with values of 96 ± 47 µg and 62 ± 50 µg at the 4 mg and 8 mg spray amount a substantial increase in the variance was observable. Silicone oil level for the 16 mg spray amount matched the FTIR results with 84 ± 12 µg per barrel. Based on silicone oil layer thickness measurements the silicone amount of the non-autoclaved SC samples was in the range of the 8 mg IHC samples with 100 ± 7 µg per barrel and less silicone oil after autoclavation with 65 ± 5 µg.

3.3 Silicone Oil Layer Characterization

3.3.1 Silicone Oil Layer Morphology

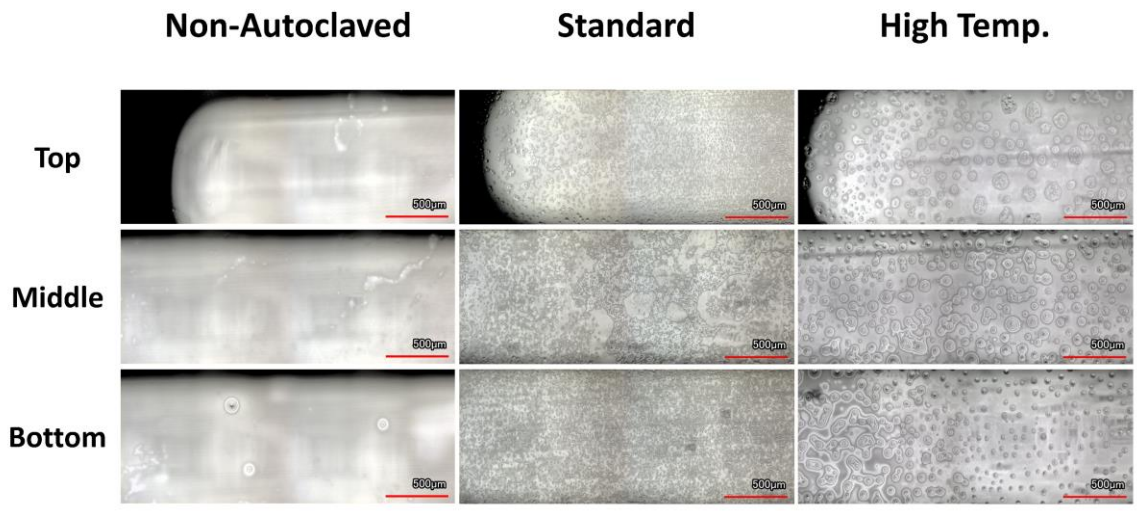

Figure IV-4: 3D-LSM images of IHC (Spray Amount: 4 mg), non-autoclaved and autoclaved, from outside.

The morphology of the silicone layer before and after autoclavation was evaluated by 3D-LSM without breakage from outside the barrel. Non-autoclaved cartridges showed a smooth, coherent silicone oil layer on the glass surface (Figure IV-4/Figure IV-5/ Supplementary Data - Figure S IV-1). After autoclavation islands like silicone accumulations could be detected along the complete length of the container. The change in

structure occurred regardless of the spray amount and the autoclavation process parameters. The higher autoclavation temperatures resulted in fewer but larger spots with sizes up to 100 µm.

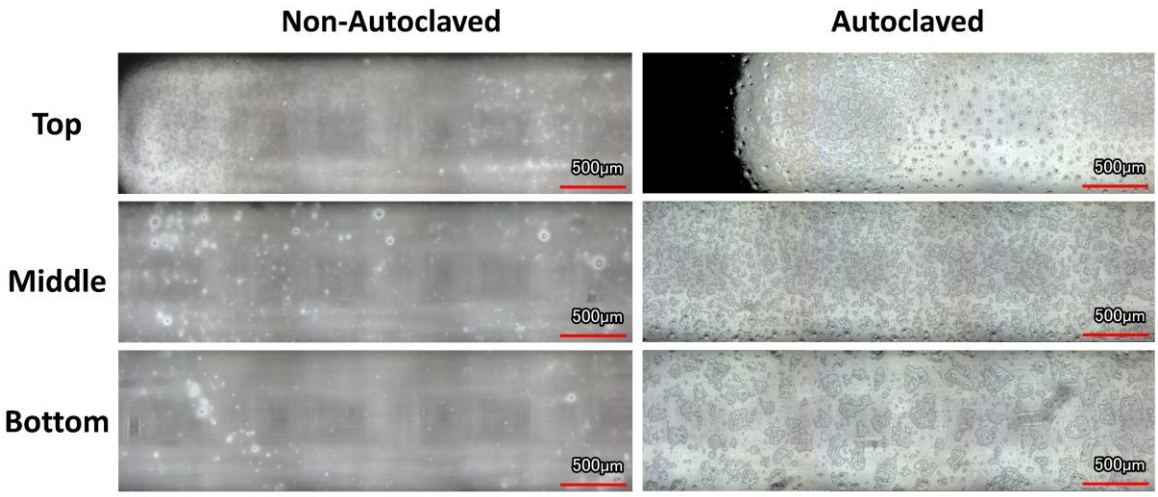

Figure IV-5: 3D-LSM images of SC, non-autoclaved and autoclaved, from outside.

3.3.2 Silicone Oil Layer Analysis

The chemical composition of the silicone oil layer of SC samples was evaluated by Raman microscopy as silicone oil and glass can be distinguished well by their Raman spectra. The arrow in Figure IV-6 A represents the scanned area of the silicone surface. The depth scan was clustered in 5 subareas of similar spectra which showed an uneven distribution of silicone oil on the surface (Figure IV-6, B). At the bottom, the large area (area 5) was attributed to the glass material of the primary container since the spectra showed high similarity to aluminum silicate based on the KnowItAll spectral library. For area 3 and 4 the intensity for signals between 2800 and 3000 cm^{-1} significantly increased which can be attributed to the stretching vibration bands of the C-H groups of silicone oil [29]. Additionally, the typical fingerprint of silicone oil between 490 and 1000 cm^{-1} induced by Si-O-Si and Si-CH_3 stretching vibrations [29] was observable (Figure IV-6, C). A high similarity with a polydimethylsiloxane reference spectrum of the KnowItAll spectral library was detected. Area 1 and 2 showed spectra resembling the glass spectra without the Si-O-Si and Si-CH_3 stretching vibrations and lower signal intensities between 2800 and 3000 cm^{-1}. The results indicate an uneven distribution of silicone oil on the glass surface with higher silicone oil levels at the beginning of the scan displayed as hill like structure in the 2D optical image.

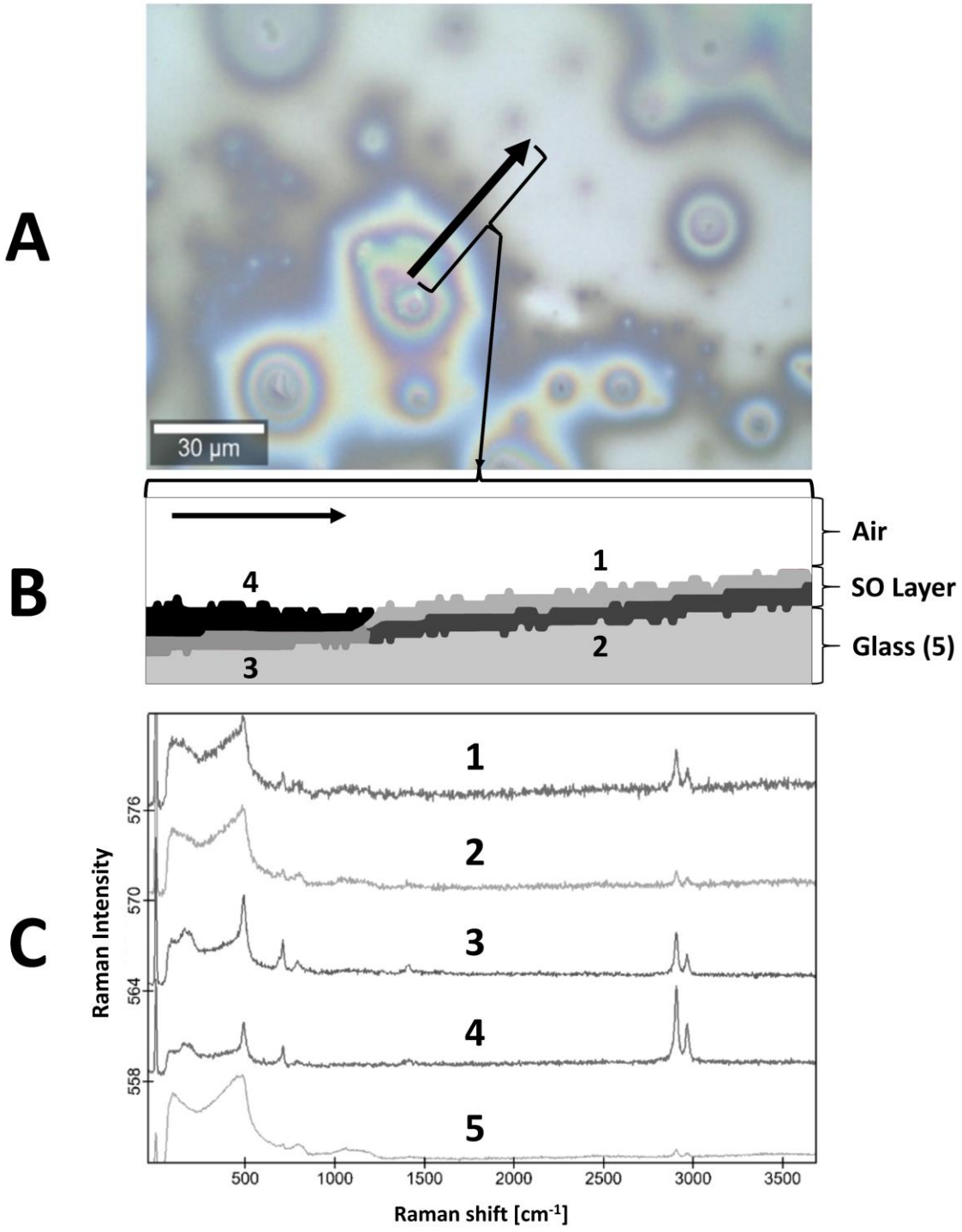

Figure IV-6: Image of SC silicone surface scanned with Raman microscope [A] and corresponding clustered 2D heat map [B] and Raman signals of the depth scan [C].

3.3.3 Surface Roughness

The silicone layer was furthermore examined with 3D-laser scanning microscopy after breakage of the container to obtain surface roughness data. The general appearance of the silicone layer was in line with the images from the outside of the container (Figure IV-7). The autoclavation process led to an increased roughness of the silicone oil layer. Non-autoclaved containers (IHC) showed initial Sa medians between 0.017 µm and 0.022 µm independent of the spray amount but higher Sz values results with higher spray amounts (Sz medians of 1.08 µm and 1.36 µm for the 8 mg and 16 mg resp. compared to 0.34 µm for the 4 mg spray amount). With autoclavation the roughness increased as indicated by the median values and the interquartile ranges (IQR) of the roughness parameters. The effect was more pronounced with higher autoclavation temperature. Also, for the SC containers the roughness increased with autoclavation, from median Sa 0.018 µm (IQR: 0.02 µm) to 0.128 µm (IQR: 0.09 µm) and median Sz 0.39 µm (IQR: 0.6 µm) to 1.5 µm (IQR: 0.7 µm).

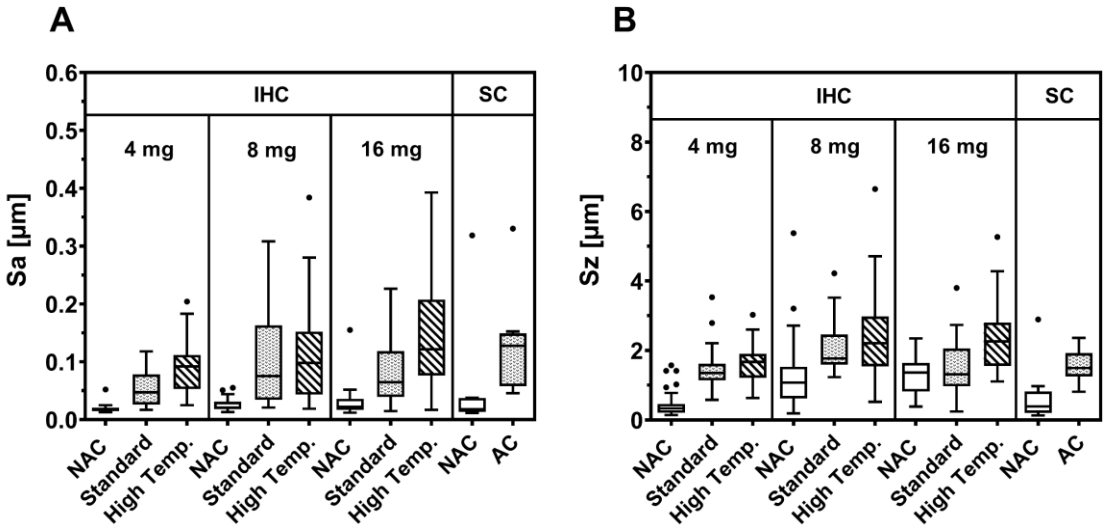

Figure IV-7: Surface arithmetic mean height (Sa) [A] and surface maximum height (Sz) [B] of siliconized IHCs and SCs non-autoclaved (NAC) and after autoclavation (AC) at 121 °C 15 min (Standard) or 130 °C 15 min (High Temp.). Box-whisker plots are displayed following Tukey.

3.3.4 Frictional Force

Additionally, impact of the silicone oil layer treatment on the performance of IHC samples was analyzed. The force required to push a plunger through an empty, uncapped container was measured which is predominantly dependent on the friction coefficient of the rubber plunger on the surface [30,31]. The BLF of empty cartridges ranged between 3.2 N and 4.3 N on average independent of the spray amount and was unchanged upon autoclavation

(Figure IV-8, A). In contrast the GF was increased for all spray amounts after standard autoclavation (Figure IV-8, B) from approximately 0.6 to 0.8 N before to 1.6 ± 0.1 N, 1.2 ± 0.2 N and 1.8 ± 0.2 N for 4 mg, 8 mg and 16 mg spray amount. Higher autoclavation temperatures did not enhance the effect, instead the values were less increased.

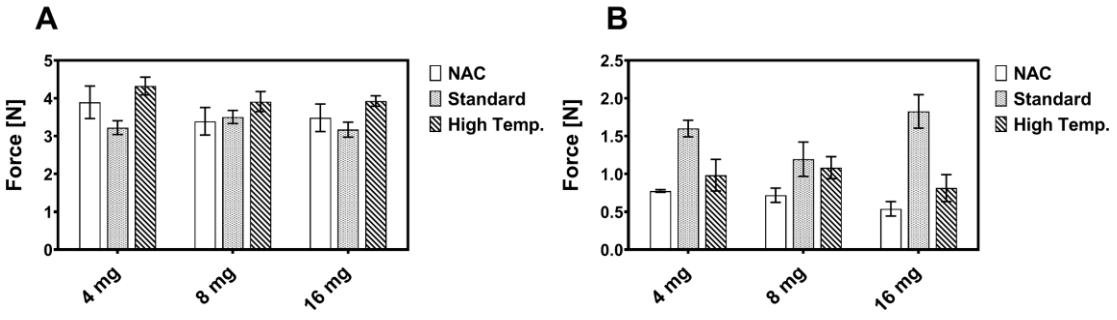

Figure IV-8: Break-Loose [A] and Gliding [B] forces of empty IHCs non-autoclaved (NAC) and after autoclavation at 121 °C 15 min (Standard) or 130 °C 15 min (High Temp.).

3.4 Further Characteristics of the Silicone Layer

Additionally, we analyzed the SFE of the silicone oil layer surfaces were determined before and after autoclavation via contact angle (CA) measurements. The silicone oil was baked-on to flat microscopic slides for analysis. After autoclavation it showed a microstructure with spots indicating silicone oil accumulation similar to the one observed with the cartridges (Figure IV-9 – I). The CA for water decreased from 110.2 ± 0.7° to 102.8 ± 3.3° and 66.7 ± 36.9° resp. upon autoclavation at 121 °C and 130 °C (Figure IV-9 – II, A). For ethylene glycol the CA values also decreased from 87.9 ± 2.0° bevor to 84.8 ± 5.7° and 63.8 ± 26.4° respectively after autoclavation, whereas the CA of diiodomethane was consistent between 72° and 77°. The data showed a higher variability after autoclavation especially after 130 °C treatment for the more polar solvents. The SFE values obtained by Owens-Wendt-Rabel-Kaelble (OWRK) analysis based on the CA data (R^2 = 0.92 and 0.93) [32] demonstrated an increase in the polar component for the autoclaved surfaces (Figure IV-9-II, B).

3.5 Adsorption to the Silicone Oil Layer

Surface characteristics like surface roughness and SFE are known to influence protein interactions with solid surfaces [33]. Therefore, protein adsorption to the inner container surface was quantified for a mAb. A protein concentration of 2 mg/mL was used for the incubation as it showed a saturation of the surface (Supplementary Data, Figure S IV-2)

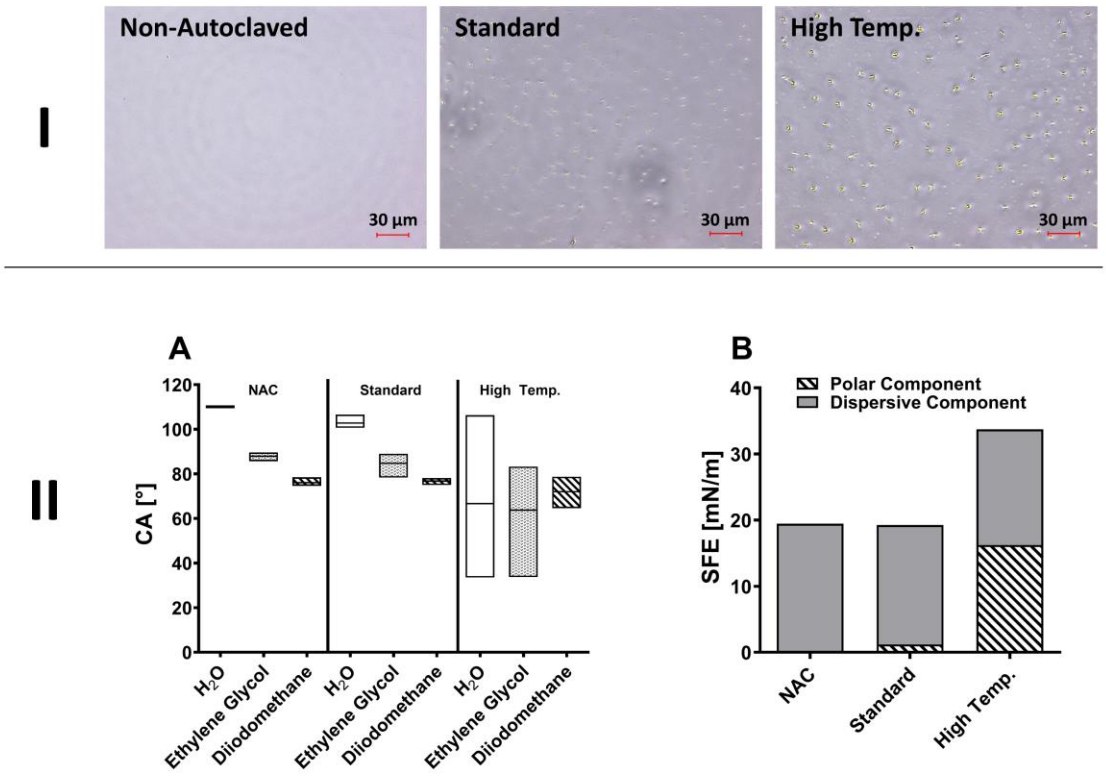

Figure IV-9: Optical images of baked-on silicone oil layers on microscopic slides before (NAC) and after autoclavation at 121 °C, 15 min (Standard) and 130 °C, 15 min (High Temp.) [I] as well as CAs of different liquids on the slides (floating bars display min to max values with the line at mean) [II, A] and corresponding SFE [II, B].

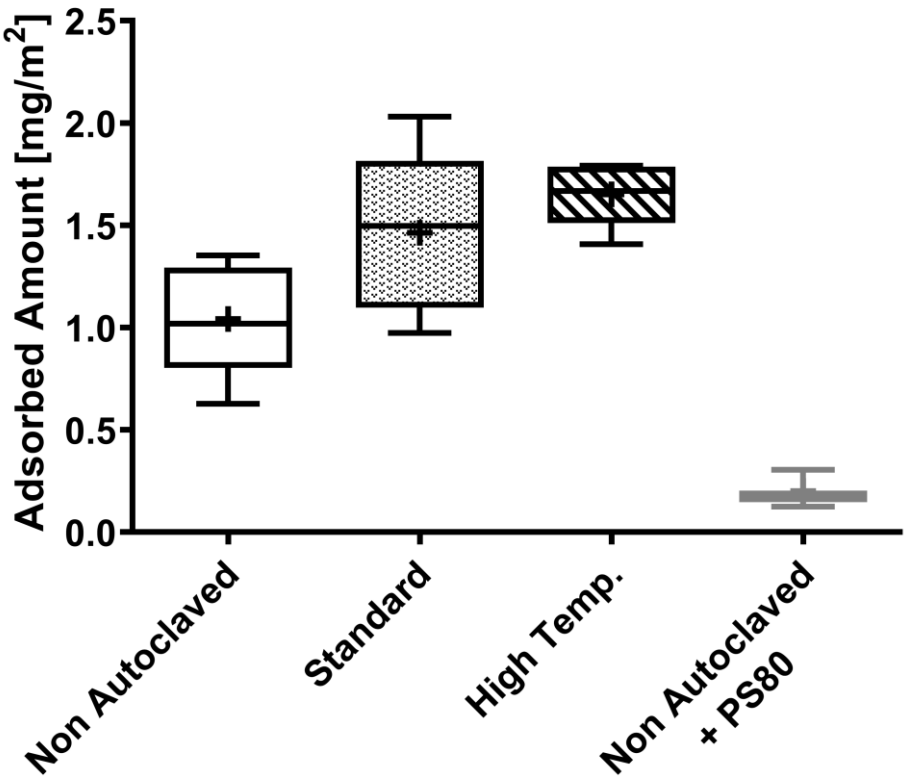

Figure IV-10: MAb adsorption at 2 mg/mL onto baked-on silicone oil layers before and after autoclavation at 121 °C, 15 min (Standard) or 130 °C, 15 min (High Temp.). Whiskers represent Min to Max, median and mean displayed by line and "+".

in line with previous results [23,33,34]. The amount of mAb adsorbed was higher for autoclaved containers with 1.5 ± 0.4 mg/m^2 (121 °C, 15 min) and 1.7 ± 0.2 mg/m^2 (130 °C, 15 min) compared to 1.0 ± 0.3 mg/m^2 before autoclavation (Figure IV-10). The addition of 0.04 % (w/v) PS80 to the initial solution massively reduced adsorption to 0.2 ± 0.1 mg/m^2.

3.6 Short-Term Stability Testing of Filled Cartridges

The stability of cartridges, pre-siliconized by the supplier and filled with WFI and His-Buffer, was monitored in regards of container functionality and particle formation upon storage for 12 weeks at 40 °C.

3.6.1 Functionality

Overall, both non-autoclaved and autoclaved cartridges showed low BLGF with BLFs of around 2 N and a GF between 1.5 N and 2 N (Figure IV-11) at T0, well suited for the development of a drug/device combination product [21]. The BLF values increased to

roughly 4 N upon storage independent of autoclavation for both surrogate solutions. The GF did not change upon storage.

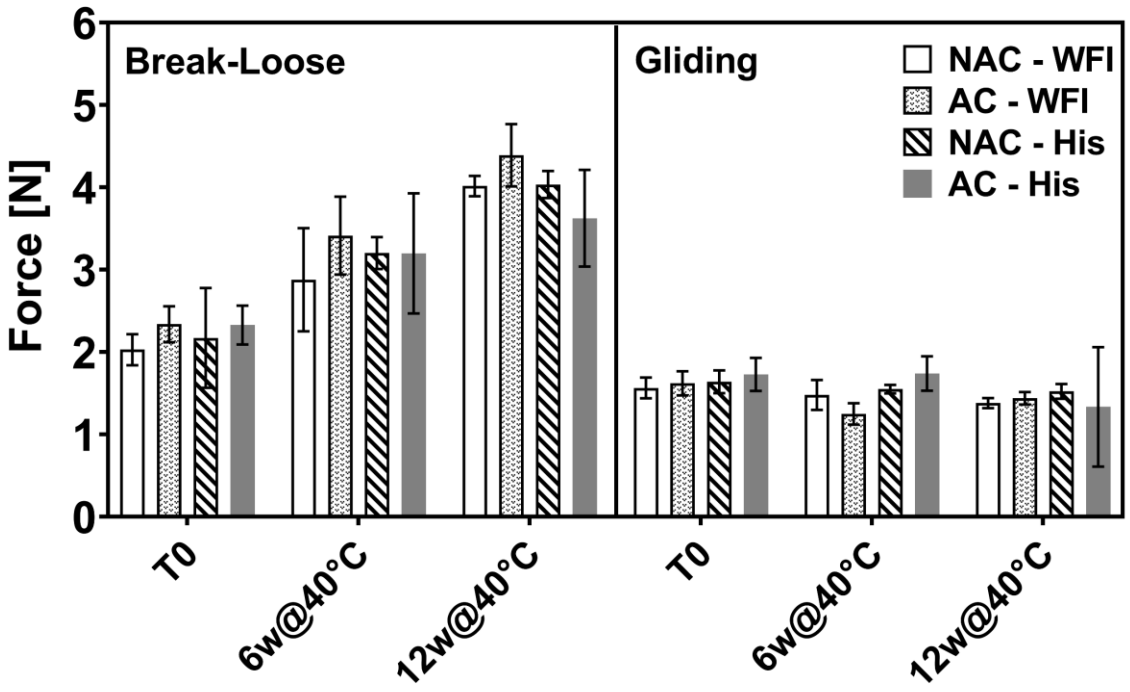

Figure IV-11: Break-loose and gliding forces of siliconized SCs not autoclaved (NAC) and autoclaved (AC) filled with WFI and 20mM His-Buffer containing 0.04 % PS80 upon storage at 40 °C.

3.6.2 Particle Formation

The number of SvPs as indicator for free silicone oil droplets in the filled solutions was overall very low in expelled samples (Figure 12) with 1600 - 8100 > 1µm per mL in FI und 500 - 2700 particles > 1µm per mL in LO without a trend with autoclavation. The number of particles ≥ 10 µm and ≥ 25 µm were well below the requirements for the approval of parenteral drugs and did not show any effect of autoclavation (Supplementary Data, Table S IV-1) [14,21,35]. Furthermore, turbidity was below 1 FNU for all samples over storage regardless of the autoclavation post siliconization.

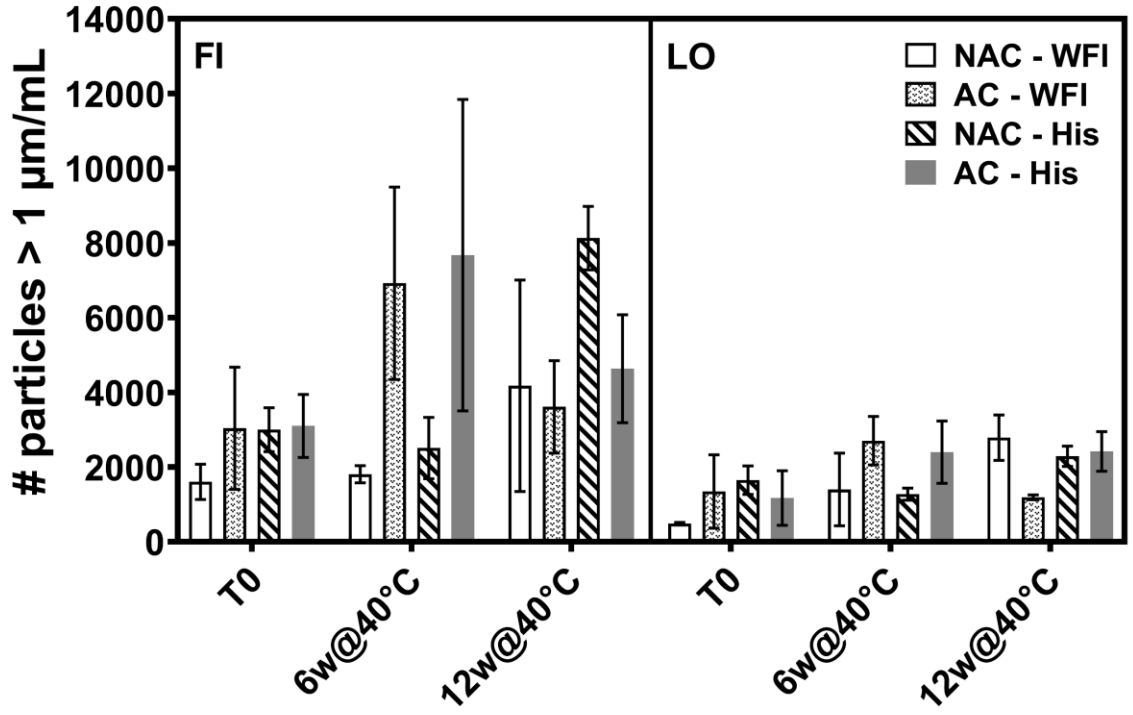

Figure IV-12: Number of SvPs > 1µm/mL of siliconized SCs not autoclaved (NA) and autoclaved (A) filled with WFI and 20mM His-Buffer containing 0.04 % PS80 upon storage at 40 °C and expelling analyzed by FI and LO.

4 Discussion

Functionality and silicone oil transfer into drug product are key aspects in the development of syringes and cartridges as primary packaging material for biopharmaceuticals. The silicone oil on the inner surface of the barrel acts as a lubricant to reduce the friction force between plunger and glass surface ensuring consistent and easy movement of the plunger during administration [1,3,30,36]. A change or depletion of this lubricant layer upon storage may lead to an increase of the BLGF to the point that the functionality is at stake [20,21]. Furthermore, a change of the structure or the surface chemistry of the silicone oil layer may result in a more pronounced formation of silicone oil droplets in the drug product. Silicone oil microdroplets are known to interact with protein molecules forming mixed aggregates which are considered critical [20,37,38]. Autoclavation is a potential step in the manufacturing of ready-to-fill containers. In this study we aimed to thoroughly investigate the impact autoclavation has on the silicone oil layer and its consequences for functionality and silicone oil droplet formation in the drug product. The silicone layer characterization protocol was extended for IHC samples due to limited availability of SC material. For the subsequent short-term stability study (see section 4.5.2) SC samples were filled and stored.

4.1 Silicone Layer Characterization

The silicone oil layer thickness of baked-on siliconized IHC samples was not affected by autoclavation according to WLI and quantification of the silicone oil amount per barrel by FTIR. WLI hereby proved to be a valuable, non-destructive, and fast method matching the FTIR results. After autoclavation at the high temperature of 130 °C the silicone oil layer was more affected with a higher percentage of datapoints below LOD and the variance of WLI was increased. WLI only covers a small area of the silicone oil surface and remains an approximation based on the silicone oil layer thickness data, which can be biased especially for a container with an uneven silicone oil distribution, a low silicone oil amount, and a high number of datapoints below LOD. Whereas the silicone oil distribution across the container was not affected by autoclavation, a substantial change of the silicone oil layer morphology on a microscale level could be noticed, especially for samples autoclaved at 130 °C. Silicone oil was accumulated at certain spots as indicated by 3D-LSM and Raman microscopy resulting in a higher surface roughness. The increase in surface roughness was more pronounced for thicker silicone oil layers. The impact of autoclavation

on the lubricant layer was reflected in a small increase of the GF by approximately 1 N analyzing empty cartridges. The forces recorded are the result of the frictional forces between freshly emerged contact areas of glass and the rubber of the plunger during plunger movement [30,39]. Overall, the increase in GFs was negligibly small compared to reported upper force limits between 15 and 30 N [12,21,40]. In comparison, the SC samples used for the stability study showed the same change in the surface characteristics for autoclaved samples. The silicone oil layer morphology of autoclaved samples was reminiscent to IHC samples autoclaved at 121 °C, 15 min. The number of datapoints below LOD and the surface roughness were in the same range as well as similarly increased for autoclaved samples. The average silicone layer thickness of non-autoclaved samples resembled the 8 mg spray amount. Autoclaved SC samples showed slightly lower silicone layer thicknesses, but the overall range was comparable to the IHC samples.

Contact angle measurements indicated a change in surface properties towards a more polar surface as consequence of the autoclavation process. Since polydimethylsiloxane creates a predominantly hydrophobic surface [12,13,33,41] the results may point to a removal of silicone oil at certain microspots. The glass surface is hydrophilic [33,42,43] and able to bind water molecules during the autoclavation process [44]. We observed a higher variance in the contact angle measurements of autoclaved material which could be due to a higher surface roughness, known to interfere with contact angle measurements [45,46]. Given the non-uniformity of the surface morphology observed by 3D-LSM it seems likely that there is a less consistent energy level present at the surface. Overall, changes were more distinct for samples autoclaved at the higher temperature.

Protein adsorption to surfaces is rather complex and depends on many different factors including formulation and surface properties which impact the hydrophobic and electrostatic interactions [24,47–50]. Overall, the amount of mAb adsorbed was low compared to previously reported amounts for siliconized primary packaging material. Protein adsorption is in general considered to be more pronounced towards hydrophobic surfaces compared to hydrophilic ones [51]. Specifically, the adsorption of mAbs to siliconized primary packaging materials is higher compared to non-siliconized [33,34,52]. We could show that more protein was adsorbed to autoclaved silicone layers. On the one hand the hydrophilicity of the silicone layer increased with autoclavation, which may lead to less protein adsorption. On the other hand, the morphology was changed and the surface roughness increased upon autoclavation, which can enhance protein adsorption,

specifically for large “soft” proteins [22,23]. As expected, the samples containing PS 80 showed a distinct decrease in the adsorption tendency [21,53,54]. The changed adsorption behavior with autoclavation could be relevant for proteins with higher binding tendency, at lower protein concentrations, for formulations without surfactant, and if containers with a higher surface to volume ratio are used [55].

4.2 Short-Term Stability Study

We also evaluated whether an effect of autoclavation on the lubricant layer can be seen upon storage. Therefore, we stressed SCs filled with surrogate solution at 40 °C for 12 weeks and analyzed functionality and particle formation. Despite the obvious impact of autoclavation on the silicone layer the performance and stability of the primary container was not diminished. Stability data did not imply higher silicone oil detachment tendencies for the autoclaved samples. The increase in BL-Forces over time was detectable for both, non-autoclaved and autoclaved, samples and can be explained through a constant de-wetting of the surface of silicone oil [36,56]. No significant increase in number of SvPs was observed over storage. The samples not only fulfilled the requirements for parenteral products (≤ 6000 particles/container ≥ 10 µm and ≤ 600 particles/container ≥ 25 µm [35]), but even met the tighter limits of ocular products according to USP <789> (≤ 50 particles/mL ≥ 10 µm, ≤ 5 particles/mL ≥ 25 µm and ≤ 2 particles/mL ≥ 50 µm [21,57,58]). In comparison to sprayed-on packaging material [59–62] particle concentrations were very low and consistent. The stability in terms of functionality and SvP formation indicates a high integrity of the silicone layer which is not impacted by autoclavation [63,64].

5 Conclusion

In this work the impact of autoclavation on baked-on silicone oil layers in primary packaging containers for biopharmaceuticals was investigated for the first time. Autoclavation changed the surface morphology on a microscale level from a homogenous silicone coating into a structured surface with spots of silicone oil enrichment at the expense of the local silicone oil layer thickness. Interferometry indicates redistribution at a larger scale. These changes come along with an increase in the surface roughness, hydrophilicity, protein adsorption and frictional force. But all effects were minor and were less pronounced after autoclavation at 121 °C compared to 130 °C. It is important to note that the total silicone oil amount was not reduced by the autoclavation process, and that the silicone oil was still distributed evenly along the complete length of the barrel. Thus, functionality of the container system was fully preserved. Additionally, autoclavation did not affect container stability in terms of functionality and particle formation in a 12 week stress study at 40 °C. Accordingly, we conclude that an autoclavation of baked-on siliconized containers at 121 °C for 15 min will not impact the functionality, stability and safety of biopharmaceutical products in drug/device combinations.

Supplementary Data

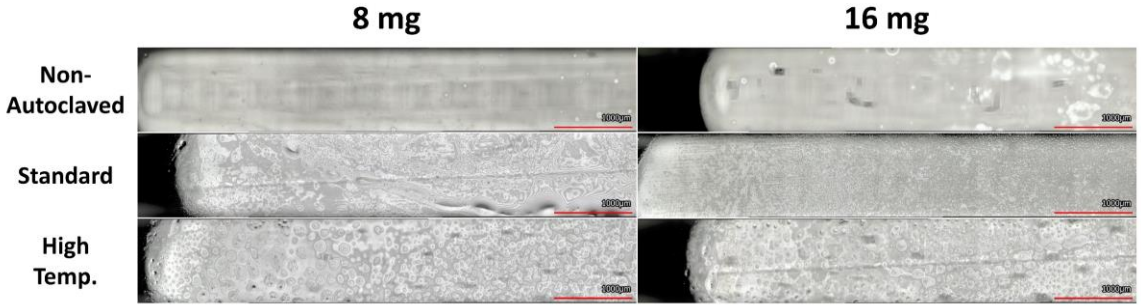

Figure S IV-1: 3D-LSM images from outside of siliconized IHCs non-autoclaved and after autoclavation at 121 °C,15 min (Standard) and 130 °C, 15 min (High Temp.) siliconized with 8 mg and 16 mg spray amount.

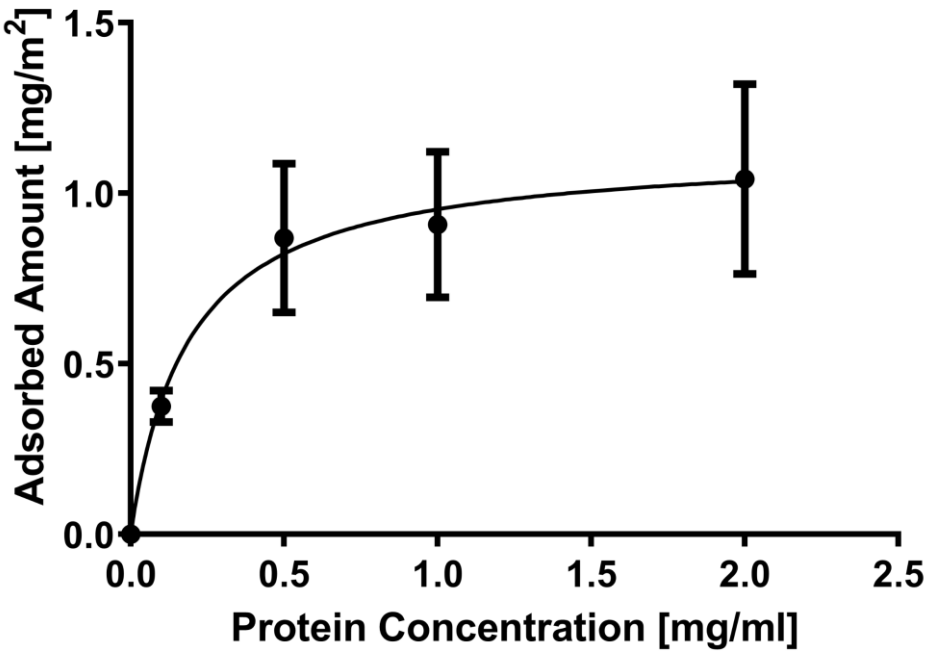

Figure S IV-2: Adsorption isotherm (R^2=0.83) of mAb at 2 mg/mL at a bake-on siliconized non-autoclaved container surface. Line represents fit for one site specific binding model.

Material	Fill Medium	Particle Size	T0	6 w.	12 w.
NAC	WFI	≥ 10 µm/mL	5 ± 2	13 ± 11	26 ± 11
		≥ 25 µm/mL	0 ± 0	3 ± 2	< 1 ± < 1
		≥ 50 µm/mL	0 ± 0	< 1 ± < 1	0 ± 0
	His	≥ 10 µm/mL	33 ± 16	32 ± 1	33 ± 11
		≥ 25 µm/mL	4 ± 4	3 ± 3	1 ± 1
		≥ 50 µm/mL	0 ± 0	< 1 ± < 1	0 ± 0
AC	WFI	≥ 10 µm/mL	6 ± 5	8 ± 1	5 ± 1
		≥ 25 µm/mL	0 ± 0	1 ± 1	1 ± 1
		≥ 50 µm/mL	0 ± 0	< 1 ± < 1	< 1 ± < 1
	His	≥ 10 µm/mL	22 ± 10	42 ± 16	40 ± 15
		≥ 25 µm/mL	3 ± 3	2 ± 1	4 ± 5
		≥ 50 µm/mL	< 1 ± < 1	< 1 ± < 1	< 1 ± < 1

Table S IV-1: Subvisible Particle Concentration ≥ 10 µm, ≥ 25 µm and ≥ 50 µm per mL obtained by LO of expelled cartridges non-autoclaved (NAC) and after autoclavation (AC) stored at 40 °C for 12 weeks.

Abbreviations

3D-LSM	3D – Laser Scanning Microscope
AC	Autoclaved
BLF	Break-Loose Force
BLGF	Break-Loose Gliding Force
FTIR	Fourier Transform Infrared (Spectroscopy)
GF	Gliding Force
HPW	Highly Purified Water
IHC	In-house Cartridges
IQR	Interquartile Range
LOD	Limit of Detection
NAC	Non-Autoclaved
n.d.	Not Detectable
OWRK	Owens-Wendt-Rabel-Kaelble
Sa	Surface Arithmetic Mean Height
SC	Supplier’s Cartridges
SFE	Surface Free Energy
SvP	Subvisible Particle
Sz	Surface Maximum Height
WFI	Water for Injection

References

[1] Sacha, G.; Rogers, J. A.; Miller, R. L. Pre-Filled Syringes: A Review of the History, Manufacturing and Challenges. Pharm. Dev. Technol. 2015, 20 (1), 1–11. https://doi.org/10.3109/10837450.2014.982825.

[2] Nuova Ompi Srl. EZ-Fill® - A Fully Ready-to-Use Solution for Your Aseptic Manufacturing - Brochure; 2020.

[3] Sacha, G. A.; Saffell-Clemmer, W.; Abram, K.; Akers, M. J. Practical Fundamentals of Glass, Rubber, and Plastic Sterile Packaging Systems. Pharm. Dev. Technol. 2010, 15 (1), 6–34. https://doi.org/10.3109/10837450903511178.

[4] Kiminami, H.; Krueger, A. B.; Abe, Y.; Yoshino, K.; Carpenter, J. F. Impact of Sterilization Method on Protein Aggregation and Particle Formation in Polymer-Based Syringes. J. Pharm. Sci. 2017, 106 (4), 1001–1007. https://doi.org/10.1016/j.xphs.2016.12.007.

[5] Mendes, G. C. C.; Brandão, T. R. S.; Silva, C. L. M. Ethylene Oxide Sterilization of Medical Devices: A Review. Am. J. Infect. Control 2007, 35 (9), 574–581. https://doi.org/10.1016/j.ajic.2006.10.014.

[6] Yu, B. L.; Han, J.; Hammond, M.; Wang, X.; Zhang, Q.; Clausen, A.; Forster, R.; Eu, M. Kinetic Modeling of the Release of Ethylene Oxide from Sterilized Plastic Containers and Its Interaction with Monoclonal Antibodies. PDA J. Pharm. Sci. Technol. 2017, 71 (1), 11–19. https://doi.org/10.5731/pdajpst.2015.005819.

[7] Chen, L.; Sloey, C.; Zhang, Z.; Bondarenko, P. V.; Kim, H.; Sekhar Kanapuram, D. R. Chemical Modifications of Therapeutic Proteins Induced by Residual Ethylene Oxide. J. Pharm. Sci. 2015, 104 (2), 731–739. https://doi.org/10.1002/jps.24257.

[8] Funatsu, K.; Kiminami, H.; Abe, Y.; Carpenter, J. F. Impact of Ethylene Oxide Sterilization of Polymer-Based Prefilled Syringes on Chemical Degradation of a Model Therapeutic Protein During Storage. J. Pharm. Sci. 2019, 108 (1), 770–774. https://doi.org/10.1016/j.xphs.2018.09.029.

[9] Advanced Optics; SCHOTT AG. Radiation Resistant Optical Glasses - Technical Information Advanced Optics https://www.schott.com/d/advanced_optics/0bdd65d7-4d93-4d35-927a-a22fc6044d8e/1.4/schott_tie-42_radiation_resistant_optical_glasses_row.pdf (accessed Mar 26, 2020).

[10] Fruit, M.; Berghmans, F.; Ulbrich, G.; Gussarov, A.; Doyle, D. Radiation Impact on the Characteristics of Optical Glasses Test Results on a Selected Set of Materials. In International Conference on Space Optics — ICSO 2000; Otrio, G., Ed.; SPIE, 2017; Vol. 10569, p 56. https://doi.org/10.1117/12.2307918.

[11] Funke, S.; Matilainen, J.; Nalenz, H.; Bechtold-Peters, K.; Mahler, H.-C.; Friess, W. Optimization of the Bake-on Siliconization of Cartridges. Part I: Optimization of the Spray-on Parameters. Eur. J. Pharm. Biopharm. 2016, 104, 200–215. https://doi.org/10.1016/j.ejpb.2016.05.007.

[12] Funke, S.; Matilainen, J.; Nalenz, H.; Bechtold-Peters, K.; Mahler, H.-C.; Vetter, F.; Müller, C.; Bracher, F.; Friess, W. Optimization of the Bake-on Siliconization of Cartridges. Part II: Investigations into Burn-in Time and Temperature. Eur. J. Pharm. Biopharm. 2016, 105, 209–222. https://doi.org/10.1016/j.ejpb.2016.05.015.

[13] Mundry, A. T. Einbrennsilikonisierung Bei Pharmazeutischen Glaspackmitteln - Analytische Studien Eines Produktionsprozesses, Humboldt-Universität zu Berlin, 1999. https://doi.org/10.18452/14348.

[14] Funke, S.; Matilainen, J.; Nalenz, H.; Bechtold-Peters, K.; Mahler, H.-C.; Friess, W. Silicone Migration From Baked-on Silicone Layers. Particle Characterization in Placebo and Protein Solutions. J. Pharm. Sci. 2016, 105 (12), 3520–3531. https://doi.org/10.1016/j.xphs.2016.08.031.

[15] Gerhardt, A.; Nguyen, B. H.; Lewus, R.; Carpenter, J. F.; Randolph, T. W. Effect of the Siliconization Method on Particle Generation in a Monoclonal Antibody Formulation in Pre-Filled Syringes. J. Pharm. Sci. 2015, 104 (5), 1601–1609. https://doi.org/10.1002/jps.24387.

[16] Jones, L. S.; Kaufmann, A.; Middaugh, C. R. Silicone Oil Induced Aggregation of Proteins. J. Pharm. Sci. 2005, 94 (4), 918–927. https://doi.org/10.1002/jps.20321.

[17] Thirumangalathu, R.; Krishnan, S.; Ricci, M. S.; Brems, D. N.; Randolph, T. W.; Carpenter, J. F. Silicone Oil- and Agitation-Induced Aggregation of a Monoclonal Antibody in Aqueous Solution. J. Pharm. Sci. 2009, 98 (9), 3167–3181. https://doi.org/10.1002/jps.21719.

[18] Basu, P.; Blake-Haskins, A. W.; O'Berry, K. B.; Randolph, T. W.; Carpenter, J. F. Albinterferon A2b Adsorption to Silicone Oil–Water Interfaces: Effects on Protein Conformation, Aggregation, and Subvisible Particle Formation. J. Pharm. Sci. 2014, 103 (2), 427–436. https://doi.org/10.1002/jps.23821.

[19] Li, J.; Pinnamaneni, S.; Quan, Y.; Jaiswal, A.; Andersson, F. I.; Zhang, X. Mechanistic Understanding of Protein-Silicone Oil Interactions. Pharm. Res. 2012, 29 (6), 1689–1697. https://doi.org/10.1007/s11095-012-0696-6.

[20] Badkar, A.; Wolf, A.; Bohack, L.; Kolhe, P. Development of Biotechnology Products in Pre-Filled Syringes: Technical Considerations and Approaches. AAPS PharmSciTech 2011, 12 (2), 564–572. https://doi.org/10.1208/s12249-011-9617-y.

[21] Warne, N. W.; Mahler, H. C. Challenges in Protein Product Development. AAPS Advances in the Pharmaceutical Sciences Series Vol. 38; Springer, Cham, 2018. https://doi.org/10.1007/978-3-319-90603-4.

[22] Rechendorff, K.; Hovgaard, M. B.; Foss, M.; Zhdanov, V. P.; Besenbacher, F. Enhancement of Protein Adsorption Induced by Surface Roughness. Langmuir 2006, 22 (26), 10885–10888. https://doi.org/10.1021/la0621923.

[23] Saller, V. Interactions of Formulation and Disposables in Biopharmaceutical Drug Product Manufacturing. Ph.D. Thesis, LMU Munich, 2015.

[24] Rabe, M.; Verdes, D.; Seeger, S. Understanding Protein Adsorption Phenomena at Solid Surfaces. Adv. Colloid Interface Sci. 2011, 162 (1–2), 87–106. https://doi.org/10.1016/j.cis.2010.12.007.

[25] Norde, W. Driving Forces for Protein Adsorption at Solid Surfaces. Macromol. Symp. 1996, 103, 5–18. https://doi.org/10.1002/masy.19961030104.

[26] Lee, H. J.; McAuley, A.; Schilke, K. F.; McGuire, J. Molecular Origins of Surfactant-Mediated Stabilization of Protein Drugs. Adv. Drug Deliv. Rev. 2011, 63 (13), 1160–1171. https://doi.org/10.1016/j.addr.2011.06.015.

[27] Dow Corning Corporation. Product Information Dow Corning ® 360 Medical Fluid; Form No. 51-0374O-01.

[28] Moll, F.; Bechtold-Peters, K.; Mellman, J.; Sigg, J.; Friess, W. Replacing the Emulsion for Bake-on Siliconization of Containers − Comparison of Emulsion Stability and Container Performance in the Context of Protein Formulations. PDA J. Pharm. Sci. Technol. 2021, pdajpst.2021.012640. https://doi.org/10.5731/pdajpst.2021.012640.

[29] Deiringer, N.; Haase, C.; Wieland, K.; Zahler, S.; Haisch, C.; Friess, W. Finding the Needle in the Haystack: High-Resolution Techniques for Characterization of Mixed Protein Particles Containing Shed Silicone Rubber Particles Generated During Pumping. J. Pharm. Sci. 2021, 110 (5), 2093–2104. https://doi.org/10.1016/j.xphs.2020.12.002.

[30] Rathore, N.; Pranay, P.; Eu, B.; Ji, W.; Walls, E. Variability in Syringe Components and Its Impact on Functionality of Delivery Systems. PDA J. Pharm. Sci. Technol. 2011, 65 (5), 468–480. https://doi.org/10.5731/pdajpst.2011.00785.

[31] Allmendinger, A.; Fischer, S.; Huwyler, J.; Mahler, H. C.; Schwarb, E.; Zarraga, I. E.; Mueller, R. Rheological Characterization and Injection Forces of Concentrated Protein Formulations: An Alternative Predictive Model for Non-Newtonian Solutions. Eur. J. Pharm. Biopharm. 2014, 87 (2), 318–328. https://doi.org/10.1016/j.ejpb.2014.01.009.

[32] Owens, D. K.; Wendt, R. C. Estimation of the Surface Free Energy of Polymers. J. Appl. Polym. Sci. 1969, 13 (8), 1741–1747. https://doi.org/10.1002/app.1969.070130815.

[33] Mathes, J. M. Protein Adsorption to Vial Surfaces – Quantification , Structural and Mechanistic Studies. Ph.D. Thesis, LMU Munich, 2010.

[34] Höger, K.; Mathes, J.; Frieß, W. IgG1 Adsorption to Siliconized Glass Vials-Influence of PH, Ionic Strength, and Nonionic Surfactants. J. Pharm. Sci. 2015, 104 (1), 34–43. https://doi.org/10.1002/jps.24239.

[35] Singh, S. K.; Afonina, N.; Awwad, M.; Bechtold-Peters, K.; Blue, J. T.; Chou, D.; Cromwell, M.; Krause, H.-J.; Mahler, H.-C.; Meyer, B. K.; Narhi, L.; Nesta, D. P.; Spitznagel, T. An Industry Perspective on the Monitoring of Subvisible Particles as a Quality Attribute for Protein Therapeutics. J. Pharm. Sci. 2010, 99 (8), 3302–3321. https://doi.org/10.1002/jps.22097.

[36] Persson, B. N. J.; Prodanov, N.; Krick, B. A.; Rodriguez, N.; Mulakaluri, N.; Sawyer, W. G.; Mangiagalli, P. Elastic Contact Mechanics: Percolation of the Contact Area and Fluid Squeeze-Out. Eur. Phys. J. E 2012, 35 (1). https://doi.org/10.1140/epje/i2012-12005-2.

[37] Gerhardt, A.; Mcgraw, N. R.; Schwartz, D. K.; Bee, J. S.; Carpenter, J. F.; Randolph, T. W. Protein Aggregation and Particle Formation in Prefilled Glass Syringes. J. Pharm. Sci. 2014, 103 (6), 1601–1612. https://doi.org/10.1002/jps.23973.

[38] Majumdar, S.; Ford, B. M.; Mar, K. D.; Sullivan, V. J.; Ulrich, R. G.; D'souza, A. J. M. Evaluation of the Effect of Syringe Surfaces on Protein Formulations. J. Pharm. Sci. 2011, 100 (7), 2563–2573. https://doi.org/10.1002/jps.22515.

[39] Yoshino, K.; Nakamura, K.; Yamashita, A.; Abe, Y.; Iwasaki, K.; Kanazawa, Y.; Funatsu, K.; Yoshimoto, T.; Suzuki, S. Functional Evaluation and Characterization of a Newly Developed Silicone Oil-Free Prefillable Syringe System. J. Pharm. Sci. 2014, 103 (5), 1520–1528. https://doi.org/10.1002/jps.23945.

[40] Burckbuchler, V.; Mekhloufi, G.; Giteau, A. P.; Grossiord, J. L.; Huille, S.; Agnely, F. Rheological and Syringeability Properties of Highly Concentrated Human Polyclonal Immunoglobulin Solutions. Eur. J. Pharm. Biopharm. 2010, 76 (3), 351–356. https://doi.org/10.1016/j.ejpb.2010.08.002.

[41] Marinova, K. G.; Christova, D.; Tcholakova, S.; Efremov, E.; Denkov, N. D. Hydrophobization of Glass Surface by Adsorption of Poly(Dimethylsiloxane). Langmuir 2005, 21 (25), 11729–11737. https://doi.org/10.1021/la051690t.

[42] Jurak, M.; Chibowski, E. Topography and Surface Free Energy of DPPC Layers Deposited on a Glass, Mica, or PMMA Support. Langmuir 2006, 22 (17), 7226–7234. https://doi.org/10.1021/la060585w.

[43] Chibowski, E.; Delgado, A. V; Rudzka, K.; Szcześ, A.; Hołysz, L. Surface Modification of Glass Plates and Silica Particles by Phospholipid Adsorption. J. Colloid Interface Sci. 2011, 353 (1), 281–289. https://doi.org/10.1016/j.jcis.2010.09.028.

[44] Razouk, R. I.; Salem, A. S. The Adsorption of Water Vapor on Glass Surfaces. J. Phys. Colloid Chem. 1948, 52 (7), 1208–1227. https://doi.org/10.1021/j150463a013.

[45] Wenzel, R. N. Resistance of Solid Surfaces to Wetting by Water. Ind. Eng. Chem. 1936, 28 (8), 988–994. https://doi.org/10.1021/ie50320a024.

[46] Tamai, Y.; Aratani, K. Experimental Study of the Relation between Contact Angle and Surface Roughness. J. Phys. Chem. 1972, 76 (22), 3267–3271. https://doi.org/10.1021/j100666a026.

[47] Nakanishi, K.; Sakiyama, T.; Imamura, K. On the Adsorption of Proteins on Solid Surfaces, a Common but Very Complicated Phenomenon. J. Biosci. Bioeng. 2001, 91 (3), 233–244. https://doi.org/10.1016/S1389-1723(01)80127-4.

[48] Brash, J. L.; Horbett, T. A. Proteins at Interfaces; UTC, 1995; Vol. 16, pp 1–23. https://doi.org/10.1021/bk-1995-0602.ch001.

[49] Bremer, M. G. E. G.; Duval, J.; Norde, W.; Lyklema, J. Electrostatic Interactions between Immunoglobulin (IgG) Molecules and a Charged Sorbent. Colloids Surfaces A Physicochem. Eng. Asp. 2004, 250 (1-3 SPEC. ISS.), 29–42. https://doi.org/10.1016/j.colsurfa.2004.05.026.

[50] Malmsten, M. Ellipsometry Studies of the Effects of Surface Hydrophobicity on Protein Adsorption. Colloids Surfaces B Biointerfaces 1995, 3 (5), 297–308. https://doi.org/10.1016/0927-7765(94)01139-V.

[51] Andrade, J. D.; Hlady, V. Protein Adsorption and Materials Biocompatibility: A Tutorial Review and Suggested Hypoteheses. Adv. Polym. Sci. 1987, 1–63. https://doi.org/10.1007/3-540-16422-7_6.

[52] Rabe, M.; Verdes, D.; Seeger, S. Understanding Protein Adsorption Phenomena at Solid Surfaces. Adv. Colloid Interface Sci. 2011, 162 (1), 87–106. https://doi.org/10.1016/j.cis.2010.12.007.

[53] Khan, T. A.; Mahler, H. C.; Kishore, R. S. K. Key Interactions of Surfactants in Therapeutic Protein Formulations: A Review. Eur. J. Pharm. Biopharm. 2015, 97, 60–67. https://doi.org/10.1016/j.ejpb.2015.09.016.

[54] Zhang, Z.; Marie Woys, A.; Hong, K.; Grapentin, C.; Khan, T. A.; Zarraga, I. E.; Wagner, N. J.; Liu, Y. Adsorption of Non-Ionic Surfactant and Monoclonal Antibody on Siliconized Surface Studied by Neutron Reflectometry. J. Colloid Interface Sci. 2020, 584, 429–438. https://doi.org/10.1016/j.jcis.2020.09.110.

[55] Gervasi, V.; Dall Agnol, R.; Cullen, S.; McCoy, T.; Vucen, S.; Crean, A. Parenteral Protein Formulations: An Overview of Approved Products within the European Union. Eur. J. Pharm. Biopharm. 2018, 131 (December 2017), 8–24. https://doi.org/10.1016/j.ejpb.2018.07.011.

[56] Lorenz, B.; Krick, B. A.; Rodriguez, N.; Sawyer, W. G.; Mangiagalli, P.; Persson, B. N. J. Static or Breakloose Friction for Lubricated Contacts: The Role of Surface Roughness and Dewetting. J. Phys. Condens. Matter 2013, 25 (44), 445013. https://doi.org/10.1088/0953-8984/25/44/445013.

[57] Gühlke, M.; Hecht, J.; Böhrer, A.; Hawe, A.; Nikels, F.; Garidel, P.; Menzen, T. Taking Subvisible Particle Quantitation to the Limit: Uncertainties and Statistical Challenges With Ophthalmic Products for Intravitreal Injection. J. Pharm. Sci. 2020, 109 (1), 505–514. https://doi.org/10.1016/j.xphs.2019.10.061.

[58] Peláez, S. S.; Mahler, H.-C.; Koulov, A.; Joerg, S.; Matter, A.; Vogt, M.; Chalus, P.; Zaeh, M.; Sediq, A. S.; Jere, D.; Mathaes, R. Characterization of Polymeric Syringes Used for Intravitreal Injection. J. Pharm. Sci. 2020, 109 (9), 2812–2818. https://doi.org/10.1016/j.xphs.2020.06.003.

[59] Chillon, A.; Pace, A.; Zuccato, D. Introducing the Alba ® Primary Packaging Platform. Part 1: Particle Release Evaluation . PDA J. Pharm. Sci. Technol. 2018, 72 (4), 382–392. https://doi.org/10.5731/pdajpst.2018.008623.

[60] Jiao, N.; Barnett, G. V.; Christian, T. R.; Narhi, L. O.; Joh, N. H.; Joubert, M. K.; Cao, S. Characterization of Subvisible Particles in Biotherapeutic Prefilled Syringes: The Role of Polysorbate and Protein on the Formation of Silicone Oil and Protein Subvisible Particles After Drop Shock. J. Pharm. Sci. 2020, 109 (1), 640–645. https://doi.org/10.1016/j.xphs.2019.10.066.

[61] Depaz, R. A.; Chevolleau, T.; Jouffray, S.; Narwal, R.; Dimitrova, M. N. Cross-Linked Silicone Coating: A Novel Prefilled Syringe Technology That Reduces Subvisible Particles and Maintains Compatibility with Biologics. J. Pharm. Sci. 2014, 103 (5), 1383–1393. https://doi.org/10.1002/jps.23947.

[62] Richard, C. A.; Wang, T.; Clark, S. L. Using First Principles to Link Silicone Oil / Formulation Interfacial Tension with Syringe Functionality in Pre-Filled Syringes Systems. J. Pharm. Sci. 2020. https://doi.org/10.1016/j.xphs.2020.06.014.

[63] Wang, T.; Richard, C. A.; Dong, X.; Shi, G. H. Impact of Surfactants on the Functionality of Prefilled Syringes. J. Pharm. Sci. 2020, 1–10. https://doi.org/10.1016/j.xphs.2020.07.033.

[64] Shi, G. H.; Gopalrathnam, G.; Shinkle, S. L.; Dong, X.; Hofer, J. D.; Jensen, E. C.; Rajagopalan, N. Impact of Drug Formulation Variables on Silicone Oil Structure and Functionality of Prefilled Syringe System. PDA J. Pharm. Sci. Technol. 2018, 72 (1), 50–61. https://doi.org/10.5731/pdajpst.2017.008169.

Chapter V Evaluation of a Novel Silicone Oil Free Primary Packaging System with PTFE-Based Barrier Stopper for Biologics

Graphical Abstract

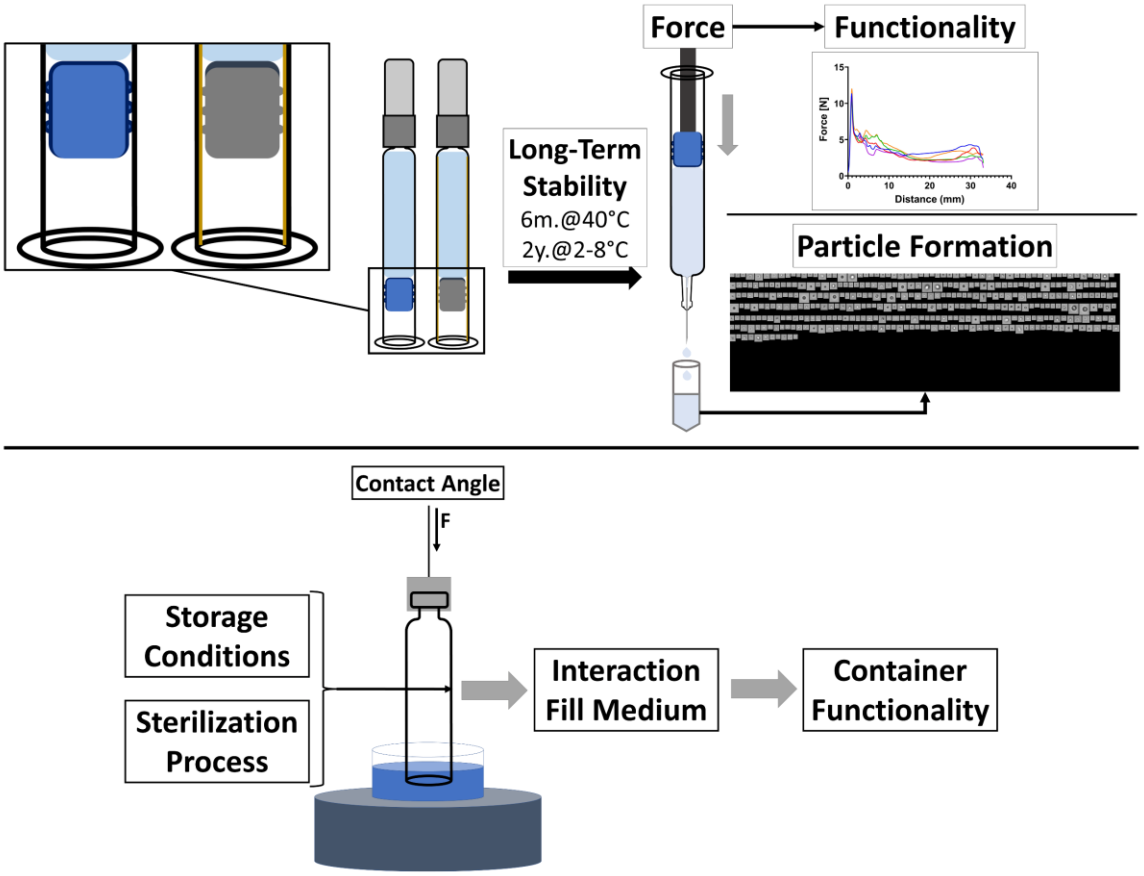

Abstract

In order to overcome silicone oil related problems for biopharmaceuticals, novel container systems are of interest with a focus on the reduction, fixation or complete avoidance of silicone oil in the primary container. Ultimately, silicone oil free (SOF) container systems made from cyclic olefin (co-)polymer or glass combined with the respective silicone-oil free plungers were developed. In the following study we evaluated the potential of a SOF container system based on a glass barrel in combination with a fluoropolymer coated syringe plunger. In a long-term stability study, the system was compared to other alternative container systems in terms of functionality and particle formation when filled with placebo buffers. The system proved to be a valuable alternative to marketed siliconized container systems with acceptable and consistent break-loose gliding forces and it was clearly superior in terms of particle formation over storage time. Additionally, we evaluated the importance of the glass barrel surface for functionality. The interaction of the fill medium with the glass surface significantly impacted friction forces. Consequently, storage conditions and production processes like washing and sterilization, which can easily alter the surface properties, should be carefully evaluated and controlled. The novel combination of non-lubricated glass barrel and fluoropolymer coated plunger provides a highly valuable SOF packaging alternative for biopharmaceuticals.

Keywords

Pre-Filled Syringe – Silicone oil free container systems – Silicone oil – Biopharmaceuticals – PTFE stopper – Container functionality – DDCP

1 Introduction

With the growing importance of biopharmaceuticals in therapy various new primary packaging challenges were identified including leachables and extractables [1,2], tungsten [3,4], needle clogging [5], and silicone oil (SO) interaction [6–8]. With respect to the siliconization of containers, the functionality of the device as well as the stability of the drug product in the primary container have to be assured [9–14]. The most common setup is a sprayed-on siliconized pre-filled glass syringe [9,13]. SO on the inner barrel acts as a lubricant to ensure an easy and consistent gliding of the plunger during administration. As the SO is not fixed entirely to the glass, it tends to migrate into solution, which can lead to a reduced or even failing functionality of the container system [15,16]. The silicone in solution forms microdroplets [17,18], which potentially interact with the API [6,19–21]. Furthermore, SO microdroplets contribute to the overall subvisible particulate burden, which is undesirable for parenterals, and specifically for intravitreal injections [22,23]. In addition, the SO between the plunger and glass barrel is known to be gradually squeezed-out of the contact area causing a steady increase of the break-loose forces over storage [24,25].

Consequently, substantial efforts were made in recent years to develop novel robust packaging materials with fixation, reduction, or even complete abandonment of SO which are less prone for drug product interactions. SO can be either baked-on or cross-linked after the siliconization process leading to packaging material with thinner and more stable SO layers, less prone for detachment [17,18,26,27]. In the following study we compare baked-on and cross-linked siliconized pre-filled glass syringes to a newly developed SOF system still based on glass. A special fluoropolymer (polytetrafluoroethylene (PTFE)) coating of the plunger allows the use of non-siliconized/lubricated barrels. Moving completely away from glass barrels, SO free (SOF) containers were introduced to the market consisting of plastic syringes based on cyclic olefin (co-)polymer (COP or COC) in combination with specially coated plungers [28,29]. However, glass is still the almost exclusive material used for pre-filled syringes both in the European and in the US market [9,30]. Compared to plastic it is more transparent, less scratch sensitive and it shows stronger gas/water vapour barrier properties which is relevant for oxygen sensitive and low volume (e.g. 0.2 mL) pharmaceuticals [31]. In addition, switching from a vial to an SOF glass based syringe in the course of product development would come without a change in the contact material giving less raise for compatibility concerns. Hence, an SOF glass

syringe without any extra barrel coating displays a highly interesting novel container concept to overcome the SO related challenges.

The purpose of this study was to evaluate the quality and performance of the newly introduced SOF glass packaging system. To this end we compared the SOF glass container in a 24-month stability study to baked-on siliconized containers with two different SO levels and two cross-linked siliconized syringes from different suppliers as currently marketed. The SOF plunger was tested in a co-marketed non-siliconized syringe as well as in a non-siliconized glass cartridge to investigate robustness. All container systems were stored at 40 °C and 2-8 °C, and subvisible particle (SvP) formation and break-loose gliding forces (BLGF) were monitored over storage time. In addition, baked-on and cross-linked silicone layers were monitored for silicone oil migration by 3D-laser scanning microscopy (3D-LSM). A previous report compared SOF glass containers in combination with PTFE coated plungers to standard sprayed-on syringes in terms of particle generation during agitation [32]. The SOF system would show significantly less particle formation. However, a long-term stability study under static storage conditions including functionality data is still lacking and it remains unclear how the container system performs compared to novel alternative packaging systems with reduced SO migration risk.

Next to stability we investigated the factors influencing the extrusion force of an SOF glass container system. Scanning electron microscopy (SEM) allowed us to understand the general setup of the new PTFE coated plunger. For siliconized containers, the friction between plunger and barrel is a function of the silicone oil amount and distribution on the barrel [33,34]. Yet, little is known about factors influencing the friction forces in SOF container systems. Our stability study revealed a decline in gliding forces (GF) for one fill medium and different extrusion force profiles dependent on the container used. We found that surface polarity of the glass and the resulting contact angles of the fill media towards the container impacted the extrusion forces of a SOF glass container system. In the following, we tested the importance of the glass surface free energy (SFE) as it is affected by treatments like steam and heat sterilization on container functionality. The SFE was determined with a Tensiometer via dynamic contact angle measurements and the SFE was monitored during a short-term stability study for empty as well as for containers filled with different fill media.

2 Materials and Methods

2.1 Materials

Chemicals

Chemicals used were L-histidine monohydrochloride, L-histidine, sucrose, polysorbate 80 (Sigma-Aldrich Chemie GmbH, Taufkirchen, Germany), ethylene glycol (Grüssing GmbH, Filsum, Germany), diiodomethane, ethanol absolute ≥ 99.5 % (VWR International GmbH, Darmstadt, Germany).

Packaging Materials

Packaging included baked-on siliconized 1mL long glass cartridges with two different SO levels (BOSC I and II) as well non-siliconized 1 mL long glass cartridges (SOFC) from the same glass cartridge batch provided by Nuova Ompi S.r.l. (Piombino Dese, Italy). This material is referred to as "standard material" throughout the publication. In a second short-term stability study two cross-linked silicone coated syringe systems (XS I and II) as well as non-siliconized 1 mL long glass syringes (SOFS) from Schott AG (Mainz, Germany) were compared.

Container System	Container Material	Container type	Inner Surface	Plunger	Storage	Group	Abbreviation
Baked-On	Glass Type I	1 mL long cartridge	Baked-On SO (2 SO Levels)	West NovaPure®	- 6m.@40 °C - 2y.@2-8 °C	Standard	BOSC
Cross-Linked		1 mL long syringe	Cross-Linked SO (2 Suppliers)		- 12w.@40 °C - 1y.@2-8 °C	Exploratory	XS
Silicone Oil Free		1 mL long cartridge	Glass Type I	GORE® IMPROJECT®	- 6m.@40 °C - 2y.@2-8 °C	Standard	SOFC
		1 mL long syringe			- 12w.@40 °C - 1y.@2-8 °C	Exploratory	SOFS

Table V-1 Overview of the packaging material included in the stability studies.

The packaging material included in the short-term stability study is referred to as "exploratory material" (Table V-1). All syringes in use came with 27G ½" staked-in needles. NovaPure® Syringe Plungers (West Pharmaceutical Services, Inc., Exton, PA, USA) were inserted in siliconized container systems after filling. The SOF container systems were closed with GORE® IMPROJECT® Plunger (W. L. Gore & Associates, Inc., Newark, DE, USA). Glass cartridges were closed with Weststar® 8 mm lined seal metal caps (West Pharmaceutical Services, Inc. Exton, PA USA). Both plunger types were

inserted with a bench top insertion jig resulting with the same headspace for all packaging material of 5.9 mm.

2.2 Stability Study

Sample Preparation

After manual filling with sterile filtrated 0.95 mL of water for injection (WFI) or 20 mM histidine-buffer (His) containing 240 mM sucrose and 0.04 % polysorbate 80 (w/v), pH 5.5, the plunger was inserted, and the samples were stored at 40 °C and 2-8 °C. Filling and plunger insertion were executed under laminar air flow. Samples included in the long-term stability study (standard material) were stored up to 6 months at 40 °C as well as 2 years at 2-8 °C. The short-term stability study (exploratory material) was completed after 12 weeks at 40 °C and 1-year at 2-8 °C, respectively. Functionality and particle formation were monitored over the storage time at different timepoints. BOSC I data for T0, 6 weeks, and 12 weeks at 40 °C were already reported previously but included here for comparison (see chapter IV).

Container Functionality

A Texture Analyzer TA.XT Plus (Stable Micro Systems Ltd., Surrey, UK) was used to determine container functionality (n = 5). Containers were expelled at 190.2 mm/min and the resulting force distance diagrams were used to determine break-loose (BLF) and gliding force (GF). The BLF was hereby defined as the maximum value between 0 and 2 mm, whereas the GF represents the average force required between 5 and 32.5 mm. For cartridges, piercing needles (Cambridge Consultant Ltd, Cambridge, UK) were connected via a male luer integral lock ring to ¼-28 UNF thread adapter (Cole Parmer GmbH, Wertheim, Germany) to BD Microlance 3 27G x 1/2 " (0.4 x 13 mm) cannulas as previously reported [35].

To investigate the impact of the surface energy on functionality, the BLGFs were determined as stated above either with empty, wet, or filled containers. In the case of wet conditions, the fill medium was manually poured out of the cartridges through the uncapped top immediately prior to the measurement. Filled containers in this case were capped and connected to NovoFine 8 - 0,30 x 8 mm (30G) pen piercing needles (Novo Nordisk A/S, Bagsværd, Denmark) attached with a holding clamp for the expelling.

Subvisible Particle Analysis (SvP-Analysis)

The subvisible particles (SvPs) in expelled samples were analyzed using a FlowCam 8100 (Fluid Imaging Technologies, Inc., Scarborough, ME, USA) and a PAMAS SVSS (Partikel- und Analysensysteme GmbH, Rutesheim, Germany) as describe before [35]. The samples were expelled at a constant extrusion speed of 190.2 mm/min into pre-cleaned Eppendorf tubes. ($n \geq 3$)

Silicone Layer Analysis (3D-Laser Scanning Microscope)

The silicone layer of the packaging material was monitored with a Keyence VK-X250 3D-Laser Scanning Microscope (Keyence International NV/SA, Mechelen, Belgium). Prior to 3D-LSM scans filled containers were emptied by removing the stopper with pincers and pouring out the content through the bottom followed by 3 times rinsing with 1 mL highly purified water (HPW) and final drying at 80 °C for at least 1h. A Nikon CF Plan 10x/0.30 OFN WD 16.5 objective was used for large area measurements from outside the barrel. The silicone layer thickness measurements as well as surface roughness measurements of the plunger surfaces were conducted with a Nikon CF Plan 100x/0.80 EWLD ∞/0 Epi OFN 25 WD 2.0 objective. Silicone layer thickness measurements were performed by scanning the inner container surface after breakage of the glass barrel based on a method developed by Funke et al. ($n = 3$) [36]. Scratches were made with Sterican® 20G x 1½" cannulas vertically to the barrel length and the surface height differences between the uncovered glass surface and the surrounding silicone surface was determined with the MultiFileAnalyzer software from Keyence (Version 1.3.1.120) using the average step height tool. For thickness measurements at least 2 images were stitched together using the VK Image Stitching software (version 2.1.1.0) provided by Keyence International NV/SA (Mechelen, Belgium).

2.3 Plunger Characterization

Scanning Electron Microscope (SEM)

Surface and coating of syringe plungers was examined with an FEI Helios G3 UC (Hillsboro, Oregon, USA) scanning electron microscope (SEM). The plungers were cut into thin pieces and sputtered with carbon. SEM micrographs of the plunger cross sections were taken at 5.0 kV and at 71x, 200x, 650x and 1000x magnifications.

2.4 Impact Glass Surface Energy

Glass Surface Treatment

After washing with HPW, SOFCs were either autoclaved, heat sterilized, or heat treated to alter the glass surface properties. Autoclavation was performed with a Varioklav 65T (H+P Labortechnik AG, Oberschleißheim, Germany) at 121 °C for 15 min, followed by drying at 80 °C for 1 h. Heat sterilization was performed at 250 °C for 1 h and 3 h in a FED 53 oven (BINDER GmbH, Tuttlingen, Germany), heat treatment at 400 °C and 600 °C for 1 h in a Carbolite ELF 11/6B oven (Carbolite GmbH, Ubstadt-Weiher, Germany). Alternatively, SOFCs were stored in HPW in a beaker at 40 °C for 4 weeks. 24 h after the glass treatment the containers were capped, filled with 0.95 mL HPW and the plungers were inserted. The functionality was evaluated after another 24 h. To investigate the persistence of changes induced by autoclavation, cartridges were wrapped in sterilization foil and stored empty at 25 °C for 6 weeks before filling and analysis.

Contact Angle and Surface Free Energy Analysis

Contact angles (CA) of HPW and diiodomethane on the inner glass surface of SOFC and SOFS containers were obtained with a Drop Shape Analyzer (DSA) (Krüss GmbH, Hamburg, Germany). 2 µl of the liquid were pipetted manually onto the inner container surface at the bottom of the container and images were taken 20 s after the deposition of the droplet. A curved baseline was set manually, and CA values were obtained in the ellipse (tangent-1) mode using the Krüss Advance software (version 1.6.2.0.). Staked-in syringe needles were removed prior to measurements with pincers to enable the light to pass the inner barrel. The CA values were used to calculate the inner surface free energies (SFE) following the method of Owens-Wendt-Raebel and Kaelble (OWRK). (n = 3)

The dynamic CA values of HPW, ethylene glycol and diodomethane, as well as different ethanol-water and ethylene glycol-water mixtures on the glass container were obtained using a K100MK2 tensiometer (Krüss GmbH, Hamburg, Germany) controlled at 25 °C. The container bottoms were cut off and the containers cleaned. Containers stored filled were emptied and dried at 80 °C prior to analysis. The wetted length was set according to the inner and outer perimeter of the glass barrel following the ISO 11040-4 standard dimensions with immersion depth between 2 and 10 mm [12]. The SFE was calculated following OWRK. The surface tension of the ethanol-water and the ethylene glycol-water mixtures was determined with a Wilhelmy Plate using the same tensiometer. (n = 3)

Statistical Evaluation

Data is presented as average values and with standard deviation ($n \geq 3$) unless otherwise described. Two-sided unpaired t-tests were conducted using the Graphpad Prism (Version 9.0.2) with a confidence level of 95 %.

3 Results

3.1 Long-Term Stability Study of Different Container Systems

3.1.1 Container Functionality of Standard Material

At first a head-to-head comparison of the baked-on siliconized cartridges with two silicone levels (BOSC I and BOSC II) and silicone oil free glass cartridges (SOFC) filled with WFI and a His-Buffer containing 0.04 % (w/v) polysorbate 80 was performed. Focus was on functionality, which may potentially be at risk especially for the new configuration, and on particle formation, which may be less critical with the new container system. The containers were stored at 40 °C and 2-8 °C for up to 6 months respectively 2 years. Both container systems, the BOSC and the SOFC, were stable with respect to functionality (Figure V-1). Overall, the functionality of the SOF system showed a higher variability compared to BOSC container systems.

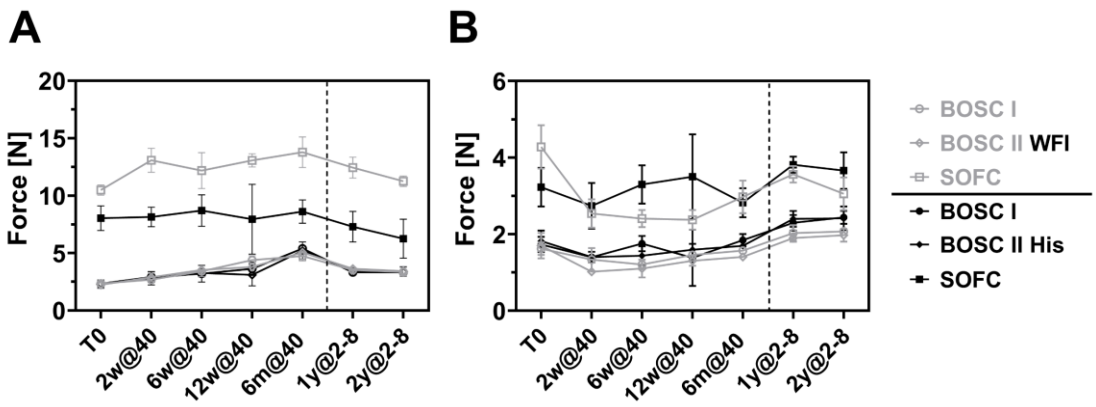

Figure V-1: Break-loose [A] and gliding forces [B] of bake-on siliconized cartridges (BOSC I/II) and SOF cartridges (SOFC) after storage at 40 °C and 2-8 °C filled with WFI or His buffer.

Only a trend towards an increase from approximately 2.3 N to 5.3 N in BLF for the BOSC cartridges could be observed upon storage at elevated temperature for both fill media. Overall, the silicone level did not influence the BLF. BLF of the SOFCs was markedly higher already at T0 with 10.5 ± 0.5 N in average and varied more over storage time with average values up to 13.8 N (6 months, 40 °C). Maximum values for individual system of 15.2 N were observed. Whereas the fill medium did not impact the BLGF of the BOSCs, the SOFCs showed significantly higher BLF values with water compared to His-Buffer.

The GF values of BOSCs were very low with 1-2 N and did not change over storage time (max. 2.4 N after 24 months at 2-8 °C). The GF with His buffer was marginally but

significantly higher than with water. The SOF cartridges showed higher but still well acceptable GF values between 2.5 N and 4 N; the GF values did not increase over storage time (maximum at T0 with WFI of 4.3 ± 0.6 N).

3.1.2 Particle Formation in Standard Material

Particle shedding from the container systems was monitored by SvP analysis of expelled samples utilizing flow imaging (FI) and light obscuration (LO) (Figure V-2). All samples showed low particle numbers independent of the fill medium which did not change upon storage. A significantly lower number of a few hundred particles > 1µm could be observed for the SOF system compared to both BOSCs with a few thousand particles > 1µm/mL.

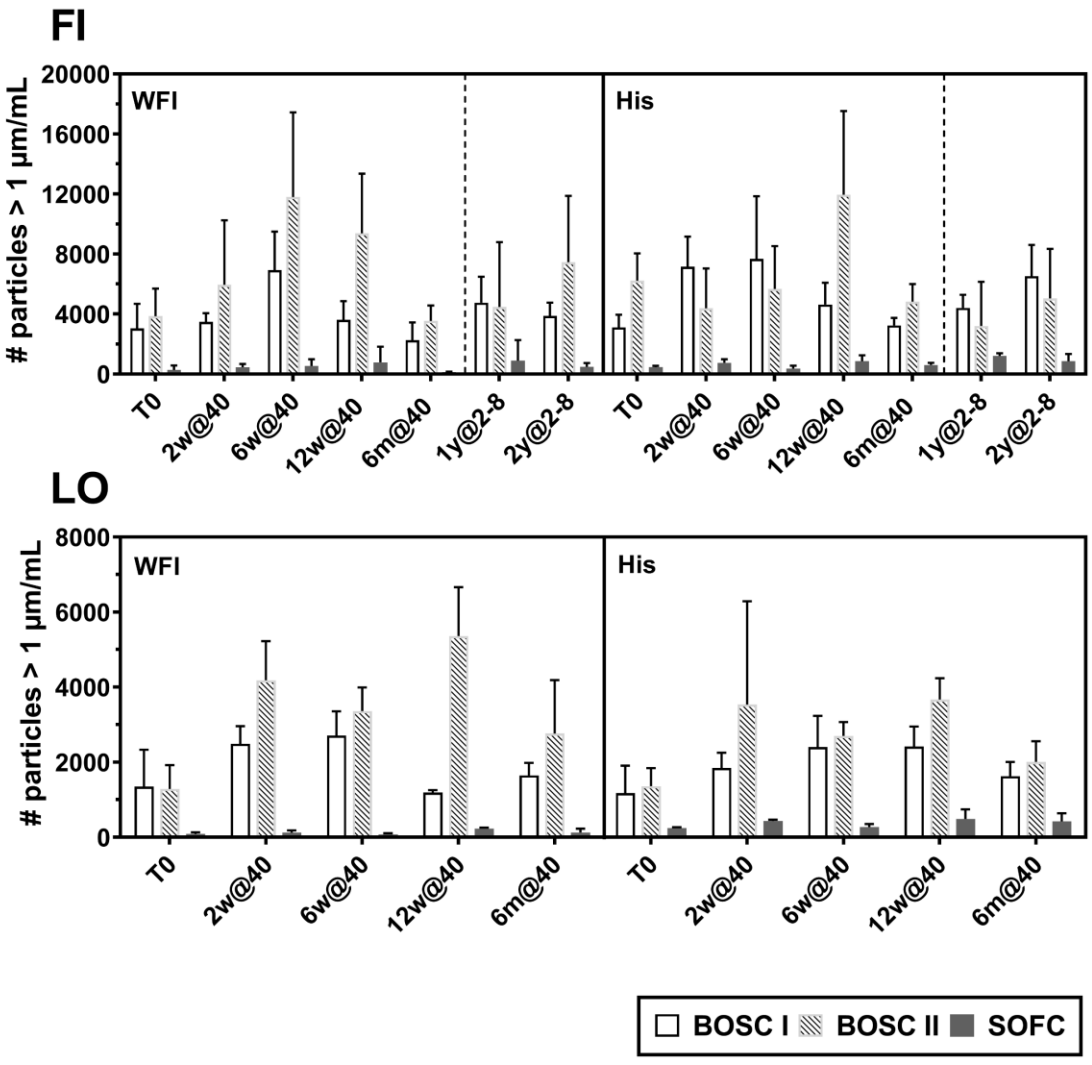

Figure V-2: Particle concentration > 1µm/mL measured with flow imaging [FI] and light obscuration [LO] of expelled bake-on siliconized cartridges (BOSC I/II) and SOF cartridges (SOFC) after storage at 40 °C and 2-8 °C filled with WFI and His buffer.

showed the same overall picture, with lower absolute particle numbers compared to flow imaging, which is in line with literature [37]. The vast majority of particles detected were smaller than 5 µm making it difficult to differentiate them based on their form or morphology. Thus, we did not observe obvious difference in particle images between samples from different container systems.

3.1.3 Functionality of Exploratory Material

An additional 1-year study was performed with cross-linked siliconized containers from two suppliers (XS I and II) to benchmark the container performance. Furthermore, a fluoropolymer coated plunger was inserted in the non-siliconized glass syringe (SOFS) to test the robustness of the packaging system.

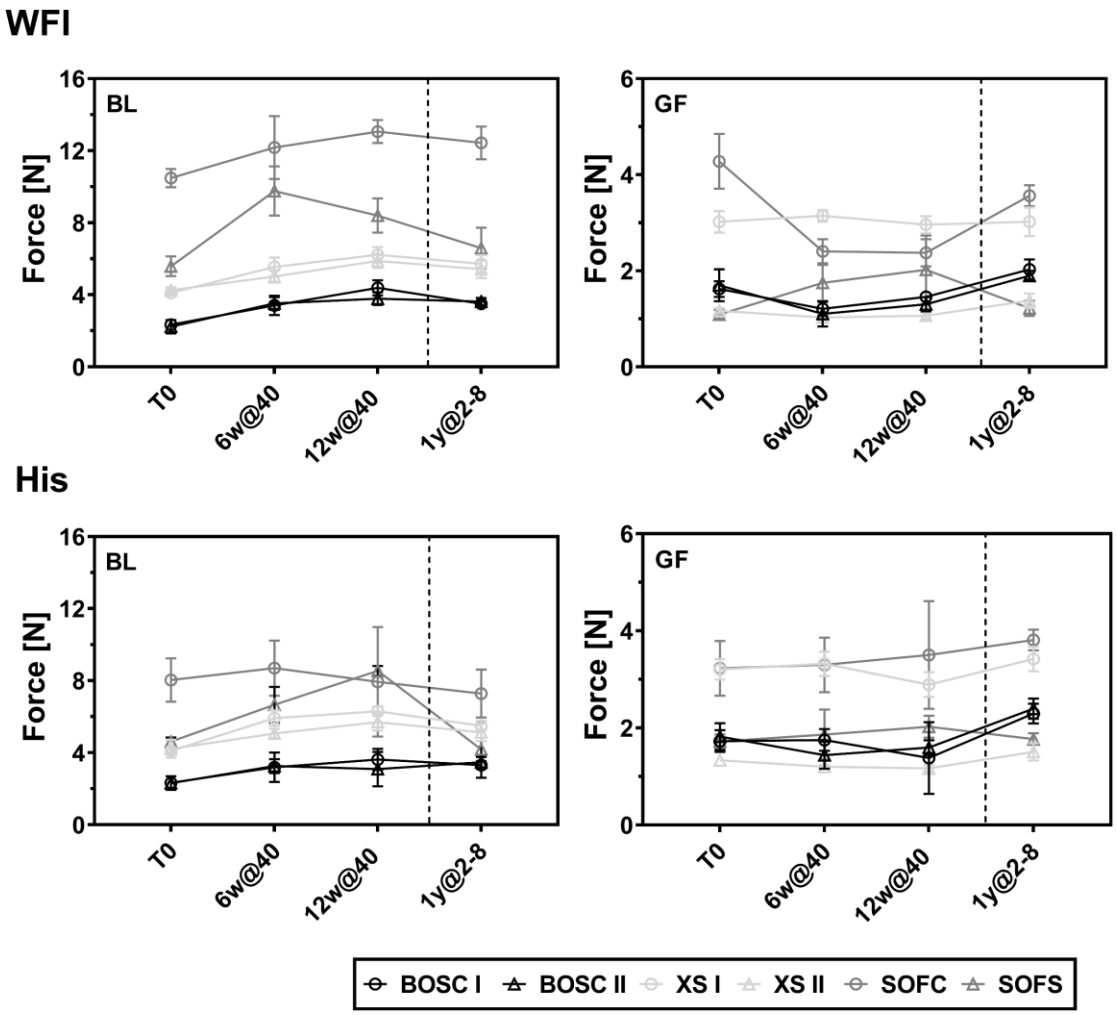

Figure V-3: Break-loose [A] and gliding forces [B] of bake-on siliconized cartridges (BOSC I/II) and SOF cartridges (SOFC) as well as cross-linked siliconized (XS I/II) and SOF syringes (SOFS) after storage at 40 °C and 2-8 °C filled with WFI or His buffer.

The container stability in terms of functionality and particle formation was monitored over a shorter time of 1-year at 2-8 °C as well as 12 weeks at 40 °C. Both cross-linked container systems showed slightly higher BLF compared to the BOSCs. A steady increase from 4 N to values of approx. 6 N was observable as well (Figure V-3). The BLF of SOF container systems ranged between 4 N and 8.5 N without a distinctive trend upon storage. Noticeably, the BLF values were higher for the SOF cartridges. Overall, the BLF values were independent of the fill medium for the exploratory material unlike the difference observable for SOFCs.

The GF of the exploratory material did not change upon storage, whereas the SOF systems slightly varied between the timepoints. Overall, the values were low with approx. 1.5 - 2 N for the siliconized materials and approx. 3- 4 N for the SOF containers.

3.1.4 Particle Formation of Exploratory Material

The expelled fill media were analyzed for SvPs (Figure 4). Overall, the particle counts were low without an impact of the fill medium, as seen in the first study. Particle numbers of XSs and BOSCs were overall similar with a few thousand > 1µm/mL. Sporadically XS II showed higher numbers e.g. 57.000 particles > 1µm/mL for a syringe filled with His buffer stored for 6 weeks. Particle numbers of the SOF container systems were significantly lower ranging from 220 to 1310 particles > 1µm/mL. LO measurements underlined the FI results.

Regardless of fill medium and storage timepoint the container systems were well within the limits of 600 particles per container for particles ≥ 25 µm and 6000 particles per container ≥ 10 µm (Ph. Eur 2.9.19) (Figure 5) for injectables. The USP <789> monograph regarding particulate matter of products for intravitreal injection is more challenging with not more than 50, 5, and 2 particles per mL of 10, 25, and 50 µm respectively [9,23]. Essentially no particles larger than 50 µm were observed. Overall, WFI showed less particles ≥10 µm and ≥ 25 µm compared to the surfactant containing His buffer. Whereas the WFI filled systems matched the criteria initially and upon storage in all containers, His buffer filled non-SOF containers slightly exceeded the numbers of particles ≥ 10µm and ≥ 25µm limits. In contrast, His buffer filled SOF container systems met the specifications even for intravitreal application at all time points.

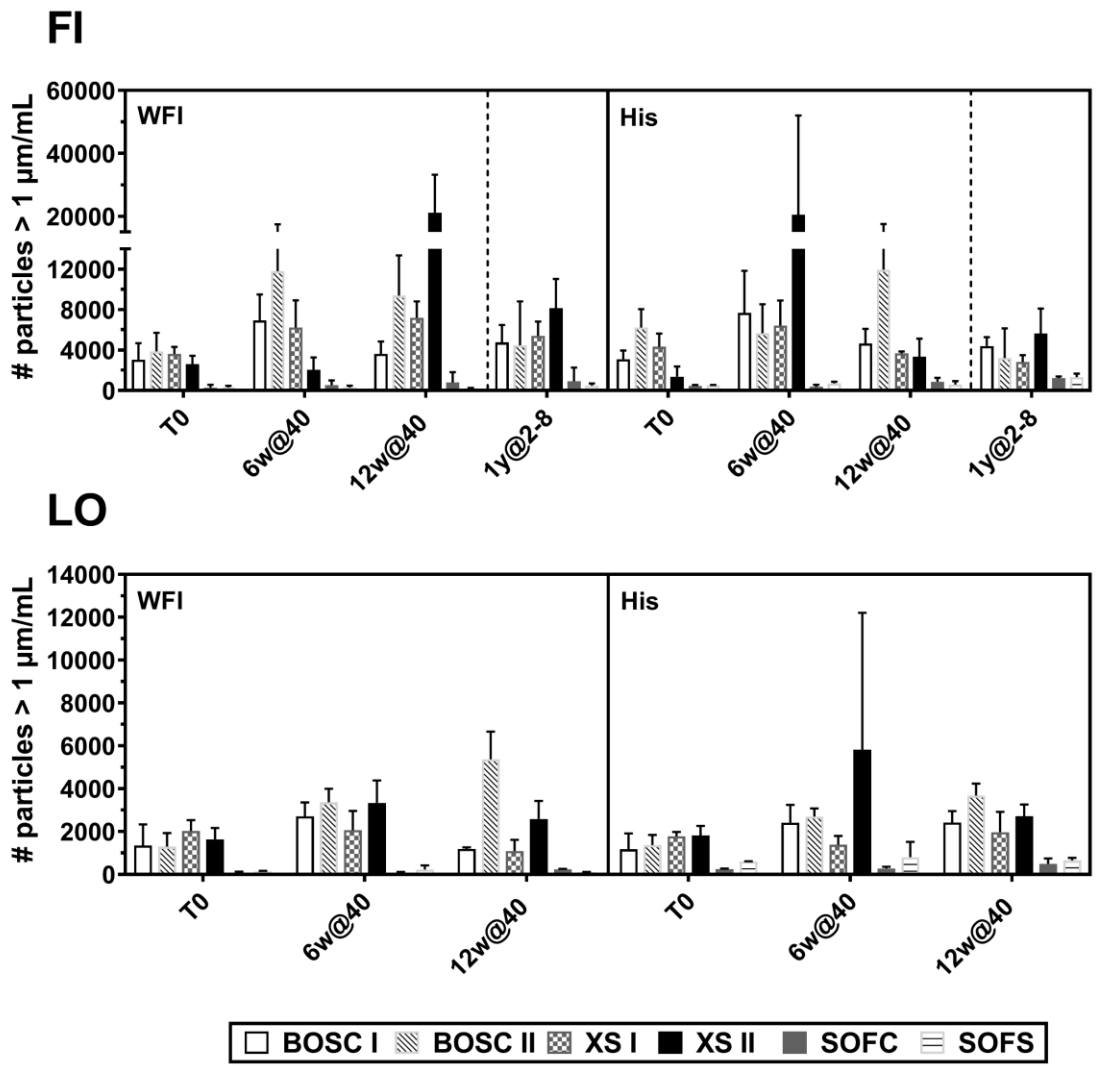

Figure V-4: Particle concentration > 1µm/mL measured with flow imaging and light obscuration of bake-on siliconized cartridges (BOSC I/II) and SOF cartridges (SOFC) as well as cross-linked siliconized (XS I/II) and SOF syringes (SOFS) after storage at 40 °C and 2-8 °C filled with WFI and His buffer.

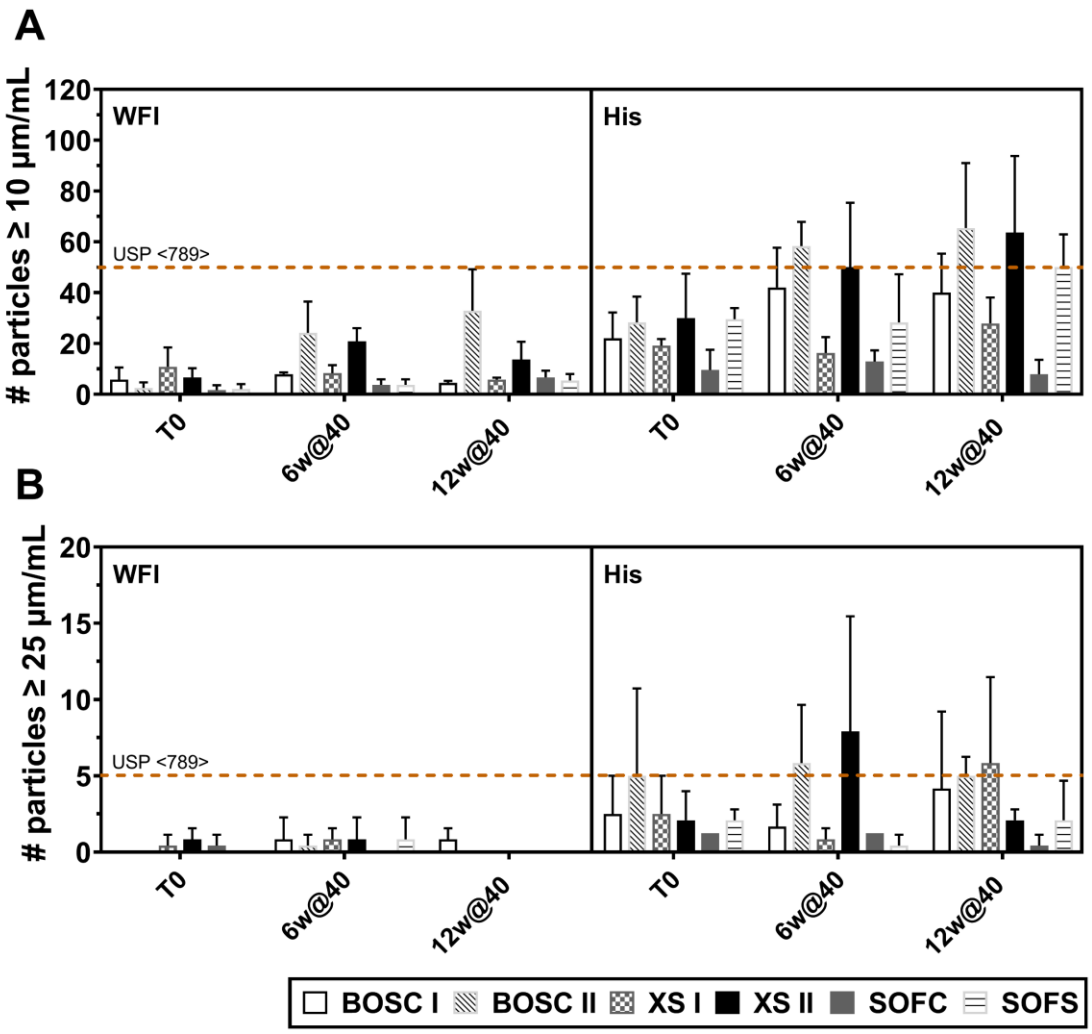

Figure V-5: SvP concentration ≥ 10 µm/mL [A] and ≥ 25 µm/mL [B] measured with light obscuration of expelled bake-on siliconized cartridges (BOSC I/II) and SOF cartridges (SOFC) as well as cross-linked siliconized (XS I/II) and SOF syringes (SOFS) after storage at 40 °C for 12 weeks filled with WFI and His buffer.

3.1.5 Silicone Surface Characterization

Thickness and morphology of the silicone oil layers were characterized before and after long-term storage. The XS I and II showed a layer thickness of 159 ± 49 nm and 291 ± 94 nm resp. and the baked-on containers of 104 ± 25 nm and 125 ± 27 nm respectively. As the baked-on siliconized containers were autoclaved prior filling, the surface was rather incoherent at start with spots of silicone oil (see chapter IV). After storage a trend for removal of the silicone oil in the middle of the container was observed for the His buffer, which was more pronounced at 40 °C compared to 2-8 °C (Figure V-6). No changes were

obvious for the WFI filled baked-on siliconized containers (Supplementary Data - Figure S V-1).

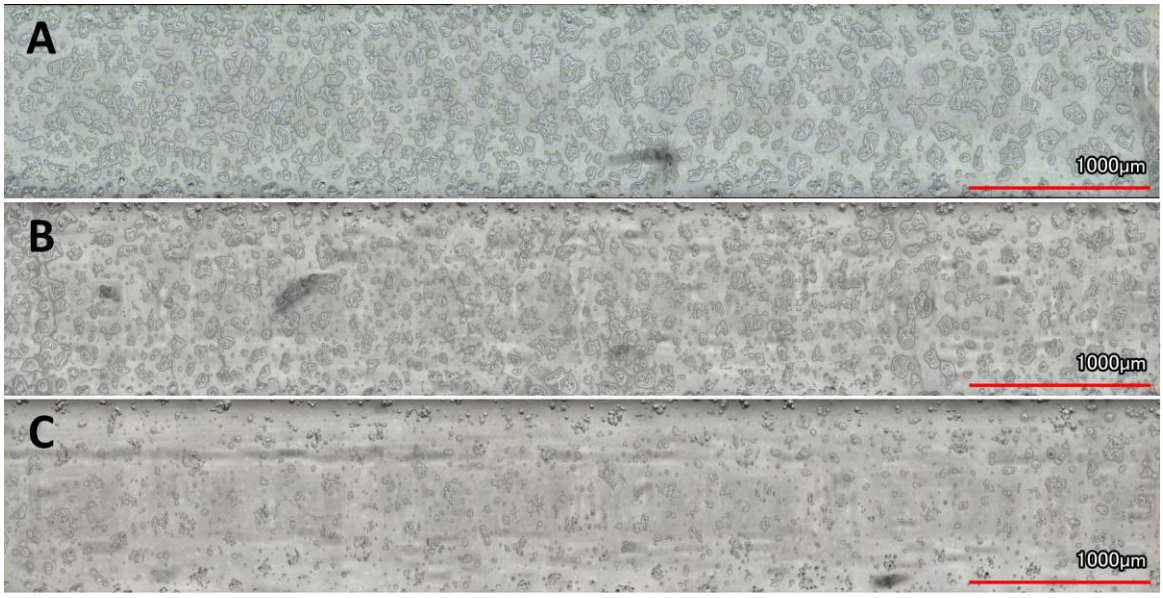

Figure V-6: 3D-LSM images of BOSC I surface before [A] and after storage at 2-8 °C [B] and 40 °C [C] for 10 months filled with His buffer.

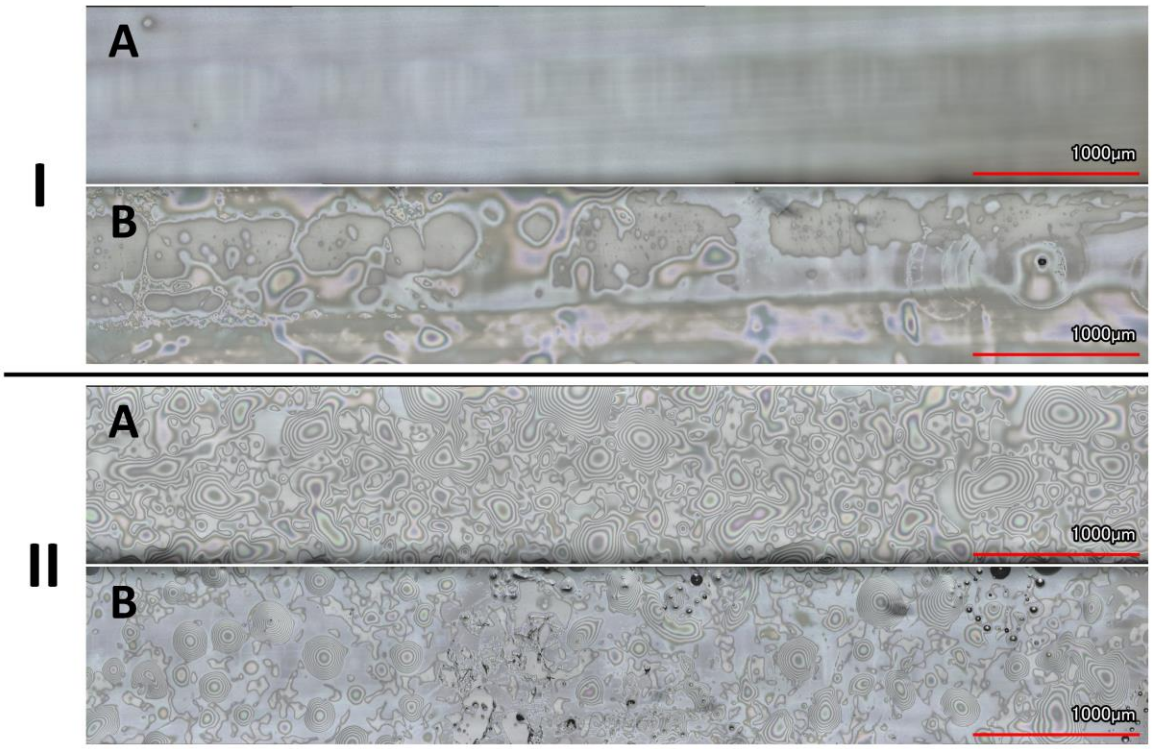

Figure V-7: 3D-LSM images of XS I and XS II surface before [A] and after storage at 2-8 °C [B] for 7 months filled with His buffer.

The XS II showed an uneven but coherent surface with a multitude of colored fringes whereas XS I had a rather smooth surface (Figure V-7). Interestingly, the morphology changed for both container systems after long-term storage at 2-8 °C. For XS II, with both fill media, parts of the top silicone layer surface were shoved to the side without being dissolved, revealing the glass surface underneath (Supplementary Data - Figure S V-2), and the silicone layer showed less irregularities and colored fringes. The silicone layer became partially removed and less coherent for the XS I filled with His Buffer, but not with WFI.

3.2 Plunger Characterization

Cross-sections of both syringe plungers were characterized with SEM to understand their setup. Both plungers show a thin film coating on top of the rubber basis (Figure V-8). The coating of the West NovaPure® plunger is thicker and only detectable at the top of the plunger, the area of contact with drug product. At the transition between top and side the coating ends with a small edge (Figure V-8 e). The GORE® IMPROJECT® plunger coating also covers the sides including the ribs (Figure V-8 b/c).

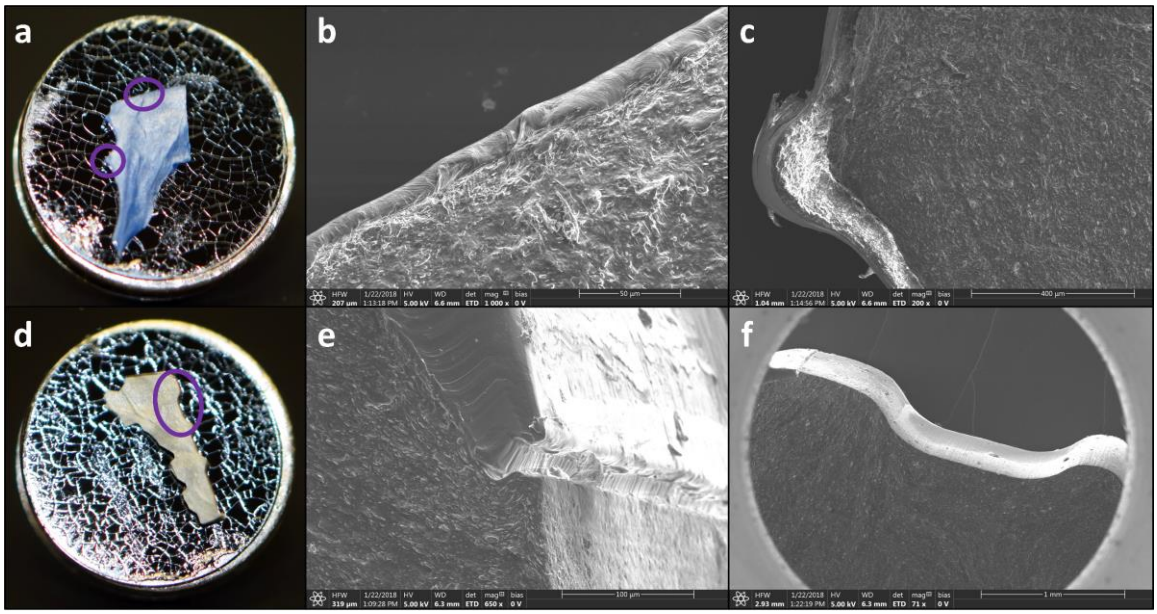

Figure V-8: Slices of the GORE® IMPROJECT® Plunger [a] and West NovaPure® plunger [d] fixed to a bracket prior to SEM measurements. SEM images of the cross-sections were taken at the top [b] and at the ribs of the Gore™ plunger [c] as well as at the side [e; f] of the West plunger as indicated by blue marks in [a] and [b].

3.3 Impact of Surface Free Energy on Functionality

The functionality of the SOF container systems, despite basically the same container setup, differed significantly with BLF of 10.5 ± 0.5 N and 5.6 ± 0.5 N and GF of 4.3 ± 0.6 N and

1.1 ± 0.1 N for SOFC and SOFS respectively (Supplementary Data - Figure S V-3) for WFI fill. The difference in BLF was consistent over storage whereas the GF of SOFC would eventually level out upon storage. The His filled containers showed less pronounced differences and both BLF and GF were eventually in the same range. To understand this difference, we further characterized the systems. Micro-computed tomography did not reveal any differences in the container dimensions including the cannula inner diameter. Furthermore, surface roughness did not differ. However, contact angle measurements on the inner barrel demonstrated a higher polar component of 23.5 mN/m and total SFE of 54.5 mN/m for the SOFS compared to 12.3 mN/m and 47.2 mN/m resp. for the SOFC (Figure V-9).

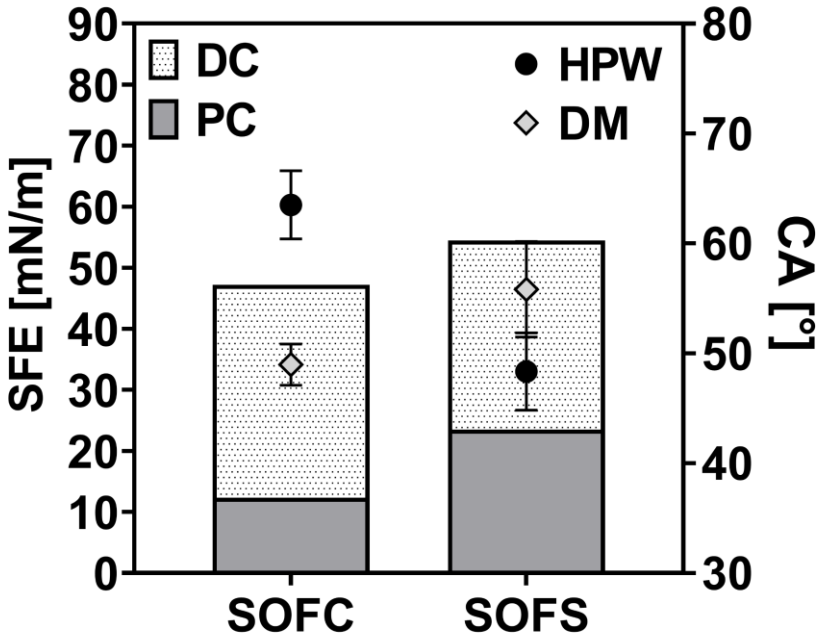

Figure V-9: Surface free energy (SFE) divided into dispersive (DC) and polar component (PC) of the inner glass container surface prior filling as well as corresponding contact angles of highly purified water (HPW) and diiodomethane (DM) determined with DSA.

Consequently, we investigated the impact of SFE on functionality further. In a first setup we altered the surface characteristics of the glass by steam sterilization, which is widely used for glass container preprocessing in parenterals fill and finish and known to alter the glass surface properties [38]. Autoclavation increased the wettability of the glass surface with water drastically and a contact angle could not be determined anymore by DSA (Figure V-10). Dynamic CA measurements showed a surface energy increase from

40.7 mN/m to 58.9 mN/m and an enhanced surface polarity from 11.5 mN/m to 26.6 mN/m (Figure V-12). Correspondingly, the gliding force of the plunger in the glass barrel was increased from 7.2 ± 1.1 N to 11.5 ± 1.4 N in autoclaved dry and unfilled container systems (Figure V-11, A).

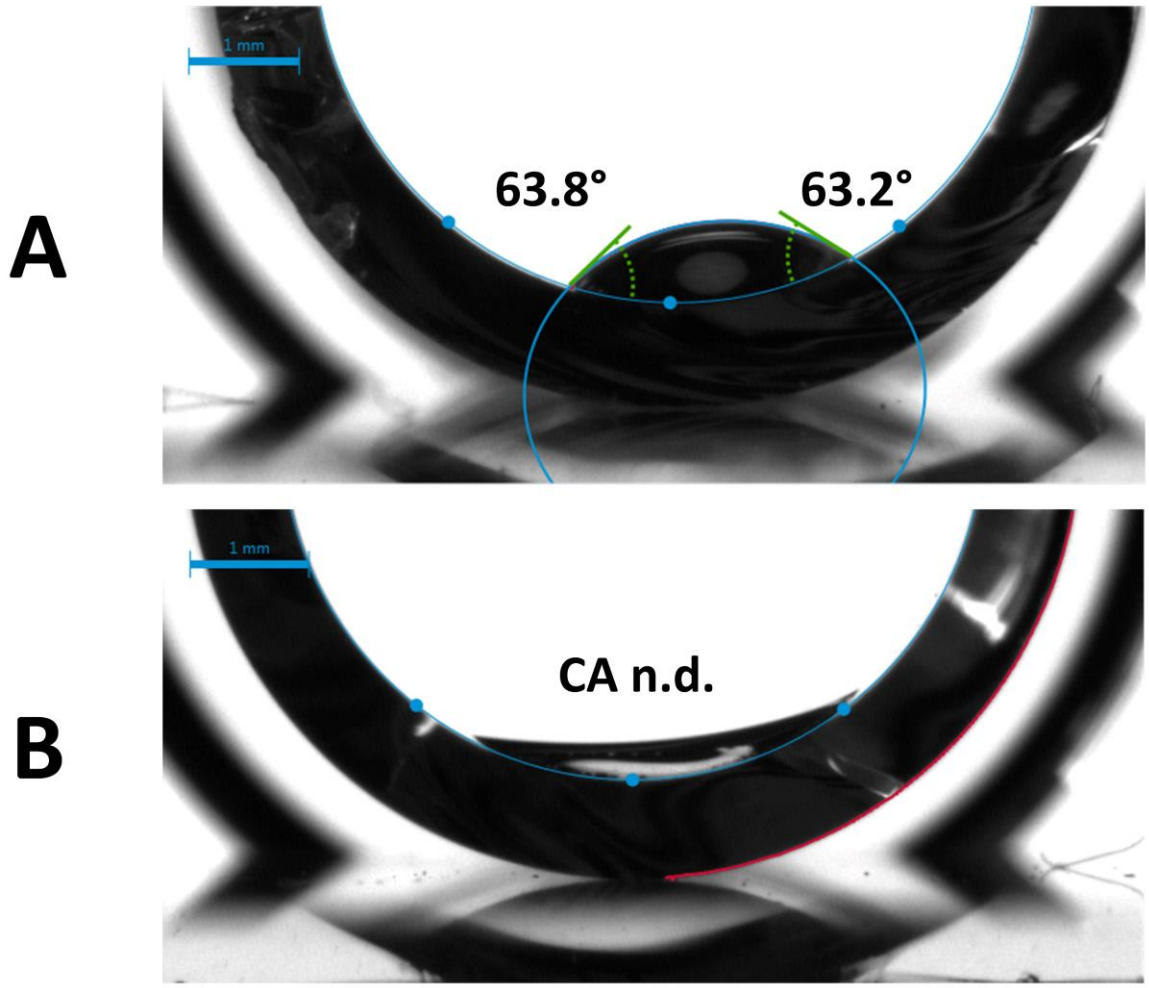

Figure V-10: Contact angles of HPW on the glass container surface before [A] and after [B] steam sterilization of the container at 121 °C for 15 min.

Also, the BLF was enhanced with 15.6 ± 1.7 N compared to 11.9 ± 0.8 N for the untreated container. However, this turned around when the container system was filled (Figure V-11, B/C); BLF and GF were drastically reduced by autoclavation. The autoclavation effect was pronounced for systems both with and without cannula.

Additionally, we heat treated the glass barrels at 250 °C for 1 h and 3 h as well as at 400 °C and 600 °C for 1 h. In contrast to autoclavation, heat sterilization at 250 °C and 400 °C caused a significant decrease of the polar component (Figure V-12). Heating the container system to 600 °C for 1 h resulted in surface characteristics similar to autoclavation. The

dispersive component was mostly unchanged and only after 3 h at 250 °C an increase to 38.0 mN/m was observed. Also, this dry heat induced changes of the surface polarity affected the functionality of the container system. A higher polar component led to a reduction of both, the BLF and GF, of the filled container. Cartridges heat-treated cartridges at 600 °C showed similar BLF values as autoclaved systems. On the contrary, glass containers treated at 250 °C and 400 °C with lower polar component showed a slight increase in BLF and GF by up to 2 N as compared to untreated containers. The polarity could be also enhanced by incubation of the glass containers in water at 40 °C for 4 weeks with the same impact on BLGFs.

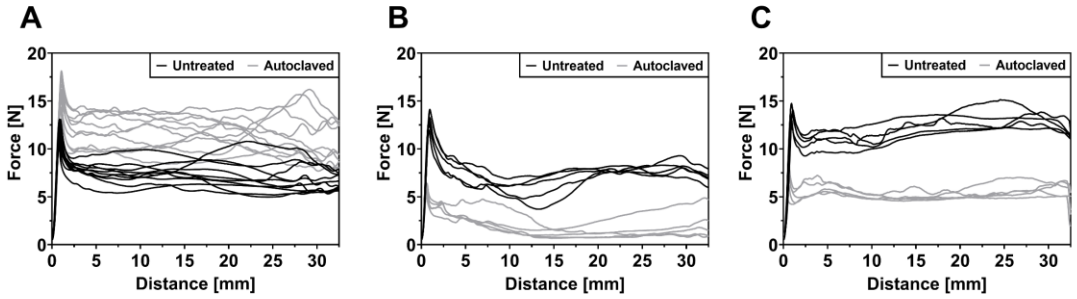

Figure V-11: Impact of autoclavation on extrusion force profiles of silicone oil free cartridges (SOFC) in the dry [A] and wet [B] state or with HPW filled containers [C].

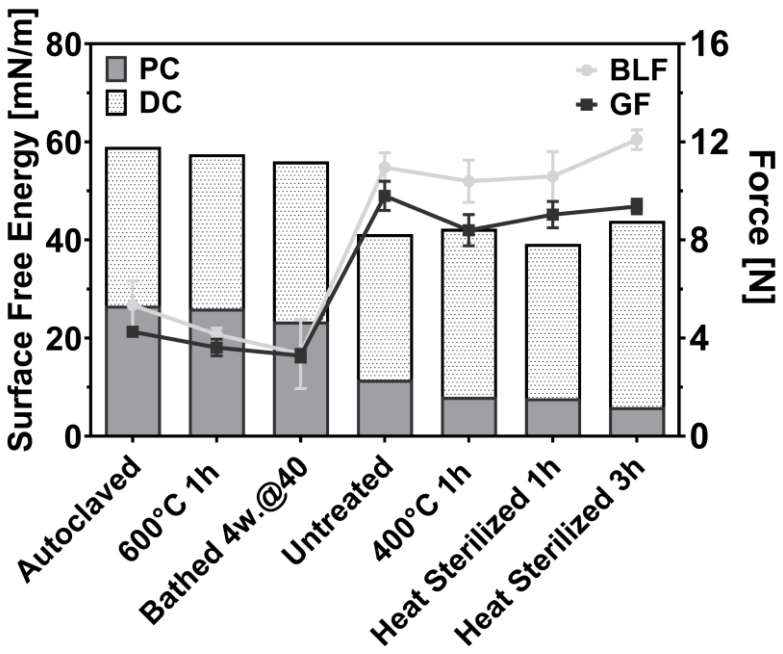

Figure V-12: Surface free energy (SFE) divided into dispersive (DC) and polar component (PC) of glass container surface after different treatments based on dynamic contact angle measurements and break-loose (BLF) and gliding forces (GF) of the HPW filled containers.

Additionally, we filled different water-ethanol and water-ethylene glycol mixtures to gradually change wettability and contact angle with the fill medium (Figure V-13). Interestingly, the contact angle correlated with both the BLF and the GF values. For pure ethanol, which showed the lowest dynamic contact angle of 0°, a BLF of 5.3 ± 1.1 N and a GF of 2.7 ± 0.5 N were determined which steadily increased with higher water fraction to 13.3 ± 0.9 N and 7.1 ± 0.4 N respectively for HPW. Also, for water - ethylene glycol mixtures the BLGF values increased with higher contact angle.

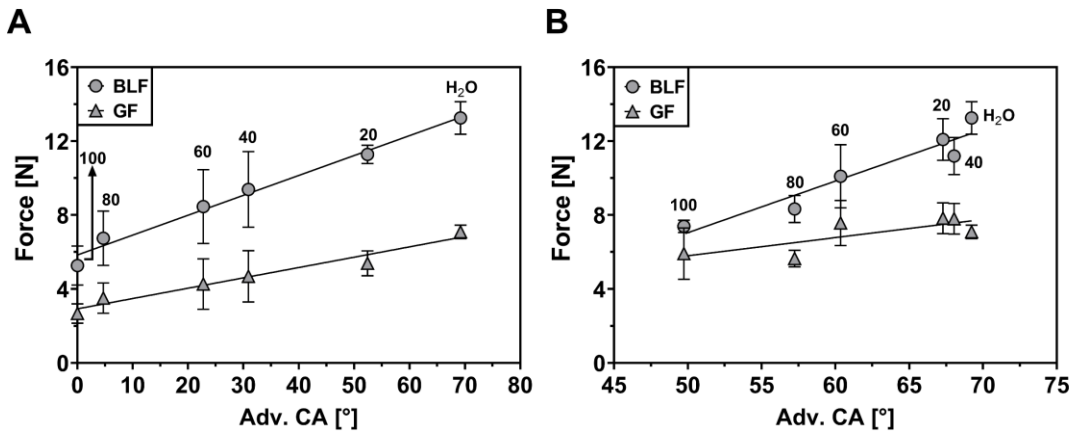

Figure V-13: Correlation between advancing contact angles and break-loose (BLF) and gliding (GF) forces of wet containers using different water-ethanol [A] and water-ethylene glycol mixtures [B]. Numbers represent the mass fraction of ethanol and ethylene glycol.

3.4 Impact of Storage on Surface Free Energy

3.4.1 Storage of Empty Containers

The change in functionality after autoclavation of the glass containers did not persist for a long time (Figure V-14) and the contact angle for HPW correspondingly increased. After 6 weeks in air the contact angle of water was back at 43.8 ± 3.2° and the BLG values at approximately 10 N. The contact angle did not differ along the barrel length indicating a homogenous surface energy in the container.

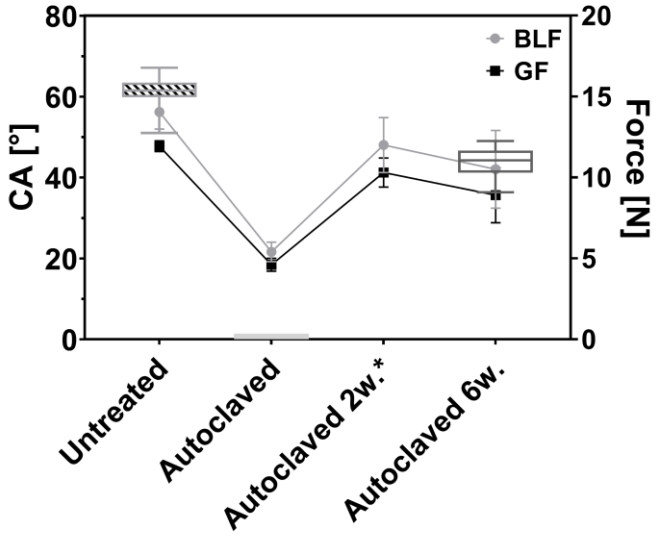

Figure V-14: Contact angles (CA) of HPW determined by DSA and break-loose (BLF) and gliding forces (GF) of HPW filled containers before and after autoclavation as well as after empty storage at 25 °C in air atmosphere. * = no CA data available

3.4.2 Storage of Filled Containers

Functionality and surface characteristics over storage were further evaluated with HPW filled containers (Figure V-15). The contact of the glass surface with water induced an increase in polarity and the container functionality changed correspondingly. As seen in the long-term stability study the GF dropped from 12.0 ± 0.7 N to 7.1 ± 1.7 N and 5.2 ± 0.5 N after storage at 40 °C for 2 and 4 weeks respectively. On the other hand, the BLF was consistent at approx. 13.5 N over the 4 weeks. A similar change of the functionality could be induced by pretreating empty containers in water at 40 °C prior to filling; however not only the GF was decreased but also the BLF.

Dynamic contact angle measurements demonstrated an increase of the polar component of the containers filled with HPW from approx. 11 mN/m to 17 mN/m after storage. For containers bathed in HPW the increase was even more pronounced with 23.4 mN/m. We specifically analyzed the cartridge area where the plunger is positioned. At this spot, the wettability significantly increased compared to samples with a plunger in position as well as the initial material.

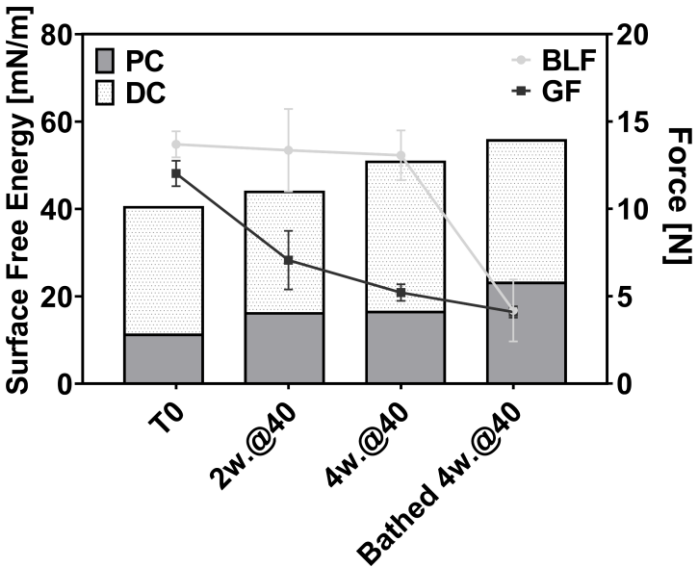

Figure V-15: Surface free energy divided in polar (PC) and dispersive component (DC) after filled storage as well as bathing based on dynamic contact angle measurements and break-loose (BLF) and gliding forces (GF) of the HPW filled containers.

4 Discussion

4.1 Long-Term Stability Study of SOF and SO Container Systems

We compared a novel SOF glass container/PTFE coated plunger system to siliconized container/FluroTec® coated plunger systems either with a baked-on or cross-linked silicone layers. The system is the first ready-to use SOF product based on a glass barrel on the market and the long-term stability of such a system regarding container functionality and particle formation was not reported so far. Advantages and disadvantages of the SOF approach became evident. After filling higher BLGF values as well as less smooth extrusion force profiles were observed. However, this was still in an acceptable range regarding typical target extrusion forces of < 25 N in the development of ready-to use combination products [9]. Apart from that, samples expelled from SOFs showed drastically lower particle numbers. SOF containers are a more static and less prone to changes over storage. We did not observe an increase in BLGF values or particle numbers even after 2 years of storage. The GF values decreased for WFI filled systems upon storage. In contrast, both baked-on and cross-linked silicone oil lubrification on the inner glass surface remains a highly viscous liquid with the ability to move. The silicone oil layer is prone to move under gravity, to migrate into solution [9,17,18] or to be squeezed-out of the area between the stopper and the glass [25]. We observed the latter, as all siliconized container systems showed a small but consistent increase of the BLF. Only for the baked-on container systems after 1- or 2-years long-term storage we noticed an increase of the GF values. Both changes were not critical for application but underline the differences between the SOF and the siliconized container systems. Given a different fill medium, longer storage times, different storage conditions or different container dimensions, those changes could be enhanced and under worst case conditions create an inappropriate container system lacking long-term stability. A fundamental difference between SOF and siliconized container systems lies in the number of subvisible particles formed in the filled medium. The SOF containers show a 10 times lower number of particles ≥ 1 µm. It should be noted that the extent of silicone detachment into solution for all packaging material was rather low so that all the container systems would meet the requirements for particulate matter of the Ph. Eur. and USP for parenterals (≥ 10µm 6000 particles per container/≥ 25 µm 600 particles per container). Considering the more challenging specifications of the USP <789> for intravitreal administration, the SOF container systems were superior. Hence, the system may overcome SO related issues for biopharmaceuticals. As the barrel is based on glass, it

constitutes an important SOF alternative for oxygen sensitive pharmaceuticals and could be beneficial compared to plastic-based SOF systems [31]. 3D-LSM images of the silicone layer revealed a change in microstructure of the silicone oil layer upon storage, indicating silicone oil detachment even at low temperatures for all SO container systems and reflecting the slight changes upon long-term stability [39,40]. In our case, the morphological change was more obvious for baked-on siliconized containers filled with His buffer containing 0.04 % polysorbate 80 as compared to WFI. This change is not reflected in SvP numbers, but the GF significantly increased. An enhanced migration into the product due to the presence of surfactant was previously reported for spray-on siliconized container systems and linked to a lower interfacial tension of the formulation [15,16,41]. To the best of our knowledge, this has not been reported for baked-on siliconized container systems so far.

The study did not only clarify the differences between a SOF and a SO containing container system but also revealed differences within the SO group. Despite the high consistency of functionality, XS II occasionally showed rather high particle counts. Microscopy suggests that the thicker silicone layer of the systems is rather uneven and that after storage, the top silicone oil layer folds aside uncovering potentially less or non-cross-linked silicone oil prone for detachment into solution. The finding underlines the differences among cross-linked siliconized container systems reported before [40]. Potentially, the overall degree of cross-linking is higher for a thinner silicone layer which could explain the higher stability of the silicone layer of XS I. In general, cross-linked SO container systems contain a rather high amount of 0.2 – 1 mg of pure silicone oil similar to the standard spray-on configuration [9,40,42–44]. In contrast, the bake-on siliconization process allows a homogenous distribution for SO amounts of less than 0.1 mg per barrel. The heat treatment increases the molecular weight distribution of the siloxane chains potentially also promoting cross-linking [18,44–46].

4.2 Plunger Characterization

The characterization of the PTFE based plunger used for SOF revealed its different conception compared to the standard ethylene tetrafluoroethylene (ETFE) FluroTec® coated plunger for siliconized containers [47,48]. Both stoppers show a fluoropolymer based coating [49,50]. The ETFE coating is only present on the top of the stopper as it serves as an inert barrier to prevent interactions with the drug product [9,51]. The coating decreases the risk of leachates which e.g. may be associated with higher protein instabilities and higher immunogenicity [2,52,53]. Since silicone oil on the inside of the barrels acts as

highly viscous lubricant reducing the friction coefficient, the plunger side wall does not require a coating [28]. In contrast, the stopper needs to glide without an extra lubricant in the SOF syringes and therefore shows a coating, which covers the sides as well and which is composed of polytetrafluoroethylene (PTFE) [49]. It not only acts as a barrier but reduces the friction between the elastomeric rubber and the glass. This allows to avoid silicone oil on the barrel without compromising functionality [54]. PTFE is a well-known for its exceptionally low friction coefficient compared to other polymers, specifically on glass surfaces [55–57]. It is considered a solid lubricant forming a rodlike structure, which allows the molecules to slip among each other forming kind of a thin, coherent transfer film [55,56]. According to Persson [58], a PTFE coating on elastic rubber material creates a stiff layer that hinders the rubber to fully adapt to the surface roughness of a rigid solid.

4.3 Impact of Surface Properties on Functionality

The stability study revealed differences in force-distance diagrams depending on the glass container. Furthermore, the GF of WFI filled SOF cartridges decreased with storage time. Changes in functionality over storage time or differences due to the glass containers were not reported before for SOF systems. Neither the roughness of the inner glass surface nor the component dimensions differed between the two SOF container systems. These would be factors known to influence extrusion forces respectively friction force in general [59,60]. Instead, we could link the phenomenon to the surface free energy and the interaction of the fill medium with the glass surface. A higher polarity of the glass surface reflected in lower contact angle with the fill medium water results in lower extrusion forces. The glasses surface characteristic may easily change with the handling steps involved in the preparation of primary packaging material like washing, depyrogenation, and sterilization. Each treatment of the glass can be considered as a potential cause for a change of the surface properties. For instance, the autoclavation process most likely increases the amount of physically bound water thereby enhancing the glass container polarity. Water molecules are well known to adsorb to silicate glass predominantly at the hydroxyl groups altering the surface wetting properties [61–64]. After autoclavation the BLGF values of SOF containers were significantly reduced when filled with water. Dry heat treatment induces different processes at the glass surface including evaporation of physisorbed water, dehydroxylation and formation of siloxane bonds, which in general increases the hydrophobicity of the glass surface [64–67]. At temperatures above 600 °C the polarity of the glass surface can increase again which could be explained by pyrolytic removal of organic residues from the surface

[39, 68]. The induced increase in hydrophobicity did not markedly impair the performance of the container but higher surface polarities led to significantly lower BLGF values. Hence, a container surface with high interaction propensities with the fill medium i.e. lower contact angle results in lower extrusion forces. This explains the lower BLGF values of SOF cartridges after filling with His buffer as compared to WFI. Potentially, the fill medium can act as liquid lubricant as the plunger moves along the glass wall reducing the glide force and potentially also the break-loose force. As compared to siliconized container systems, the fill medium, and its interaction with the SOF container material influences the friction force from the beginning. Thus, both excipients and API can impact the friction forces of SOF glass containers; an effect that also holds true for siliconized containers upon storage as excipients and API impact silicone oil detachment upon storage [16,39,41]. Further studies will have to clarify this impact, especially of surface-active molecules, like surfactants or proteins which decrease surface tension, increase wettability and interact with the primary packaging material through adsorption processes [52,69–71].

We also found the physico-chemical properties of the glass container surface changed during storage, depending on the storage environment. The increased surface polarity of samples induced by autoclavation was already declined after 2 weeks storage in air atmosphere resulting in BLGFs comparable to untreated glass containers. The increased surface hydrophobicity upon storage of empty containers is in general attributed to the contamination of the surface with organic impurities present in the surrounding air atmosphere [68,72,73]. A change was also substantiated for glass in contact with water. Untreated glass containers showed increased glass surface polarity and lower GFs after filling and storage. In line with the long-term stability data the BLF values did not change, because the plunger at its very position prevented the contact of the glass surface with water and there the surface polarity did not change. In contrast, container systems pretreated in a water bath for the same storage time showed a higher polarity also at the plunger area and corresponding lower BLF values.

5 Conclusion

SOF glass container systems are a valuable alternative packaging system for biopharmaceuticals. With the introduction of a fluoropolymer coating as a solid lubricant on the plunger stopper's sides, the friction force between stopper and barrel is strongly reduced. This allows to waive the use of silicone oil as lubricant. Although the extrusion forces at T0 are significantly higher they are still in an acceptable range. In the following, the container system showed high stability upon long-term storage of 24 months with exceptionally low particle formation. The SOF container systems are more potent than other novel siliconization approaches like bake-on and cross-linked siliconization compared to spray-on in reducing the SvP burden of the product. The system is especially interesting for products sensitive to silicone oil interactions as well as for products with strict requirements regarding the particle burden e.g for ophthalmic use. The use of a glass barrel would be beneficial to avoid protein oxidation as compared to plastic-based SOF systems.

The BLGF values of the SOF glass containers correlate with the contact angle of the fill medium which could be influenced by a change of the glass surface polarity or the fill medium itself. The surface properties of glass are easily altered by production processes like washing and steam or heat sterilization. In contact with water the surface polarity of the glass increased as well, which induced a decrease in gliding forces for WFI filled SOF containers upon storage. In consequence, the impact of storage conditions and production processes on the glass surface energy should be carefully evaluated during the development of a ready-to use combination product with an integrated SOF glass container.

Supplementary Data

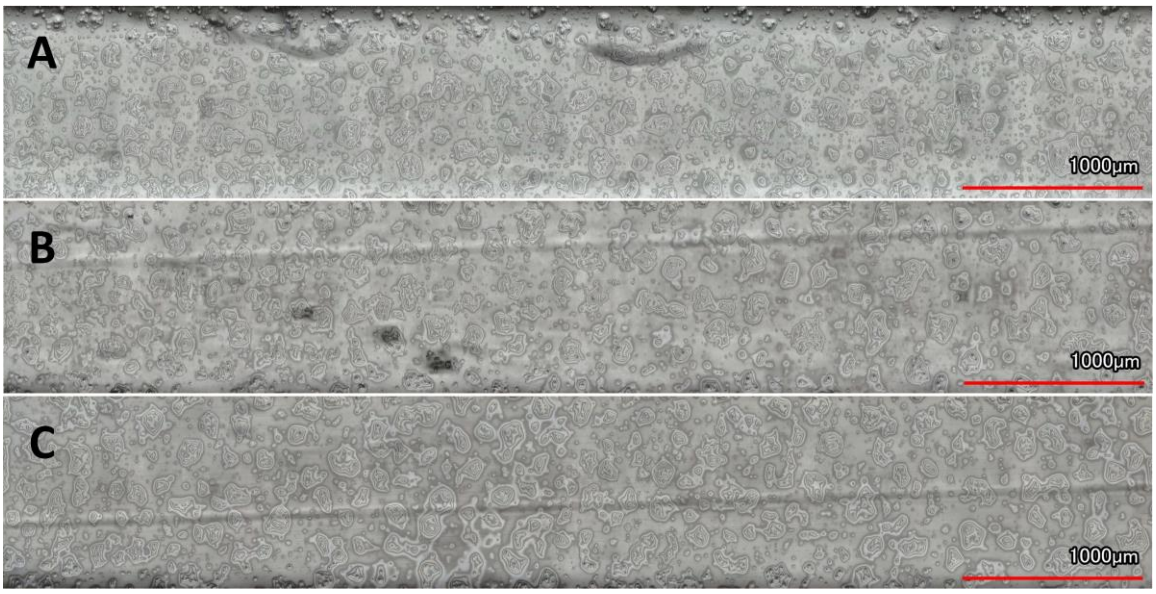

Figure S V-1: 3D-LSM images of BOSC I before [A] and after storage at 2-8 °C [B] and 40 °C [C] for 10 months filled WFI.

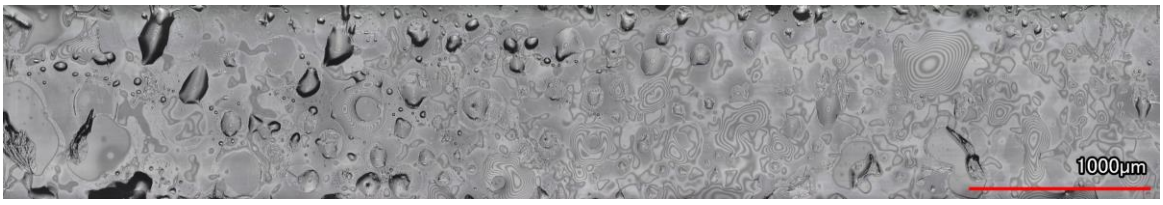

Figure S V-2: 3D-LSM images of XS I after storage at 2-8 °C for 7 months filled with WFI.

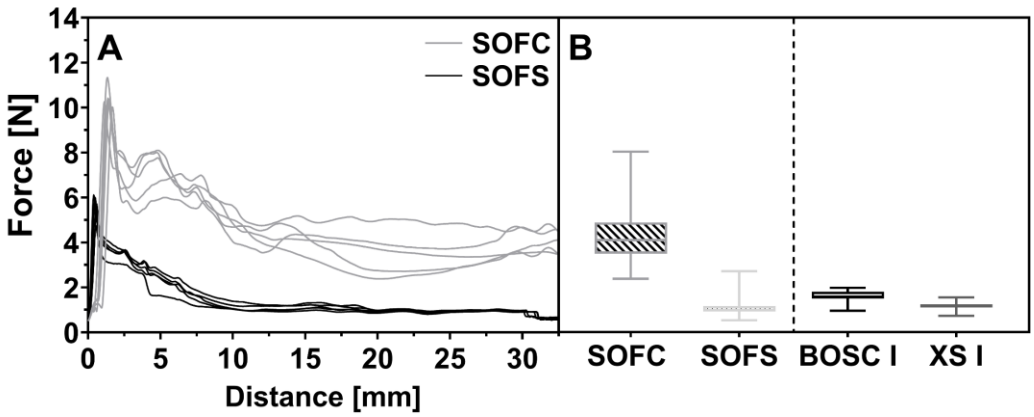

Figure S V-3: Extrusion force profiles of SOF cartridge (SOFC) and syringe (SOFS) filled with WFI at T0 of the stability study [A] as well as gliding forces displayed as boxplots including BOSC I and XS I (Min-Max) [B].

Abbreviations

3D-LSM	3D-Laser Scanning Microscope
BLF	Break-Loose Force
BLGF	Break-Loose Gliding Force
BOSC	Baked-on Siliconized Cartridge
CA	Contact Angle
COP/COC	Cyclic olefin (co-)polymer
DSA	Drop Shape Analyzer
ETFE	Ethylene Tetrafluoroethylene
FI	Flow Imaging
GF	Gliding Force
His	Histidine
HPW	Highly Purified Water
LO	Light Obscuration
PTFE	Polytetrafluoroethylene
SEM	Scanning Electron Microscope
SFE	Surface Free Energy
SO	Silicone Oil
SOF	Silicone Oil Free
SOFC	Silicone Oil Free Cartridge
SOFS	Silicone Oil Free Syringe
SvP	Subvisible Particle
WFI	Water for Injection
XS	Cross-Linked Siliconized Syringe

References

[1] Jenke, D. R. Extractables and Leachables Considerations for Prefilled Syringes. Expert Opin. Drug Deliv. 2014, 11 (10), 1591–1600. https://doi.org/10.1517/17425247.2014.928281.

[2] Bee, J. S.; Randolph, T. W.; Carpenter, J. F.; Bishop, S. M.; Dimitrova, M. N. Effects of Surfaces and Leachables on the Stability of Biopharmaceuticals. J. Pharm. Sci. 2011, 100 (10), 4158–4170. https://doi.org/10.1002/jps.22597.

[3] Liu, W.; Swift, R.; Torraca, G.; Nashed-Samuel, Y.; Wen, Z. Q.; Jiang, Y.; Vance, A.; Mire-Sluis, A.; Freund, E.; Davis, J.; Narhi, L. Root Cause Analysis of Tungsten-Induced Protein Aggregation in Pre-Filled Syringes. PDA J. Pharm. Sci. Technol. 2010, 64 (1).

[4] Seidl, A.; Hainzl, O.; Richter, M.; Fischer, R.; Böhm, S.; Deutel, B.; Hartinger, M.; Windisch, J.; Casadevall, N.; London, G. M.; Macdougall, I. Tungsten-Induced Denaturation and Aggregation of Epoetin Alfa during Primary Packaging as a Cause of Immunogenicity. Pharm. Res. 2012, 29 (6), 1454–1467. https://doi.org/10.1007/s11095-011-0621-4.

[5] De Bardi, M.; Müller, R.; Grünzweig, C.; Mannes, D.; Rigollet, M.; Bamberg, F.; Jung, T. A.; Yang, K. Clogging in Staked-in Needle Pre-Filled Syringes (SIN-PFS): Influence of Water Vapor Transmission through the Needle Shield. Eur. J. Pharm. Biopharm. 2018, 127 (February), 104–111. https://doi.org/10.1016/j.ejpb.2018.02.016.

[6] Gerhardt, A.; Mcgraw, N. R.; Schwartz, D. K.; Bee, J. S.; Carpenter, J. F.; Randolph, T. W. Protein Aggregation and Particle Formation in Prefilled Glass Syringes. J. Pharm. Sci. 2014, 103 (6), 1601–1612. https://doi.org/10.1002/jps.23973.

[7] Gerhardt, A.; McUmber, A. C.; Nguyen, B. H.; Lewus, R.; Schwartz, D. K.; Carpenter, J. F.; Randolph, T. W. Surfactant Effects on Particle Generation in Antibody Formulations in Pre-Filled Syringes. J. Pharm. Sci. 2015, 104 (12), 4056–4064. https://doi.org/10.1002/jps.24654.

[8] Basu, P.; Blake-Haskins, A. W.; O'Berry, K. B.; Randolph, T. W.; Carpenter, J. F. Albinterferon A2b Adsorption to Silicone Oil–Water Interfaces: Effects on Protein Conformation, Aggregation, and Subvisible Particle Formation. J. Pharm. Sci. 2014, 103 (2), 427–436. https://doi.org/10.1002/jps.23821.

[9] Warne, N. W.; Mahler, H. C. Challenges in Protein Product Development. AAPS Advances in the Pharmaceutical Sciences Series Vol. 38; Springer, Cham, 2018. https://doi.org/10.1007/978-3-319-90603-4.

[10] Badkar, A.; Wolf, A.; Bohack, L.; Kolhe, P. Development of Biotechnology Products in Pre-Filled Syringes: Technical Considerations and Approaches. AAPS PharmSciTech 2011, 12 (2), 564–572. https://doi.org/10.1208/s12249-011-9617-y.

[11] Adler, M. Challenges in the Development of Pre-Filled Syringes for Biologics from a Formulation Scientist's Point of View. American Pharmaceutical Review. 2012. (Accessed 26 September 2019) https://www.americanpharmaceuticalreview.com/Featured-Articles/38372-Challenges-in-the-Development-of-Pre-filled-Syringes-for-Biologics-from-a-Formulation-Scientist-s-Point-of-View/

[12] Sacha, G.; Rogers, J. A.; Miller, R. L. Pre-Filled Syringes: A Review of the History, Manufacturing and Challenges. Pharm. Dev. Technol. 2015, 20 (1), 1–11. https://doi.org/10.3109/10837450.2014.982825.

[13] Jezek, J.; Darton, N. J.; Derham, B. K.; Royle, N.; Simpson, I. Biopharmaceutical Formulations for Pre-Filled Delivery Devices. Expert Opin. Drug Deliv. 2013, 10 (6), 811–828. https://doi.org/10.1517/17425247.2013.780023.

[14] Jameel, F.; Skoug, J. W.; Nesbitt, R. R. Development of Biopharmaceutical Drug-Device Products; Jameel, F., Skoug, J. W., Nesbitt, R. R., Eds.; AAPS Advances in the Pharmaceutical Sciences Series; Springer International Publishing: Cham, 2020; Vol. 35. https://doi.org/10.1007/978-3-030-31415-6.

[15] Richard, C. A.; Wang, T.; Clark, S. L. Using First Principles to Link Silicone Oil / Formulation Interfacial Tension with Syringe Functionality in Pre-Filled Syringes Systems. J. Pharm. Sci. 2020. https://doi.org/10.1016/j.xphs.2020.06.014.

[16] Wang, T.; Richard, C. A.; Dong, X.; Shi, G. H. Impact of Surfactants on the Functionality of Prefilled Syringes. J. Pharm. Sci. 2020, 1–10. https://doi.org/10.1016/j.xphs.2020.07.033.

[17] Funke, S.; Matilainen, J.; Nalenz, H.; Bechtold-Peters, K.; Mahler, H.-C.; Friess, W. Silicone Migration From Baked-on Silicone Layers. Particle Characterization in Placebo and Protein Solutions. J. Pharm. Sci. 2016, 105 (12), 3520–3531. https://doi.org/10.1016/j.xphs.2016.08.031.

[18] Gerhardt, A.; Nguyen, B. H.; Lewus, R.; Carpenter, J. F.; Randolph, T. W. Effect of the Siliconization Method on Particle Generation in a Monoclonal Antibody Formulation in Pre-Filled Syringes. J. Pharm. Sci. 2015, 104 (5), 1601–1609. https://doi.org/10.1002/jps.24387.

[19] Majumdar, S.; Ford, B. M.; Mar, K. D.; Sullivan, V. J.; Ulrich, R. G.; D'souza, A. J. M. Evaluation of the Effect of Syringe Surfaces on Protein Formulations. J. Pharm. Sci. 2011, 100 (7), 2563–2573. https://doi.org/10.1002/jps.22515.

[20] Gerhardt, A.; Bonam, K.; Bee, J. S.; Carpenter, J. F.; Randolph, T. W. Ionic Strength Affects Tertiary Structure and Aggregation Propensity of a Monoclonal Antibody Adsorbed to Silicone Oil-Water Interfaces. J Pharm Sci 2013, 102, 429–440. https://doi.org/10.1002/jps.23408.

[21] Jones, L. S.; Kaufmann, A.; Middaugh, C. R. Silicone Oil Induced Aggregation of Proteins. J. Pharm. Sci. 2005, 94 (4), 918–927. https://doi.org/10.1002/jps.20321.

[22] Peláez, S. S.; Mahler, H.-C.; Koulov, A.; Joerg, S.; Matter, A.; Vogt, M.; Chalus, P.; Zaeh, M.; Sediq, A. S.; Jere, D.; Mathaes, R. Characterization of Polymeric Syringes Used for Intravitreal Injection. J. Pharm. Sci. 2020, 109 (9), 2812–2818. https://doi.org/10.1016/j.xphs.2020.06.003.

[23] Gühlke, M.; Hecht, J.; Böhrer, A.; Hawe, A.; Nikels, F.; Garidel, P.; Menzen, T. Taking Subvisible Particle Quantitation to the Limit: Uncertainties and Statistical Challenges With Ophthalmic Products for Intravitreal Injection. J. Pharm. Sci. 2020, 109 (1), 505–514. https://doi.org/10.1016/j.xphs.2019.10.061.

[24] Persson, B. N. J.; Prodanov, N.; Krick, B. A.; Rodriguez, N.; Mulakaluri, N.; Sawyer, W. G.; Mangiagalli, P. Elastic Contact Mechanics: Percolation of the Contact Area and Fluid Squeeze-Out. Eur. Phys. J. E 2012, 35 (1). https://doi.org/10.1140/epje/i2012-12005-2.

[25] Lorenz, B.; Krick, B. A.; Rodriguez, N.; Sawyer, W. G.; Mangiagalli, P.; Persson, B. N. J. Static or Breakloose Friction for Lubricated Contacts: The Role of Surface Roughness and Dewetting. J. Phys. Condens. Matter 2013, 25 (44), 445013. https://doi.org/10.1088/0953-8984/25/44/445013.

[26] Depaz, R. A.; Chevolleau, T.; Jouffray, S.; Narwal, R.; Dimitrova, M. N. Cross-Linked Silicone Coating: A Novel Prefilled Syringe Technology That Reduces Subvisible Particles and Maintains Compatibility with Biologics. J. Pharm. Sci. 2014, 103 (5), 1383–1393. https://doi.org/10.1002/jps.23947.

[27] Chillon, A.; Pace, A.; Zuccato, D. Introducing the Alba ® Primary Packaging Platform. Part 1: Particle Release Evaluation . PDA J. Pharm. Sci. Technol. 2018, 72 (4), 382–392. https://doi.org/10.5731/pdajpst.2018.008623.

[28] Yoshino, K.; Nakamura, K.; Yamashita, A.; Abe, Y.; Iwasaki, K.; Kanazawa, Y.; Funatsu, K.; Yoshimoto, T.; Suzuki, S. Functional Evaluation and Characterization of a Newly Developed Silicone Oil-Free Prefillable Syringe System. J. Pharm. Sci. 2014, 103 (5), 1520–1528. https://doi.org/10.1002/jps.23945.

[29] Waxman, L.; Vilivalam, V. D. A Comparison of Protein Stability in Prefillable Syringes Made of Glass and Plastic. PDA J. Pharm. Sci. Technol. 2017, 71 (6), 462–477. https://doi.org/10.5731/pdajpst.2016.007146.

[30] Nakamura, K.; Abe, Y.; Kiminami, H.; Yamashita, A.; Iwasaki, K.; Suzuki, S.; Yoshino, K.; Dierick, W.; Constable, K. A Strategy for the Prevention of Protein Oxidation by Drug Product in Polymer-Based Syringes. PDA J. Pharm. Sci. Technol. 2015, 69 (1), 88–95. https://doi.org/10.5731/pdajpst.2015.01009.

[31] Werner, B. P.; Schöneich, C.; Winter, G. Silicone Oil-Free Polymer Syringes for the Storage of Therapeutic Proteins. J. Pharm. Sci. 2019, 108 (3), 1148–1160. https://doi.org/10.1016/j.xphs.2018.10.049.

[32] Teska, B. M.; Brake, J. M.; Tronto, G. S.; Carpenter, J. F. Aggregation and Particle Formation of Therapeutic Proteins in Contact With a Novel Fluoropolymer Surface Versus Siliconized Surfaces: Effects of Agitation in Vials and in Prefilled Syringes. J. Pharm. Sci. 2016, 105 (7), 2053–2065. https://doi.org/10.1016/j.xphs.2016.04.015.

[33] Funke, S.; Matilainen, J.; Nalenz, H.; Bechtold-Peters, K.; Mahler, H.-C.; Friess, W. Optimization of the Bake-on Siliconization of Cartridges. Part I: Optimization of the Spray-on Parameters. Eur. J. Pharm. Biopharm. 2016, 104, 200–215. https://doi.org/10.1016/j.ejpb.2016.05.007.

[34] Chan, E.; Hubbard, A.; Sane, S.; Maa, Y. F. Syringe Siliconization Process Investigation and Optimization. PDA J. Pharm. Sci. Technol. 2012, 66 (2), 136–150. https://doi.org/10.5731/pdajpst.2012.00856.

[35] Moll, F.; Bechtold-Peters, K.; Mellman, J.; Sigg, J.; Friess, W. Replacing the Emulsion for Bake-on Siliconization of Containers − Comparison of Emulsion Stability and Container Performance in the Context of Protein Formulations. PDA J. Pharm. Sci. Technol. 2021, pdajpst.2021.012640. https://doi.org/10.5731/pdajpst.2021.012640.

[36] Funke, S.; Matilainen, J.; Nalenz, H.; Bechtold-Peters, K.; Mahler, H.-C.; Friess, W. Analysis of Thin Baked-on Silicone Layers by FTIR and 3D-Laser Scanning Microscopy. Eur. J. Pharm. Biopharm. 2015, 96, 304–313. https://doi.org/10.1016/j.ejpb.2015.08.009.

[37] Ripple, D. C.; Hu, Z. Correcting the Relative Bias of Light Obscuration and Flow Imaging Particle Counters. Pharm. Res. 2016, 33 (3), 653–672. https://doi.org/10.1007/s11095-015-1817-9.

[38] Mathes, J. M. Protein Adsorption to Vial Surfaces – Quantification , Structural and Mechanistic Studies. Ph.D. Thesis, LMU Munich, 2010.

[39] Shi, G. H.; Gopalrathnam, G.; Shinkle, S. L.; Dong, X.; Hofer, J. D.; Jensen, E. C.; Rajagopalan, N. Impact of Drug Formulation Variables on Silicone Oil Structure and Functionality of Prefilled Syringe System. PDA J. Pharm. Sci. Technol. 2018, 72 (1), 50–61. https://doi.org/10.5731/pdajpst.2017.008169.

[40] Thakare, V.; Schmidt, T.; Rupprechter, O.; Leibold, J.; Stemmer, S.; Mischo, A.; Bhattacharjee, D.; Prazeller, P. Can Cross-Linked Siliconized PFS Come to the Rescue of the Biologics Drug Product? J. Pharm. Sci. 2020, 109 (11), 3340–3351. https://doi.org/10.1016/j.xphs.2020.08.018.

[41] Jiao, N.; Barnett, G. V.; Christian, T. R.; Narhi, L. O.; Joh, N. H.; Joubert, M. K.; Cao, S. Characterization of Subvisible Particles in Biotherapeutic Prefilled Syringes: The Role of Polysorbate and Protein on the Formation of Silicone Oil and Protein Subvisible Particles After Drop Shock. J. Pharm. Sci. 2020, 109 (1), 640–645. https://doi.org/10.1016/j.xphs.2019.10.066.

[42] Group, S. Patent OMPI Cross-Linked Syringes. 2016, 1 (19).

[43] Becton Dickinson France, L. P. de C. (F.; Becton Dickinson France, L. P. de C. (F.). Patent XSi. 2018, 2.

[44] Funke, S.; Matilainen, J.; Nalenz, H.; Bechtold-Peters, K.; Mahler, H.-C.; Vetter, F.; Müller, C.; Bracher, F.; Friess, W. Optimization of the Bake-on Siliconization of Cartridges. Part II: Investigations into Burn-in Time and Temperature. Eur. J. Pharm. Biopharm. 2016, 105, 209–222. https://doi.org/10.1016/j.ejpb.2016.05.015.

[45] Mundry, A. T. Einbrennsilikonisierung Bei Pharmazeutischen Glaspackmitteln - Analytische Studien Eines Produktionsprozesses, Humboldt-Universität zu Berlin, 1999. https://doi.org/10.18452/14348.

[46] Camino, G.; Lomakin, S. .; Lazzari, M. Polydimethylsiloxane Thermal Degradation Part 1. Kinetic Aspects. Polymer (Guildf). 2001, 42 (6), 2395–2402. https://doi.org/10.1016/S0032-3861(00)00652-2.

[47] Sacha, G. A.; Saffell-Clemmer, W.; Abram, K.; Akers, M. J. Practical Fundamentals of Glass, Rubber, and Plastic Sterile Packaging Systems. Pharm. Dev. Technol. 2010, 15 (1), 6–34. https://doi.org/10.3109/10837450903511178.

[48] Services, A.; Health, A.; Technology, C.; Products, C.; Health, C.; Integrity, C. C.; Improvement, C. What ' s the difference between a Teflon film-coated and a FluroTec film-coated stopper ? https://www.westpharma.com/en/blog/2014/January/Whats-the-difference-between-a-Teflon-film-coated-and-a-FluroTec-film-coated-stopper.

[49] Silicone-Free Plungers To Enable Delivery of Complex, Sensitive Biologics. W. L. Gore & Associates, Inc. 2019.

[50] Cote, S.; Brockett, R. Responding to Market Trends in Prefilled Delivery - A Review of Component Assessment and Selection. West Pharmaceutical Services, Inc.

[51] Wang, M.; Li, Y.; Srinivasan, P.; Hu, Z.; Wang, R.; Saragih, A.; Repka, M. A.; Murthy, S. N. Interactions Between Biological Products and Product Packaging and Potential Approaches to Overcome Them. AAPS PharmSciTech 2018, 19 (8), 3681–3686. https://doi.org/10.1208/s12249-018-1184-z.

[52] Boven, K.; Stryker, S.; Knight, J.; Thomas, A.; Van Regenmortel, M.; Kemeny, D. M.; Power, D.; Rossert, J.; Casadevall, N. The Increased Incidence of Pure Red Cell Aplasia with an Eprex Formulation in Uncoated Rubber Stopper Syringes. Kidney Int. 2005, 67 (6), 2346–2353. https://doi.org/10.1111/j.1523-1755.2005.00340.x.

[53] Sharma, B. Immunogenicity of Therapeutic Proteins. Part 2: Impact of Container Closures. Biotechnol. Adv. 2007, 25 (3), 318–324. https://doi.org/10.1016/j.biotechadv.2007.01.006.

[54] Ashmead, E.; Gunzel, E.; Moritz, M. Syringe Stopper Coated with Expanded PTFE. WO 2011/059823, 2012.

[55] Bhushan, B. Introduction to Tribology; John Wiley & Sons, Ltd: The Atrium, Southern Gate, Chichester, West Sussex, PO19 8SQ, UK, 2013. https://doi.org/10.1002/9781118403259.

[56] Biswas, S. K.; Vijayan, K. Friction and Wear of PTFE - a Review. Wear 1992, 158 (1–2), 193–211. https://doi.org/10.1016/0043-1648(92)90039-B.

[57] Busch, C. Solid Lubrication. In Lubricants and Lubrication; Dresel, W., Mang, T., Eds.; Wiley-VCH Verlag GmbH & Co. KGaA: Weinheim, Germany, 2017; Vol. 95, pp 843–880. https://doi.org/10.1002/9783527645565.ch17.

[58] Persson, B. N. J. Contact Mechanics for Layered Materials with RandomLy Rough Surfaces. J. Phys. Condens. Matter 2012, 24 (9). https://doi.org/10.1088/0953-8984/24/9/095008.

[59] Persson, B. N. J. Sliding Friction (Review). Surf. Sci. Rep. 1999, 33 (3), 85–119.

[60] Rathore, N.; Pranay, P.; Eu, B.; Ji, W.; Walls, E. Variability in Syringe Components and Its Impact on Functionality of Delivery Systems. PDA J. Pharm. Sci. Technol. 2011, 65 (5), 468–480. https://doi.org/10.5731/pdajpst.2011.00785.

[61] Lin, Y. T.; Smith, N. J.; Banerjee, J.; Agnello, G.; Manley, R. G.; Walczak, W. J.; Kim, S. H. Water Adsorption on Silica and Calcium-Boroaluminosilicate Glass Surfaces—Thickness and Hydrogen Bonding of Water Layer. J. Am. Ceram. Soc. 2021, 104 (3), 1568–1580. https://doi.org/10.1111/jace.17540.

[62] Engländer, T.; Wiegel, D.; Naji, L.; Arnold, K. Dehydration of Glass Surfaces Studied by Contact Angle Measurements. J. Colloid Interface Sci. 1996, 179 (2), 635–636. https://doi.org/10.1006/jcis.1996.0260.

[63] Bernett, M. K.; Zisman, W. A. Effect of Adsorbed Water on Wetting Properties of Borosilicate Glass, Quartz, and Sapphire. J. Colloid Interface Sci. 1969, 29 (3), 413–423. https://doi.org/10.1016/0021-9797(69)90120-9.

[64] Lamb, R. N.; Furlong, D. N. Controlled Wettability of Quartz Surfaces. J. Chem. Soc. Faraday Trans. 1 Phys. Chem. Condens. Phases 1982, 78 (1), 61–73. https://doi.org/10.1039/F19827800061.

[65] Zhuravlev, L. T. Concentration of Hydroxyl Groups on the Surface of Amorphous Silicas. Langmuir 1987, 3 (3), 316–318. https://doi.org/10.1021/la00075a004.

[66] Zhuravlev, L. T. The Surface Chemistry of Amorphous Silica. Zhuravlev Model. Colloids Surfaces A Physicochem. Eng. Asp. 2000, 173 (1–3), 1–38. https://doi.org/10.1016/S0927-7757(00)00556-2.

[67] Suzuki, T.; Sekine, T.; Yamamoto, K.; Fukutani, K. Change in the Surface OH Group on Soda Lime Silicate Glass and Silica Glass after Heat Treatment in Nitrogen Atmosphere. J. Non. Cryst. Solids 2017, 464, 89–91. https://doi.org/10.1016/j.jnoncrysol.2017.03.014.

[68] Mills, A.; Crow, M. A Study of Factors That Change the Wettability of Titania Films. Int. J. Photoenergy 2008, 2008. https://doi.org/10.1155/2008/470670.

[69] Szymczyk, K.; Zdziennicka, A.; Jańczuk, B. Effect of Polysorbates on Solids Wettability and Their Adsorption Properties. Colloids and Interfaces 2018, 2 (3), 26. https://doi.org/10.3390/colloids2030026.

[70] Rabe, M.; Verdes, D.; Seeger, S. Understanding Protein Adsorption Phenomena at Solid Surfaces. Adv. Colloid Interface Sci. 2011, 162 (1–2), 87–106. https://doi.org/10.1016/j.cis.2010.12.007.

[71] Khan, T. A.; Mahler, H. C.; Kishore, R. S. K. Key Interactions of Surfactants in Therapeutic Protein Formulations: A Review. Eur. J. Pharm. Biopharm. 2015, 97, 60–67. https://doi.org/10.1016/j.ejpb.2015.09.016.

[72] So, L.; Ng, N.; Bilek, M.; Pigram, P. J.; Brack, N. X-Ray Photoelectron Spectroscopic Study of the Surface Chemistry of Soda-Lime Glass in Vacuum. Surf. Interface Anal. 2006, 38 (4), 648–651. https://doi.org/10.1002/sia.2222.

[73] Durán, I. R.; Laroche, G. Current Trends, Challenges, and Perspectives of Anti-Fogging Technology: Surface and Material Design, Fabrication Strategies, and Beyond. Prog. Mater. Sci. 2019, 99, 106–186. https://doi.org/10.1016/j.pmatsci.2018.09.001.

Chapter VI The Silicone Depletion in Combination Products Induced by Biologics

Graphical Abstract

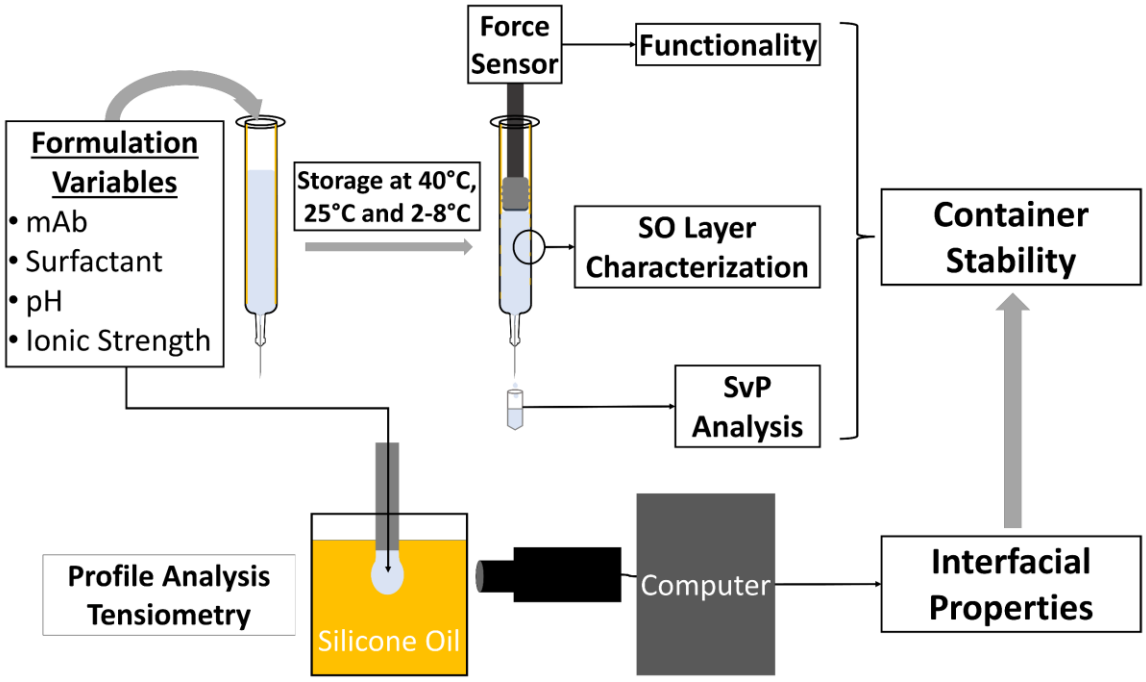

Measurements for the formulation dependent stability study as well as interfacial tension measurements were partly performed by Omaima Missaoui during her Master thesis project ("Formulation Dependent Silicone Depletion From Sprayed-On Siliconized Pre-Filled Syringes", 2020).

Abstract

Silicone oil (SO) migration into the drug product of combination products for biopharmaceuticals during storage is a common challenge. As the inner barrel surface is depleted of SO the extrusion forces can increase compromising the container functionality. In this context we investigated the impact of different formulations on the increase in gliding forces in a spray-on siliconized pre-filled syringe upon storage at 2-8 °C, 25 °C and 40 °C for up to 6 months. We tested the formulation factors such as surfactant type, pH, and ionic strength in the presence of one monoclonal antibody (mAb) as well as compared three mAbs in one formulation. After 1 month at 40 °C, the extrusion forces were significantly increased due to SO detachment dependent on the fill medium. The storage at 40 °C enhanced the SO migration process but it could also be observed at lower storage temperatures. Regarding the formulation factors the tendency for SO migration was predominantly dependent on the presence and type of surfactant. Interestingly, when varying the mAb molecules, one of the proteins showed a rather stabilizing effect on the SO layer resulting into higher container stability. In contrast to the formulation factors, those different stability outcomes could not be explained by interfacial tension (IFT) measurements at the SO interface. Further characterization of the mAb molecules regarding interfacial rheology and conformational stability were not adequately able to explain the observed difference. Solely a hydrophobicity ranking of the molecules correlated to the stability outcome. Further investigations are needed to clarify the role of the protein in the SO detachment process and to understand the cause for the stabilization. However, the study clearly demonstrated that the protein itself plays a critical role in the SO detachment process and underlined the importance to include verum for container stability.

Keywords: Syringe Functionality – Silicone Oil – Protein Formulations – Biopharmaceuticals – Pre-filled Syringes – Surface Rheology – Silicone Oil Detachment

1 Introduction

Ready-to use primary packaging systems like pre-filled syringes are of particular importance for biopharmaceuticals as they enable the patient to administer the drug by himself, ease application for health care professionals and improve drug safety. A critical aspect in this context is the presence of silicone oil (SO) in the drug product [1–3]. SO is sprayed-on the inner barrel of glass containers to reduce the friction force between the rubber plunger and the glass barrel thereby enabling an easy and consistent administration of the drug [4,5]. However, SO is known to migrate into solution where it forms microdroplets that add up to the overall particle count and potentially interact with the API [6,7]. SO is discussed to increase the immunogenicity of injectables [8,9] and there have been numerous reports about SO microdroplets found in the vitreous after injections into the eye potentially causing adverse effects [10]. Hence, trends in the development of novel packaging materials are to fix the applied SO by baking-on, cross-linking, or to reduce the sprayed-on amount of SO [11–14]. Unfortunately, lower SO levels in the barrel potentially result in higher extrusion forces already after filling or during storage, thus it is important to better understand the process of SO detachment to define packaging materials that ensure functionality and safety of the combination product over the complete storage time.

The functionality of combination products over storage is impacted by the fill medium [15,16]. The increase in friction force caused by SO depletion from the container surface is triggered by surface active ingredients. The presence and a higher concentration of polysorbate 80 (PS 80) negatively impact the container stability and induce higher particle formation [17]. Furthermore, formulations containing poloxamer 188 (Px188) exhibit a lower tendency to detach SO compared to PS 80 [16,18]. This effect is linked to the interfacial properties of the fill medium. With increasing PS 80 concentrations the interfacial tension (IFT) between the formulation and SO decrease. In addition, PS80 decreases the IFT more effectively than Px188 [16,19–21]. Besides the surfactant, Fang et al. reported that the buffer system, pH and tonicity agents impact syringe functionality upon storage [18]. However, this was demonstrated predominantly for placebo and without monitoring the state of the SO layer or IFT. Therapeutic proteins constitute surface active molecules which adsorb to interfaces, decrease the IFT as well as form viscoelastic films and are known to interact with the SO layer [6,22–28]. Correspondingly, a monoclonal antibody (mAb) verum shows higher SO particle concentrations in the drug product as compared to a placebo and a mAb concentration dependent increase in gliding forces has

been reported [6,16,29]. Although protein adsorption can be inhibited in formulations by surfactants, co-adsorption of mAbs at the interface occurs [19,26,30–32]. The interfacial storage modulus of the mAb film formed the SO interface correlates with the mAb adsorption and aggregation propensity at the SO interface [25,33]. But further thorough investigation of the formulation variables including the protein properties are still necessary.

The purpose of this study was to further identify formulation related factors which lead to a reduced stability in siliconized syringes due to SO migration. Compared to previous reports, we systematically tested different formulation variables a mAb and compared 3 different mAbs in the same formulation. We hypothesized that the IFT between formulation and SO to correlate with the increase in extrusion forces upon storage, also in the presence of the proteins. Formulation factors included protein concentration, pH, surfactant type (polysorbate 20 (PS20) and Px188) and concentration as well as ionic strength. A change of the pH and ionic strength are known to influence adsorption behavior of proteins to accessible surfaces and thus the container stability in terms of functionality could be influenced indirectly [34–37]. We monitored the extrusion forces upon storage at 2-8 °C, 25 °C and 40 °C for up to 6 months. The residual SO amount and the SO layer thickness in the barrels were determined by Fourier-transform infrared spectroscopy (FTIR) and interferometry measurements. 3D-laser scanning microscopy (3D-LSM) was utilized to take images of the silicone layer from outside the barrel at all the study timepoints. The IFT between the formulations and SO were obtained with a profile analysis tensiometer (PAT). We further characterized the formulations and mAbs in terms of interfacial rheology properties. As an impact of the mAb on the SO detachment became obvious, the proteins were further characterized in terms of hydrophobicity and conformational stability with the aim to find protein characteristics which explain and potentially predict the protein induced SO detachment. Both parameters are considered important in the adsorption process of mAbs to surfaces [35,38–40].

2 Materials and Methods

2.1 Materials and Methods

Chemicals

Following chemicals were used: L-histidine, L-histidine monohydrochloride monohydrate, polysorbate 20 (PS20), NaCl (Merck KGaA, Darmstadt, Germany), trehalose (Ferro Pfanstiehl, Waukegan, IL, USA), sucrose (Sigma-Aldrich Chemie GmbH, Steinheim, Germany) and Poloxamer 188 (BASF, Ludwigshafen, Germany).

Sample Preparation

Four different IgG1 monoclonal antibodies were kindly provided by Novartis AG (Basel, Switzerland). mAb 2, 3 and 4 were obtained in histidine-buffers without further excipients. mAb 1 was obtained already finally formulated at 120 mg/mL in histidine buffer (His) containing trehalose and 0.02 % (w/v) PS20. Vivaflow® 50 cross flow cassettes with a 50 kDa MWCO PES membrane (Sartorius AG, Goettingen, Germany) were used to concentrate the other protein solutions or exchange the buffer system. Buffer solutions were prepared with highly purified water and pH was checked with a Mettler Toledo MP220 pH meter (Mettler Toledo, Greifensee, Switzerland). After final formulation, concentration was checked using UV-Vis spectrophotometer NanoDrop™ (Thermo Scientific, Wilmington, Delaware, USA). To investigate the impact of formulation variables, mAb 4 was formulated varying protein concentration, pH, ionic strength, and surfactant type and concentration (Table VI-1). mAb 2 and 3 were formulated according to the formulation of mAb 1 including 0.02 % (w/v) PS 20. For all protein formulation, an accordingly formulated placebo was prepared. The protein solutions were filled into 1 mL long BD Neopak™ syringes with 27G ½" staked-in needles (BD Medical – Pharmaceutical Systems, Le Pont-de-Claix, France) and containers were closed with NovaPure® Syringe Plungers (West Pharmaceutical Services, Inc., Exton, PA, USA) under laminar air flow. The plungers were all set to the same height using an insertion jig. Prior filling all solutions were sterile filtrated using vacuum filtration units with a 0.2 µm PES filter membrane (VWR International GmbH, Darmstadt, Germany).

Abbreviation	Protein Concentration	pH	Ionic Strength	Surfactant
Standard	**75 mg/mL**	6	-	0.06 % (w/v) PS20
Low mAb	**5 mg/mL**	6	-	0.06 % (w/v) PS20
Middle mAb	**40 mg/mL**	6	-	0.06 % (w/v) PS20
High mAb	**120 mg/mL**	6	-	0.06 % (w/v) PS20
Low pH	75 mg/mL	**5**	-	0.06 % (w/v) PS20
High Ion	75 mg/mL	6	**140 mM**	0.06 % (w/v) PS20
High Surfactant	75 mg/mL	6	-	**0.12 % (w/v) PS20**
W/o Surfactant	75 mg/mL	6	-	**-**
Px188	75 mg/mL	6	-	**0.06 % (w/v) Px188**
High Px188*	75 mg/mL	6	-	**0.40 % (w/v) Px188**

Table VI-1: Overview of verum and placebo formulations of mAb 4 tested (30 mM His, 270 mM sucrose). *Only tested as placebo.

2.2 Stability Study

Syringes filled with mAb 1 – 3 were stored without agitation at 40 °C and 2-8 °C for up to 6 months as well as at 25 °C for up to 3 months, mAb 4 formulations were stored for up to 3 months at 40 °C. At designated timepoints functionality, particle formation, silicone distribution and content per barrel as well as silicone layer morphology were investigated.

Functionality

Functionality was investigated using a Texture Analyzer TA.XT Plus (Stable Micro Systems Ltd., Surrey, UK). The containers were expelled with a velocity of 190.2 mm/min until a trigger force of 30 N. The maximum force required for the distance 0 – 35 mm was set as the maximum extrusion force (Fmax). Extrusion was automatically stopped, when the upper limit of 30 N was reached and such container systems were declared as “failed“. ($n \geq 5$)

Subvisible Particle Analysis (SvP-Analysis)

Particles in the product were monitored using a using FlowCam 8100 (Fluid Imaging Technologies, Inc., Scarborough, ME, USA) equipped with a 10x magnification lens. Samples were collected during the functionality measurements in pre-rinsed Eppendorf® tubes and particle > 1µm concentration was evaluated using 150 µl at a flowrate of 100 µl/min. ($n \geq 4$)

Silicone Oil Distribution

A RapID Layer Explorer UT (rap.ID Particle Systems GmbH, Berlin, Germany) was used to evaluate the silicone oil distribution in the barrel. Prior to measurements, the syringes were emptied after carefully removing the plunger with tweezers. The barrels were subsequently rinsed with 1 mL highly purified water (HPW) at least 3 times and firmLy dried. After baseline recording of a non-siliconized syringe 8 lines of 40 mm per barrel with a resolution of 0.4 mm/step were recorded to determine the silicone layer thickness along the barrel. In the study evaluating the mAb effect combined white light and laser interferometry (WLI) was used (UT Mode/LOD = 20 nm), whereas in the formulation effect study syringes were evaluated using white light interferometry (WI) (BI Mode/ LOD = 80 nm). Calculating the silicone layer thickness silicone depletion was evaluated based on the datapoints 35 – 100. Datapoints below limit of detection were counted as 20 nm respectively 80 nm depending on the method used. Samples declared as T0 display syringes not filled. (n = 3)

Silicone Layer Morphology

The silicone layer of syringes emptied and cleaned as described above was assessed with a Keyence VK-X250 3D-Laser Scanning Microscope (Keyence International NV/SA, Mechelen, Belgium). After focusing on the silicone layer from outside images were taken alongside the barrel with a CF Plan 10x/0.30 Nikon OFN WD 16.5 objective. Seven images in the middle of the barrel were stitched together with the VK Image Stitching software (version 2.1.1.0).

Silicone Oil Quantification

The silicone oil amount per barrel was quantified using a FTIR Tensor 27 (Bruker Corp., Billerica, MA, USA) after emptying and cleaning the syringes as described above and following a method developed by Funke et al. [41]. Briefly, the silicone oil was extracted twice per barrel with 700 µl n-heptane. Therefore, plungers were inserted with the same jig used for the stability study and the syringes were rotated overhead for 20 min at 18 rpm. The solvent extracts were pooled in 2R vials and heptane was removed with a Flowtherm Evaporator (Barkey GmbH & Co.KG, Leopoldshöhe, Germany) at 100 °C and nitrogen flow of 100 mL/min. The dried extract was redissolved with 500 µl n-heptane and filled into a 250 µm path length transmission liquid cell. To obtain transmittance spectrum 100 scans with a resolution of 4 cm^{-1} were recorded between the wavelengths 3000 to 900 cm^{-1}.

After calibration (R^2 = 0.9999), silicone oil was quantified based on the area under the curve of the symmetrical Si-CH_3 deformation between 1280 and 1240 cm^{-1} obtained by the Brukers OPUS software (Version 7.5.18). Samples declared as T0 display syringes not filled. (n = 3)

2.3 Interfacial Behavior at Silicone Oil Interface

The interfacial tension (IFT) at the silicone interface of the various fill mediums was determined with a PAT1M profile analysis tensiometer (SINTERFACE Technologies e.K., Berlin, Germany). A droplet was formed with a single capillary (2.1 mm) immersed in silicone oil (Dow Corning® 360 Medical Fluid 100 cSt, Dow Corning GmbH, Wiesbaden, Germany). Dynamic interfacial tension was recorded based on the captures of a video camera for at least 5000 s. For the samples mAb 1 – 3 the droplet volume was oscillated after 5000s (Amplitude 10 %) at 0.01 Hz, 0.02 Hz, 0.05 Hz, 0.1 Hz and 0.2 Hz. Fourier Transformation enabled the calculation of viscoelastic properties of the adsorbed surfactant and protein layers (storage modulus E' and imaginary modulus E''). Protein concentration was adjusted to 5 mg/mL for all PAT measurements. (n = 3)

2.4 Conformational Stability

The mAb unfolding was studied by nano differential scanning fluorimetry (nanoDSF) at 1 mg/mL using a Prometheus® NT.48 (nanoTemper Technologies, Munich, Germany) at 1 °C/min from 20 °C to 100 °C. Fluorescence intensity at 350 nm was plotted against temperature and the apparent melting temperature of the protein was obtained from the maximum of the first derivative using the PR.ThermControl V2.1 software (nanoTemper Technologies, Munich, Germany). (n = 3)

Additionally, isothermal chemical denaturation (ICD) was used to characterize the protein physical stability following a method developed by Svilenov et al. [42]. Protein stock solutions (10 mg/mL in His-Buffer) were pipetted into a non-binding surface 384 well plate (Corning, USA) and mixed with the buffer and a denaturant stock solution (6 M guanidine hydrochloride) resulting in different denaturant concentration and a constant protein concentration of 1 mg/mL. Pipetting and mixing were performed with a 12.5 µL and 125 µL Viaflo pipette and the Viaflo Assist (Integra Biosciences, Konstanz, Germany). After sealing the microplate, the samples were incubated at room temperature for 27 h and intrinsic fluorescence was determined at 350 nm with a Fluostar Omega microplate reader (BMG Labtech, Ortenberg, Germany). The data was plotted against denaturant

concentration with the CDpal software (Version 2.15) [43] and the autofit function was used to evaluate the approximate Cm values of the curves. (n = 3)

2.5 Hydrophobicity

Hydrophobic interaction chromatography (HIC) was used to evaluate protein hydrophobicity. Protein samples were analyzed on an Agilent 1200 device (Agilent Technologies GmbH, Böblingen, Germany). MAb samples were diluted with ammonium sulphate buffer to a final concentration of 0.33 mg/mL prior analysis. A total mAb amount of 20 µg was injected onto a 35 x 4.6 mm TSKgel Butyl-NR column from Tosoh Bioscience GmbH (Darmstadt, Germany) and eluted at a flow rate of 1 mL/min at 25 °C. After the equilibration of the column for 2 min with buffer A (20 mM His/HCl, pH 5.4 containing 1.5 M $(NH_4)_2SO_4$, concentration of buffer B (20 mM His/HCl, pH 5.4) was increased linearly from 0 – 100 % in the following 66 min ($t_{gradient}$). MAbs were detected with a G1314B UV detector at 280 nm. The results are presented as the quotient of retention time and $t_{gradient}$.

3 Results

3.1 Stability Study – Variation of Formulation

After filling spray-on siliconized syringes with mAb 4 formulations differing in protein concentration, pH, surfactant type, concentration as well as ionic strength (Table VI-1), containers were stored at 40 °C for 3 months. Next to the progress in gliding forces, SvP count of expelled samples was evaluated. SO migration was monitored by quantifying residual SO amount per barrel after extraction and SO layer thickness measurements. Both results were supported by 3D-LSM of the inner SO surface.

3.1.1 Functionality

The Fmax of the protein and placebo samples increased over storage dependent study. This included the functionality failure of a broad number of syringes at the end of the stability study after 3 months at 40 °C (Figure VI-1). The increase in extrusion force was dependent on the formulation filled in. At T0 all samples showed similar Fmax values between 2.1 N and 2.5 N, which increased to 6 N and 10 N for most of the samples after 1 month at 40 °C. The samples without surfactant and with Px188 showed a smaller increase towards values of 3.2 ± 0.2 N and 4.0 ± 0.8 N respectively. Interestingly, also the syringes containing a formulation with higher ionic strength were still easier to expel with Fmax values of 3.1 ± 0.2 N. After 3 months, the extrusion force was massively increased to 25 N to 30 N for the syringes except for the ones containing either no surfactant or Px188, which staged at approximately 3 N, and the high ionic strength formulation with 15.6 ± 2.1 N.

These results agree with the Fmax results of the corresponding placebos. In some cases, the placebos solution showed higher extrusion force values after storage. For instance, the lower pH placebo formulation showed an increase from 2.0 ± 0.1 N to 28.6 ± 2.5 N already after 1 month at 40 °C and for the Px188 placebo sample a higher Fmax of 7.6 ± 7.0 N was detected after 3 months. An additional formulation with a higher Px188 concentration (0.4 % (w/v)) resulted in Fmax of 17.1 ± 10.8 N, which was higher than with 0.06 % (w/v) Px188, but still lower compared to the PS20 containing samples.

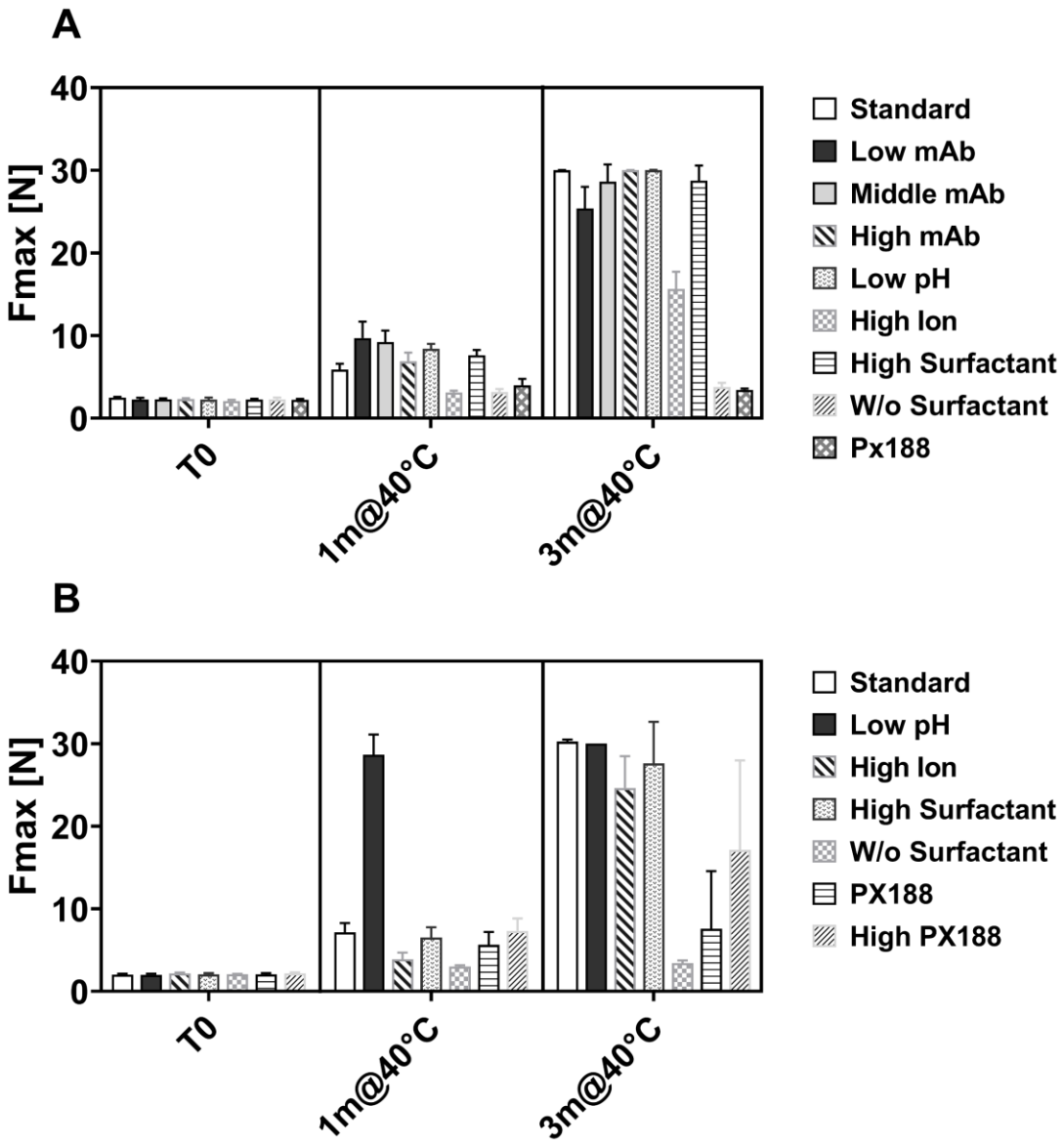

Figure VI-1: Maximum extrusion forces (Fmax) of syringes after storage at 40 °C of different mAb 4 [A] and placebo [B] formulations.

3.1.2 SvP-Analysis

The particle count of the expelled samples was assessed with flow imaging and served as indicator for silicone oil migration into the product (Figure VI-2). Formulations without PS20 or containing Px188 did not show an increase in particle concentration upon storage at all. At maximum 66.000 ± 19.000 particles > 1µm/mL were detected in verum and 36.000 ± 25.000 particles > 1µm/mL in placebo. All PS20 containing samples showed enhanced particle concentrations after expelling. In general, placebo solutions for this group showed lower particle counts compared to protein containing solutions as they did

not exceed values > 3.5 x 10^5 particles > 1µm/mL. In comparison, 5 out of the 7 protein samples showed values of > 1x10^6 particles > 1µm/mL. Particularly high particle concentrations were detected for the protein formulation with a higher PS20 concentration (High Surfactant/ 0.12 % (w/v)), which reached values up to 4.8 x 10^6 particles > 1µm/mL after 3 months storage. Lower particle concentrations were found for the solution containing higher mAb concentration (120 mg/mL) and the lower pH 5.

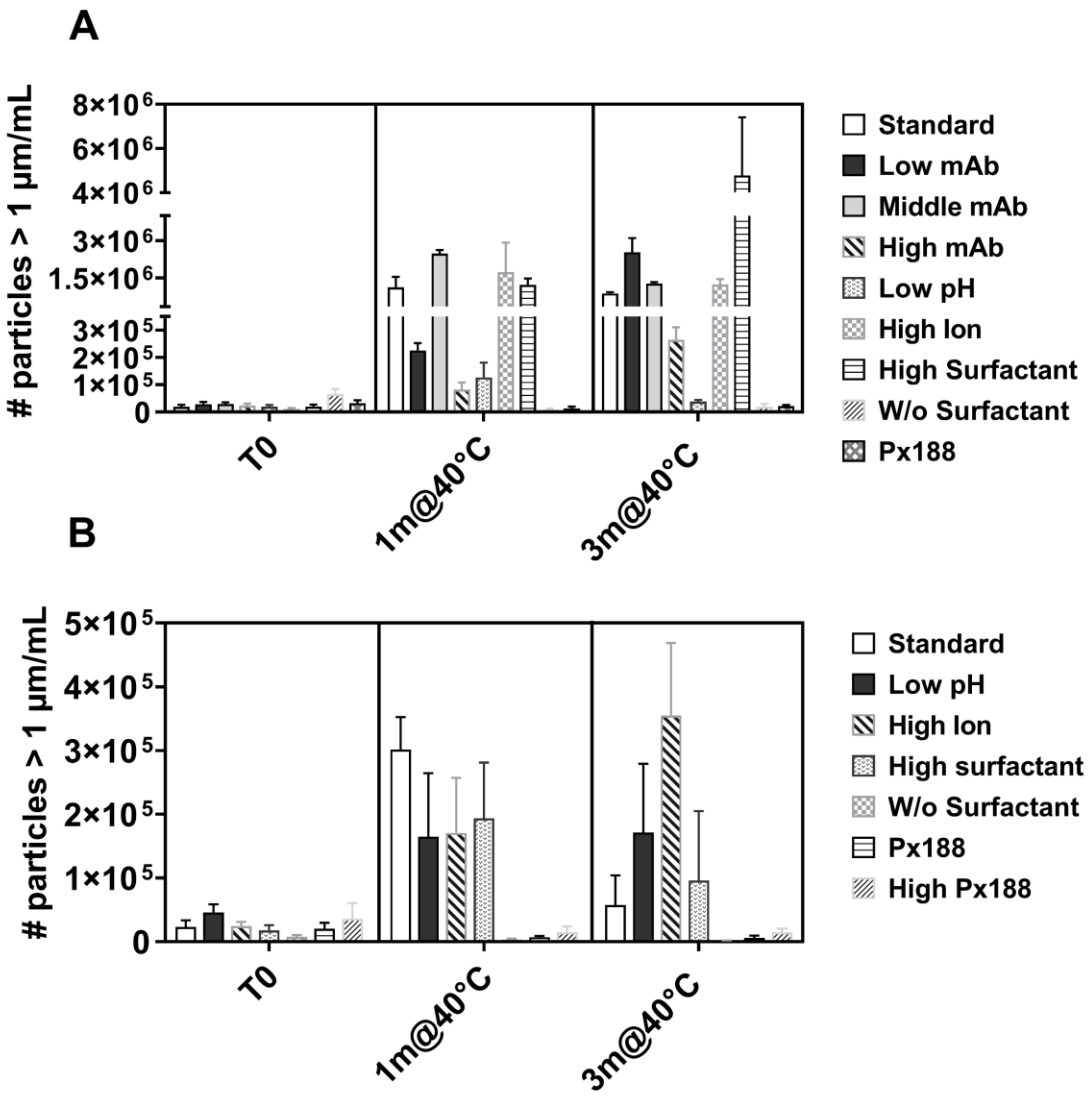

Figure VI-2: Number of particles> 1µm/mL after storage at 40 °C for different mAb 4 [A] and placebo [B] formulations.

3.1.3 Silicone Layer Characterization

Silicone layer detachment upon storage could be demonstrated by silicone oil quantification with FTIR as well as by interferometry measurements at the silicone layer to determine its

thickness. The solutions without PS20 or containing Px188 also at higher concentration showed a reduction of the silicone oil from approximately 200 µg SO per barrel to 120 – 160 µg after storage for 1 or 3 months (Figure VI-3). For PS20 containing formulations the amount decreased to 50 – 80 µg after 1 month and approximately 30 µg after 3 months. Overall, the effect was similar for the verum and the placebo.

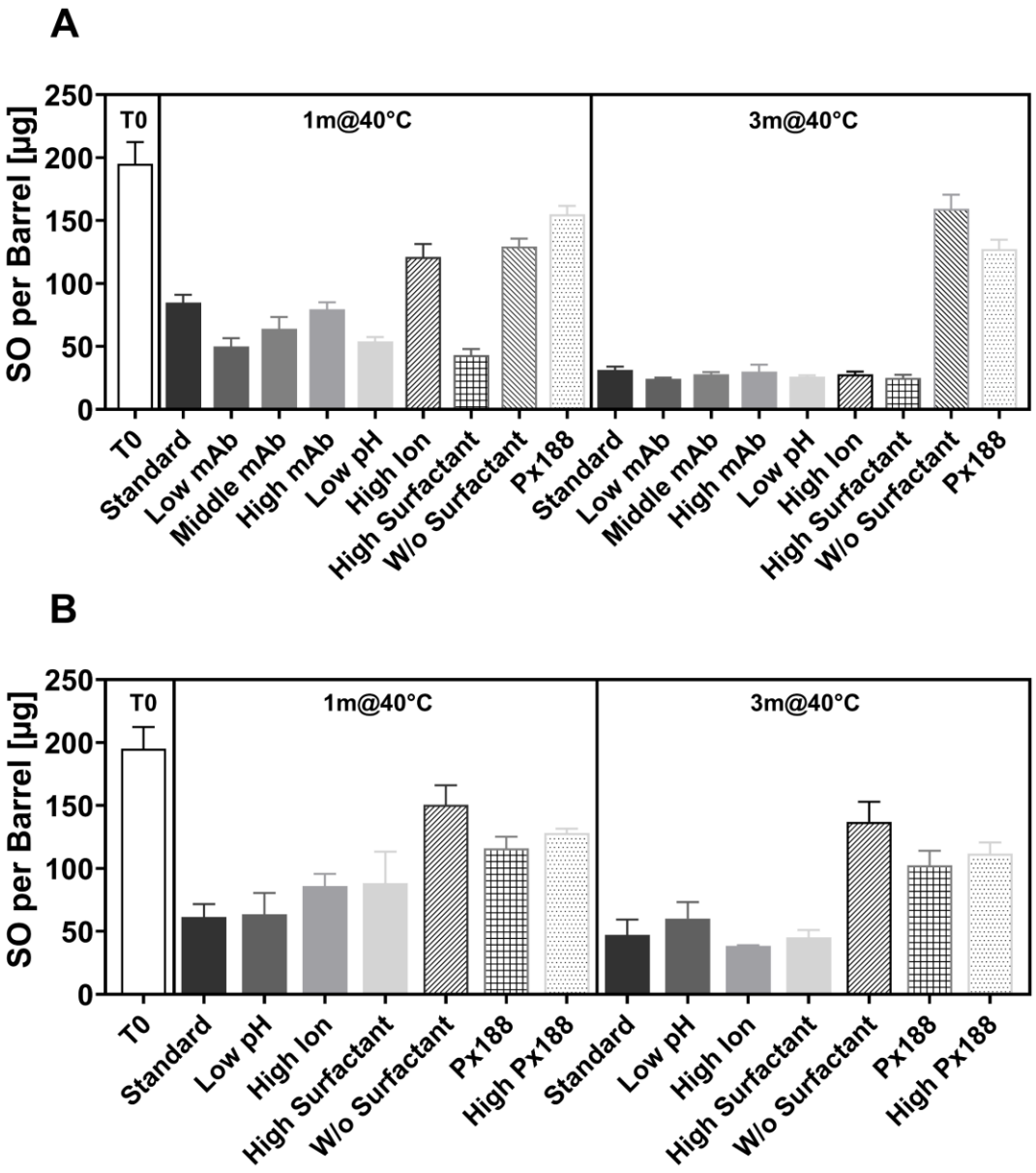

Figure VI-3: SO amount per barrel after storage at 40 °C of different mAb 4 [A] and placebo [B] formulations.

The results were reflected by silicone layer thickness measurements (Figure VI-4). Silicone oil was hardly detectable in the samples except for the surfactant free and the Px188 containing formulations with most of the datapoints < LOD already after 1 month at 40 °C.

As all datapoints < LOD were calculated as 80 nm, the boxes of samples with obvious depletion appear as a flat line. The Px188 concentration did not impact the change in silicone layer thickness. After 3 months the silicone layer height was further decreased for both the protein and placebo. In general, the presence of protein enhanced the decline of the layer thickness. Furthermore, silicone layer thickness for the Px188 containing as well as the standard formulation stored for 3 months was examined in UT mode (Supplementary Data - Figure S VI-1); the majority of the datapoints detected for the standard formulation was < LOD as well indicating no silicone at all at the inner barrel surface. The Px188 showed more silicone oil left and less depletion occurred with placebo.

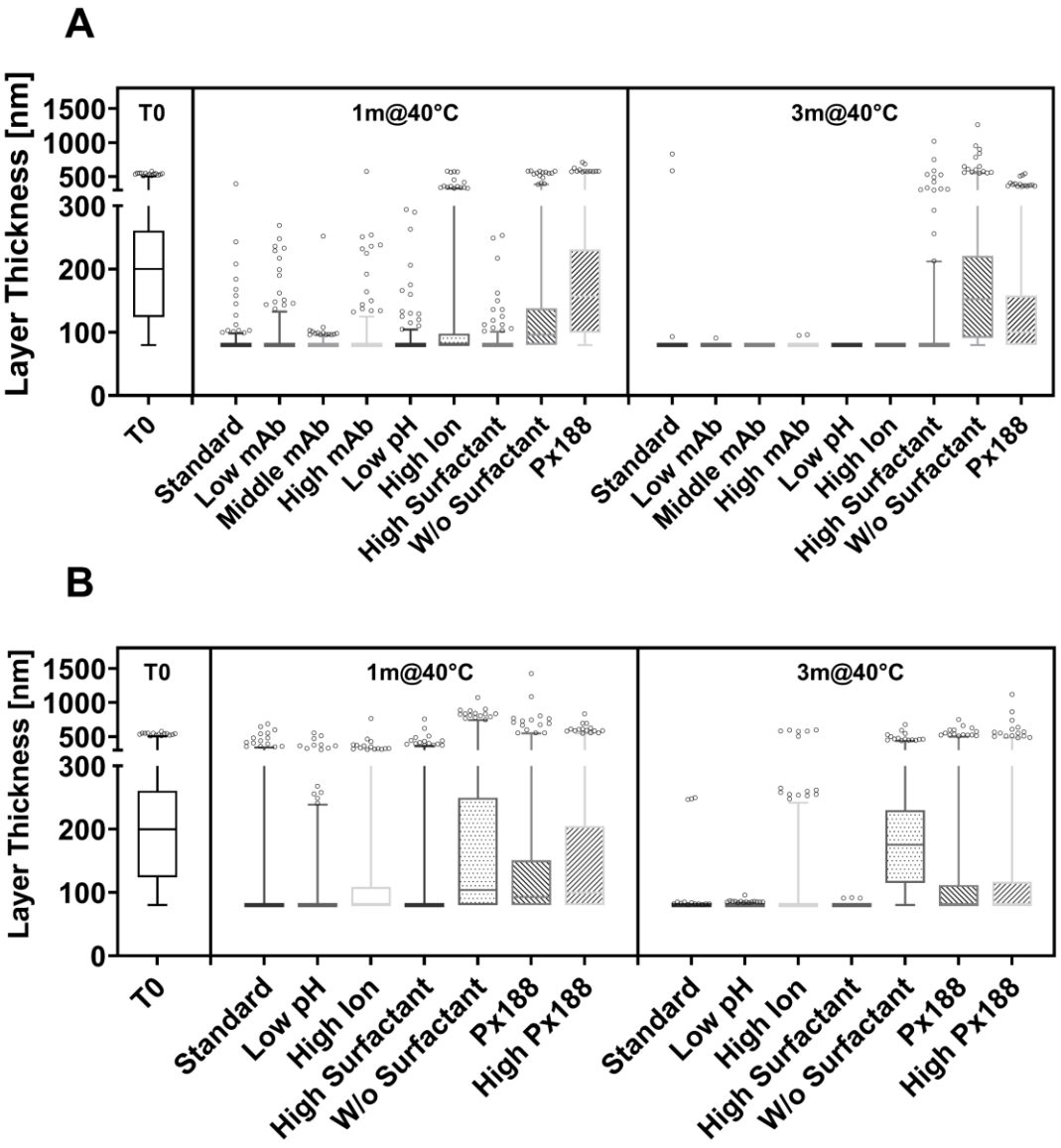

Figure VI-4: SO layer thickness after storage at 40 °C of different mAb 4 [A] and placebo [B] formulations displayed as box plots (Box: 25th – 75th percentile; Whiskers: 1th – 99th percentile/LOD: 80 nm).

3D-LSM confirmed the findings. At start, the SO formed blurred structures (Figure VI-5), which were still partially present after 1 month (Supplementary Data - Figure S VI-2) and vanished for PS20 containing samples after 3 months storage. Remainders of SO were still visible for the surfactant free and Px188 containing formulations.

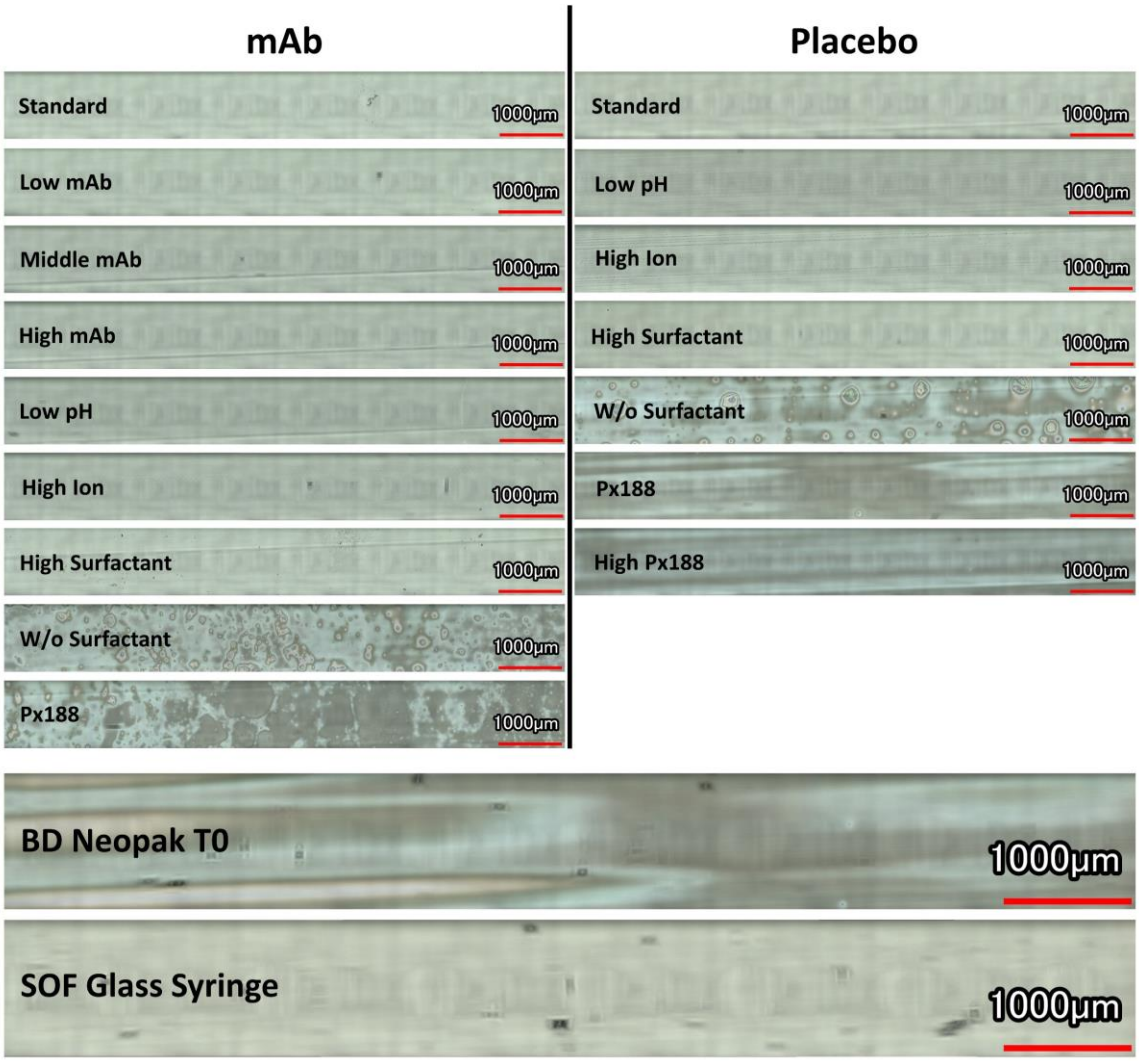

Figure VI-5: 3D-LSM images of the inner surface of syringes after storage at 40 °C for 3 months of different mAb 4 and placebo formulations compared to T0 and non-siliconized syringes.

3.2 Stability Study – Variation of the mAb Molecule

After filling spray-on siliconized syringes with one formulation (Formulation mAb 1) but 3 different mAbs (mAb 1 – 3), containers were stored for up to 6 months at 40 °C, 25 °C and 2-8 °C. Container stability as well as SO migration upon storage was monitored as abovementioned.

3.2.1 Functionality

Extrusion forces at T0 were low for all syringes with Fmax between 2.3 N and 4.7 N. Fmax of the mAb 1 - 3 solution and placebo filled syringes increased with storage (Figure VI-6). Overall, the syringes filled with mAb 1 showed the most pronounced increase of Fmax followed by placebo and mAb 2. Fmax of syringes filled with mAb 3 increased least and was still acceptable even after 6 months storage at 40 °C.

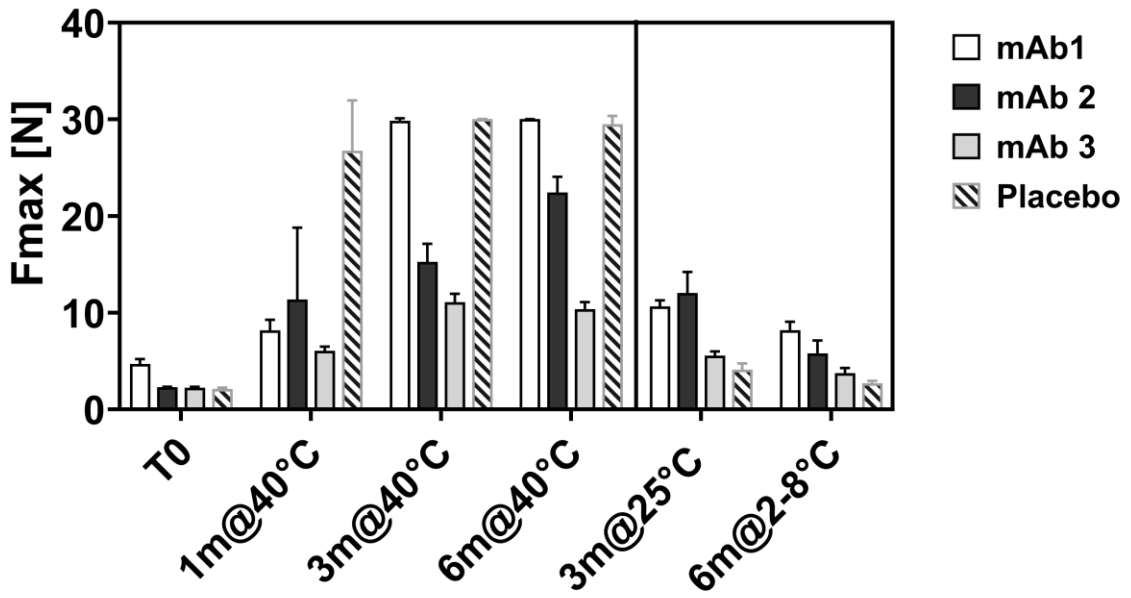

Figure VI-6: Maximum extrusion forces (Fmax) of syringes after storage at 40 °C, 25 °C or 2-8 °C of mAb 1, 2 and 3 as well as placebo formulations.

After one month storage at 40 °C, already two placebo solution samples failed respectively they showed a Fmax > 30N (average Fmax of 26.8 ± 5.2 N/ Figure VI-6). After 3 months at 40 °C, 4 out of 6 syringes filled with mAb 1 failed reaching an Fmax average of 29.8 ± 0.3 N; placebo solutions completely failed at that timepoint. An increase became also evident for mAb 2 (Fmax 15.3 ± 1.9 N) and mAb 3 (Fmax 11.1 ± 0.9 N). The results after 6 months at 40 °C were similar to the 3-month timepoint except for a further increase of Fmax for the mAb 2 formulation to 22.4 ± 1.6 N. Also, at lower storage temperatures

Fmax increased but no syringe failed after 6 months. The trend of the mAb effect observed at 40 °C could also be noticed at 2-8 and 25 °C. In general, mAb 1 and 2 showed markedly higher Fmax values compared to T0 than mAb 3. For the placebo only a small increase could be noticed.

3.2.2 SvP-Analysis

The concentration of particles > 1µm increased after storage at all temperatures (Figure VI-7). After filling mAb 2, mAb 3, and placebo samples showed 18.000 to 25.000 particles > 1µm/mL and mAb 1 70.000 ± 29.000 particles > 1µm/mL on average. After 1 month at 40 °C, mAb 1 and placebo samples contained around 200.000 particles > 1µm/mL and mAb 2 samples 380.000 ± 95.000 particles > 1µm/mL, whereas mAb 3 samples stayed much lower with 40.500 ± 10.000 particles > 1µm/mL. The particle concentrations did increase further at the 3- and 6-month timepoint for the mAb 2 and 3 samples. As the extrusion was not conducted completely for the mAb 1 and placebo at those timepoints, the results cannot be further compared (marked as x in Figure 8). The failing of the syringes obviously decreased the particle count in the collected samples. After 3 months storage at 25 °C mAb 1, 2 and placebo showed increased particles levels and mAb 3 no change. At 2-8 °C after 6 months, the particle count was marginally increased in all samples at a similar level.

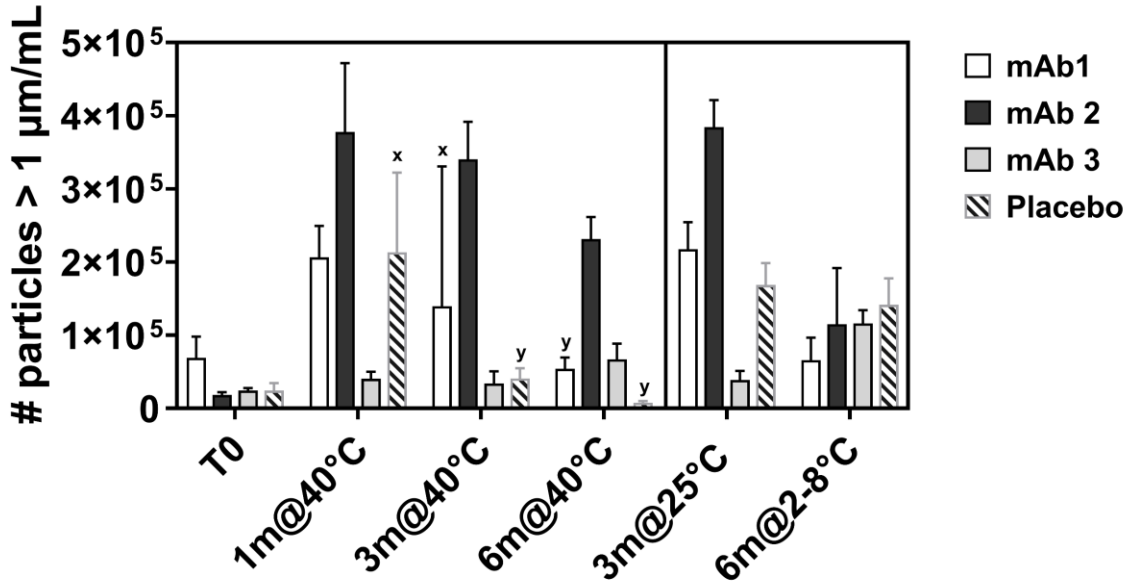

Figure VI-7: Number of particles > 1µm/mL after storage at 40 °C, 25 °C or 2-8 °C of mAb 1, 2 and 3 as well as placebo formulations. x: Samples with incomplete extrusion due to functionality failure; y: all syringes failed.

3.2.3 Silicone Layer Characterization

As shown for the variation of the formulation the increase in extrusion forces for syringes filled with different mAbs was linked to a steady decrease of the SO layer height on the inner barrel surface. Syringes filled with mAb 1, mAb 2 and placebo showed a rather similar decline of the SO amount over storage (Figure VI-8) reaching values around 30 µg per barrel after 6 months at 40 °C. In contrast, the lowest values obtained for mAb 3 samples were around 90 µg per barrel. Results for the samples stored for 3 months at 25 °C were comparable to the 1-month timepoint at 40 °C. After 6 months at 2-8 °C the SO level for all samples was only half of the T0 value without obvious differences between the samples.

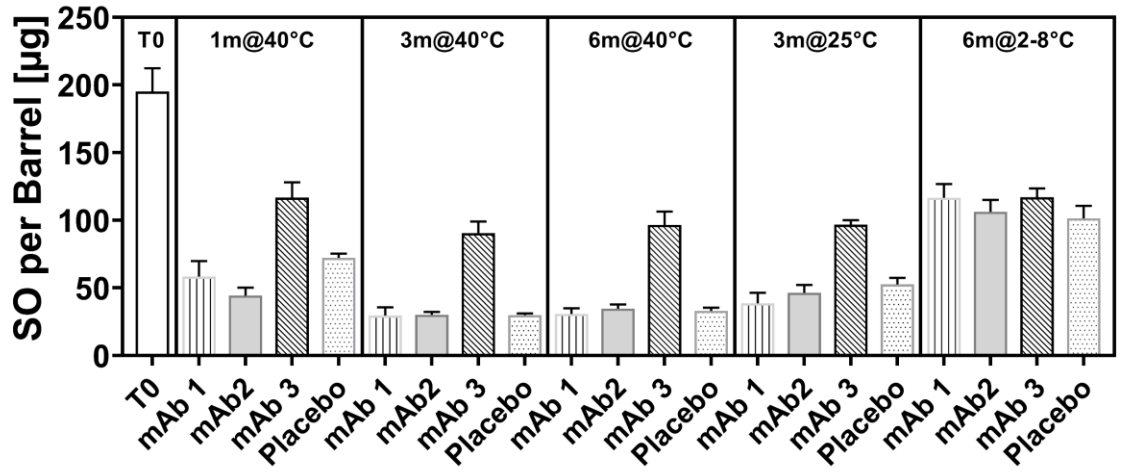

Figure VI-8: SO amount per barrel after storage at 40 °C, 25 °C or 2-8 °C of mAb 1, 2 and 3 as well as placebo formulations.

Corresponding results were obtained with interferometry. For mAb 1, mAb 2 and placebo solutions SO was hardly detectable after storage at 40 °C and 25 °C (Figure VI-9). Starting at a median of approximately 160 nm for unfilled syringed the thickness dropped to 20 nm representing the LOD of the method. In contrast, the medians of syringes filled with mAb 3 ranged roughly between 58 and 73 nm throughout the stability study. Silicone oil detachment was less pronounced at 2-8 °C; still the decrease was less distinct for mAb 3. Furthermore, the inner barrel of syringes filled with mAb 1, mAb 2 or placebo showed the appearance of the surface of a silicone oil free glass syringe in 3D-LSM already after 1 month storage at 40 °C (Figure VI-10/ Supplementary Data - Figure S VI-3). In contrast, the images of syringes filled with mAb 3 indicated presence of a SO layer although the inner surface appeared less smooth and congruent. After 3 months at 25 °C, SO still was

visible for mAb 3 and placebo solution; after 6 months at 2-8 °C SO was still clearly visible for all samples.

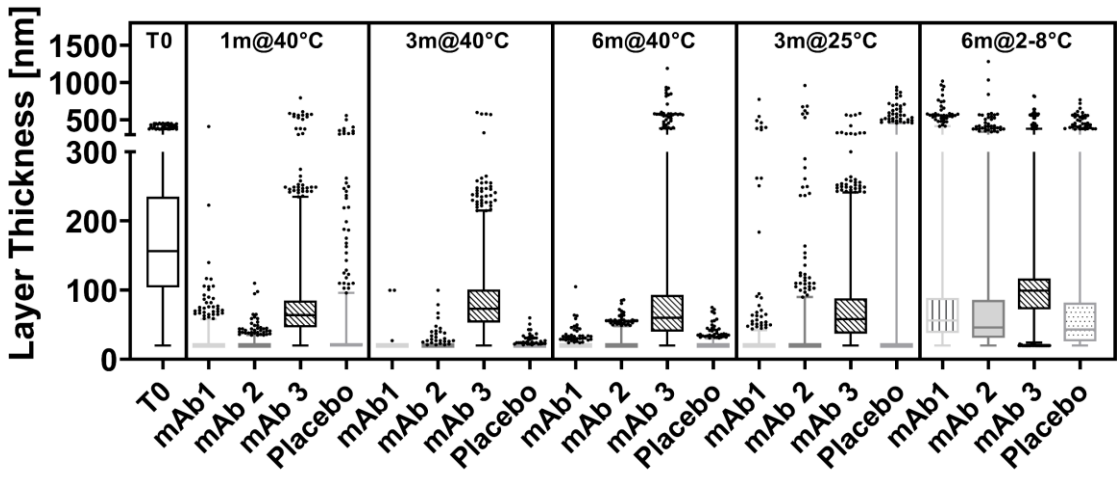

Figure VI-9: SO layer thickness after storage at 40 °C, 25 °C or 2-8 °C of mAb 1, 2 and 3 as well as placebo formulations displayed as box plots (Box: 25th – 75th percentile; Whiskers: 2.5th – 97.5th percentile/LOD: 20 nm).

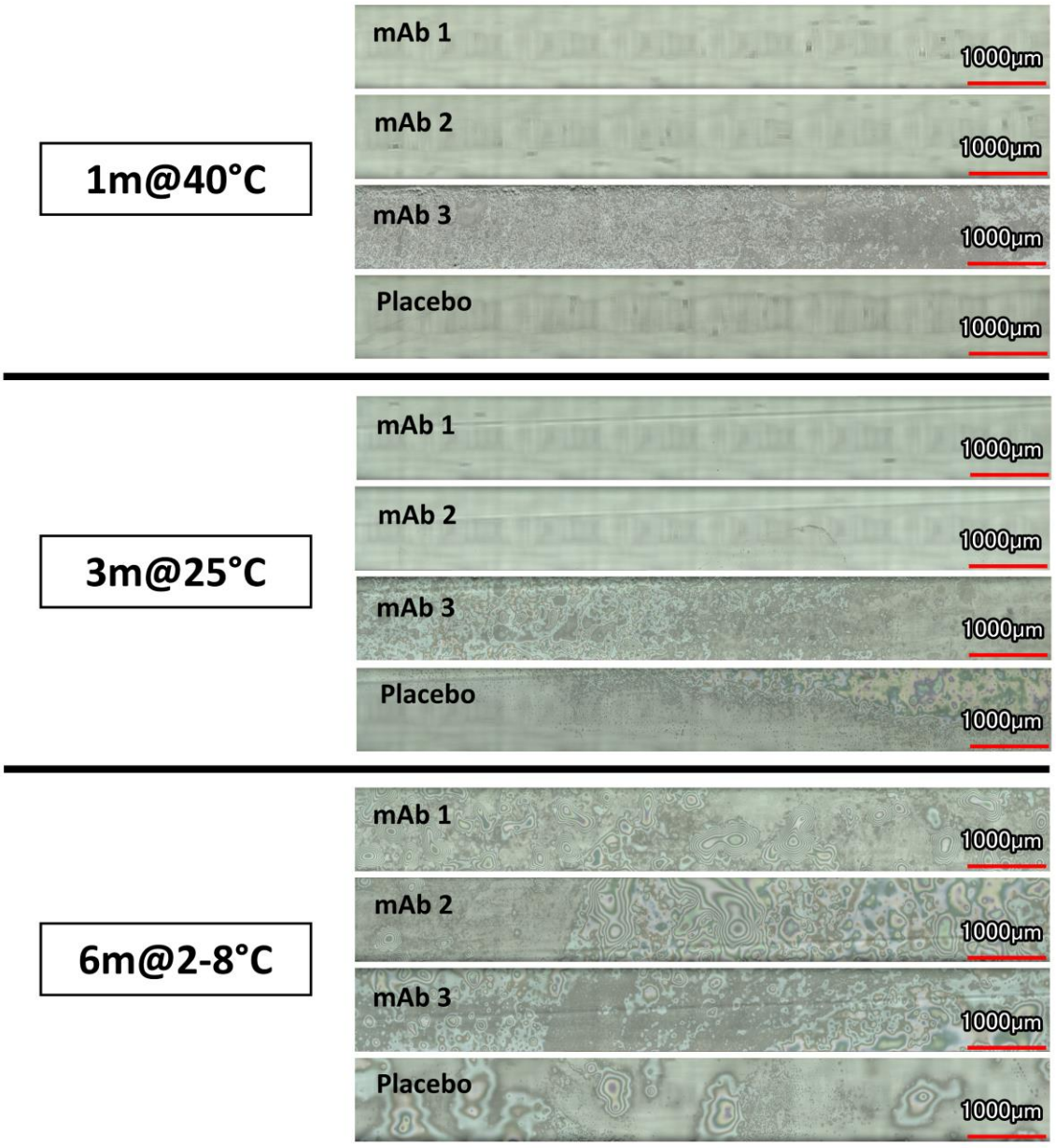

Figure VI-10: 3D-LSM images of the inner surface of syringes after storage at 40 °C, 25 °C or 2-8 °C of mAb 1, 2 and 3 as well as placebo formulations.

3.3 Interfacial Behavior Silicone Oil Interface

Interfacial tension and rheological measurements between the formulations and SO were performed looking for explanations of the difference in the outcome of the stability study with respect to both the formulation and the mAb effect.

3.3.1 Variation of the Formulation

All polysorbate containing samples showed the same progression of the IFT at the SO interface over time with a fast decline in the first 100s to values of around 9 mN/m, which continued to decrease to 7 mN/m after 5000 s (Figure VI-11). The corresponding placebo solution showed the same progression with slightly but consistently higher values. In contrast, Px188 containing samples induced IFT to decrease instantly to higher values of 20 mN/m without further change after the first 100 s and lower IFT values for the placebo solution. The formulations without surfactant showed a rather slow decline to values of 22.9 ± 0.7 mN/m after 5000 s, whereas the IFT was stable for the surfactant free placebo at a value of 34 mN/m.

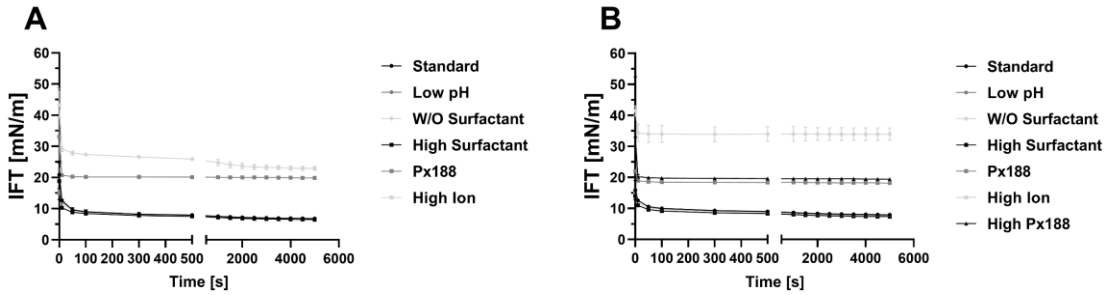

Figure VI-11: IFT of different mAb 4 [A] and placebo [B] formulations at the SO interface.

3.3.2 Variation of the mAb Molecule

As seen for the formulation study, the presence of the surfactant predominantly determined the progression of the IFT at the SO interface over time thus resulting in a decline to 8 mN/m after 5000 s for all samples including the placebo compared to 37 mN/m of the surfactant free buffer (Figure VI-12). Furthermore, no significant difference was observable in between the surfactant free mAb solutions (mAb 1 – 3) as they all decreased the IFT to approximately 26 mN/m after 5000 s. Dilational rheology measurements indicated the same viscoelastic properties of the films formed at the silicone interface for the actual formulations (Figure VI-13, A) as there was no distinct difference in the storage

(E') and loss modulus (E'') at different frequencies observable. Without the surfactant the elasticity of the different mAb films was similarly increased (Figure VI-13, B).

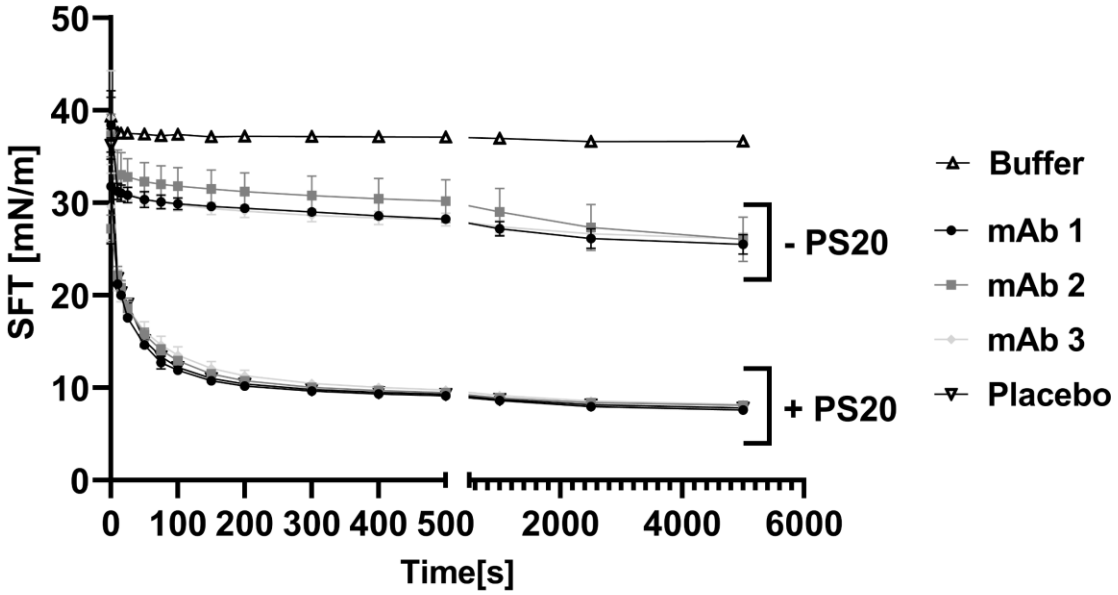

Figure VI-12: IFT of formulations containing mAb 1, 2 and 3 and placebo with (+) and without (-) 0.02 % (w/v) PS20.

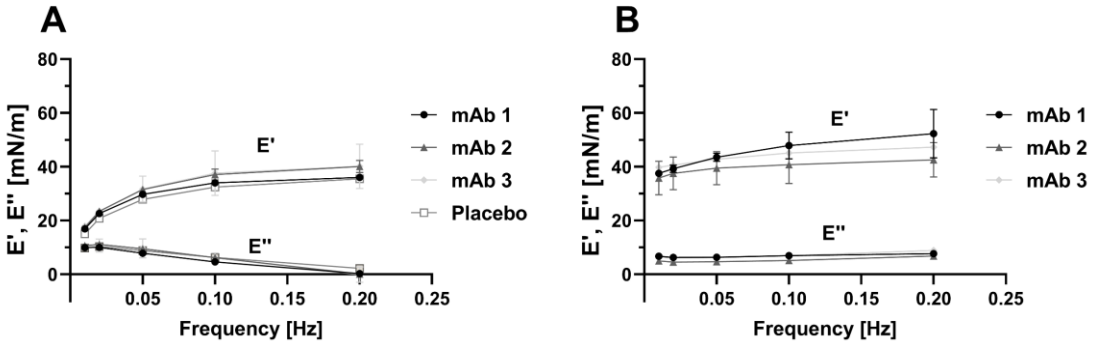

Figure VI-13: Dilatational storage (E') and loss modulus (E'') of the interfacial film between SO and formulations containing mAb 1, 2 and 3 and placebo with [A] and without [B] 0.02 % (w/v) PS20 at different oscillation frequencies.

3.4 Further mAb Properties

The three different mAbs were further characterized and ranked in terms of solution viscosity, hydrophobicity, and conformational stability. The viscosity of the mAb 1 formulation was significantly higher with 14.2 ± 0.0 mPa*s compared to 5.8 ± 0.2 mPa*s and 5.0 ± 0.0 mPa*s for mAb 2 and 3. In addition, mAb 1 showed the highest

hydrophobicity with a retention time quotient in HIC of 0.57 followed by mAb 2 and mAb 3 with 0.49 and 0.44 respectively.

The ranking in terms of conformational stability obtained by isothermal chemical denaturation matched the results by thermal unfolding of the proteins with nDSF (Supplementary Data - Figure S VI-4). mAb 1 was least stable with the earliest unfolding with a Tm of 71.6 ± 0.0 °C and a Cm of 2.1 ± 0.1 M, followed by mAb 3 with a Tm of 76.8 ± 0.1 °C and Cm of 2.3 ± 0.0 M, and mAb 2 showing a Tm of 79.0 ± 0.0 °C and Cm of 2.7 ± 0.1 M.

4 Discussion

The aim of the present study was to identify mAb formulation factors, which contribute to reduced storage stability by enhancing SO detachment from the container surface. To this end, we investigated the impact of different fill media upon long-term storage of spray-on siliconized pre-filled syringes.

At first, we varied the mAb formulations in terms of excipient type and concentration. Two formulations, the one lacking a surfactant and the one containing Px188, showed clearly less tendency for SO detachment. Subsequently, higher container stability was obtained with these formulations without a significant increase of extrusion forces or even failure of the syringe. The trend was observed with verum and placebo. The extrusion force results were well in line with the residual SO amount analyzed by FTIR, and the layer thickness analyzed by interferometry and 3D-LSM. 3D-LSM turned out to be a quick, non-destructive, and reliable method to identify SO removal from the inner barrel surface. Additionally, SvP analysis showed less particles for those two formulations compared to all other formulations after expelling. Hence as reported for PS80 [16–18], also PS20 shows higher tendency to remove SO from the container surface and to increase gliding forces in siliconized syringes compared to Px188. In comparison, a higher mAb concentration, different pH or higher ionic strength did not markedly affect the syringe stability as all PS20 containing formulations showed the same SO depletion and a distinct increase in gliding forces at the 3 months timepoint. However, for the verum the SO removal was slightly enhanced compared to placebo. The stability correlated with the IFT between formulation and SO. All PS20 containing samples displayed a lower IFT compared to the surfactant free and Px188 formulation. As the IFT decreases the energy necessary to overcome the interfacial tension is lowered and hence a SO migration is more likely to occur [17]. The formulation with highest IFT, in our case the placebo solution without surfactant, showed least silicone oil removal followed by the protein formulation without surfactant and the formulations containing Px188. The fact that a higher PS20 concentration in the formulation did not accelerate the increase in gliding forces was also reflected in the IFT as a minimum value was already reached by the lowest PS20 concentration. The PS20 concentration of 0.06 % (w/v) is well above the critical micelle concentration (CMC) [44,45]. Px188 is less hydrophobic than PS20 with an HLB value of around 29 [30] compared to 16.7 [46], making it less surface active. Furthermore, the Px188 adsorption rate is less compared to PS20 due to its higher a molecular size around 8 kDa compared to

1.2 kDa for PS20 [16,19,21,30,47–51]. A higher amount of protein co-adsorbed to the interface was observed for Px188 compared to polysorbates [19,25,34,50–52]. According to our results Px188 is advantageous for protein formulations in combination products. Not only did it show higher container stability but by decreasing SO migration into solution the interfacial area for mAbs to adsorb to is lower. Hence, protein stability is potentially less diminished in this case [25]. Nevertheless, the choice of surfactant needs to be evaluated based on the product itself. Recently, visible protein-SO particles were detected after long term storage specifically in mAb formulations containing Px188.[48] After all, the occurrence of SO depletion can be also overcome by the appropriate choice of the primary packaging material [3,11,53].

In the second setup, only the mAb was varied instead of the formulation factors (Formulation mAb 1). The stability was found to depend on the mAb molecule. mAb 3 formulations were more stable compared to mAb 1 and 2 formulations as well as placebo at 40 °C, 25 °C and 2-8 °C. In general, SO migration was less pronounced after storage at lower temperature. But an increase in extrusion forces and a reduction of the SO layer thickness were observed, following the 40 °C results except for placebo solutions. In contrast to the formulation factor study, the outcome of the stability did not correlate to the IFT results. We assume a decreased IFT between the formulation and SO as one of the basic requirements for SO detachment. Nonetheless the protein effect on SO detachment was not reflected in IF. Additional dilational surface rheology measurements did not show any differences in the behavior of the mAb molecules at the SO interface. mAbs are known to form viscoelastic films upon adsorption at hydrophobic interfaces as a result of unfolding and increasing intermolecular interactions [22,24,25,54]. The presence of surfactant equally decreased elasticity regardless of the mAb type. A lower elasticity for protein-surfactant mixtures was expected as PS20 prevents the adsorption of the protein and thereby the formation of a protein network at the interface [27,28,50,52,55]. As the values matched the placebo, we assume the SO interface to be predominantly occupied by PS20 for all formulations. Further characterization of the protein molecules failed to identify clear predictive parameters related to SO detachment. Conformational stability, as tested via thermal unfolding, did not correlate with the stability of the syringes. Upon adsorption conformational changes of proteins can occur and an increased conformational stability tested both by thermal and chemical means is in general associated with a lower adsorption tendency [35,38]. Only the relative hydrophobicity ranking was in line with the stability

data. Hydrophobic interactions play a substantial role for protein adsorption to solid surfaces and thus an increased surface hydrophobicity could potentially enhance the interaction between the mAb and the SO interface respectively SO microdroplets in solution [34,40,56,57].

However, a different adsorption behavior of the mAb molecules was not indicated by the dynamic IFT measurements. Thus, the mechanism behind the stabilization respectively destabilization remains unclear at this point. A broad variety of different methods can be applied to further investigate the adsorption behavior of the protein and surfactant at the SO interface as well as the reversibility of the adsorption process [35,58,59]. Especially quartz crystal microbalance with dissipation monitoring (QCM-D) has been utilized to study the absorption of proteins and surfactants to siliconized surfaces and it also offers to determine a viscoelasticity of the adsorbed film [19,30,40]. In general, the monitoring of adsorption and desorption kinetics of the proteins to hydrophobic surfaces by methods like ellipsometry [60], optical waveguide lightmode spectroscopy [21], surface plasmon resonance [61] or biolayer interferometry [62] could help identify key differences for the molecules. Also, neutron reflectometry has been used to study the adsorption behavior to hydrophobic surfaces as it can provide detailed information about the molecule orientation and composition of the adsorbed film by determining layer thickness in the sub nanometer range [50,51,63,64]. The inclusion of more proteins with a broader variety of physico-chemical and surface-active properties is needed to identify the key factors influencing the SO detachment from the inner barrel surface. As all mAbs included in this study belonged to the IgG_1 subclass we expect no significant difference of the Fc fragment between the molecules [65]. A focus on the characterization of the Fab fragments could potentially facilitate the identification of predictive molecule properties. Finally, we suggest studies that focus on the interaction of the surfactants, SO and the protein beyond the interfacial properties of the formulations as the surface rheology measurements indicated the absence of the mAb molecule at the interface. Potentially, the ability to emulsify SO microdroplets plays a role in the SO migration enhancing tendency of certain formulations and mAb molecules. This could explain the lower stabilities of placebo formulations at higher storage temperature as the CMC of PS decreases and the micelle size increases at elevated temperatures [66,67]. In addition, mAbs were shown to increase the CMC of PS20 and PS80 due to interaction between protein and surfactant [68,69]. The fact that Px188 exhibits

a significantly higher CMC then PS may also be in line with a higher SO layer stability due to less microdroplet formation [16,34,70].

5 Conclusion

In the course of this study the dependency of the container stability on the fill medium systems became evident for standard spray-on siliconized container. In general, extrusion forces increased due to SO migration into the drug product at all storage temperatures including samples stored at 2-8 °C. Differences between formulations were already detectable after one month storage at 40 °C, which was predictive for storage at 25 °C and 2-8 °C. The silicone layer characterization revealed a complete SO removal from the inner barrel surface for specific formulations. Not only surfactant type but interestingly also the mAb present in formulation were found to impact container stability. Px188 containing formulations showed less SO detachment compared to PS20 containing formulations. mAb 3 samples were significantly more stable compared to syringes filled with mAb 1 and 2 and compared to placebo. In the case of formulation variables, a lower container stability could be correlated with a lower IFT, but the IFT did not differ with the mAb utilized. Also, interfacial rheology measurements as well as protein characterization in terms of conformational stability could not explain the difference between the mAbs in the very same formulation. Although the hydrophobicity ranking indicates that the observed SO depletion can be linked to intrinsic molecule properties, further studies are necessary to better understand the role of the protein in the SO detachment process and identify key factors for the occurrence of SO depletion. Overall, the studies underline the importance of testing container stability with verum.

Supplementary Data

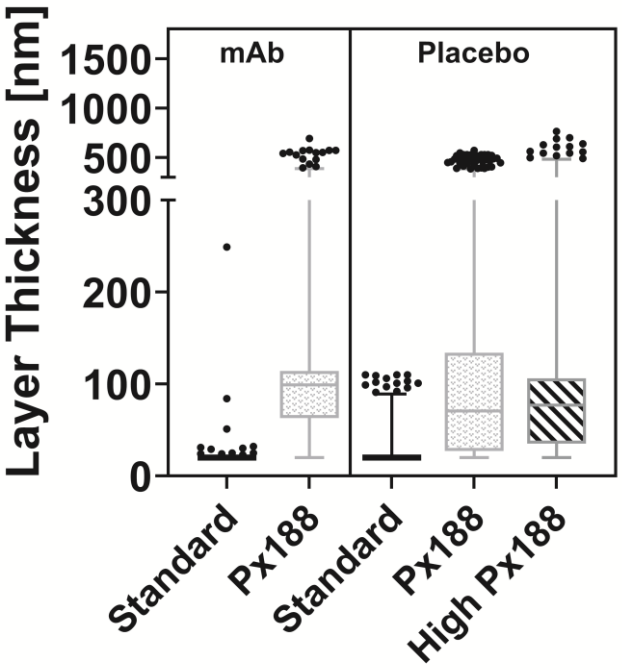

Figure S VI-1: SO layer thickness after storage at 40 °C for 3 months of different mAb 4 [A] and placebo [B] formulations displayed as box plots (Box: 25th – 75th percentile; Whiskers: 2.5th – 97.5th percentile/LOD: 20 nm).

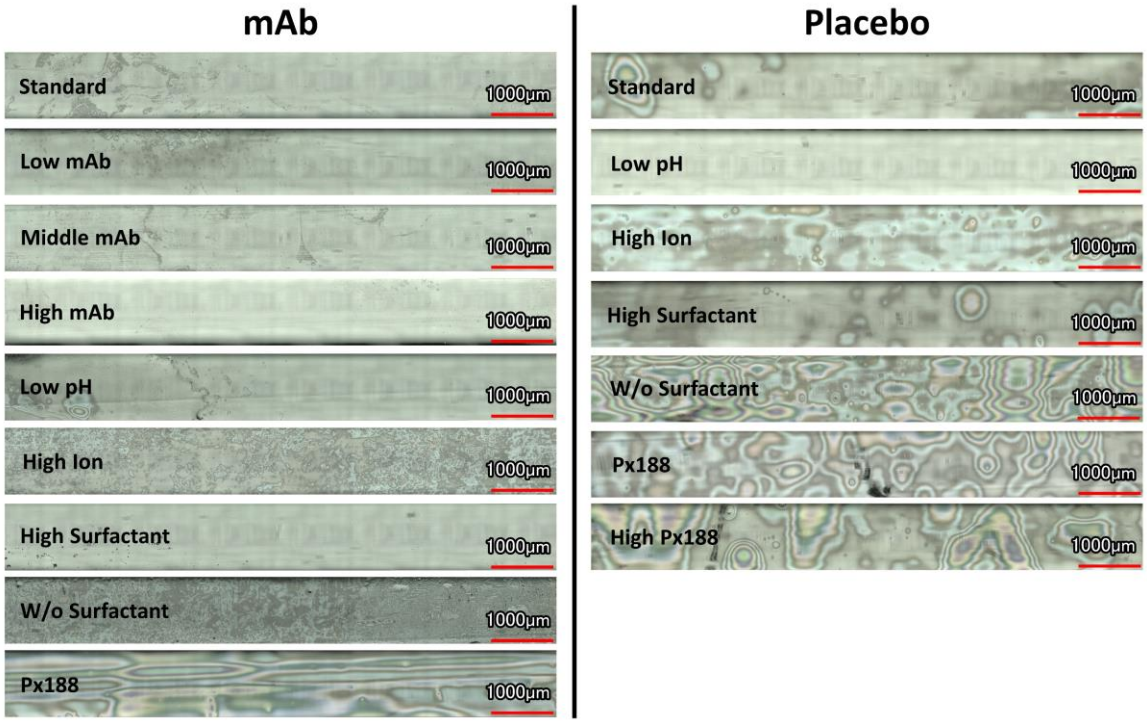

Figure S VI-2: 3D-LSM images of the inner surface of syringes after storage at 40 °C for 1 month of different mAb 4 and placebo formulations.

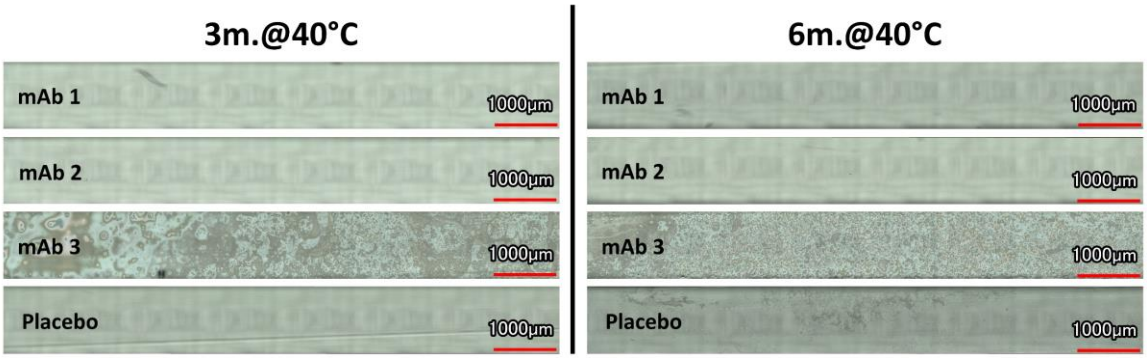

Figure S VI-3: 3D-LSM images of the inner surface of syringes after storage at 40 °C of mAb 1, 2 and 3 as well as placebo formulations.

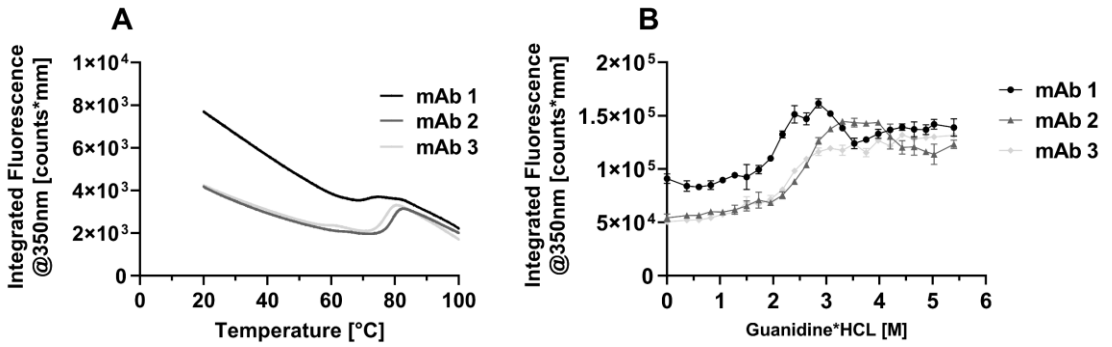

Figure S VI-4: Thermal unfolding [A] and chemical denaturation [B] of mAb 1, 2 and 3 detected by intrinsic fluorescence at 350 nm.

Abbreviations

3D-LSM	3D-Laser Scanning Microscope
CMC	Critical Micelle Concentration
E’	Storage Modulus
E’’	Loss Modulus
Fmax	Maximum Extrusion Force
FTIR	Fourier Transform Infrared Spectroscopy
HIC	Hydrophobic Interaction Chromatography
HPW	Highly Purified Water
IFT	Interfacial Tension
mAb	Monoclonal Antibody
PAT	Profile Analysis Tensiometer
PS	Polysorbate
Px	Poloxamer
SO	Silicone Oil
WI	White Light Interferometry
WLI	Combined White Light and Laser Interferometry

References

[1] Warne, N. W.; Mahler, H. C. Challenges in Protein Product Development. AAPS Advances in the Pharmaceutical Sciences Series Vol. 38; Springer, Cham, 2018. https://doi.org/10.1007/978-3-319-90603-4.

[2] Jameel, F.; Skoug, J. W.; Nesbitt, R. R. Development of Biopharmaceutical Drug-Device Products; Jameel, F., Skoug, J. W., Nesbitt, R. R., Eds.; AAPS Advances in the Pharmaceutical Sciences Series; Springer International Publishing: Cham, 2020; Vol. 35. https://doi.org/10.1007/978-3-030-31415-6.

[3] Yoneda, S.; Torisu, T.; Uchiyama, S. Development of Syringes and Vials for Delivery of Biologics: Current Challenges and Innovative Solutions. Expert Opin. Drug Deliv. 2021, 18 (4), 459–470. https://doi.org/10.1080/17425247.2021.1853699.

[4] Sacha, G.; Rogers, J. A.; Miller, R. L. Pre-Filled Syringes: A Review of the History, Manufacturing and Challenges. Pharm. Dev. Technol. 2015, 20 (1), 1–11. https://doi.org/10.3109/10837450.2014.982825.

[5] Sacha, G. A.; Saffell-Clemmer, W.; Abram, K.; Akers, M. J. Practical Fundamentals of Glass, Rubber, and Plastic Sterile Packaging Systems. Pharm. Dev. Technol. 2010, 15 (1), 6–34. https://doi.org/10.3109/10837450903511178.

[6] Gerhardt, A.; Mcgraw, N. R.; Schwartz, D. K.; Bee, J. S.; Carpenter, J. F.; Randolph, T. W. Protein Aggregation and Particle Formation in Prefilled Glass Syringes. J. Pharm. Sci. 2014, 103 (6), 1601–1612. https://doi.org/10.1002/jps.23973.

[7] Basu, P.; Blake-Haskins, A. W.; O'Berry, K. B.; Randolph, T. W.; Carpenter, J. F. Albinterferon A2b Adsorption to Silicone Oil–Water Interfaces: Effects on Protein Conformation, Aggregation, and Subvisible Particle Formation. J. Pharm. Sci. 2014, 103 (2), 427–436. https://doi.org/10.1002/jps.23821.

[8] Chisholm, C. F.; Baker, A. E.; Soucie, K. R.; Torres, R. M.; Carpenter, J. F.; Randolph, T. W. Silicone Oil Microdroplets Can Induce Antibody Responses Against Recombinant Murine Growth Hormone in Mice. J. Pharm. Sci. 2016, 105 (5), 1623–1632. https://doi.org/10.1016/j.xphs.2016.02.019.

[9] Chisholm, C. F.; Soucie, K. R.; Song, J. S.; Strauch, P.; Torres, R. M.; Carpenter, J. F.; Ragheb, J. A.; Randolph, T. W. Immunogenicity of Structurally Perturbed Hen Egg Lysozyme Adsorbed to Silicone Oil Microdroplets in Wild-Type and Transgenic Mouse Models. J. Pharm. Sci. 2017, 106 (6), 1519–1527. https://doi.org/10.1016/j.xphs.2017.02.008.

[10] Melo, G. B.; Cruz, N. F. S. da; Emerson, G. G.; Rezende, F. A.; Meyer, C. H.; Uchiyama, S.; Carpenter, J.; Shiroma, H. F.; Farah, M. E.; Maia, M.; Rodrigues, E. B. Critical Analysis of Techniques and Materials Used in Devices, Syringes, and Needles Used for Intravitreal Injections. Prog. Retin. Eye Res. 2021, 80 (March). https://doi.org/10.1016/j.preteyeres.2020.100862.

[11] Funke, S.; Matilainen, J.; Nalenz, H.; Bechtold-Peters, K.; Mahler, H.-C.; Friess, W. Silicone Migration From Baked-on Silicone Layers. Particle Characterization in Placebo and Protein Solutions. J. Pharm. Sci. 2016, 105 (12), 3520–3531. https://doi.org/10.1016/j.xphs.2016.08.031.

[12] Gerhardt, A.; Nguyen, B. H.; Lewus, R.; Carpenter, J. F.; Randolph, T. W. Effect of the Siliconization Method on Particle Generation in a Monoclonal Antibody Formulation in Pre-Filled Syringes. J. Pharm. Sci. 2015, 104 (5), 1601–1609. https://doi.org/10.1002/jps.24387.

[13] Depaz, R. A.; Chevolleau, T.; Jouffray, S.; Narwal, R.; Dimitrova, M. N. Cross-Linked Silicone Coating: A Novel Prefilled Syringe Technology That Reduces Subvisible Particles and Maintains Compatibility with Biologics. J. Pharm. Sci. 2014, 103 (5), 1383–1393. https://doi.org/10.1002/jps.23947.

[14] Chillon, A.; Pace, A.; Zuccato, D. Introducing the Alba ® Primary Packaging Platform. Part 1: Particle Release Evaluation . PDA J. Pharm. Sci. Technol. 2018, 72 (4), 382–392. https://doi.org/10.5731/pdajpst.2018.008623.

[15] Shi, G. H.; Gopalrathnam, G.; Shinkle, S. L.; Dong, X.; Hofer, J. D.; Jensen, E. C.; Rajagopalan, N. Impact of Drug Formulation Variables on Silicone Oil Structure and Functionality of Prefilled Syringe System. PDA J. Pharm. Sci. Technol. 2018, 72 (1), 50–61. https://doi.org/10.5731/pdajpst.2017.008169.

[16] Wang, T.; Richard, C. A.; Dong, X.; Shi, G. H. Impact of Surfactants on the Functionality of Prefilled Syringes. J. Pharm. Sci. 2020, 1–10. https://doi.org/10.1016/j.xphs.2020.07.033.

[17] Richard, C. A.; Wang, T.; Clark, S. L. Using First Principles to Link Silicone Oil / Formulation Interfacial Tension with Syringe Functionality in Pre-Filled Syringes Systems. J. Pharm. Sci. 2020. https://doi.org/10.1016/j.xphs.2020.06.014.

[18] Fang, L.; Richard, C. A.; Shi, G. H.; Dong, X.; Rase, M. C.; Wang, T. Physicochemical Excipient-Container Interactions in Prefilled Syringes and Their Impact on Syringe Functionality. PDA J. Pharm. Sci. Technol. 2021, pdajpst.2020.012278. https://doi.org/10.5731/pdajpst.2020.012278.

[19] Dixit, N.; Maloney, K. M.; Kalonia, D. S. Protein-Silicone Oil Interactions: Comparative Effect of Nonionic Surfactants on the Interfacial Behavior of a Fusion Protein. Pharm. Res. 2013, 30 (7), 1848–1859. https://doi.org/10.1007/s11095-013-1028-1.

[20] Begum, F.; Amin, S. Investigating the Influence of Polysorbate 20/80 and Polaxomer P188 on the Surface & Interfacial Properties of Bovine Serum Albumin and Lysozyme. Pharm. Res. 2019, 36 (7). https://doi.org/10.1007/s11095-019-2631-6.

[21] Kim, H. L.; Mcauley, A.; Livesay, B.; Gray, W. D.; Mcguire, J. Modulation of Protein Adsorption by Poloxamer 188 in Relation to Polysorbates 80 and 20 at Solid Surfaces. J. Pharm. Sci. 2014, 103 (4), 1043–1049. https://doi.org/10.1002/jps.23907.

[22] Mehta, S. B.; Lewus, R.; Bee, J. S.; Randolph, T. W.; Carpenter, J. F. Gelation of a Monoclonal Antibody at the Silicone Oil-Water Interface and Subsequent Rupture of the Interfacial Gel Results in Aggregation and Particle Formation. J. Pharm. Sci. 2015, 104 (4), 1282–1290. https://doi.org/10.1002/jps.24358.

[23] Thirumangalathu, R.; Krishnan, S.; Ricci, M. S.; Brems, D. N.; Randolph, T. W.; Carpenter, J. F. Silicone Oil- and Agitation-Induced Aggregation of a Monoclonal Antibody in Aqueous Solution. J. Pharm. Sci. 2009, 98 (9), 3167–3181. https://doi.org/10.1002/jps.21719.

[24] Freer, E. M.; Yim, K. S.; Fuller, G. G.; Radke, C. J. Interfacial Rheology of Globular and Flexible Proteins at the Hexadecane/Water Interface: Comparison of Shear and Dilatation Deformation. J. Phys. Chem. B 2004, 108 (12), 3835–3844. https://doi.org/10.1021/jp037236k.

[25] Kannan, A.; Shieh, I. C.; Negulescu, P. G.; Chandran Suja, V.; Fuller, G. G. Adsorption and Aggregation of Monoclonal Antibodies at Silicone Oil-Water Interfaces. Mol. Pharm. 2021, 18 (4), 1656–1665. https://doi.org/10.1021/acs.molpharmaceut.0c01113.

[26] Kannan, A.; Shieh, I. C.; Fuller, G. G. Linking Aggregation and Interfacial Properties in Monoclonal Antibody-Surfactant Formulations. J. Colloid Interface Sci. 2019, 550, 128–138. https://doi.org/10.1016/j.jcis.2019.04.060.

[27] A. Bos, M.; van Vliet, T. Interfacial Rheological Properties of Adsorbed Protein Layers and Surfactants: A Review. Adv. Colloid Interface Sci. 2001, 91 (3), 437–471. https://doi.org/10.1016/S0001-8686(00)00077-4.

[28] Mcauley, W. J.; Jones, D. S.; Kett, V. L. Characterisation of the Interaction of Lactate Dehydrogenase With Tween-20 Using Isothermal Titration Calorimetry, Interfacial Rheometry and Surface Tension Measurements. J. Pharm. Sci. 2009, 98 (8), 2659–2669. https://doi.org/10.1002/jps.21640.

[29] Jiao, N.; Barnett, G. V.; Christian, T. R.; Narhi, L. O.; Joh, N. H.; Joubert, M. K.; Cao, S. Characterization of Subvisible Particles in Biotherapeutic Prefilled Syringes: The Role of Polysorbate and Protein on the Formation of Silicone Oil and Protein Subvisible Particles After Drop Shock. J. Pharm. Sci. 2020, 109 (1), 640–645. https://doi.org/10.1016/j.xphs.2019.10.066.

[30] Li, J.; Pinnamaneni, S.; Quan, Y.; Jaiswal, A.; Andersson, F. I.; Zhang, X. Mechanistic Understanding of Protein-Silicone Oil Interactions. Pharm. Res. 2012, 29 (6), 1689–1697. https://doi.org/10.1007/s11095-012-0696-6.

[31] Köpf, E. Antibody drugs at the liquid-air interface: physicochemical characteristics, aggregation & the impact of formulation. Ph.D. Thesis, LMU Munich, 2017.

[32] Dixit, N.; Maloney, K. M.; Kalonia, D. S. The Effect of Tween® 20 on Silicone Oil-Fusion Protein Interactions. Int. J. Pharm. 2012, 429 (1–2), 158–167. https://doi.org/10.1016/j.ijpharm.2012.03.005.

[33] Kannan, A.; Shieh, I. C.; Leiske, D. L.; Fuller, G. G. Monoclonal Antibody Interfaces: Dilatation Mechanics and Bubble Coalescence. Langmuir 2018, 34 (2), 630–638. https://doi.org/10.1021/acs.langmuir.7b03790.

[34] Höger, K.; Mathes, J.; Frieß, W. IgG1 Adsorption to Siliconized Glass Vials-Influence of PH, Ionic Strength, and Nonionic Surfactants. J. Pharm. Sci. 2015, 104 (1), 34–43. https://doi.org/10.1002/jps.24239.

[35] Rabe, M.; Verdes, D.; Seeger, S. Understanding Protein Adsorption Phenomena at Solid Surfaces. Adv. Colloid Interface Sci. 2011, 162 (1–2), 87–106. https://doi.org/10.1016/j.cis.2010.12.007.

[36] Gerhardt, A.; Bonam, K.; Bee, J. S.; Carpenter, J. F.; Randolph, T. W. Ionic Strength Affects Tertiary Structure and Aggregation Propensity of a Monoclonal Antibody Adsorbed to Silicone Oil-Water Interfaces. J Pharm Sci 2013, 102, 429–440. https://doi.org/10.1002/jps.23408.

[37] Ludwig, D. B.; Carpenter, J. F.; Hamel, J.-B.; Randolph, T. W. Protein Adsorption and Excipient Effects on Kinetic Stability of Silicone Oil Emulsions. J. Pharm. Sci. 2010, 99 (4), 1721–1733. https://doi.org/10.1002/jps.

[38] Karlsson, M.; Ekeroth, J.; Elwing, H.; Carlsson, U. Reduction of Irreversible Protein Adsorption on Solid Surfaces by Protein Engineering for Increased Stability. J. Biol. Chem. 2005, 280 (27), 25558–25564. https://doi.org/10.1074/jbc.M503665200.

[39] Norde, W. Driving Forces for Protein Adsorption at Solid Surfaces. Macromol. Symp. 1996, 103, 5–18. https://doi.org/10.1002/masy.19961030104.

[40] Oom, A.; Poggi, M.; Wikström, J.; Sukumar, M. Surface Interactions of Monoclonal Antibodies Characterized by Quartz Crystal Microbalance with Dissipation: Impact of Hydrophobicity and Protein Self-Interactions. J. Pharm. Sci. 2012, 101 (2), 519–529. https://doi.org/10.1002/jps.22771.

[41] Funke, S.; Matilainen, J.; Nalenz, H.; Bechtold-Peters, K.; Mahler, H.-C.; Friess, W. Analysis of Thin Baked-on Silicone Layers by FTIR and 3D-Laser Scanning Microscopy. Eur. J. Pharm. Biopharm. 2015, 96, 304–313. https://doi.org/10.1016/j.ejpb.2015.08.009.

[42] Svilenov, H.; Markoja, U.; Winter, G. Isothermal Chemical Denaturation as a Complementary Tool to Overcome Limitations of Thermal Differential Scanning Fluorimetry in Predicting Physical Stability of Protein Formulations. Eur. J. Pharm. Biopharm. 2018, 125 (January), 106–113. https://doi.org/10.1016/j.ejpb.2018.01.004.

[43] Niklasson, M.; Andresen, C.; Helander, S.; Roth, M. G. L.; Zimdahl Kahlin, A.; Lindqvist Appell, M.; Mårtensson, L.-G.; Lundström, P. Robust and Convenient Analysis of Protein Thermal and Chemical Stability. Protein Sci. 2015, 24 (12), 2055–2062. https://doi.org/10.1002/pro.2809.

[44] Deechongkit, S.; Wen, J.; Narhi, L. O.; Jiang, Y.; Park, S. S.; Kim, J.; Kerwin, B. A. Physical and Biophysical Effects of Polysorbate 20 and 80 on Darbepoetin Alfa. J. Pharm. Sci. 2009, 98 (9), 3200–3217. https://doi.org/10.1002/jps.21740.

[45] Horiuchi, S.; Winter, G. CMC Determination of Nonionic Surfactants in Protein Formulations Using Ultrasonic Resonance Technology. Eur. J. Pharm. Biopharm. 2015, 92, 8–14. https://doi.org/10.1016/j.ejpb.2015.02.005.

[46] Rowe, R.; Sheskey, P.; Quinn, M. Handbook of Pharmaceutical Excipients; Pharmaceutical Press: London, 2009; Vol. Sixth Edit.

[47] Kolliphor, P.; Poloxamer, M.; Poloxamer, M. Technical Information Sheet Kolliphor ® P 188; BASF SE, 2021; pp 1–4.

[48] Grapentin, C.; Müller, C.; Kishore, R. S. K.; Adler, M.; ElBialy, I.; Friess, W.; Huwyler, J.; Khan, T. A. Protein-Polydimethylsiloxane Particles in Liquid Vial Monoclonal Antibody Formulations Containing Poloxamer 188. J. Pharm. Sci. 2020, 109 (8), 2393–2404. https://doi.org/10.1016/j.xphs.2020.03.010.

[49] Sigma-Aldrich Chemie GmbH. Sicherheitsdatenblatt Gemäß Verordnung (EG) Nr. 1907/2006 Tween® 20; 2021; pp 1–9.

[50] Tein, Y. S.; Zhang, Z.; Wagner, N. J. Competitive Surface Activity of Monoclonal Antibodies and Nonionic Surfactants at the Air-Water Interface Determined by Interfacial Rheology and Neutron Reflectometry. Langmuir 2020, 36 (27), 7814–7823. https://doi.org/10.1021/acs.langmuir.0c00797.

[51] Zhang, Z.; Marie Woys, A.; Hong, K.; Grapentin, C.; Khan, T. A.; Zarraga, I. E.; Wagner, N. J.; Liu, Y. Adsorption of Non-Ionic Surfactant and Monoclonal Antibody on Siliconized Surface Studied by Neutron Reflectometry. J. Colloid Interface Sci. 2020, 584, 429–438. https://doi.org/10.1016/j.jcis.2020.09.110.

[52] Narváez, A. R.; Vaidya, S. V. Protein—Surfactant Interactions at the Air-Water Interface. In Excipient Applications in Formulation Design and Drug Delivery; Springer International Publishing: Cham, 2015; pp 139–166. https://doi.org/10.1007/978-3-319-20206-8_6.

[53] Yoshino, K.; Nakamura, K.; Yamashita, A.; Abe, Y.; Iwasaki, K.; Kanazawa, Y.; Funatsu, K.; Yoshimoto, T.; Suzuki, S. Functional Evaluation and Characterization of a Newly Developed Silicone Oil-Free Prefillable Syringe System. J. Pharm. Sci. 2014, 103 (5), 1520–1528. https://doi.org/10.1002/jps.23945.

[54] Burgess, D. J.; Sahin, N. O. Interfacial Rheological and Tension Properties of Protein Films. J. Colloid Interface Sci. 1997, 189 (1), 74–82. https://doi.org/10.1006/jcis.1997.4803.

[55] Blomqvist, B. R.; Ridout, M. J.; Mackie, A. R.; Wärnheim, T.; Claesson, P. M.; Wilde, P. Disruption of Viscoelastic β-Lactoglobulin Surface Layers at the Air-Water Interface by Nonionic Polymeric Surfactants. Langmuir 2004, 20 (23), 10150–10158. https://doi.org/10.1021/la0485475.

[56] Vermeer, A. W. P.; Giacomelli, C. E.; Norde, W. Adsorption of IgG onto Hydrophobic Teflon. Differences between the Fab and Fc Domains. Biochim. Biophys. Acta - Gen. Subj. 2001, 1526 (1), 61–69. https://doi.org/10.1016/S0304-4165(01)00101-5.

[57] Kanthe, A. D.; Krause, M.; Zheng, S.; Ilott, A.; Li, J.; Bu, W.; Bera, M. K.; Lin, B.; Maldarelli, C.; Tu, R. S. Armoring the Interface with Surfactants to Prevent the Adsorption of Monoclonal Antibodies. ACS Appl. Mater. Interfaces 2020, 12 (8), 9977–9988. https://doi.org/10.1021/acsami.9b21979.

[58] Li, J.; Krause, M. E.; Chen, X.; Cheng, Y.; Dai, W.; Hill, J. J.; Huang, M.; Jordan, S.; LaCasse, D.; Narhi, L.; Shalaev, E.; Shieh, I. C.; Thomas, J. C.; Tu, R.; Zheng, S.; Zhu, L. Interfacial Stress in the Development of Biologics: Fundamental Understanding, Current Practice, and Future Perspective. AAPS J. 2019, 21 (3). https://doi.org/10.1208/s12248-019-0312-3.

[59] Nakanishi, K.; Sakiyama, T.; Imamura, K. On the Adsorption of Proteins on Solid Surfaces, a Common but Very Complicated Phenomenon. J. Biosci. Bioeng. 2001, 91 (3), 233–244. https://doi.org/10.1016/S1389-1723(01)80127-4.

[60] Malmsten, M. Ellipsometry Studies of the Effects of Surface Hydrophobicity on Protein Adsorption. Colloids Surfaces B Biointerfaces 1995, 3 (5), 297–308. https://doi.org/10.1016/0927-7765(94)01139-V.

[61] Nault, L.; Guo, P.; Jain, B.; Bréchet, Y.; Bruckert, F.; Weidenhaupt, M. Human Insulin Adsorption Kinetics, Conformational Changes and Amyloidal Aggregate Formation on Hydrophobic Surfaces. Acta Biomater. 2013, 9 (2), 5070–5079. https://doi.org/10.1016/j.actbio.2012.09.025.

[62] Ramadan, M. H.; Prata, J. E.; Karácsony, O.; Dunér, G.; Washburn, N. R. Reducing Protein Adsorption with Polymer-Grafted Hyaluronic Acid Coatings. Langmuir 2014, 30 (25), 7485–7495. https://doi.org/10.1021/la500918p.

[63] Ruane, S.; Li, Z.; Campana, M.; Hu, X.; Gong, H.; Webster, J. R. P.; Uddin, F.; Kalonia, C.; Bishop, S. M.; Van Der Walle, C. F.; Lu, J. R. Interfacial Adsorption of a Monoclonal Antibody and Its Fab and Fc Fragments at the Oil/Water Interface. Langmuir 2019, 35 (42), 13543–13552. https://doi.org/10.1021/acs.langmuir.9b02317.

[64] Couston, R. G.; Skoda, M. W.; Uddin, S.; Van Der Walle, C. F. Adsorption Behavior of a Human Monoclonal Antibody at Hydrophilic and Hydrophobic Surfaces. MAbs 2013, 5 (1), 126–139. https://doi.org/10.4161/mabs.22522.

[65] Chennamsetty, N.; Helk, B.; Voynov, V.; Kayser, V.; Trout, B. L. Aggregation-Prone Motifs in Human Immunoglobulin G. J. Mol. Biol. 2009, 391 (2), 404–413. https://doi.org/10.1016/j.jmb.2009.06.028.

[66] Nayem, J.; Zhang, Z.; TomLinson, A.; Zarraga, I. E.; Wagner, N. J.; Liu, Y. Micellar Morphology of Polysorbate 20 and 80 and Their Ester Fractions in Solution via Small-Angle Neutron Scattering. J. Pharm. Sci. 2020, 109 (4), 1498–1508. https://doi.org/10.1016/j.xphs.2019.12.016.

[67] Garidel, P.; Blech, M.; Buske, J.; Blume, A. Surface Tension and Self-Association Properties of Aqueous Polysorbate 20 HP and 80 HP Solutions: Insights into Protein Stabilisation Mechanisms. J. Pharm. Innov. 2021, 16 (4), 726–734. https://doi.org/10.1007/s12247-020-09488-4.

[68] Mahler, H.-C.; Senner, F.; Maeder, K.; Mueller, R. Surface Activity of a Monoclonal Antibody. J. Pharm. Sci. 2009, 98 (12), 4525–4533. https://doi.org/10.1002/jps.21776.

[69] Dixit, N.; Zeng, D. L.; Kalonia, D. S. Application of Maximum Bubble Pressure Surface Tensiometer to Study Protein-Surfactant Interactions. Int. J. Pharm. 2012, 439 (1–2), 317–323. https://doi.org/10.1016/j.ijpharm.2012.09.013.

[70] Wan, L. S. C.; Lee, P. F. S. CMC of Polysorbates. J. Pharm. Sci. 1974, 63 (1), 136–137. https://doi.org/10.1002/jps.2600630136.

Chapter VII Summary and Outlook

With the success of biopharmaceuticals as well as novel injectable API formats like gene therapy and RNA based drugs the development of drug device combination products (DDCPs) became increasingly important in the last years. As the drug product and device interact in the primary container the choice of the adequate container system is to be considered individually. In this context, several new container systems have been developed to overcome the issues originating from silicone oil (SO) applied in the standard spray-on siliconized container systems. Despite the obvious superiority for SO particle burden and interaction potential, long hands-on experience for most of the alternative container system in marketed product is still lacking. The thesis aimed to analyze and understand different challenges in the context of the development of DDCPs for biopharmaceuticals.

At first, the impact of a change of the emulsion used for bake-on siliconization due to REACh regulations was evaluated in chapter III. The change of the formulation did not negatively impact the stability of the newly introduced emulsion Liveo™ 366 as well as the dilution used for spraying compared to the current gold standard emulsion Liveo™ 365. Particle size and distribution were identical and did not significantly change upon storage or freezing and thawing of the dilutions. The emulsions showed comparable creaming behavior and redistribution could easily be achieved by slight shaking. By thermogravimetric analysis and 1H-NMR measurements we could show that both the newly added surfactant Undeceth-5 and the preservative Phenoxyethanol were completely removed by the bake-on process. Surface morphology and roughness as well as surface free energy of the different baked-on SO layers did not differ. Container systems siliconized with either of one of the emulsions showed exceptionally low subvisible particle formation and break-loose gliding forces (BLGF) upon storage at 40 °C for 12 weeks. Consequently, the change of the emulsion does not to significantly affect the quality and safety of a final DDCP.

In addition, we studied the effect of autoclavation on baked-on SO, as it is used in the context of preparation of ready to use containers for biopharmaceuticals in chapter IV. Autoclavation significantly impacted the SO layer morphology as it turned from a homogenous coating to a structured surface with spots of SO enrichment leading to local increase in SO layer thickness. Interferometry measurements showed a SO redistribution

along the complete length of the barrel. The change was more pronounced at higher autoclavation temperatures of 130 °C. We additionally found an increase in surface roughness, hydrophilicity, frictional force, and protein adsorption with autoclavation. Nevertheless, the total SO amount per barrel was not significantly reduced upon autoclavation and SO was still distributed evenly along the barrel as assessed with interferometry and 3D-laser scanning microscopy (3D-LSM) measurements. A stability study comparing autoclaved and non-autoclaved containers showed no difference in SvP formation and BLGF upon storage at 40 °C for 12 weeks. Hence, autoclavation at standard process parameters does not negatively impact the stability and safety of DDCP for biopharmaceuticals.

A recently marketed new silicone oil free (SOF) container system was evaluated in chapter V. The SOF system proofed to be a valuable alternative to the existing container systems. It exhibited significantly lower particle formation as well as constant and acceptable BLGFs upon storage at accelerated (40 °C) and long-term storage conditions (24 months). Although the siliconized systems showed reliable container stability, the SO layer morphology changed upon storage. SEM images of cross sections of the SOF plunger compared to standard plungers for siliconized systems showed that the PTFE coating of the plungers for the SOF container system was applied on the complete plunger. This includes the sides in contact with the glass thereby reducing the friction force. The SOF container functionality correlated with contact angle measurements of the fill medium. A change in surface polarity of the glass or the filled medium significantly affected the friction force. Thus, storage conditions or manufacturing processes like washing and sterilization need to be carefully evaluated regarding their impact on the glass surface properties during the development of a DDCP.

Not only does the container mitigate the drug product stability but also the formulation itself has an impact on the container stability as described in Chapter VI. Open storage of spray-on siliconized containers we observed an increase in the extrusion forces which was dependent on the formulation of a mAb. We also found an effect of the protein itself when comparing three mAbs in the very same formulation. Based on SO layer thickness measurements, 3D-LSM images of the silicone layer and quantification of residual SO amounts the in some cases massive increase in gliding force after 1 month could be explained by a removal of SO from the inner surface of the glass barrel during storage. Results obtained at 40 °C correlated with changes upon storage at 25 °C and 2-8 °C.

Polysorbate 20 containing formulations showed significantly higher gliding forces compared to samples without surfactant or Poloxamer 188. This correlated with the lower interfacial tension (IFT) between formulation and SO. Further formulation factors like the pH, ionic strength or the protein concentration did not clearly affect the container stability. However, the stability of the container system varied depending on the mAb present in the formulation. Whereas in two cases performance was worse compared to placebo, one mAb stabilized the container system compared to placebo. We could not correlate this different container stability with either a difference in IFT or with the mAb hydrophobicity and conformational stability. The studies underlined the importance to include the verum for container stability studies as well as the complexity of the SO detachment process.

Overall, this work focused on different aspects in the development of DDCPs. As the variety of primary container types increased over the last years the challenges involved in the development will be more versatile in the future. It remains unclear if the cost-efficient standard spray-on siliconized container system already served its time given that a variety of drug products show low SO sensitivity. The studies showed the superiority SOF container systems and those with fixed SO layers in terms of subvisible particle formation and container stability.